

AD-A098 636

GEORGIA INST OF TECH ATLANTA ENGINEERING EXPERIMENT --ETC F/G 6/1
MILLIMETER WAVE ATMOSPHERIC RADIOMETRY OBSERVATIONS. (U)

MAR 81 J H RAINWATER, J J GALLAGHER

NO8173-78-C-0168

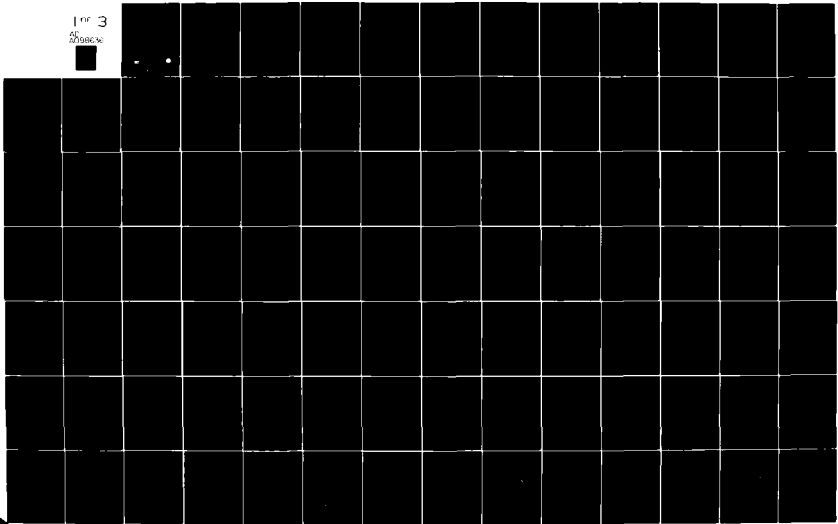
NL

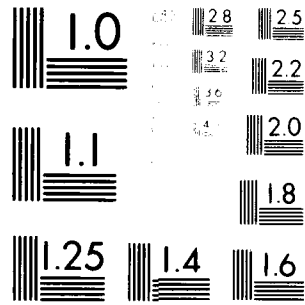
UNCLASSIFIED

617/EES-A-2173

1 of 3

50
PAGE





MICROCOPY RESOLUTION TEST CHART
NATIONAL BUREAU OF STANDARDS-1963-A

FINAL REPORT
GT/PROJECT NO. A-2173

LEVEL

2

ALU A U 9 8 6 3 6

**MILLIMETER WAVE ATMOSPHERIC
RADIOMETRY OBSERVATIONS**

By
J. H. Rainwater
J. J. Gallagher

Prepared for
THE NAVAL RESEARCH LABORATORY
WASHINGTON, D.C. 20375

DTIC
ELECTED
MAY 7 1981

Under
Contract No. N00173-78-C-0165
Contracting Project Officer: J. Hollinger

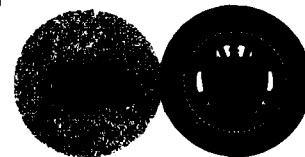
Period Covered: 1 August 1978 through 16 June 1980

27 March 1981

GEORGIA INSTITUTE OF TECHNOLOGY

Engineering Experiment Station
Atlanta, Georgia 30332

GT
EES



DISTRIBUTION STATEMENT A
Approved for public release;
Distribution Unlimited

DTIC FILE COPY

81 4 8 052

2

MILLIMETER WAVE ATMOSPHERIC
RADIOMETRY OBSERVATIONS.

Georgia Institute of Technology,
Engineering Experiment Station
Atlanta, Georgia 30332

Contract No. N00173-78-C-0165
CT/Proc. No. A-2173

WESIT/EES-A-2173

FINAL REPORT

Period Covered: 1 Aug 1978 through 16 Jun 1980

J. H. Rainwater
J. J. Gallagher

Contracting Project Officer: J. Hollinger
Prepared for
The Naval Research Laboratory
Washington, D.C. 20375

11 27 Mar 1981

2-60

DISP. BY...
Approved For...
Date...

REPORT DOCUMENTATION PAGE		READ INSTRUCTIONS BEFORE COMPLETING FORM	
1. REPORT NUMBER	2. GOVT ACCESSION NO.	3. RECIPIENT'S CATALOG NUMBER	
	AD A098 636		
4. TITLE (and Subtitle) Millimeter Wave Atmospheric Radiometry Observations		5. TYPE OF REPORT & PERIOD COVERED Final Report 1 August, 1978-16 June, 1980	
		6. PERFORMING ORG. REPORT NUMBER A-2173	
7. AUTHOR(s) J. H. Rainwater J. J. Gallagher		8. CONTRACT OR GRANT NUMBER(s) Contract No. ^{u.} N00173-78-C-0165	
9. PERFORMING ORGANIZATION NAME AND ADDRESS Georgia Institute of Technology Engineering Experiment Station Atlanta, Georgia 30332		10. PROGRAM ELEMENT, PROJECT, TASK AREA & WORK UNIT NUMBERS	
11. CONTROLLING OFFICE NAME AND ADDRESS The Naval Research Laboratory Washington, DC 20375		12. REPORT DATE 27 March, 1981	
		13. NUMBER OF PAGES	
14. MONITORING AGENCY NAME & ADDRESS (if different from Controlling Office)		15. SECURITY CLASS. (of this report) Unclassified	
		15a. DECLASSIFICATION/DOWNGRADING SCHEDULE	
16. DISTRIBUTION STATEMENT (of this Report)			
17. DISTRIBUTION STATEMENT (of the abstract entered in Block 20, if different from Report)			
18. SUPPLEMENTARY NOTES			
19. KEY WORDS (Continue on reverse side if necessary and identify by block number) Millimeter Waves Zenith Observations Atmospheric Effects 94GHz Fluctuations Radiometry			
20. ABSTRACT (Continue on reverse side if necessary and identify by block number) Observations of atmospheric emission were performed at 94GHz during a period of inclement weather in February/March, 1980. The measurements were made at the Engineering Experiment Station at Georgia Tech and were limited to zenith observations. The radiometer which was employed has been described in previous reports. Theoretical aspects of fluctuation effects are described. The observations were performed for an integration time of 0.16 seconds so that the ΔT_{\min} was in the range from approximately 0.8°K to			

1.2°K. The observed sky emission resulted in brightness temperatures approximately an order of magnitude larger than ΔT_{\min} and exceeds the theoretical sky temperature values.

Appendices give weather data and the data taken. A bibliography of pertinent references is presented as Appendix E. Conclusions and Recommendations (Section IV) are discussed. The data represents an initial effort in the observation of short-term fluctuation effects. Further work under a greater variety of weather conditions is needed.

UNCLASSIFIED

TABLE OF CONTENTS

<u>SECTION</u>	<u>PAGE</u>
PREFACE	i
I. Introduction.....	1
II. Discussion of Turbulence Effects.....	2
III. Measurements Performed.....	24
A. Radiometric Measurement System.....	24
B. Experimental Observations.....	28
C. Data and Preliminary Analysis.....	29
IV. Conclusions and Recommendations.....	38
REFERENCES	
APPENDIXES	
A. Data Taking Record.....	43
B. Weather Data for Observations.....	52
C. Ambient Load Data.....	59
D. Zenith Sky Data.....	99
E. Bibliography of Atmospheric Fluctuation Effects.....	245

Accession For
NTIS GRANT
DTIC TAB
Unannounced
Justification: _____
By _____
Distribution _____
As of _____
Dist _____
A

PREFACE

This report presents the final 94 GHz atmospheric emission measurements performed during February and March of 1980 under the terms of Contract No. N00173-780C-0165 between the Naval Research Laboratory (NRL) and the Georgia Institute of Technology Engineering Experiment Station (GTEES). Two field exercises were conducted at NRL during the program, and these have been discussed in previous reports. The measurements described herein were obtained with a slightly modified version of the radiometer used during the 1978 and 1979 measurement programs. Theoretical models of atmospheric fluctuations are briefly discussed. The data taken during February-March, 1980 are reviewed and discussed, with chosen data analyzed with current theoretical considerations. Recommendations and conclusions resulting from this work are presented.

I. INTRODUCTION

The turbulent atmosphere is an inhomogeneous medium in which the refractive index is a function of position and time. Scintillation, the observed fluctuation in intensity and apparent position of small angular size, is caused by random fluctuations in the refractive index of the earth's atmosphere through which the signals propagate. The majority of the investigations of atmospheric turbulence has been confined to the optical and the low frequency regions. Until recently, the effects of atmospheric turbulence on millimeter wave propagation have received little attention, and, in addition, most millimeter wave investigations have been directed to one-way link transmissions employing coherent transmitters. Only a few studies have concentrated on passive radiometric observations of atmospheric fluctuation effects.

The objective of these upward looking atmospheric measurements was to establish the spatial and temporal characteristics of atmospheric absorption/emission in the 94 GHz region. This atmospheric information is important for determining limitations on radio astronomy resolving power, and applications in communications, and is, in turn, necessary for providing the overall target to background clutter threshold as viewed from space, when combined with high resolution data on target signatures and surface clutter.

In this report, some of the effects expected from theory are discussed in order to provide a preliminary estimate of the effects observed in the experiments performed at Georgia Tech. Most of the theoretical considerations are extensions from optical studies; this practice is questionable until further data and analysis exist in the millimeter wavelength region. However, some millimeter wave radiometric studies have been performed, and our discussion will rely heavily on these investigations.

II. DISCUSSION OF TURBULENCE EFFECTS

The effects of atmospheric fluctuations have been extensively studied in the optical region with little consideration given to the effects in the millimeter wavelength region. Of the measurements performed at microwave frequencies and the few in the millimeter region, practically all have been for propagation between two points with coherent sources. Only a few have treated observations or relevant theory for passive radiometric observations. As a result, much of the theory and terminology must not only be adapted to a new spectral region but could be erroneously used to interpret passive observations. At the current stage of activities in the area of interest to this program, there is a need for detailed investigations of both theory and measurements. For the few investigations of atmospheric fluctuations by millimeter wave radiometry, the interest has been in slower fluctuation rates than those investigated in the measurements performed in this study.

In addition to the above considerations, the observed fluctuations originate from different causes. In the visible wavelength region, the refractive index variations are associated with the fluctuation of the temperature of the atmosphere due to turbulence. At longer radio wavelengths, the variation of the electron density in the ionosphere is the cause of scintillation. At shorter radio wavelengths, where the influence of the ionosphere is diminishing, variations in the water vapor concentration of the troposphere become increasingly important in causing fluctuations in the index of refraction. Kemp [1] has pointed out that, in all of these regions, the medium is essentially non-absorbing and attenuation of the signal in the turbulent region plays an insignificant role. For millimeter and submillimeter wavelengths, however, this is no longer the case. Thus, it is necessary to consider fluctuations in atmospheric attenuation in order to determine the amount of signal fluctuation present in a radiometric observation. In most of

the analysis performed in this spectral region [2], the model uses the properties of the dry atmosphere to conform to a standard atmosphere, e.g., the US Standard Atmosphere [3]. The water vapor concentration is assumed to have a mean profile but the concentration is allowed to fluctuate from point to point around this mean profile.

One of the earliest investigations of passive observations of the fluctuation components of the atmospheric noise temperature was performed by Orhaug [4] at 8 GHz. He employed a 12' parabolic antenna at NRAO and considered the small scale fluctuations in brightness temperature during periods with no precipitation to be an important limitation in radiometry. His short fluctuations were on the order of 1-2 °K with an average periodicity on the order of a few minutes. The system integration time was 5 seconds, long compared to our requirements. In Orhaug's observations [4], the atmospheric effects which he described were due to the thermal emission by the atmosphere, resulting from absorption characteristics of the transmission medium. The influence on phase characteristics of a wave propagating through the medium was not included. Orhaug has used results published by Hogg [5] to demonstrate the effects of changing water vapor content within the receiver beam as a function of zenith angle. Hogg used the brightness noise temperature from a standard atmosphere having a water vapor content of 10 g/m³ at ground level and from a humid atmosphere with 20 g/m³. In Figure 1, the effect of increasing the water vapor content from 10 to 20 g/m³ is indicated for 10 GHz. At the zenith direction, it is seen that the antenna noise temperature difference for the two water-vapor contents is 4°K increasing with zenith angle. The effect of different water vapor contents in the propagation path increases considerably as frequency is increased into the millimeter region.

A very rough, but interesting estimate of the variation in brightness temperature can be made for the assumption that a change in absorption coefficient occurs over a limited height interval ΔL .

$$\Delta T = T e^{-\alpha \Delta L} (\Delta \alpha \Delta L) \quad (1)$$

where the absorption coefficient is $\alpha + \Delta \alpha$ in the interval ΔL .

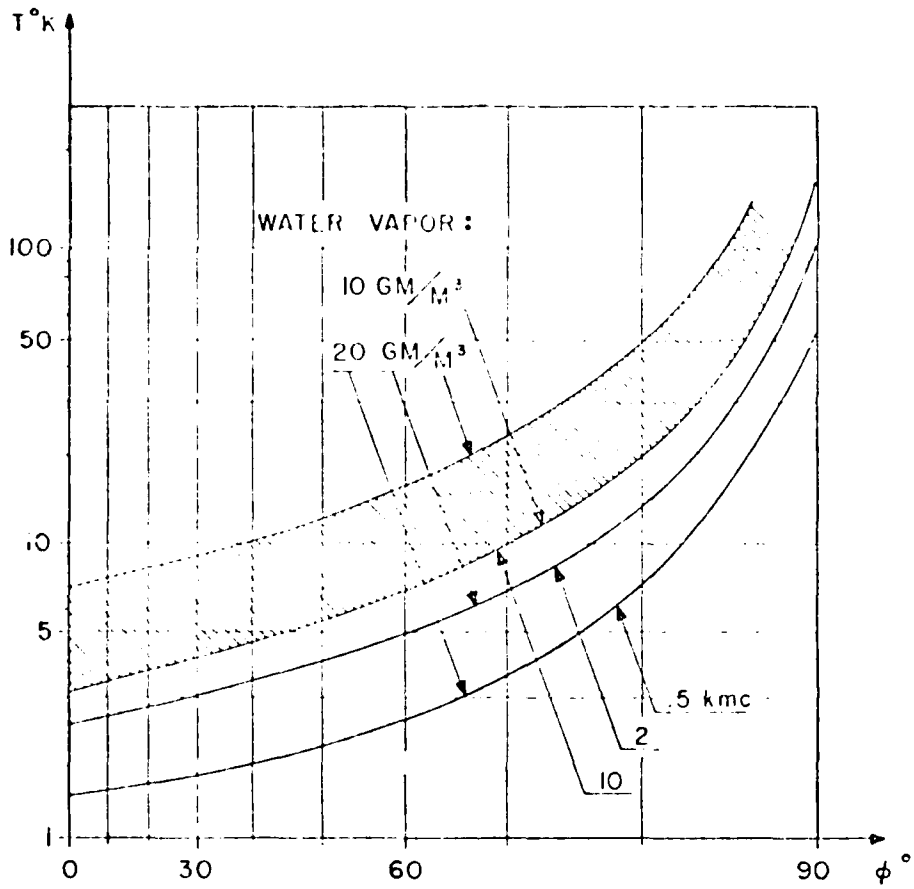


Fig. 1 -- Antenna noise temperature $T^{\circ}K$ due to atmospheric absorption as a function of antenna zenith angle for three different frequencies in the microwave region.

In this case, $\Delta\alpha$ is a function of pressure, temperature and water-vapor variation, which is the most significant parameter. Orhaug has considered the results of refractometer measurements to obtain the variation of the index of refraction as a function of the variation of the water vapor content: The index of refraction, n , is

$$n = 1 + \left(\frac{79}{T} P - \frac{10e}{T} + \frac{3.8 \times 10^5 e}{T^2} \right) 10^6 \quad (2)$$

where P is the total pressure in mb and e is the partial water-vapor pressure. With the refractivity, $N = (n-1) 10^6$, it is assumed that variation in N is caused only by variation in e , then

$$\Delta N = 4.2 \Delta e \text{ for } T = 300^\circ\text{K}$$

Orhaug indicates that refractometer measurements at different altitudes have given large-scale variations in N of the order of 50-200 N-units for the first 5 km of the earth's atmosphere. For $\Delta N=200$, the corresponding e -variation is $\Delta e=50$ mb.

The absorption coefficient for water vapor is directly proportional to the water vapor density, ρ grams/ m^3 and

$$\Delta\alpha = \alpha \frac{\Delta\rho}{\rho} = \alpha \frac{\Delta e}{e} \quad (3)$$

So the corresponding change in brightness temperature is

$$\Delta T_b = T e^{-\alpha_n \Delta L} \left(\alpha_n \frac{\Delta e}{e} \Delta L \right) \quad (4)$$

where α_n is the absorption coefficient in nepers. Orhaug has an error of a factor of 10 in his calculation so that the fluctuation ΔT_b is not as large as he indicates. In our case, with the correction made,

$$\Delta T_b = 1.75^\circ\text{K}$$

for $\alpha=0.3$ dB/km = .0345 neper/km

$$\begin{aligned} \rho &= 5 \text{ gm/m}^3 & \frac{\Delta e}{e} &\approx 0.2 \\ T &= 250 \text{ K} & \text{and } \Delta L &= 1 \text{ km} \\ \rho &= 600 \text{ mm Hg} \end{aligned}$$

This variation in the brightness temperature is observable with our system, but is not as large as was observed in some measurements.

Sollner [6] has made measurements of the frequency spectrum of fluctuations in submillimeter sky emission and absorption. The observations were for single beam techniques and double beam techniques (at fixed separation at 6 feet). The results were analyzed in terms of their power spectral density between 4×10^{-3} Hz and 0.25 Hz. For observations involving the fluctuating atmosphere, Sollner has considered the observed brightness of a source of brightness $B_s(\nu)$ propagating through an emitting and absorbing medium of brightness $B_m(\nu)$ and optical depth $\tau(\nu)$. This observed value is

$$B = \int B_s(\nu) f(\nu) e^{-\tau(\nu)} d\nu + \int B_m(\nu) f(\nu) (1 - e^{-\tau(\nu)}) d\nu \quad (5)$$

where $f(\nu)$ is the normalized response of the detector; the first term is the contribution from source (transmission term); the second term results from the intervening medium (emission term). The fluctuations in these terms are transmission noise and emission noise. If one assumes an effective optical depth, the transmission term can be written as

$$B_T = e^{-\tau} e^{\int B_s(\nu) f(\nu) d\nu} = e^{-\tau} e^{\overline{B_e}} \quad (6)$$

For a source constant in time, any fluctuations in the transmission term are due to change in τ_e . This term can be made to dominate the emission noise by choosing a sufficiently bright source. Sollner gives τ_e as $\tau_e + \Delta\tau_e(t)$ where $\Delta\tau_e(t)$ is the fluctuations of the effective

optical depth

$$B_T = \bar{B}_S \exp -[\tau_e + \Delta \tau_e] \quad (7)$$

and the power spectrum of $\Delta \tau_e$ as

$$S_{\Delta \tau_e}(f) = \mu_1 f^{-\alpha_1} \quad (8)$$

where the magnitude of B_T depends on τ_e , f is the frequency in Hz and α_1 is a constant determined from observations.

In the case of emission noise, simplifications are not possible because B_m changes with time as does τ . The physical situation of regions of differing B_m and τ passing through the observed solid angle can be represented in terms of spatial and temporal distributions for B_m and τ . In the investigations performed in this program, neither a tracking capability nor sufficient resolution to localize solar areas of constant brightness were available so that the important aspects of the absorption term could not be investigated. Such observations should be performed in the future. Further work should be performed in other well-defined observing windows and correlations should be made with temperature, water-vapor and wind velocity.

Several additional considerations can be given to millimeter fluctuation effects. In the case of millimeter wave propagation observations, theory predicts a strong dependence of the scintillation amplitude and angle of arrival variations on the humidity structure parameter C_h in addition to the temperature structure parameter C_T .

Tatarski [7] has shown that the resulting energy distribution in the turbulent atmosphere is log normal, characterized by a variance σ_E^2 that is a function of the degree of atmospheric turbulence.

Chernov [8] and Tatarski [7], in their original work, treated mainly optical fluctuations and neglected the effects of absorption on the fluctuations. Recent work of Russian workers has considered fluctuations in the millimeter and submillimeter wavelength regions, requiring the inclusion of absorption by atmospheric water vapor. Izyumov [9] has solved the wave equation to account for absorption resulting in expressions for amplitude and phase fluctuations valid for millimeter wave propagation. As a result of this work, the index of refraction N is given by

$$\begin{aligned}
 N &= n + im \\
 \text{with } n &= n_0 + \mu \\
 \text{and } m &= m_0 + \nu
 \end{aligned}
 \tag{9}$$

Here, n_0 and m_0 are mean values of the real and imaginary parts of N , and μ and ν are the fluctuating parts.

Armand [10] has given the spectra of fluctuations of the real and imaginary parts of the index of refraction and their cross-correlation in terms of the temperature and humidity fluctuations [See McMillan et al, Reference 11].

Gurvich [12] has given values of μ and ν for calculations of the spectra of fluctuations

$$\mu = (K_1 \frac{p}{T} + K_2 \frac{e}{T} + K_3 \frac{e}{T^2}) \times 10^{-6}
 \tag{10}$$

$$\nu = \gamma (p_0, T_0, e_0) \frac{e}{e_0} \frac{T_0^2}{T} \frac{p}{p_0} \frac{\lambda}{2\pi} \times 10^{-6}
 \tag{11}$$

$$K_1 = 78^\circ\text{K}/\text{mb}$$

$$K_2 = 72^\circ\text{K}/\text{mb}$$

$$K_3 = 3.7 \times 10^5 (\text{K})^2 \text{ (only weakly dependent on } \lambda \text{)}$$

p = atmospheric pressure in mb

e = partial pressure of water vapor in mb

λ = transmitted radiation wavelength

e_0, p_0, T_0 = stationary values of e, p, T

γ = absorption coefficient in nepers/km

The forms of the spectral distributions of fluctuations of temperature $\phi_T(q)$ and humidity $\phi_p(q)$ are given by Gurvich [12] (see [11]). For the relationship between C_T , the temperature structure parameter, and C_n , the index of refraction structure parameter, McMillan et al [11] have used

$$C_T = C_n(T^2/79p) \times 10^{-6} \quad (12)$$

Actually C_n^2 and C_T^2 are the meaningful parameters, but several authors quote values for C_n and C_T .

The limitations imposed by atmospheric fluctuations on the maximum linear dimensions of large telescopes have been considered by Bastin [13]. The limitation of angular resolution arises from differential phase change in radiation reaching either side of a large telescope as a result of changes in refractive index of air along the extreme rays. Bastin has considered that relatively small changes in total water-vapor in the solar direction can be determined as a function of time from small fractional variations in the transmitted solar intensity. This is the consideration that Sollner had made [6]. For deducing the fluctuation effects, it is assumed that a fixed distribution exists with random fluctuations in the concentration of water-vapor with respect to the atmosphere drifts through the antenna beam due to wind movement. This widely used assumption is in some cases referred to as the Taylor hypothesis, but is actually Tatarski's hypothesis of "Frozen-in" turbulence. Under this assumption, temporal changes can be related to spatial ones and therefore to phase changes which would be expected to occur between the spatial limits of a large telescope. Kemp [2] has extended this work by employing concepts put forth by Brooker [14].

Kemp [2] has given the absorption and refractive index of water-vapor as $\alpha(\nu)$ and $n(\nu)$ by the relations-

$$\begin{aligned} \alpha(\nu) &= K(\nu)\rho = \text{absorption coefficient} \\ n(\nu) - 1 &= L(\nu)\rho, \quad n(\nu) = \text{refractive index} \\ \text{and } \rho &= \text{density of water vapor} \end{aligned}$$

He assumes that all irregularities have essentially the same dimension D corresponding to the scale of largest significant eddies in the turbulence and uses for the variation in water-vapor density the mean square value for the deviation from the mean $(\Delta\rho)^2$. This variation produces a corresponding change in refractive index and attenuation of the signal within the region.

The fluctuation in refractive index is given by

$$\overline{(\Delta n)^2} = (L(\nu))^2 \overline{(\Delta\rho)^2} \quad (13)$$

The change in signal intensity is

$$\begin{aligned} \Delta I_\nu &= I_\nu \Delta\tau_\nu \text{ for } \Delta\tau_\nu \ll 1 \\ \text{where } I_\nu &= \text{signal intensity} \\ \Delta\tau_\nu &= K(\nu) D \Delta\rho \end{aligned}$$

$$\text{Thus, } \left[\frac{\Delta I_\nu}{I_\nu} \right]^2 = \text{change in optical depth of the region} = K(\nu) D \overline{(\Delta\rho)^2} \quad (14)$$

= relative mean square intensity fluctuation per region

The mean square fluctuation in phase of a wave of wavelength λ propagating through one region resulting from a refractive index change is

$$\begin{aligned} \overline{(\Delta\phi)^2} &= \left(\frac{2\pi D}{\lambda} \right)^2 \overline{(\Delta n)^2} \\ &= \left[\frac{2\pi}{\lambda} \frac{L(\nu)}{K(\nu)} \right]^2 \left[\frac{\Delta I_\nu}{I_\nu} \right]^2 \\ &= S^2(\nu) \left[\frac{\Delta I_\nu}{I_\nu} \right]^2 \end{aligned} \quad (15)$$

$$\text{where } S(\nu) = \frac{2\pi\nu L(\nu)}{cK(\nu)}$$

= the scintillation coefficient

If now a wave travels a distance through the fluctuation layer, it will encounter $\frac{2\ell}{D}$ regions. With the assumption that the water fluctuations are uncorrelated, the phase fluctuations will add in random walk fashion

$$\overline{(\Delta\phi)^2} = \frac{2\ell}{D} \overline{(\Delta\phi)_0^2} \quad (16)$$

Similarly, the relative fluctuations in intensity are

$$\overline{\left(\frac{\Delta I_v}{I_v}\right)^2} = \frac{2\ell}{D} \overline{\left(\frac{\Delta I_v}{I_v}\right)_0^2} \quad (17)$$

Thus, the phase fluctuation for a wave passing through a layer is related to the intensity fluctuation by

$$\overline{(\Delta\phi)^2} = S^2(\nu) \overline{\left(\frac{\Delta I_v}{I_v}\right)^2} \quad (18)$$

for $\nu \ll 1$. The scintillation coefficient $S(\nu)$ is inversely proportional to pressure and is a weak function of temperature and the concentration of water vapor. The coefficient can be taken as a constant throughout the troposphere, and the mean square fluctuation in signal phase can be determined from intensity fluctuation.

Kemp [2] has considered the practice of determining the fluctuation in phase difference for the wave arriving at two points separated by a distance d , which is perpendicular to the wave being propagated. If $C(d)$ is the correlation coefficient between the phase fluctuations at the two points, the phase difference between the signals at the two points is

$$\overline{\{\Delta(\phi_1 - \phi_2)\}_f^2} = 2\{1 - C(d)\}_f \overline{(\Delta\phi)^2} \quad (19)$$

In addition, let α_s = the angular scintillation, i.e. the fluctuation in the direction of arrival of the phase front.

$$\begin{aligned} \alpha_s^2 &= \left(\frac{\lambda}{2\pi d}\right)^2 \overline{\{\Delta(\phi_1 - \phi_2)\}_f^2} \\ &= 2\left(\frac{\lambda}{2\pi d}\right)^2 \{1 - C(d)\}_f \overline{(\Delta\phi)^2} \end{aligned} \quad (20)$$

To consider the atmospheric limits on an instrument of aperture d , σ_s compared with the minimum resolved angle due to diffraction. For the instrument to be atmospherically limited,

$$\text{or } \sigma_s \approx \frac{1.74 \pi}{d} > \frac{1.74 \pi}{(\Delta\phi)^2} \cdot (2.44\pi)^2 \quad (21)$$

Thus, when the random phase fluctuation due to the medium exceeds 1.74 π radians, for some value of d , the atmospheric angular scintillation will exceed the diffraction limit so that the instrument is atmosphere limited.

If the mean square difference coefficient $\Delta^2(d)$ is related to the correlation coefficient by

$$\Delta^2(d) = 2 \{1 - C(d)\} \quad (22)$$

$$\text{then, } \Delta^2(d) \cdot (\Delta\phi)^2 > (2.44\pi)^2 \quad (23)$$

In the millimeter wavelength region, phase fluctuations and the difference coefficients are not measured directly, but they can be determined from observable intensity fluctuations due to the variation in atmospheric attenuation.

For $\tau_v \ll 1$, the variation in phase and intensity are directly related to fluctuations in water-vapor density. Therefore, the correlation coefficient and the mean square difference coefficient for phase are identical to those for intensity fluctuations.

With equations 18 and 23,

$$\Delta^2(d) S^2(\nu) \left[\frac{\Delta I_\nu}{I_\nu} \right]^2 = (2.44\pi)^2 \quad (24)$$

where now $\Delta^2(d)$ is for intensity fluctuations.

The instrument is atmospherically limited if

$$\left[\frac{\Delta I_\nu}{I_\nu} \right]^2 = (1.74)^2 / S^2(\nu). \quad (25)$$

In addition, the limiting size of a diffraction limited instrument can be obtained from

$$\Delta^2(d) = (1.74\pi)^2 S^{-2}(\nu) \left\{ \left[\frac{\Delta I_\nu}{I_\nu} \right]^2 \right\}^{-1} \quad (26)$$

Neither the work of Kemp nor that performed in this program could measure intensity fluctuations from two positions but it has been possible to measure intensity fluctuation as a function of time at a given position. It is therefore possible to use Taylor's hypothesis to relate the mean square difference coefficient for a time interval t to the mean square difference coefficient for the spatial separation, d , by the relation

$$\Delta_d^2 = \sigma(t)^2 = \Delta_t^2 = \sigma(d)^2 \quad (27)$$

$$t = \frac{d}{v}, \quad v = \text{drift velocity of the atmosphere}$$

Kemp's work indicated that, during his measurements, the drift time interval for fluctuations was about 40 seconds, which when combined with the wind speed of 10 m/s gives the turbulent region dimension to be ~ 400 m.

In their investigations of millimeter wave atmospheric fluctuation effects, several authors have employed various concepts and methods of expressing the effects. As previously indicated, the majority of treatments applies to active one-way propagation and many discussions are not applicable to passive observations. It is important for this discussion, however, to include brief comments on these various investigations:

1.) The Kolmogorov model [15] assumes homogeneous and isotropic conditions of the atmosphere to describe the index variations. For a particular range of separation between two points, \vec{r}_1 and \vec{r}_2 , the model yields

$$\overline{|n(r_1) - n(r_2)|^2} = C_n^2 |r_1 - r_2|^{2/3} \quad (28)$$

where $\overline{\quad}$ denotes an ensemble average and C_n is the index structure constant. The separation range for validity of the model, often referred to as the inertial subrange, is

$$\ell_0 \ll |r_1 - r_2| \ll L_0 \quad (29)$$

where L_0 and ℓ_0 are the outer and inner scales of turbulence respectively. L_0 and ℓ_0 may be thought of as the approximate maximum and minimum of the eddy size. In the atmosphere, ℓ_0 ranges from a millimeter to centimeters, whereas L_0 for horizontal propagation in the low atmosphere, is about 1/3 the height above ground. For separations greater than L_0 , the mean square index fluctuation levels off to $C_n^2 L_0^{2/3}$ whereas, for separations less than ℓ_0 viscosity effects cause a very rapid decrease in index fluctuations.

2.) For intensity fluctuations in the millimeter wave region, theory requires consideration of the problem in two separate domains dependent upon the size of the outer scale of turbulence compared to the first Fresnel zone along the propagation path of length R. The cases are

$$L_0 < \sqrt{\lambda R} \quad \text{and} \quad L_0 > \sqrt{\lambda R}$$

Most rough estimates of turbulence effects in the mm wavelength region are based on Tatarski's calculations [7], valid for $L_0 > \sqrt{\lambda R}$. No simple quantitative models of amplitude fluctuations for the case of

$$L_0 < \sqrt{\lambda R}$$

exist, but Tatarski for a plane wave with $L_0 > \sqrt{\lambda R}$ gives the variance of the log-intensity fluctuations as

$$\begin{aligned} \sigma^2 &= \langle (10 \log_{10} \frac{I}{\bar{I}})^2 \rangle \\ &= 23.39 C_n^2 k^{7/6} R^{11/6} (\text{dB}^2) \end{aligned} \quad (30)$$

where $k = 2\pi/\lambda$

Worst-case estimates [16] for C_n have been made on basis of optical measurements to give $C_n^2 = 6 \times 10^{13} m^{-2/3}$ for strong turbulence.

3.) Using optical constants for obtaining estimates of millimeter wave turbulence effects, one must realize that optical turbulence is mainly dependent upon atmospheric temperature fluctuations and that varying water vapor effects are negligible. For millimeter waves, water vapor contributions to the index of refraction become important. Brown has shown that, for microwaves (> 10 GHz) statistical variations in water vapor below 8 km can produce values of C_n^2 that are more than two orders of magnitude greater than the values for the corresponding optical case; therefore, estimates of σ^2 based on optical constants may be in serious error.

4.) Armand et al [16] examined fluctuation effects near the 920 μm water line and found that on the absorption line center, the amplitude fluctuations were approximately five times less than in the 980 μm window.

5.) Mavroukoulakis et al [17] have compared the measured variances of log amplitude fluctuations at 36 and 110 GHz as a function of time and showed that the fluctuations at the different frequencies were very well correlated. Ho et al [18] have performed simultaneous mm and X-band refractivity measurements of C_n^2 obtaining over a one-hour period, respective average values of C_n^2 of $0.25 \times 10^{-14} \text{m}^{-2/3}$ and $0.32 \times 10^{-14} \text{m}^{-2/3}$.

6.) Andreyev et al [19] have made measurements at $\lambda = 2 \text{ mm}$ on a horizontal path of length 5.6 km in a strongly turbulent atmosphere. They were concerned about testing Tatarski's hypothesis of "frozen-in" turbulence and estimated the width of the spectrum on intensity fluctuations due to cross-transfer of homogeneities across the path of propagation to be

$$\Delta F = \langle v_{\perp} \rangle / \sqrt{\lambda L} \quad (31)$$

where $\langle v_{\perp} \rangle$ = the mean speed of homogeneities transfer
and L = path length

Andreyev et al found $\Delta F = 0.17 \text{ Hz}$. They divided the fluctuations into fast ($> 0.1 \text{ Hz}$) and slow ($< 0.1 \text{ Hz}$). Their conclusion was that "frozen-in" turbulence doesn't describe intensity fluctuation quite correctly. The conclusion was that "frozen-in" turbulence was confirmed when it describes intensity fast-fluctuations. Intensity slow-fluctuations are assumed to be caused by cross-transfer and evolution of large scale inhomogeneities whose sizes are more than $\sqrt{\lambda L}$. To estimate C_n^2 , Andreyev et al considered the effect of aperture averaging and obtained values for C_n^2 in the range from 0.12×10^{-6} to $0.61 \times 10^{-6} \text{m}^{-1/3}$.

In support of measurement of atmospheric turbulence, a vertical profile of the thermal structure of the atmosphere would be very important. Bufton [20] combined thermal sensor technology for microthermal measurements with radiosonde balloon systems. This resulted in an extension of turbulence sensing to heights up to 25 km above sea level. This measurement technique provides $C_T^2(h)$ data where $C_T^2(h)$ is the temperature structure coefficient and h is the altitude. The refractive index structure coefficient $C_n^2(h)$ is obtained from relationships with $C_T^2(h)$ at least for optical effects. Bufton obtained the mean-square temperature difference between two microthermal probes as a function of altitude. This is, by definition, the temperature structure function, D_T , at probe locations r_1 and r_2 :

$$D_T(r_1, r_2) = \langle [T(r_1) - T(r_2)]^2 \rangle$$

$T(r_1)$ = temperature at point r_1

$$D_T(r) = C_T^2 r^{2/3}, \quad r = |r_1 - r_2|$$

C_T^2 is a strength parameter. A larger value indicates more temperature fluctuations, which are associated with more-turbulent mixing of air. The general expression for refractive index as a function of temperature and wavelength provides the connection between C_T^2 and C_n^2 . Bufton uses the expression

$$C_n^2(h) = \left[\frac{79.9 P(h) \times 10^{-6}}{T^2(h)} \right]^2 C_T^2(h) \quad (32)$$

where $P(h)$ = atmospheric pressure (mbars)

$T(h)$ = ambient temperature ($^{\circ}$ K)

h = altitude.

This relation has been used by McMillan et al [11] [See Equation 12], but Bufton has indicated that the relation applies for $0.5 \mu\text{m}$. Therefore, caution should be exercised in using it at millimeter wavelengths.

A recent publication by Hill, Clifford and Lawrence [22] treats the effects of refractive-index and absorption fluctuations on propagation for the microwave region through the IR. This work can be adapted to the vertical radiometric observations of interest to this program. The NOAA group has investigated the dependence of fluctuations in atmospheric absorption and refraction upon fluctuations in temperature, humidity and pressure.

For the applications of interest in this report, fluctuations in atmospheric refraction are not significant. The work of Hill et al [22] has considered the contributions from line absorption by H_2O . They have developed functions, relating the fluctuations, which are necessary for evaluating degradation of electromagnetic radiation by turbulence. In the calculation of the turbulence effect, we must choose a set of mean atmospheric conditions. Since the observations are for vertical absorption effects, the mean atmospheric conditions are chosen for vertical layers of the atmosphere.

In reference [22], it is assumed that turbulent fluctuations in total pressure give a negligible contribution to absorption and refraction fluctuations. This assumption is for horizontal active system propagation, but is assumed to apply to vertical observations. Whether this is a reasonable assumption for vertical observations remains to be determined.

In the millimeter wavelength region, humidity fluctuations dominate absorption fluctuations. In order to determine the effects of absorption fluctuations on antenna temperature (ΔT), it is possible to employ the variation of atmospheric absorption as a function of fluctuations in temperature, humidity and pressure. It is necessary to provide these functions that relate the fluctuations in order to evaluate the degradation of radiation by turbulence. It is necessary to choose a set of mean atmospheric conditions.

The relations employed for the fluctuation determinations include the linestrength (S_i) for an individual i (in units of cm^{-2} per unit concentration) and the linewidth. Both the linestrength and linewidth are temperature dependent, and, in addition, the linewidth depends on pressure and humidity.

The linestrength S_i has temperature dependence arising from the partition function, Q_{PART} , and the difference of 2 Boltzmann distributions [22]

$$S_i \propto \frac{\exp(-E_i^L / CT) - \exp(-E_i^U / CT)}{Q_{\text{PART}}}$$

E^U and E^L are values of upper and lower state energies for spectral line i (in units cm^{-1}).

Then, $C = kb/hc = 0.695008 \text{ cm}^{-1} \text{ } ^\circ\text{K}^{-1}$
and $\nu_i = E^U - E^L$.

The temperature dependence of the linestrength is shown to be

$$S_i(T) = S_{oi}(T_0/T)^a \exp \left[-\frac{E_i^L}{C} \left(\frac{1}{T} - \frac{1}{T_0} \right) \right] \left(\frac{1 - \exp(-\nu_i/CT)}{1 - \exp(-\nu_i/CT_0)} \right)$$

$a = 3/2$

S_{oi} = strength of line i at the reference temperature T_0 .

Total absorption is the sum over all lines-

$$\beta = \sum_i \beta_i$$

$$n_I = \beta/4\pi\nu$$

Q = absolute humidity

The fluctuations in β_i are given by-

$$\delta\beta_i = \langle b_{T_i} \rangle \frac{\delta T}{T} + \langle b_{P_i} \rangle \frac{\delta P}{P} + \langle b_{Q_i} \rangle \frac{\delta Q}{Q}$$

$$b_{T_i} = \frac{T}{\beta_i} \left(\frac{\partial \beta_i}{\partial T} \right)_{PQ}$$

$$= \left(\frac{T}{S_i} \frac{\partial S_i}{\partial T} \right) + \left(\frac{\alpha_i}{\beta_i} \frac{\partial \beta_i}{\partial \alpha_i} \right) \left(\frac{T}{\alpha_i} \frac{\partial \alpha_i}{\partial T} \right)$$

$$b_{P_i} = \frac{P}{\beta_i} \left(\frac{\partial \beta_i}{\partial P} \right)_{TQ} = \left(\frac{\alpha_i}{\beta_i} \frac{\partial \beta_i}{\partial \alpha_i} \right) \left(\frac{P}{\alpha_i} \frac{\partial \alpha_i}{\partial P} \right)$$

$$b_{Q_i} = \frac{Q}{\beta_i} \left(\frac{\partial \beta_i}{\partial Q} \right)_{PT} = 1 + \left(\frac{\alpha_i}{\beta_i} \frac{\partial \beta_i}{\partial \alpha_i} \right) \left(\frac{Q}{\alpha_i} \frac{\partial \alpha_i}{\partial Q} \right)$$

$$\frac{T}{S_i} \frac{\partial S_i}{\partial T} = -a + \frac{E_i^L}{CT} - \frac{\nu_i}{CT} \frac{\exp(-\nu_i/CT)}{1 - \exp(-\nu_i/CT)}$$

$$\frac{T}{\alpha_i} \frac{\partial \alpha_i}{\partial T} = -b + R$$

$$\frac{P}{\alpha_i} \frac{\partial \alpha_i}{\partial P} = 1 - R$$

$$\frac{Q}{\alpha_i} \frac{\partial \alpha_i}{\partial Q} = R$$

$$\text{where } R = \frac{4kQT}{P + 4kQT}$$

$$\frac{\alpha_i}{\beta_i} \frac{\delta R_i}{\delta \alpha_i} = \frac{\alpha_i}{g} \frac{g}{\delta \alpha_i}$$

and $a = 3/2$, $b = 0.62$

If we were only concerned with β_i fluctuations due to humidity fluctuations, the result would be

$$\begin{aligned} \frac{\delta \beta_i}{\beta_i} &= -b_{Q_i} > \frac{\delta Q}{\langle Q \rangle} \\ &= 1 + \frac{\alpha_i}{\beta_i} \frac{\delta \beta_i}{\delta \alpha_i} \frac{Q}{\alpha_i} \frac{\delta \alpha_i}{\delta Q} \frac{\delta Q}{\langle Q \rangle} \\ &= 1 + \frac{\alpha_i}{g} \frac{\delta g}{\delta \alpha_i} \frac{4kQT}{p + 4kQT} \frac{\delta Q}{\langle Q \rangle} \end{aligned}$$

The total fluctuation in atmospheric absorption is

$$\begin{aligned} \delta B &= \sum_i \delta \beta_i = \sum_i \beta_i <b_{Q_i}> \frac{\delta Q}{\langle Q \rangle} \\ &= \sum_i \beta_i \left[1 + \left(\frac{\alpha_i}{g} \frac{\partial g}{\partial \alpha_i} \right) \left(\frac{4kQT}{p + 4kQT} \right) \right] \frac{\delta Q}{\langle Q \rangle} \end{aligned}$$

In the low frequency limit, $\nu_i \ll CT$, applying to the millimeter/submillimeter wavelength region,

$$S_i(T) = T^{-5/2} \exp(-E_i^L / CT)$$

The dependence of linewidth on P, Q, T is given as [22]

$$\alpha_i(P, T, Q) = \alpha_{oi} \left(\frac{P + 4kQT}{P_0} \right) \left(\frac{T_0}{T} \right)^b$$

with $b = 0.62$

α_{oi} = width of line i at reference pressure P_0 and temperature T_0 .

Hill et al used formulas for differential changes to find the fluctuations caused by turbulence (accurate to first order in fluctuations). Variables P, T and Q are written as the sum of their mean values $\langle P \rangle$, $\langle T \rangle$ and $\langle Q \rangle$ and their fluctuations caused by turbulence -

$$P = \langle P \rangle + SP$$

$$T = \langle T \rangle + ST$$

$$Q = \langle Q \rangle + SQ$$

The following relations [22] are applicable to the measurements of this investigation -

Imaginary part of refractive index attributable to a single absorption line = n_{iI}

Absorption coefficient due to the same line = β_i

$$n_{iI} = \beta_i / 4\pi\nu$$

$$\beta_i = \frac{S_i Q}{\pi} g$$

g = line-shape factor

Table I of Reference [22] gives the line shapes and their derivatives with respect to linewidth. It is possible to employ the above formulas to determine the fluctuation in the absorption coefficient over any vertical path or segment of the path as a function of the fluctuations of the three variables (P , I , O). Two approximations of the fluctuation in brightness temperature have recently been employed by R. W. McMillan of our laboratory to compare with the data reported here. He considered fluctuations in the vertical water vapor distribution to produce fluctuations in the absorption coefficient of water vapor. In one case, he considered a fluctuation in humidity at ground level and a corresponding fluctuation vertically through the atmosphere. This approach gave fluctuations in brightness temperature on the order of but less than the measured values. The use of a fluctuation throughout the atmosphere is not the most reasonable assumption. A more reasonable one is to assume that the turbulence occurred in a layer approximately 1 km wide at some altitude (used as 10 km in the case analyzed). The justification of a stratification like this might be found in the work of Bufton [21]. The calculations resulted in brightness temperature fluctuations on the order of the RMS values of fluctuation observed in the experiments, but almost an order of magnitude smaller than the peak-to-peak fluctuations which have been observed. Possibly a stratification of the turbulence in the form of layers or horizontal sheets of different amplitudes, compatible with thermosonde turbulence data [21], would be the most applicable assumption.

III-A. RADIOMETRIC MEASUREMENT SYSTEM

The atmospheric measurements conducted during this contract have been obtained with a superheterodyne, double sideband, Dicke-switched, 94 GHz radiometer. The radiometer, previously described in the Semi-Annual Report [21], is depicted in Figure 2. The most unusual feature of the radiometer front-end is the quasi-optical antenna feed which allows one of several antenna schemes to be employed. Figure 2 shows the front-end as it was operated at the prime focus of the Naval Research Laboratory's (NRL) 10 foot dish during the 1978 and 1979 measurement programs. For the 1980 measurements, the radiometer antenna feed was integrated with a 24 inch Cassegrain antenna system by connecting the conical horn's waveguide port to the feed horn of the cassegrain antenna. Antenna patterns for the modified system are shown in Figures 3 and 4.

A new sharpless wafer mixer was installed in the radiometer for the 1980 measurements which greatly improved system sensitivity at the larger post-detection bandwidths needed to observe atmospheric emission fluctuations. For most data runs, the minimum detectable temperature (ΔT_{\min}) of the radiometer was less than 1°K for a 6.25 Hz bandwidth (0.16 sec integration). The actual ΔT_{\min} for each data run is noted on the time history/spectral density plots in Appendix A.

The overall performance of the radiometric measuring system was excellent during the 1980 measurements. System sensitivity and calibration repeatability were several orders of magnitude better than that obtained during the 1978 and 1979 measurement programs at NRL, where serious radio frequency (RFI) from the ambient electrical environment degraded system performance. While some RFI was noted during operation on the Georgia Tech campus, the effect upon the system was not nearly as severe nor prolonged as that experienced at NRL.

GEORGIA TECH 94 GHz BEAM WAVEGUIDE RADIOMETER

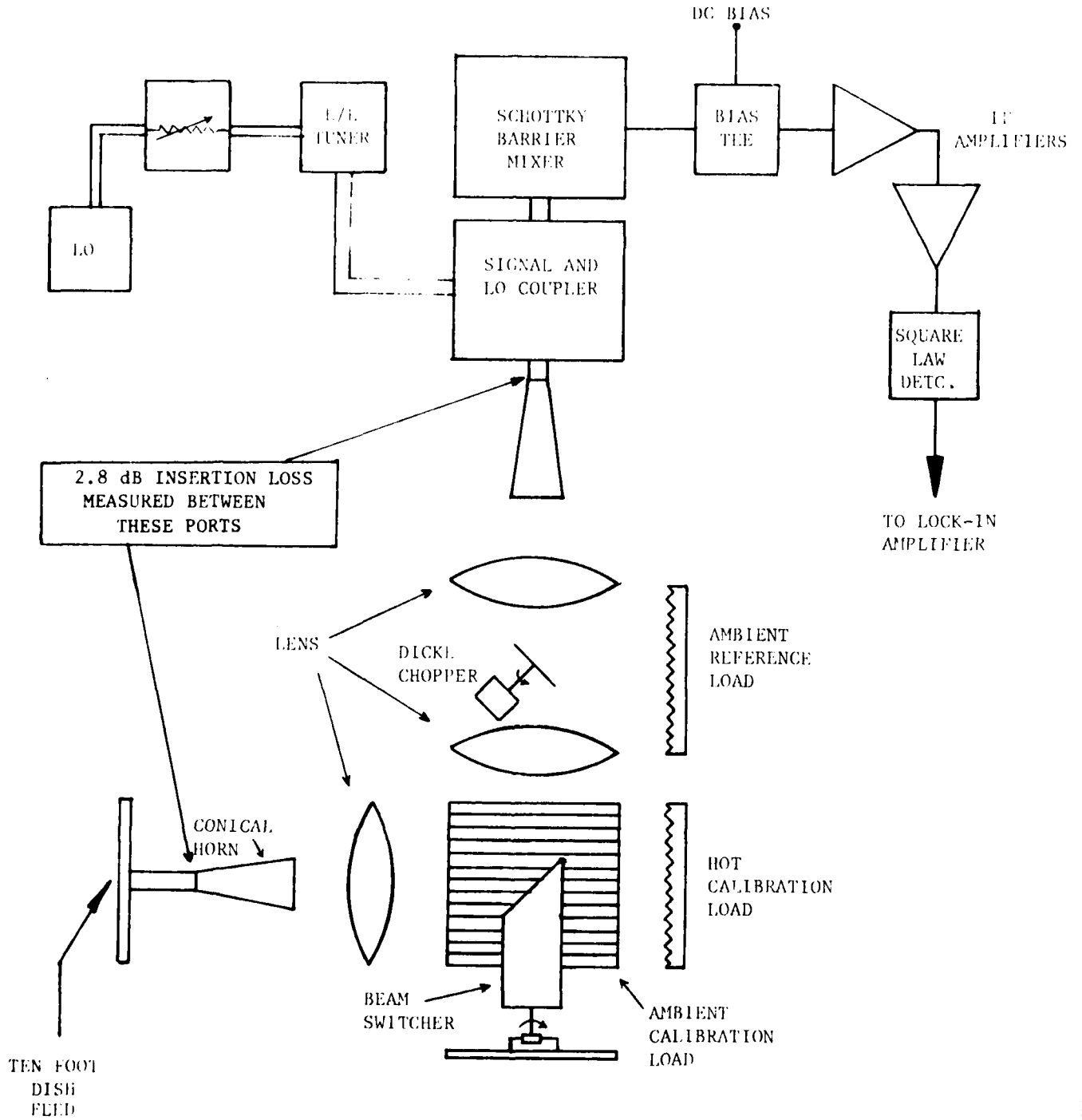


Figure 2. Radiometer RF Front-End.

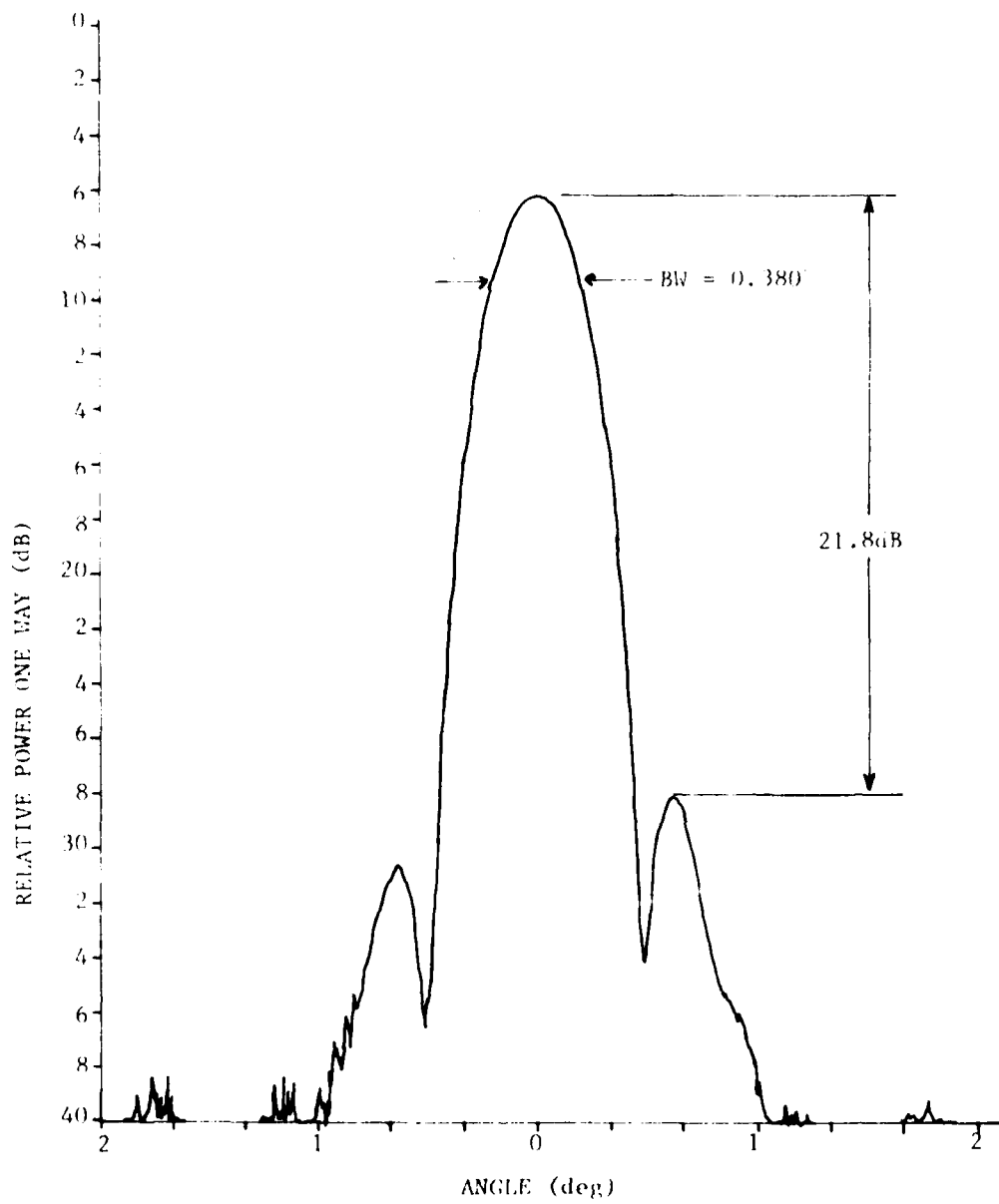


Figure 3. E-plane antenna pattern.

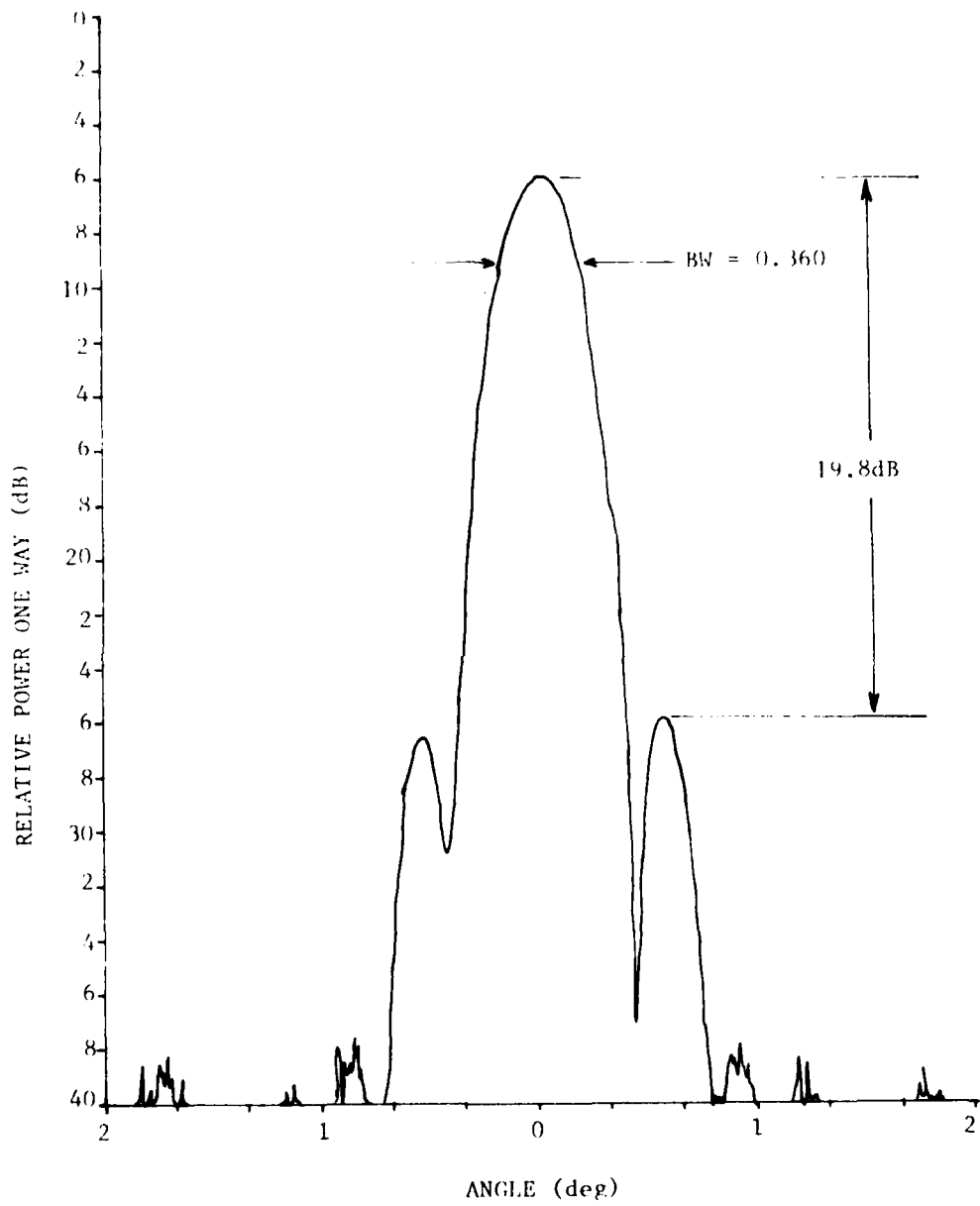


Figure 4. H-plane antenna pattern.

B. EXPERIMENTAL OBSERVATIONS

Observations of atmospheric fluctuations were made under a variety of atmospheric conditions during the period from February 28 through March 16, 1980. Appendix A lists the data taken during this period with notes on weather conditions and the approximate ΔT_{\min} existing for the observations. The minimum detectable temperature was checked periodically by observations on the ambient load, reference load and hot load, estimating the peak-to-peak noise N and from this, calculating the minimum detectable temperature, $\Delta T_{\min} = \frac{N}{6} \cdot (SF)$ where SF is a scale factor given in $^{\circ}K/\text{inch}$ of recorder paper. The weather conditions, listed in Appendix B, provided a large variety of conditions ranging from clear skies to overcast, from low humidity ($\sim 0.4 \text{ g/m}^3$) to high humidity ($\sim 15 \text{ g/m}^3$) and strong winds. The conditions of the sky (clear, overcast, etc.) can be obtained more accurately from the notes in Appendix A, since these data were derived from observations made at the site. The data in Appendix B were furnished by NOAA at the Atlanta Airport. On March 2, 1980, the weather conditions were very severe with the temperature on the order of 21° F , strong winds and snow flurries. Observations on the ambient load were made not only by the load switching scheme previously described [21] but by placing a load directly over the antenna feed horn. This allowed an observation to be made to include all losses within the system (switching, reflectors, horns, etc.) except for the antenna disk. The measurements showed no significant difference from the internal switching as far as noise level of the system was concerned. Neither technique, switching or external load observation, resulted in fluctuation levels comparable to the sky observations. These observations on the ambient load indicate that RFI or other external effects did not contribute to the large fluctuations observed during sky measurements. RFI should be the same for the external load case and the sky observations.

C. DATA AND PRELIMINARY ANALYSIS

The radiometric data taken during the period from 28 February, 1980 to 16 March, 1980 are given in Appendices C (Ambient Load Data) and D (Zenith Sky Data). The brightness temperature fluctuations for sky observation are much larger than the fluctuations obtained during observations on the ambient load. They do, in fact, exceed by a large margin the theoretically expected values. Table 1 gives the brightness temperature fluctuations as determined from the data of the Appendices. Table 1A lists the peak-to-peak temperature fluctuations and the corresponding ΔT_{RMS} . For most cases, the ambient load observations were on the order of 5 °K or less for peak-to-peak fluctuations yielding $\Delta T_{RMS} \approx 1.0$ °K. For the zenith sky measurements, the peak-to-peak fluctuations ranged between 15 °K - 30 °K as sky conditions varied considerably. The resulting ΔT_{RMS} ranged from 2.5 °K - 5 °K. The most commonly used parameters during the observations were 20 seconds for the observation time and an integration time 0.16 sec. In most cases, the fluctuation rate was much faster than $\tau = 0.16$ sec. On some observations, as for Runs 18-43 on February 28, the temperature scales were too low and fluctuations were excessive compared to the large fluctuations for zenith sky observed in other runs. It is not evident what the cause of these changes were, particularly since the characteristics returned to typical values on Run 52 of that date.

The preliminary analysis performed by R. W. McMillan was intended to provide an estimate of the fluctuations which can be expected for reasonable assumptions for atmospheric parameters. The estimate, however, results in expected fluctuations of only a few degrees maximum amplitude, an order of magnitude less than the peak-to-peak amplitudes of fluctuation that have been observed. A more accurate method of determining the meteorological conditions is needed in order to make detailed calculations of the effects.

Table IA
Brightness Temperature Fluctuations

1.) Ambient Load Observations:

Observation Time = 20 sec.

$\tau = 0.16$ sec

February 28, 1980

<u>Run #</u>	<u>ΔT Peak-Peak</u>	<u>ΔT RMS</u>
22	7.5	1.25
28	19	3.16
38	16	2.6
57	6.5	1.08
62	5	0.83
67	6	1.0

February 29, 1980

74	8.5	1.42
76	4.3	0.71
83	4.25	0.708
84	5.00	0.83
85	4.5	0.75
86	4.25	0.708
110	9.25	1.54
119	4.4	0.73
17	6.25	1.04
18	6.00	1.00

March 2, 1980

34	6.5	1.08
44	4.5	0.75
58	4.5	0.75

March 8, 1980

19	5.5	0.92
8	5.0	0.83

March 11, 1980

8	5.0	0.83	$\tau = .5 \text{ sec}$
13	5.8	0.97	slow variations
25	3.0	0.50	$\tau = 1.6 \text{ sec}$
29	2	0.33	very slow variations
42	8	1.33	$\tau = 0.5 \text{ sec}$
52	21	3.5	changed to 5 second observation
60	38	6.0	" " " $\tau = 0.016 \text{ sec}$

March 16, 1980

78	4.0	0.667	Increased back to 20 sec observation
99	3.5	0.583	$\tau = 0.16 \text{ sec}$
115	2.5	0.418	
88	1.0	0.167	5 second observation low fluctuations,
89	2.2	0.37	<u>but rapid excursions</u>
99	4.1	0.68	20 sec observation
			$\tau = 0.16 \text{ sec}$

Table 1B
Brightness Temperature Fluctuations

2.) Zenith Sky Observations
 Observation Time = 20 sec
 $\tau = 0.16$ sec

February 28, 1980

Run #	$\Delta T_{\text{Peak-Peak}}$	ΔT_{RMS}
9	24	4
10	22	3.67
11	22	3.67
12	26	4.33
13	21	3.50
18-43	see note at bottom of Table	
52	23	3.84
53	35	5.84
54	30	5.00
55	30	5.00
56	30	5.00
58	31	5.17
59	28	4.67
63	26	4.33
64	22	3.67
65	23	3.84
71	27	4.50
72	26.5	4.41
73	23.5	3.92

February 29, 1980

78	16	2.67
79	17	2.84
80	17	2.84
81	16	2.67
82	16	2.67
87	16	2.67
88	18	3.00
89	17	2.84
90	18	3.00
91	17	2.84
97	20	3.33
98	18	3.00
106	17	2.84
107	18.5	3.08
108	22	3.67
109	18	3.00
116	16.5	2.75
117	19	3.17
118	17.5	2.92
12	15.5	2.58
13	17	2.84
14	16	2.67
15	17	2.84
16	19.75	3.29

March 2, 1980

36	19.5	3.25
37	20.1	3.35
38	19	3.17
39	20	3.33
40	20	3.33
45	15.5	2.58
46	16.8	2.80
47	15.9	2.65
50	21	3.50
51	19.4	3.23
52	19.25	3.21
53	18.9	3.15
54	20	3.33
60	16.4	2.73
61	17	2.83
62	16.5	2.75
63	15.8	2.63
64	17	2.83
65	21	3.50
71	19	3.17
72	20	3.33
73	18	3.00
74	22.9	3.82
75	17	2.83

March 11, 1980

9	18	3		
10	21	3.5		
12	17	2.83		
18	9.5	1.58	$\tau = 0.5 \text{ sec}$	
21	9.5	1.58	Change in fluctuation characteristics	
22	9.0	1.5	" " " "	
23	12	2.0	" " " "	
30	4.0	0.67	$\tau = 1.6 \text{ sec}$	
31	5.0	0.83	" " " "	
32	7.0	1.17	" " " "	
33	10.00	1.67	" " " "	", slower
34	5.00	0.83	" " " "	", "
44	23	3.83	$\tau = 0.5 \text{ sec}$	", faster
45	23	3.83	" " " "	", "
46	24	4.00	" " " "	", "
47	24.4	4.07	" " " "	". "

March 16, 1980

80	16.7	2.78	$\tau 0.16 \text{ sec}$	
81	17.5	2.92	"	
82	20	3.33	"	
83	20	3.33	"	
100	7.7	1.28	60 sec observation with change in	
101	10	1.67	characteristics of fluctuation	
102	8	1.33		

117	7.5	1.25	$\tau = 1.6$ sec, 60 sec observation
118	4.0	0.67	" " " "
119	5.5	0.92	" " " "
82	10	1.67	$\tau = 5$ sec, 500 sec observation
83	6	1.0	" " " "
84	4	.67	" " " "
101	16	2.67	20 sec observation, $\tau = 0.16$ sec
102	18	3.00	" " " "
103	15	2.50	" " " "

Note: For zenith observations 18 through 43 on February 28, 1980, the temperature scale was too low and fluctuations were $\approx 30^\circ$ K.

Whereas the observations indicate that large fluctuations occur under the atmospheric conditions that prevailed during the February-March, 1980 period, a more rigorous analysis is necessary. The assumption that the atmosphere is stable during the observation period must be analyzed further. V. E. Derr of NOAA (Boulder), in a private communication to R. W. McMillan, has indicated that strong fluctuations will be observed when the atmosphere is in a state of transition, such as at the time of formation of fogs and clouds. He has observed strong return using an 8 mm radar from areas of clear sky near clouds, while simultaneous observations with a ruby lidar showed no returns. He attributes these return to refractive index inhomogeneities caused by water vapor. Such conditions could well have existed during the measurements of this program.

IV. CONCLUSIONS AND RECOMMENDATIONS

Observations performed during the period February 28 - March 16, 1960 have shown sky temperature fluctuations ranging from 15°K to 20°K peak-to-peak values with $\Delta T_{\text{RMS}} \approx 3-5^{\circ}\text{K}$. These values correspond to several sky conditions from clear to overcast. Preliminary calculations indicate that, for clear weather conditions, the expected fluctuations are smaller by a factor of approximately 4-7 than the observed fluctuations. The meteorological conditions were such that considerable instability could have existed in the atmosphere. The high rate of fluctuations is also not expected. Some sky observations appeared to have a rapid systematic variation characteristic of instability within the radiometer or from external RFI. The lack of such effects during the ambient load observations, however, does not support the contention that the observed fluctuation originated from system/RFI problems. Efforts to associate the large fluctuations with sources other than the atmosphere have not resulted in any conclusions. Some aspects of the radiometer which was used were not desirable and do present potential sources of fluctuations. This is particularly the case for the open structure beam-waveguide apparatus in the front-end of the radiometer. This structure was employed for the observations on the 10' dish at NPL but was not needed for the measurements at Georgia Tech. It did contribute to the degradation of the noise figure. For the ΔT_{min} observed with the system, the overall system noise figure was approximately 12 dB. One should expect at 94 GHz that a $\text{NF} \approx 7-8$ dB should be achievable with conventional radiometric systems for $\tau = 0.16$ sec. However, although this structure did degrade the sensitivity of the radiometer, it cannot account for the large variations (above the minimum ΔT) which were observable when viewing the sky.

The work of Kemp [2] has associated scintillation with water vapor fluctuations in the atmosphere. The suggestion of Derr, however, for the transition case of changing atmospheric conditions, would have us take into consideration refractive index changes. Kemp's observations were made during high humidity of summer months whereas the measurements of this program were made for water vapor concentrations that varied from 0.4 g/m³ to 15.3 g/m³. It is quite probable that fluctuations of the magnitude that we have observed did not originate from water vapor fluctuations alone, particularly for the case of the low water vapor concentrations.

The rapid fluctuations which have been observed in these experiments are also at variance with theoretical predictions, in that, if the Taylor hypothesis is assumed to apply, then the water vapor distribution is assumed to drift through the beam of the radiometer as a result of atmospheric movements and the rate of change in water vapor distribution is considered to be slow compared with the time taken to transit through the beam. The transit time would have to be exceptionally short for the Taylor hypothesis to hold.

The data presented provides some initial information on fluctuations at 90 GHz. It is recommended that the following tasks be performed:

- 1) Perform a more rigorous theoretical study of the fluctuation effects to define the expected effects on a passive system more accurately.

- 2) Perform more extensive measurements under a greater variety of atmospheric conditions. It is necessary to correlate observations with weather conditions; it is not evident that all reports of clear weather are for conditions void of thin visually invisible clouds.

- 3) Among the observations to be made are:

a. Simultaneous radiometric measurements at 94 GHz with two separable radiometers. Measurements as a function of the separation of radiometers are important for determining fluctuations across the face of a large antenna. Variation of the separation of the radiometers should be performed, as should interchanging of the position of radiometers. The latter test should remove the effect of immediate surroundings on the apparatus.

b. Simultaneous measurements at 140 GHz and 220 GHz to examine fluctuations as a function of frequency.

c. Measurements are needed for several different weather conditions, actually for all seasons if possible.

d. On the basis of K_a -band radar observations, V.F. Derr of NOAA has recommended that simultaneous radar and radiometry measurements be performed on the same propagation path. Radar and lidar observations would provide information on particles not observable visually.

The measurements reported here must be considered a first effort toward fluctuation effects in the millimeter region. Considerably more data are needed. The observed effects cannot be expected to occur under all measurement conditions as the prevailing conditions during the period that measurements were taken in this work were quite severe and continually changing during observations. Measurements as a function of seasonal variations over an extended period of time are needed. A more accurate method of determining the conditions of clear sky, compared to that of visual observation employed in this program, is needed.

The work of Hill et al [??] should be investigated for extension to this problem. Values of pertinent parameters of their expressions are needed for comparison with experiments.

References

1. A. J. Kemp, "A Scintillation Theory for Millimeter and Submillimeter Wavebands," Digest of the Fourth International Conference on Infrared and Millimeter Waves and Their Applications, IEEE Cat. No. 79CH1384-7 MTT, Dec. 10-15, 1979.
2. A. J. Kemp, "A Scintillation Theory for Millimetre and Submillimetre Wavebands," (preprint).
3. U. S. Standard Atmosphere Supplement, 1966, N67-37900 (NASA-CR-88870)
4. T. Orhaug, "The Effect of Atmospheric Radiation in the Microwave Region," Publication of NRAO, Vol. 1, #14, pp 215-250, (October, 1962); also "Fluctuation Component of Atmospheric Noise Temperature," Proc IEEE 51.
5. D. C. Hogg and R. A. Semplak, "The Effect of Rain and Water Vapor on Sky Noise at Centimeter Wavelengths," Bell System Technical Journal 40, pp 1331-1349, September, 1961.
6. T.C.L.G. Sollner, "Frequency Spectrum of Fluctuation in Submillimetre Sky Emission and Absorption," Astron and Astrophys. 55, 361 (1977).
7. V. I. Tatarski, "Wave Propagation in a Turbulent Medium," New York: Dover, 1961.
8. L. A. Chernov, "Wave Propagation in a Random Medium," McGraw-Hill Book Co., New York 1960.
9. A. O. Izyumov, "Amplitude and Phase Fluctuations of a Plane Monochromatic Submillimeter Wave in a Near-Ground Layer of Moisture-Containing Turbulent Air," Radio Eng. and Elec. Phys. 13, #7, pp 1009-1013 (1968).
10. N. A. Armand et al, "Fluctuations of Submillimeter Waves in a Turbulent Atmosphere," Radio Engineering and Electronics Physics 10 #8, 1257 (1971).
11. R. W. McMillan, J. C. Wiltse, and D. E. Snider, "Atmospheric Turbulence Effects on Millimeter Wave Propagation," IEEE EASCON, 1979.
12. A. S. Gurvich, "Effects of Absorption on the Fluctuation in Signal Level During Atmospheric Propagation," Radio Engineering and Electronics Physics 13, #11, 1687 (1968).
13. J. Bastin, "Atmospheric Limitations To The Size of Millimetre Telescopes," Paper Q, Joint Anglo-Soviet Seminar on Atmospheric Propagation at Millimetre and Submillimetre Wavelengths, Moscow, Nov. 1977.

14. H. G. Brooker, Proc. IRE 46, 298 (1958).
15. A. N. Kolmogorov, "The Local Structure of Turbulence in Incompressible Viscous Fluid for Very Large Reynolds' Numbers," Doklady Akad. Nauk SSSR 30, 301 (1941).
16. N. A. Armand et. al., "Fluctuations of Submillimeter Radio Waves in a Turbulent Atmosphere," Radio Engin. and Electron Physics 16 #8, 1259 (1971).
17. N. D. Mavroukoulakis et al, "Observation of Millimetre-Wave Amplitude Scintillations in a Town Environment," Electronics Letters 13, #14, 391 (1977).
18. K. L. Ho et. al., "Wavelength Dependence of Scintillation Fading at 110 and 36 GHz," Electronics Letters 13, #7, 181 (1977).
19. G. A. Andreyev et. al., "Intensity and Angle of Arrival Fluctuations of Millimetric Radiowaves in Turbulent Atmosphere," Paper R1 Joint Anglo-Soviet Seminar on Atmospheric Propagation at Millimetre and Submillimetre Wavelengths, Institute of Radioengineering and Electronics, Moscow, Nov. 1977.
20. J. L. Bufton, "A Radiosonde Thermal Sensor Technique for Measurement of Atmospheric Turbulence," NASA Technical Note, NASA TND-7867 (February, 1975).
21. J. H. Rainwater and J. J. Gallagher, "Millimeter Wave Atmospheric Radiometry Observations," Semi-Annual Report, Contract No. N00173-78-C-0165 (30 June 1978 to 30 April 1979), May 9, 1979.
22. R. J. Hill, S. F. Clifford, and R. S. Lawrence, "Refractive - Index and Absorption Fluctuations in the Infrared Caused by Temperature, Humidity, and Pressure Fluctuation", Journ. Optical Society of America 70, pp. 1192-1205 (1980).

APPENDIX A
 DATA TAKING RECORD
 28 FEBRUARY 1980

RUN	TOD	SCENE	NOTES	ΔT_{min} ($^{\circ}K$)
9	1100	SKY	Strongwind, very clear sky	1.50
10	"	"	" "	"
11	"	"	" "	"
12	"	"	" "	"
13	1200	"	" "	2.01
18	1330	"	" "	"
19		"	" "	"
20		"	" "	"
21		"	" "	"
22		AMB LOAD(INT)	" "	"
23		SKY	" "	"
24		"	" "	"
25		"	" "	"
26		"	" "	"
27		"	" "	"
28		AMB LOAD(INT)	" "	"
29		SKY	" "	"
30		"	" "	"
34		"	" "	"
35		"	" "	"
36		"	" "	"
37		"	" "	"
38		AMB LOAD(INT)	" "	"

28 FEBRUARY 1980

(CONTINUED)

RUN	TOD	SCENE	NOTES	ΔT_{min} ($^{\circ}\text{K}$)
39		SKY	Strongwind, very clear sky	2.01
40		"	" "	"
41		"	" "	"
42		"	" "	"
43		"	" "	"
52		"	" "	1.29
53		"	" "	"
54		"	" "	"
55		"	" "	"
56		"	" "	"
57	1600	AMB	" "	"
58	"	SKY	" "	"
59	"	"	" "	"
62	"	AMB LOAD (INT)	" "	"
63	"	SKY	" "	"
64	"	"	" "	"
65	"	"	" "	"
67	1730	AMB LOAD (INT)	" "	1.49
71	1830	SKY	" "	"
72		SKY	" "	"
73		"	" "	"
74		AMB LOAD (INT)	" "	"

APPENDIX A
 DATA REDUCTION RECORD
 29 FEBRUARY 1980

RUN	TOD	SCENE	NOTES	ΔT_{\min} ($^{\circ}\text{K}$)
76	1340	AMB LOAD(INT)		0.76
78		SKY	Overcast, thin cloud cover, sunny	"
79		"	" " " "	"
80		"	" " " "	"
81		"	" " " "	"
82		"	" " " "	"
83		AMB LOAD(INT)	" " " "	"
84		AMB LOAD(INT)	" " " "	"
85		AMB LOAD(EXT)	" " " "	"
86		AMB LOAD(EXT)	" " " "	"
87		SKY	" " " "	"
88		"	" " " "	"
89		"	" " " "	"
90		"	" " " "	"
91	1400	"	" " " "	"
97	15:50	"	" " " "	0.59
98		"	" " " "	"
99		"	" " " "	"
106		"	" " " "	0.90
107		"	" " " "	"
108		"	" " " "	"
109		"	" " " "	"
110		AMB LOAD(INT)	" " " "	"
116		SKY	" " " "	0.85

29 FEBRUARY 1980

(CONTINUED)

RUN	TOD	SCENE	NOTES	ΔT_{\min} (°K)
117		SKY	Overcast, thin cloud cover, sunny	0.85
118		"	" " " "	"
119	15 30	AMB LOAD (INT)	" " " "	"
12		SKY	" " " "	"
13		"	" " " "	"
14		"	" " " "	"
15		"	" " " "	"
16		"	" " " "	"
17		AMB LOAD (INT)	" " " "	"
18		AMB LOAD (INT)	" " " "	"

APPENDIX A

2 MARCH 1980

DATA REDUCTION RECORD

REN	TOD	SCENE	NOTES	ΔT_{\min} ($^{\circ}\text{K}$)
34	1430	AMB LOAD(INT)	Cloud's breaking up	0.85
36		SKY	" " "	"
37		"	" " "	"
38		"	" " "	"
39		"	" " "	"
40		"	" " "	"
44		AMB LOAD(INT)	" " "	0.83
45		SKY	Clear sky	"
46		"	" "	"
47		"	" "	"
50		"	" "	0.64
51		"	" "	"
52		"	" "	"
53		"	Slight Clouds	"
54		"	" "	"
58		AMB LOAD(INT)	" "	0.66
60		SKY	Partial clouds overhead	"
61		"	" " "	"
62		"	" " "	"
63		"	" " "	"
64		"	Very slight clouds overhead- small patches	"
65		"	" " "	"
71		"	" " "	"
72		"	" " "	"
73		"	" " "	"
74		"	" " "	"
75		"	" " "	"

(Wind from North)

APPENDIX A
 DATA REDUCTION RECORD
 8 MARCH 1980

RUN	TOD	SCENE	NOTES	ΔT_{\min} ($^{\circ}\text{K}$)
8	1640	AMB LOAD(INT)	Wind from East	0.76
10	1746	SKY	" " "	"
11		"	" " "	"
13		"	" " "	"
15		"	" " "	0.80
16		"	" " "	"
18	1755	"	" " "	"
19	1756	AMB LOAD(INT)	" " "	"
20	1756	SKY	" " "	"
22		SKY	" " "	"
23		SKY	" " "	"

APPENDIX A
 DATA REDUCTION RECORD
 11 MARCH 1980

RUN	TOD	SCENE	NOTES	ΔT_{\min} ($^{\circ}\text{K}$)
8	1728	AMB LOAD(INT)		0.76
9		SKY		"
10		"		"
12		"	All previous data @ 0.16 sec τ	"
13		AMB LOAD(INT)	" " "	"
18		SKY	New T.C. 125 ms = 0.5 sec τ	"
21		"		"
22		"		"
23		"		"
25		AMB LOAD(INT)		"
29	1757	AMB LOAD(INT)	T.C. 400 ms = 1.6 sec τ	0.29
30		SKY		"
31		"		"
32		"		"
33		"		"
42		AMB LOAD(INT)	T.C. 12.5 msec = 0.5 sec	1.18
44		SKY		"
45		"		"
46		"		"
47		"		"
52		AMB LOAD(INT)		3.65
54		SKY		"
55		"		"
56		"		"

11 MARCH 1980

(CONTINUED)

RUN	TOD	SCENE	NOTES	ΔT_{min} ($^{\circ}\text{K}$)
57		SKY		3.65
60		AMB LOAD(INT)	T.C. = 4 ms τ = 0.016 PS	6.62
62		SKY		"
63		"		"
64		"		"
65		"		"

APPENDIX A
 DATA REDUCTION RECORD
 16 MARCH 1980

RCN	TOD	SCENE	NOTES	ΔT_{\min} ($^{\circ}\text{K}$)
78	1130	AMB LOAD	Back to 40 ms or 0.16 sec τ	0.70
80		SKY		"
81		"		"
82		"		"
99	1210	AMB LOAD(INT)	T.C. to 12.5 ms = 0.05 sec	0.39
100		SKY		"
101		"		"
102		"		"
115		AMB LOAD(INT)	T.C. to 400 ms or 1.6 sec	0.17
117		SKY		"
118		"		"
119		"		"
80		AMB LOAD	T.C. = 1.25 sec τ = 5.0 sec	0.14
82		SKY		"
83		"		"
84		"		"
89		AMB LOAD	T.C. = 12.5 ms τ = 0.05 sec	4.0
91		SKY		"
92		"		"
93		"		"
99		AMB LOAD	T.C. = 40 msec τ = 0.16	0.99
101		SKY		"
102		"		"
103		"		"

APPENDIX B

WEATHER DATA FOR OBSERVATIONS

Table Weather Data: 28 Feb 80

Time of Day	Temperature (°K)	Water Vapor (g/m ³)	Wind Direction (deg)	Wind Speed (kts)	Sky Condition
0900	280.9	2.3	240	10	Clear
1000	284.2	3.3	240	12	Clear
1100	289.2	5.0	270	14	Clear
1200	292.0	6.3	240	19	Clear
1300	294.2	7.3	260	16	Clear
1400	295.4	7.7	260	16	Clear
1500	296.5	8.0	250	16	Clear
1600	296.5	8.0	250	16	Scattered Clouds
1700	295.9	8.0	250	19	Scattered Clouds
1800	294.8	7.3	250	20	Scattered Clouds
1900	293.1	6.6	240	13	Scattered Clouds
2000	291.5	6.3	240	13	Scattered Clouds
2100	290.4	5.8	230	12	Scattered Clouds

Table Weather Data: 29 Feb 80

Time of Day	Temperature (°K)	Water Vapor (g/m ³)	Wind Direction (deg)	Wind Speed (kts)	Sky Condition
0900	279.8	2.6	340	08	Overcast
1000	281.5	3.1	310	08	Overcast
1100	283.7	3.5	350	09	Overcast
1200	286.5	3.7	310	08	Overcast
1300	287.0	3.7	310	09	Overcast
1400	288.7	3.8	320	07	Overcast
1500	288.7	3.7	360	07	Overcast
1600	289.8	3.8	340	05	Overcast
1700	290.4	4.2	250	06	Broken
1800	288.7	3.8	320	08	Overcast
1900	285.9	3.3	330	10	Overcast
2000	283.1	2.4	350	10	Overcast
2100	282.0	1.9	350	09	Overcast

Table Weather Data: 2 Mar 80

Time of Day	Temperature (°K)	Water Vapor (g/m ³)	Wind Direction (deg)	Wind Speed (kts)	Sky Condition
0900	265.4	0.4	320	13	Overcast
1000	265.4	0.4	330	11	Overcast
1100	265.9	0.7	320	16	Overcast
1200	266.5	0.7	330	16	Overcast
1300	267.0	0.9	330	16	Overcast
1400	267.6	0.9	340	16	Overcast
1500	267.6	0.9	340	15	Overcast
1600	267.6	0.9	340	19	Overcast
1700	268.7	1.1	330	17	Broken
1800	268.1	0.7	310	15	Broken
1900	267.0	0.5	330	17	Scattered
2000	265.9	0.5	320	16	Clear
2100	265.4	0.4	320	15	Clear

Table Weather Data: 8 Mar 80

Time of Day	Temperature (°K)	Water Vapor (g/m ³)	Wind Direction (deg)	Wind Speed (kts)	Sky Condition
0900	290.9	9.7	210	11	Overcast
1000	290.9	9.6	220	12	Overcast
1100	292.6	10.8	230	12	Broken
1200	294.2	12.5	240	12	Overcast
1300	295.4	13.7	260	13	Overcast
1400	297.0	13.9	290	16	Overcast
1500	298.7	15.3	250	14	Overcast
1600	298.1	15.3	260	17	Overcast
1700	298.1	15.3	240	12	Overcast
1800	297.6	14.8	230	10	Overcast
1900	295.9	12.9	220	08	Overcast
2000	294.8	12.2	220	09	Overcast
2100	294.2	11.9	240	10	Overcast

Table Weather Data:11 Mar 80

Time of Day	Temperature (°K)	Water Vapor (g/m3)	Wind Direction (deg)	Wind Speed (kts)	Sky Condition
0900	281.5	3.1	330	13	Broken
1000	283.1	2.8	330	15	Broken
1100	284.8	2.4	330	15	Overcast
1200	286.5	2.8	340	17	Overcast
1300	287.6	2.4	330	16	Overcast
1400	287.6	2.1	330	16	Overcast
1500	288.7	2.1	330	11	Overcast
1600	288.1	1.9	340	12	Overcast
1700	287.0	1.7	320	11	Overcast
1800	285.4	1.6	320	10	Overcast
1900	284.2	1.0	340	10	Overcast
2000	282.6	1.0	340	11	Overcast
2100	282.0	1.0	320	08	Overcast

Table Weather Data: 16 Mar 80

Time of Day	Temperature (°K)	Water Vapor (g/m3)	Wind Direction (deg)	Wind Speed (kts)	Sky Condition
0900	284.2	3.8	130	10	Overcast
1000	285.9	4.4	160	11	Overcast
1100	289.8	6.6	160	14	Broken
1200	291.5	7.7	120	12	Broken
1300	293.1	8.7	170	16	Broken
1400	293.7	8.9	160	18	Broken
1500	294.2	9.2	170	14	Overcast
1600	294.2	8.7	170	14	Overcast
1700	293.1	8.0	170	12	Overcast
1800	292.6	8.0	180	14	Overcast
1900	291.5	7.7	170	13	Overcast
2000	290.9	7.3	170	13	Overcast
2100	291.5	7.7	170	10	Overcast

APPENDIX C

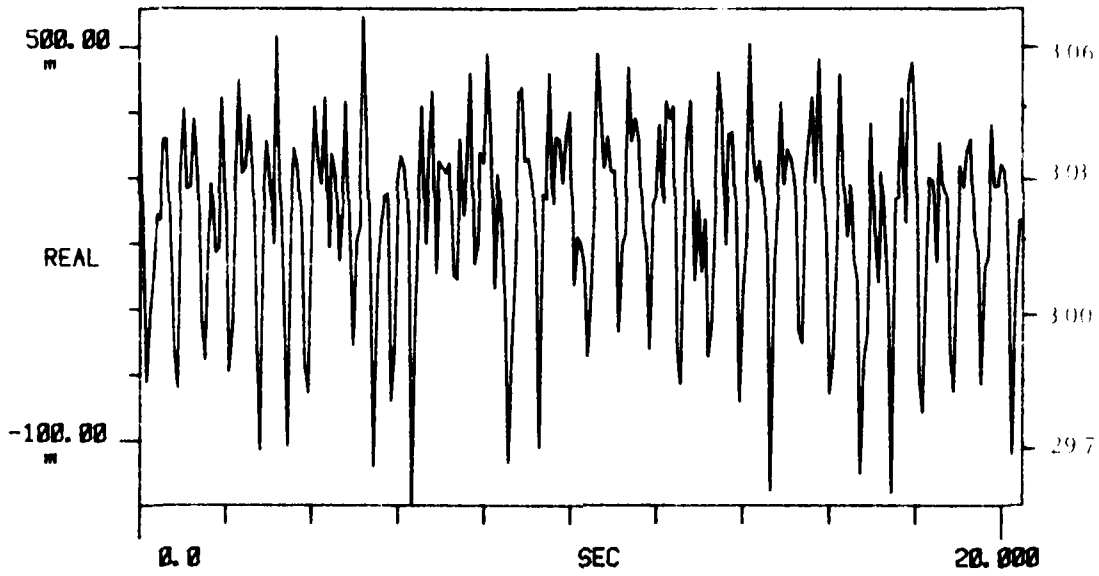
AMBIENT LOAD DATA

C-1. 28 February 1980
Ambient Load Measurements

TI AVG 1

R# 22

#A 1



TI AVG
-10.000

R# 22

#A 1

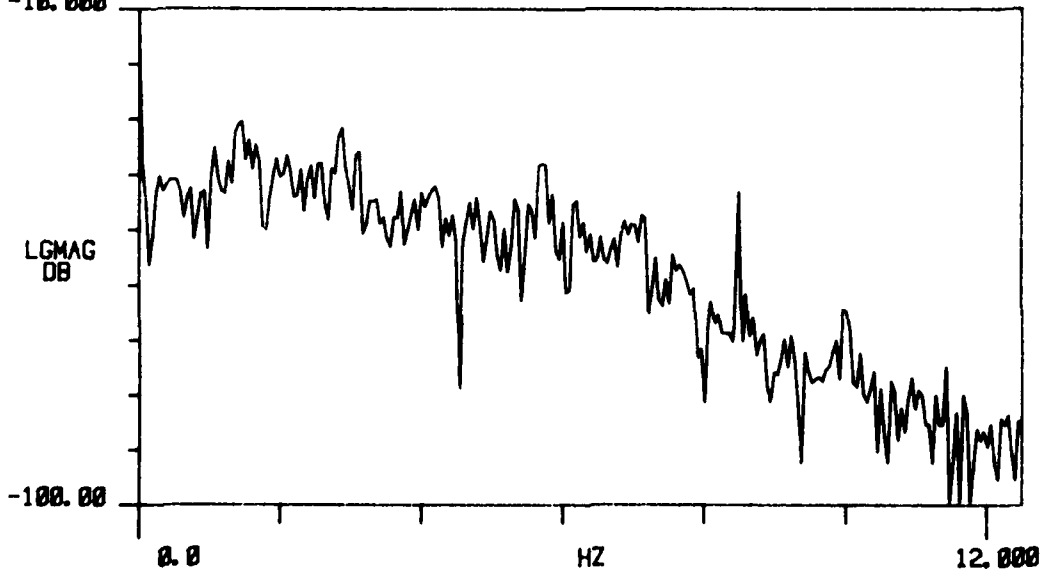
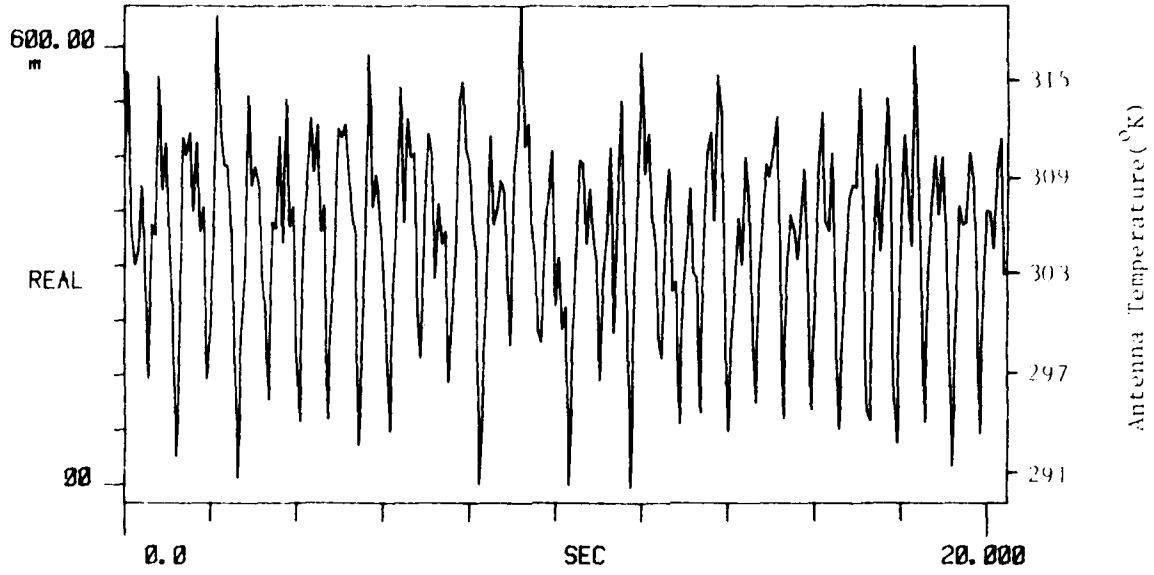


Figure C - 1. Ambient Load Measurement. 28 Feb 80

TI AVG 1

R# 28

#A 1



TI AVG
-10.000

R# 28

#A 1

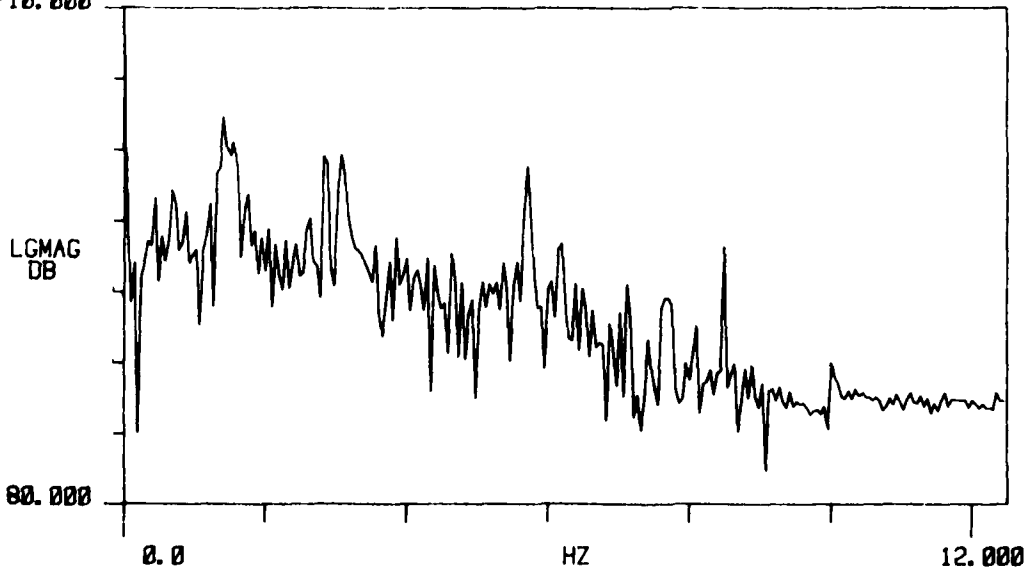
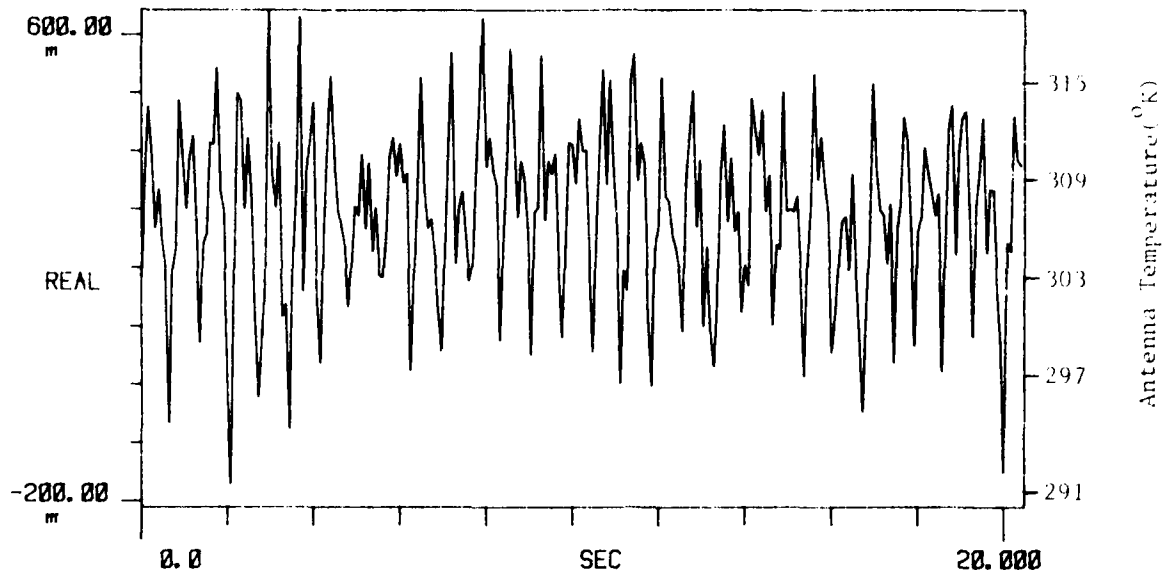


Figure C-1. Ambient Load Measurement. 28 Feb 80

TI AVG 1

R# 38

#A 1



JI AVG
-10.000

R# 38

#A 1

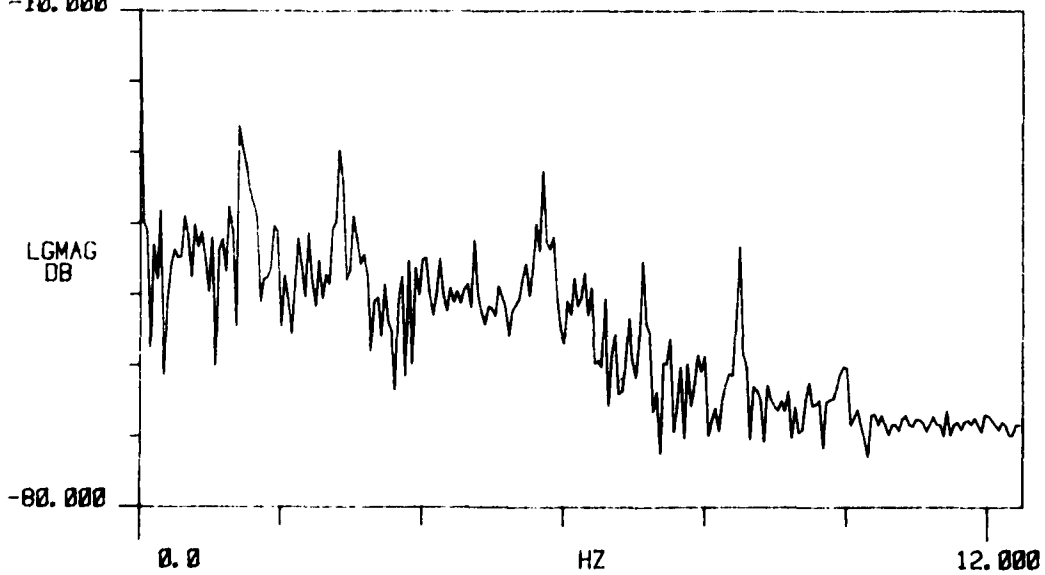


Figure C-1. Ambient Load Measurement. 28 Feb 80

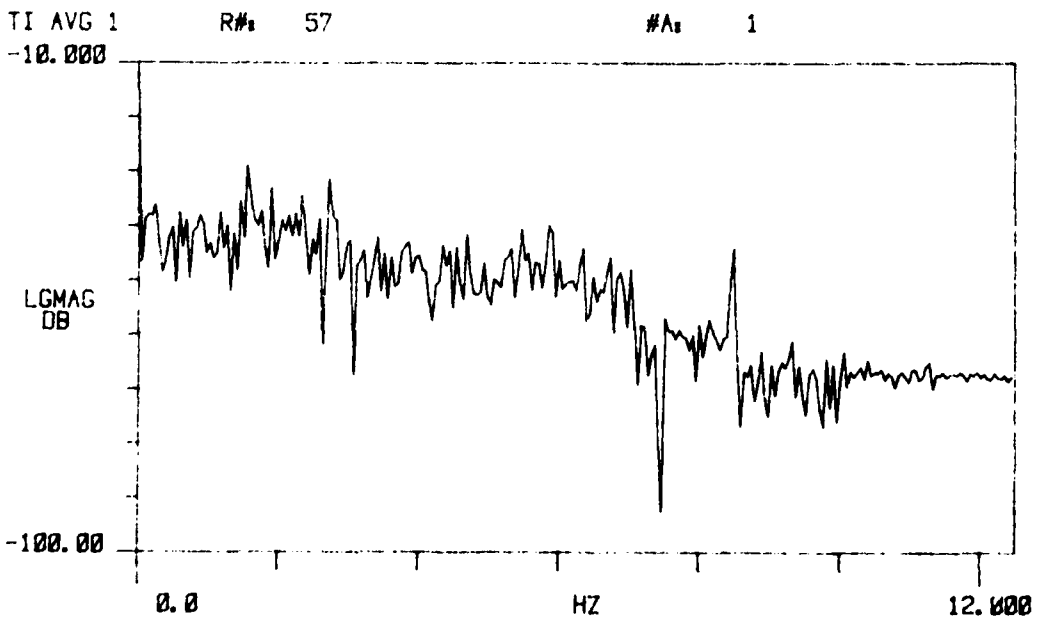
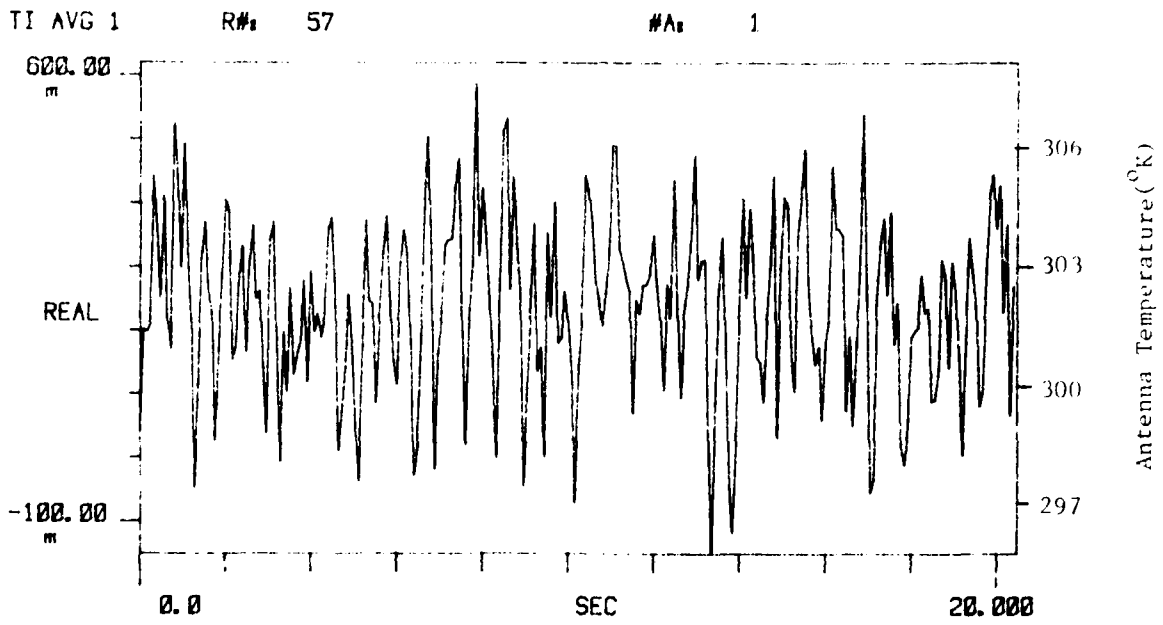
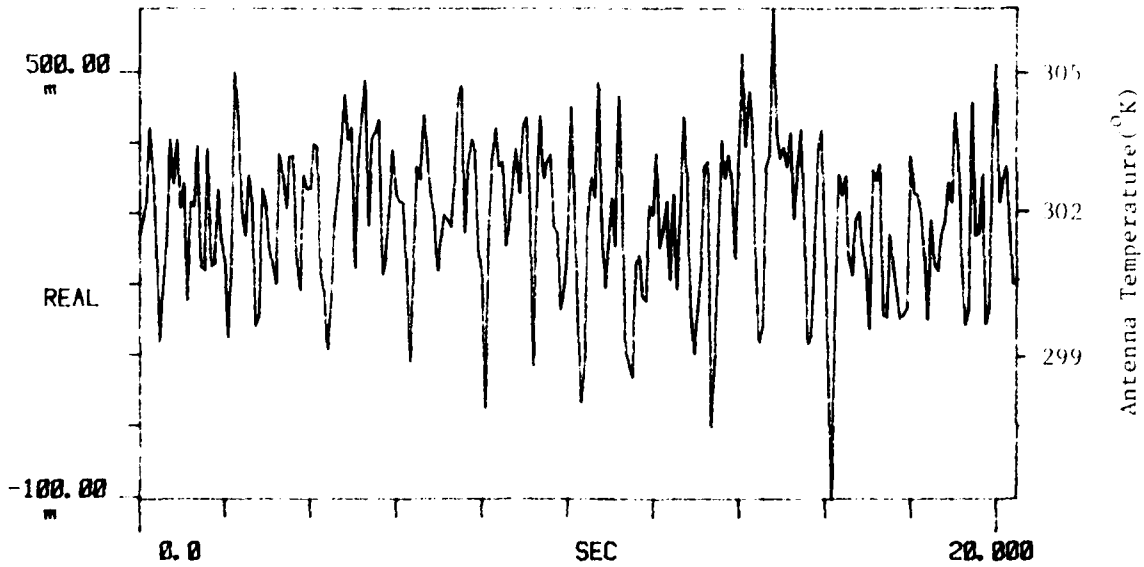


Figure C-1. Ambient Load Measurement. 28 Feb 80
64

TI AVG 1

R# 62

#A 1



TI AVG
-10.000

R# 62

#A 1

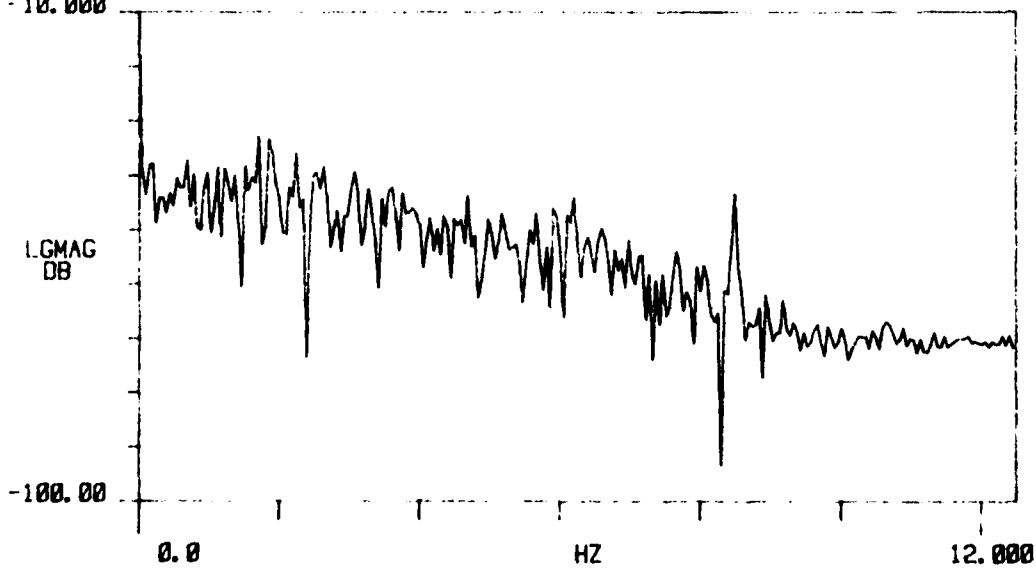
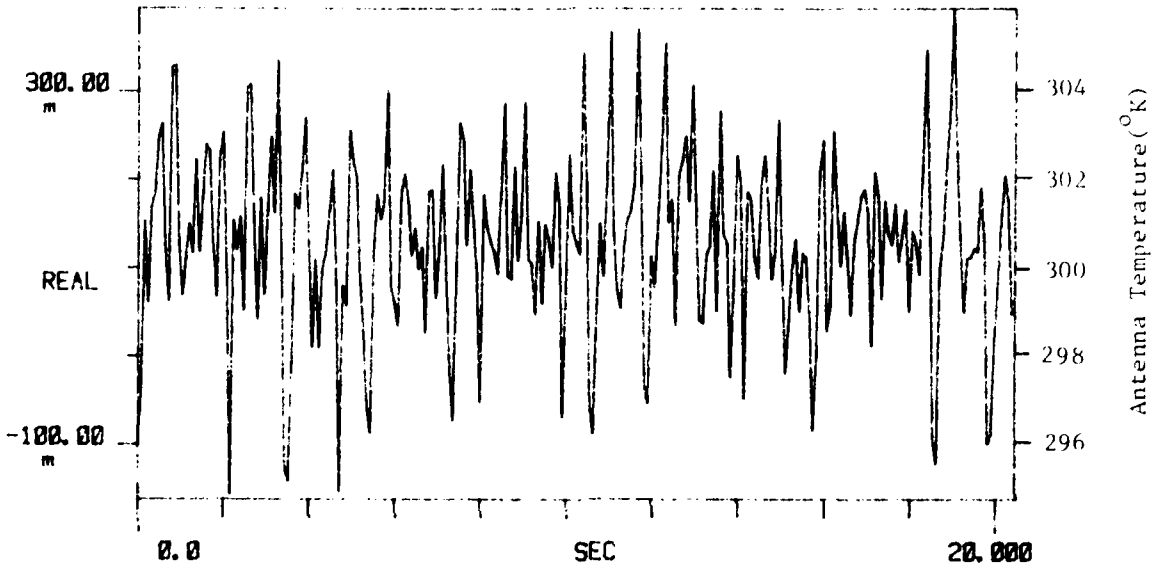


Figure C-1. Ambient Load Measurement. 28 Feb 80
65

TI AVG 1

R# 67

#A 1



TI AVG
-10.000

R# 67

#A 1

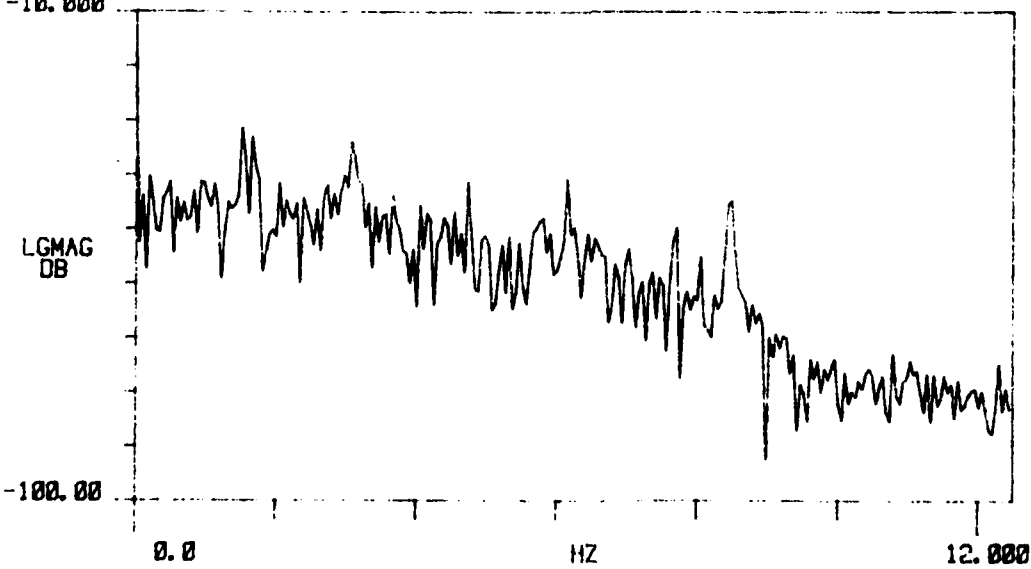


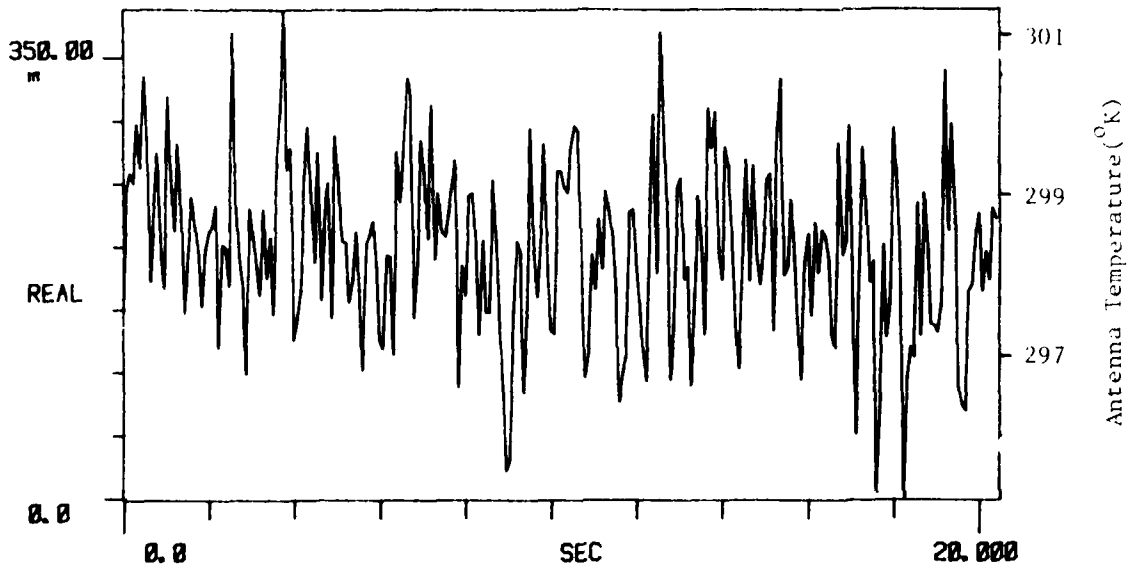
Figure C-1. Ambient Load Measurement. 28 Feb 80

C-2. 29 February 1980
Ambient Load Measurements

TI AVG 1

R# 76

#A 1



TI AVG
-10.000

R# 76

#A 1

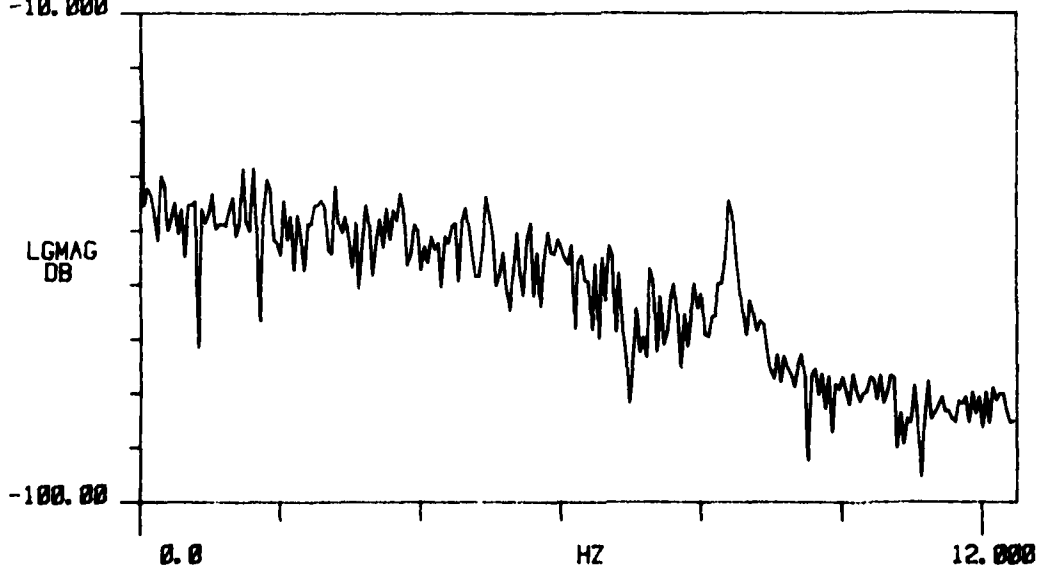
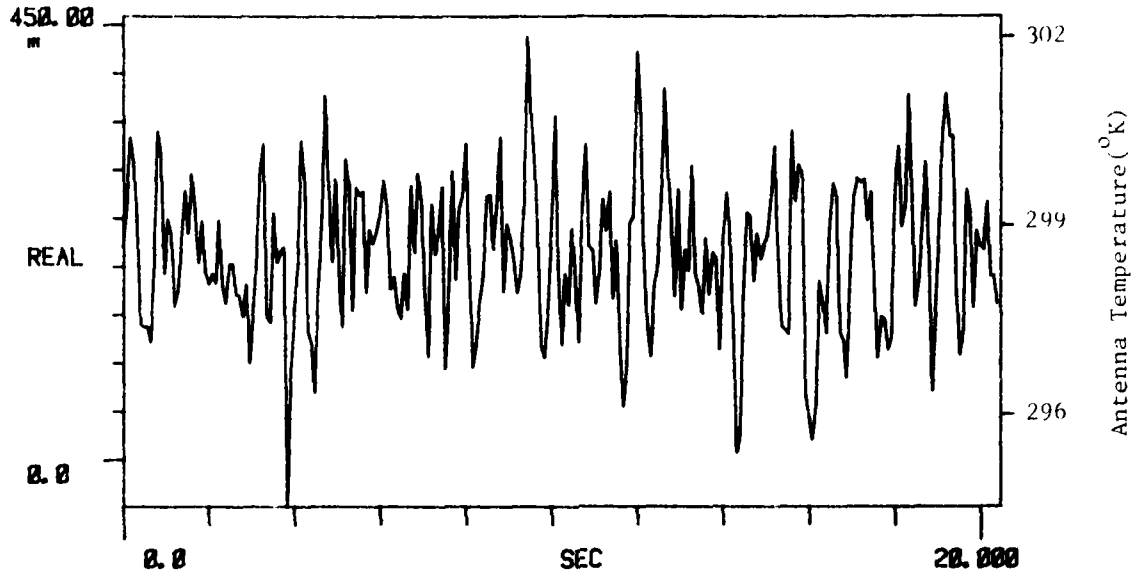


Figure C-2. Ambient Load Measurement 29 Feb 80

TI AVG 1

R# 83

#A 1



TI AVG
-10.000

R# 83

#A 1

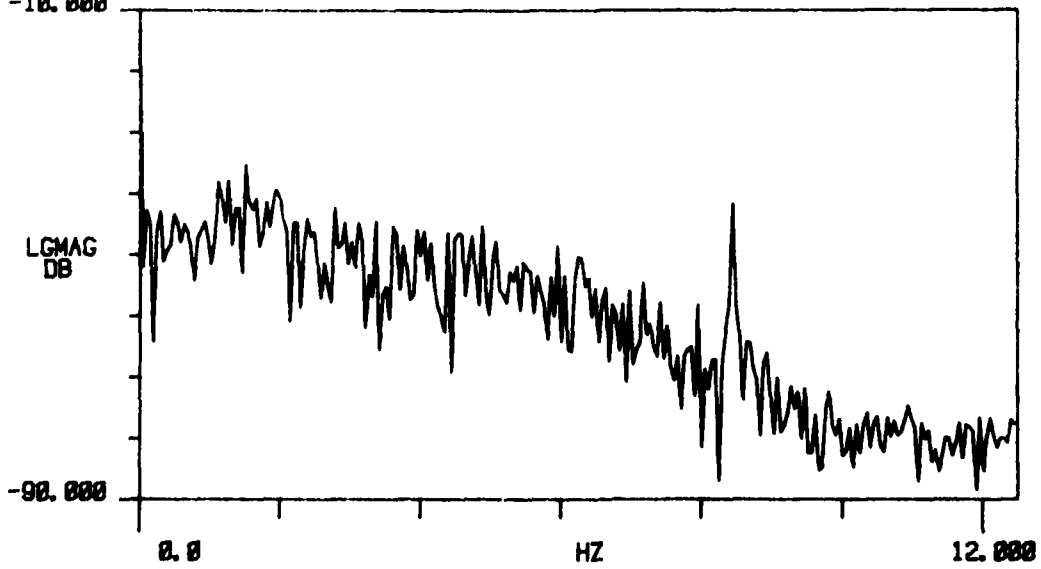
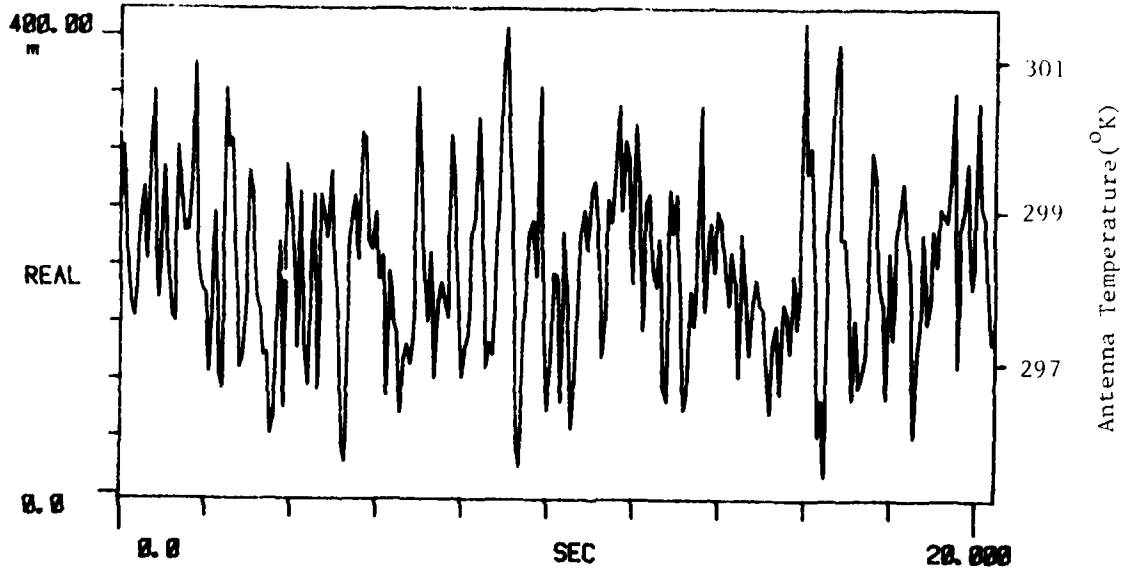


Figure C-2. Ambient Load Measurement. 29 Feb 80

TI AVG 1

R# 84

#A₀ 1



TI AVG 1

R# 84

#A₀ 1

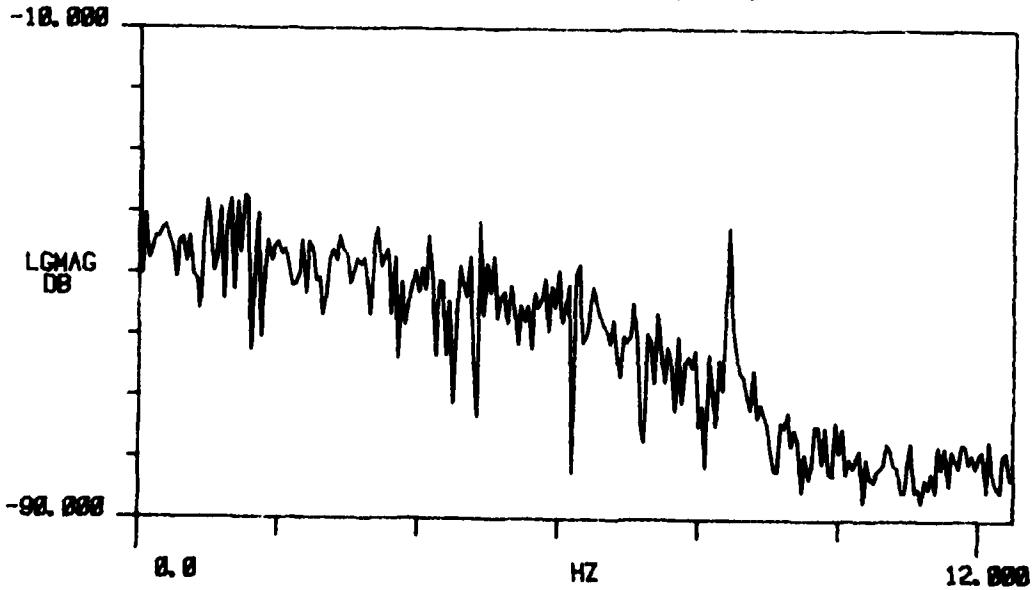


Figure C-2. Ambient Load Measurement. 29 Feb 80
70

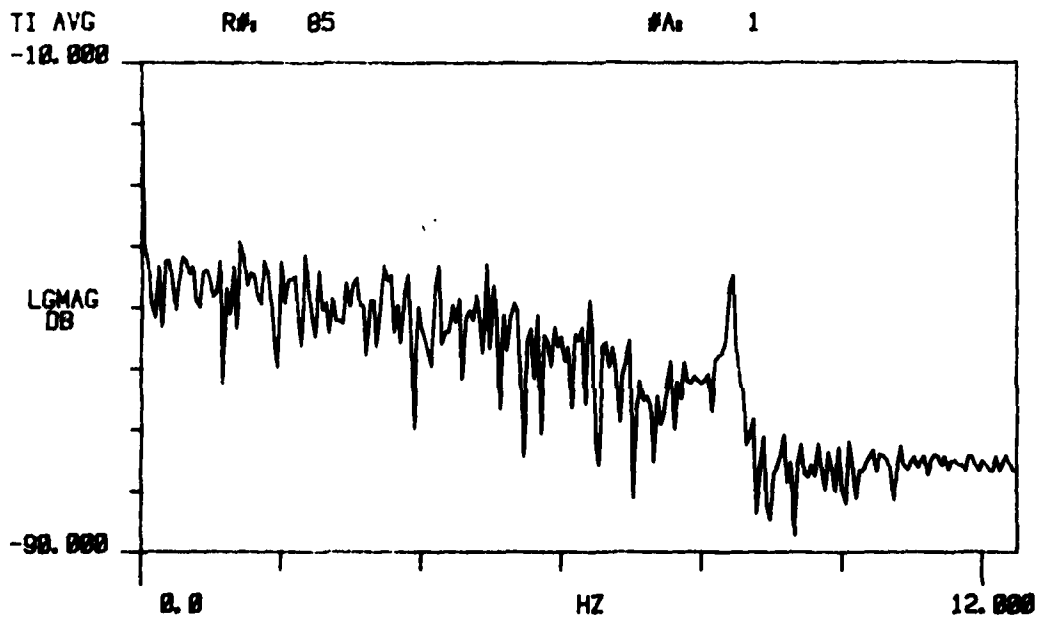
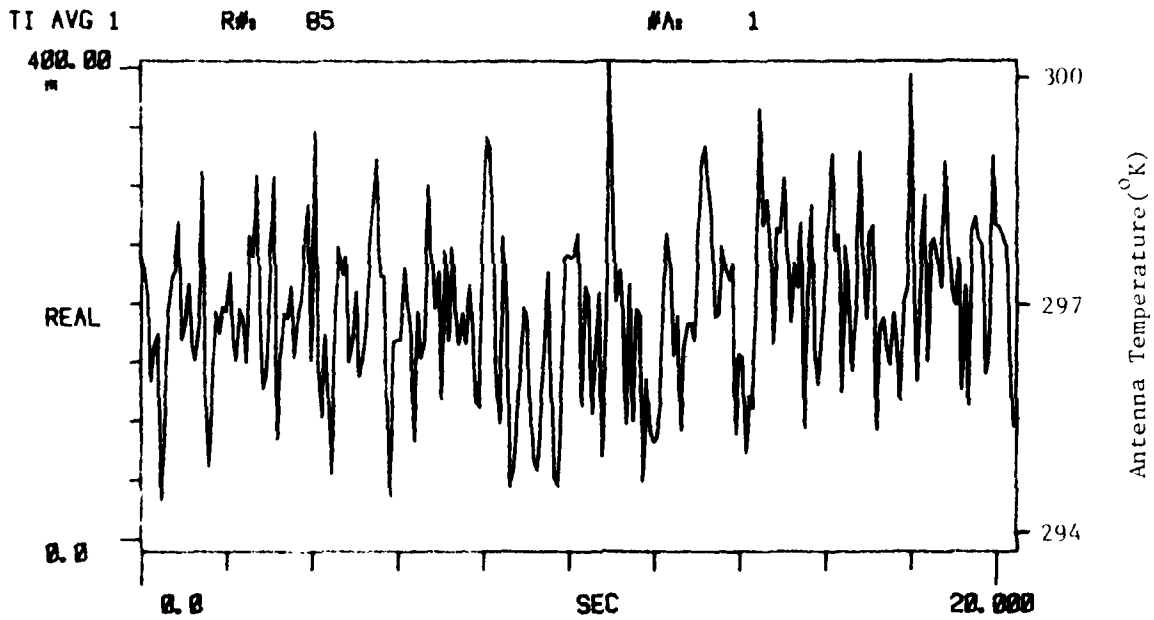
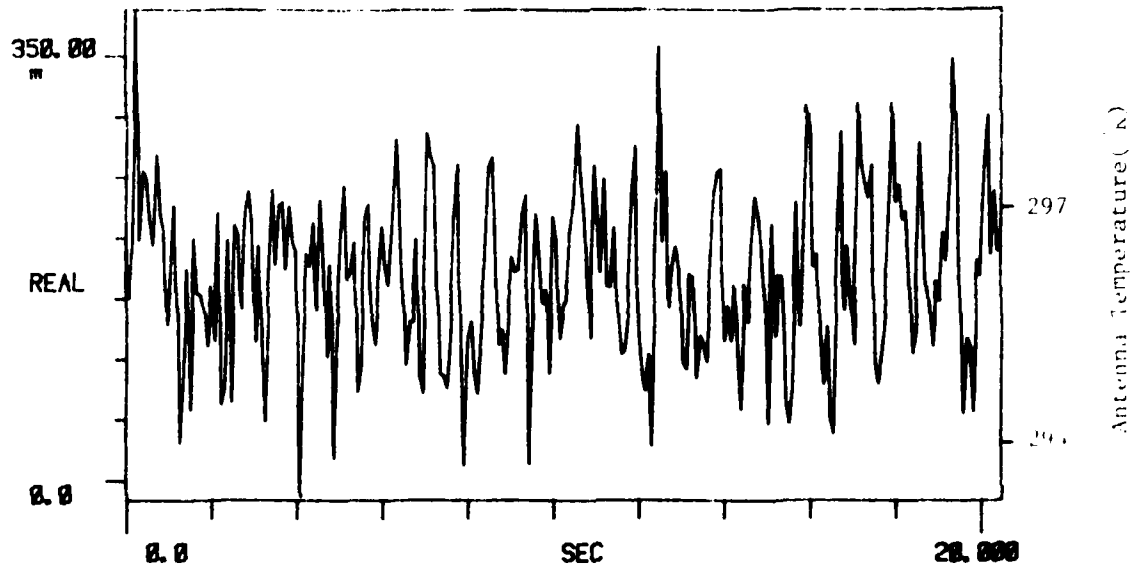


Figure C-2. Ambient Load Measurement. 29 Feb 80

TI AVG 1

R# 86

#A 1



TI AVG
-10.000

R# 86

#A 1

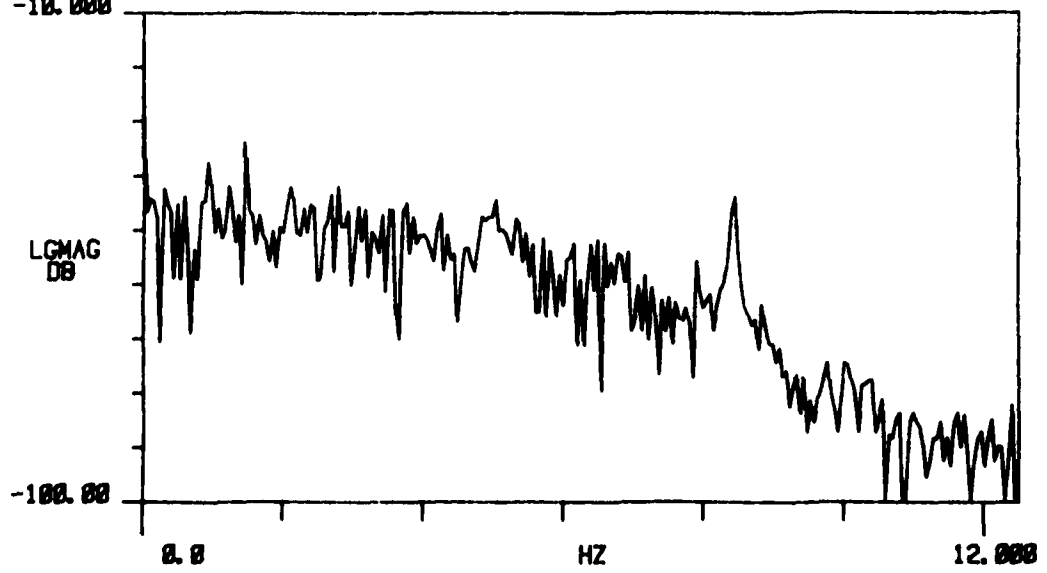


Figure C-2. Ambient Load Measurement. 29 Feb 80

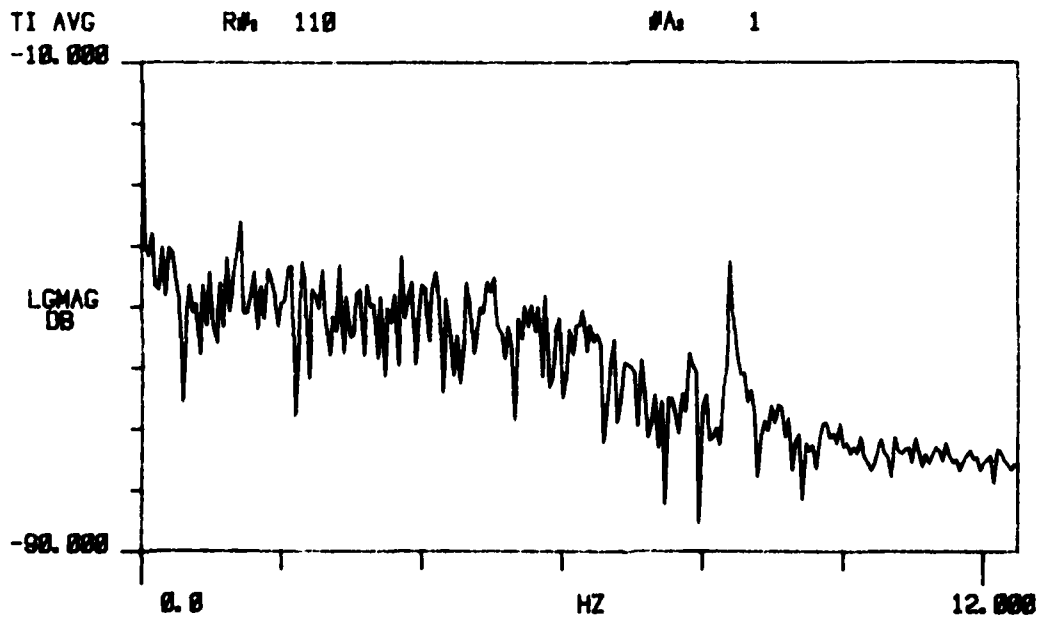
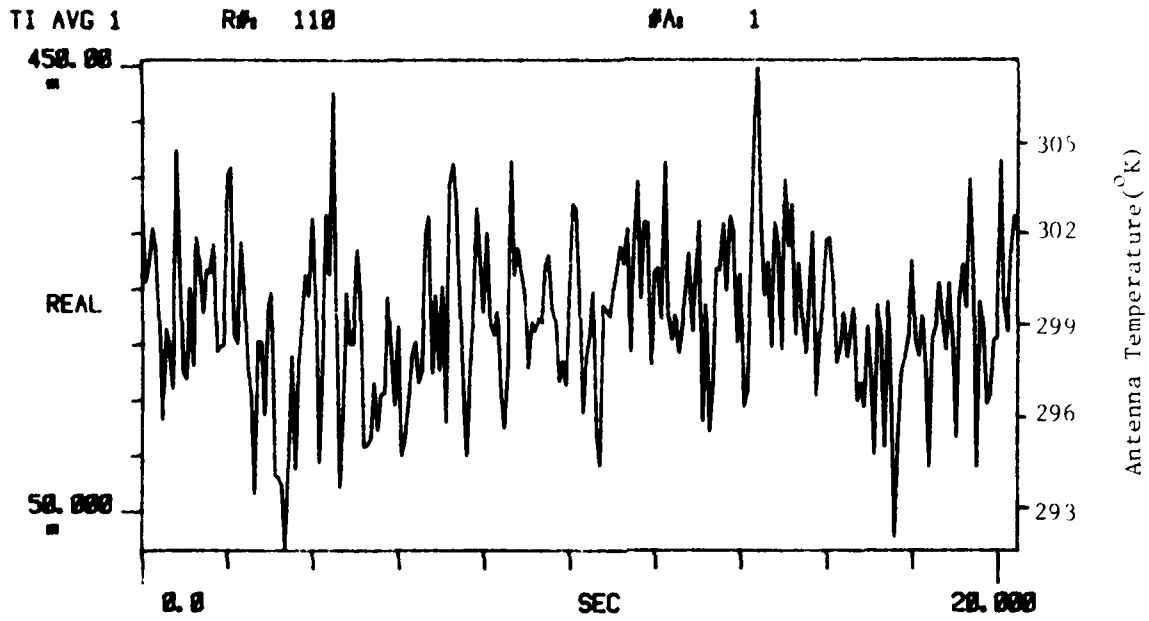
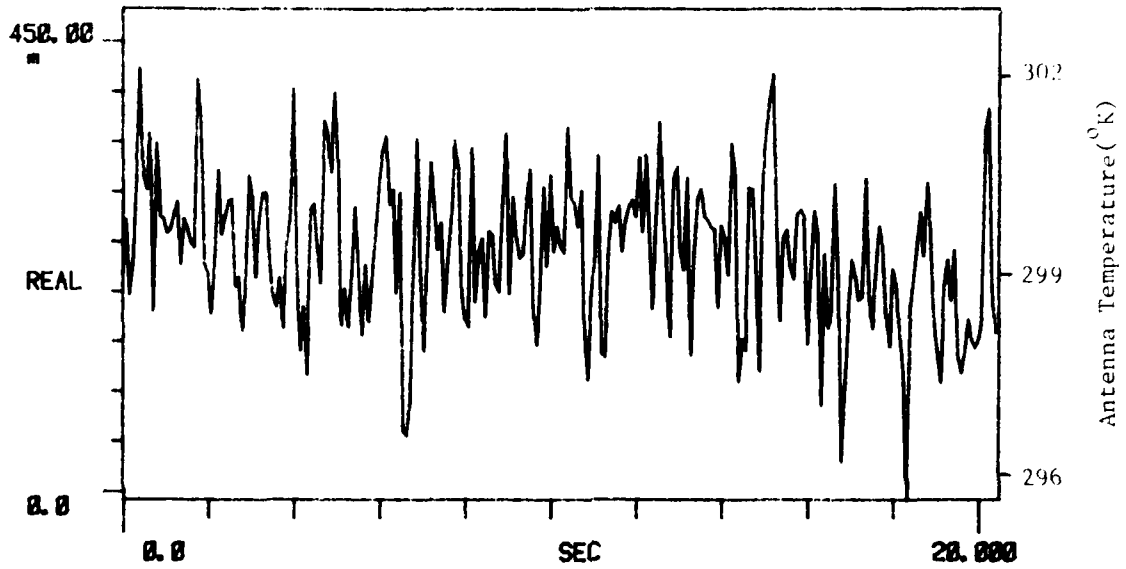


Figure C-2. Ambient Load Measurement. 29 Feb 80

TI AVG 1

R# 119

#A 1



TI AVG
-10.000

R# 119

#A 1

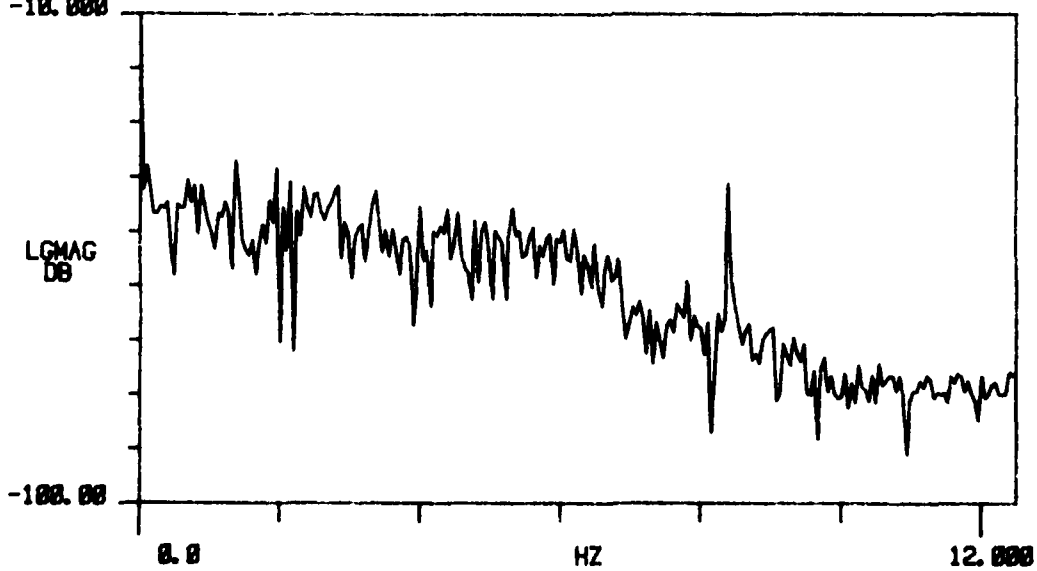
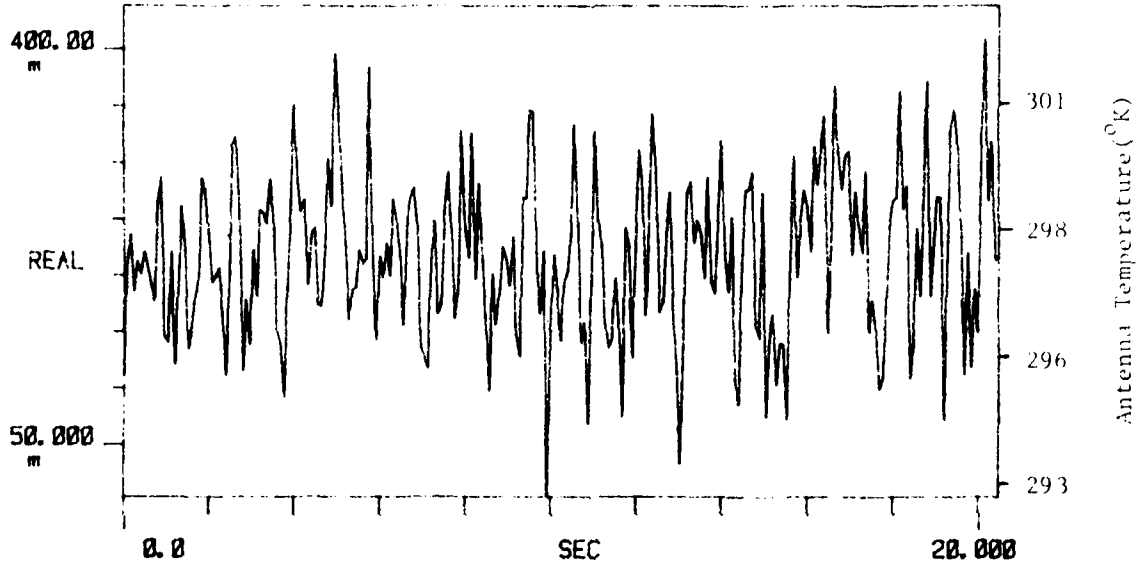


Figure C-2. Ambient Load Measurement. 29 Feb 80
74

TI AVG 1

R# 17

#A 1



TI AVG

R# 17

#A 1

-10.000

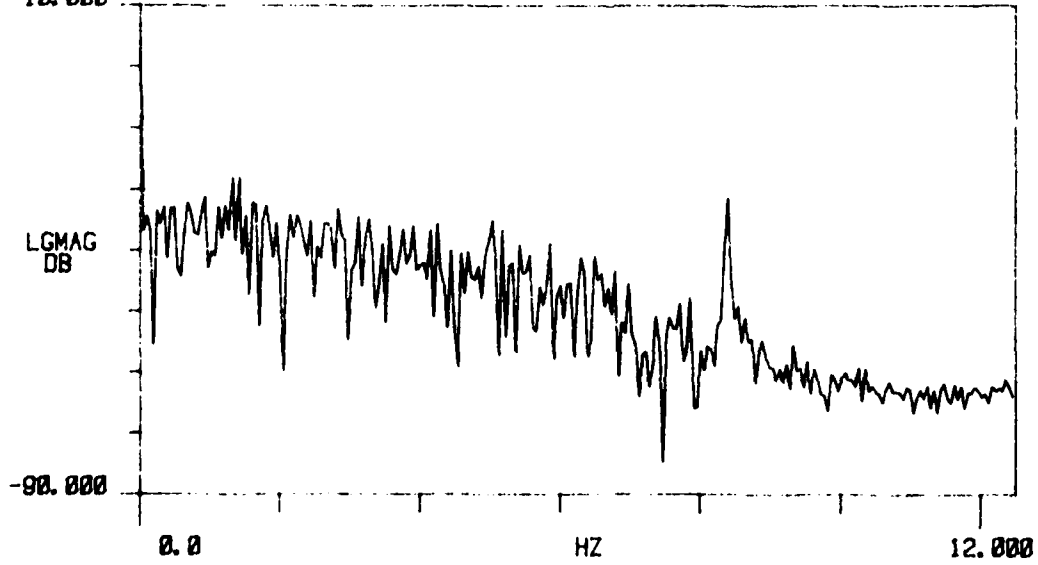


Figure C-2. Ambient Load Measurement. 29 Feb 80

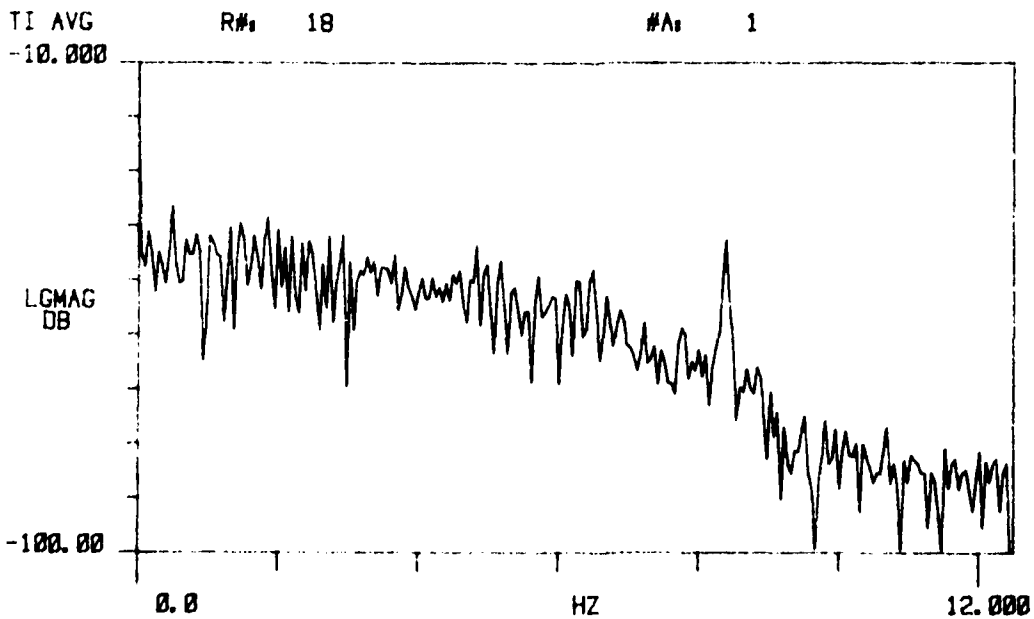
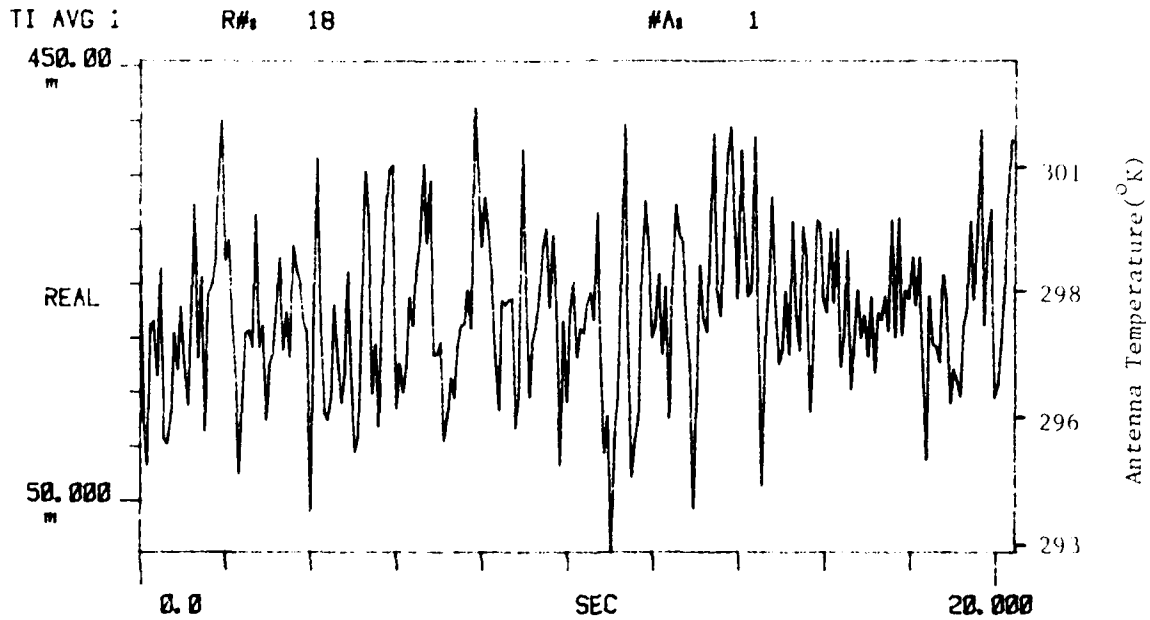


Figure C-2. Ambient Load Measurement. 29 Feb 80

C-3. 2 March 1980
Ambient Load Measurements

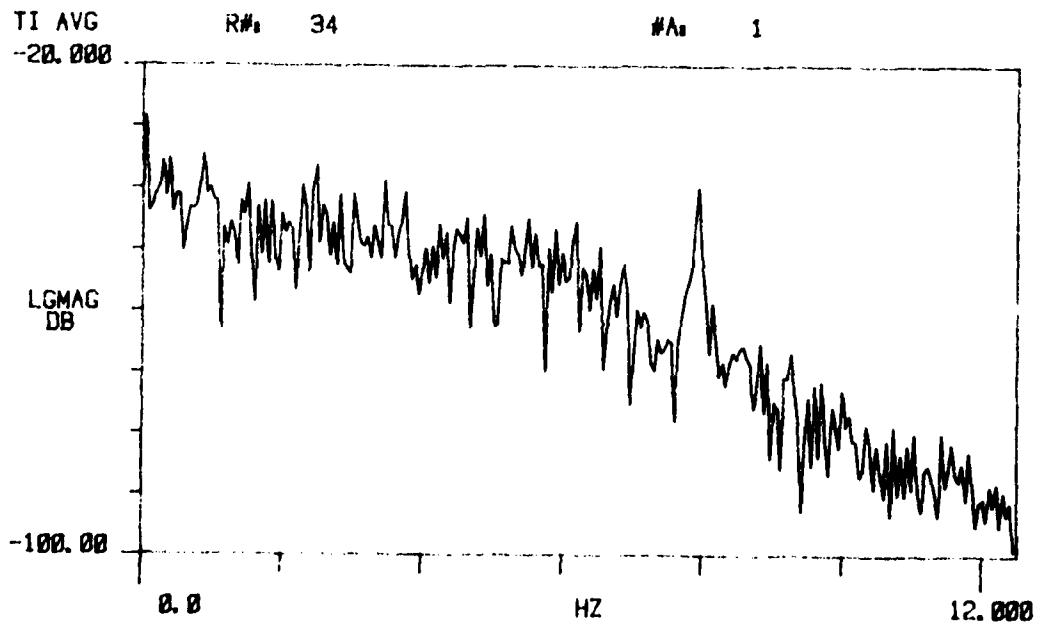
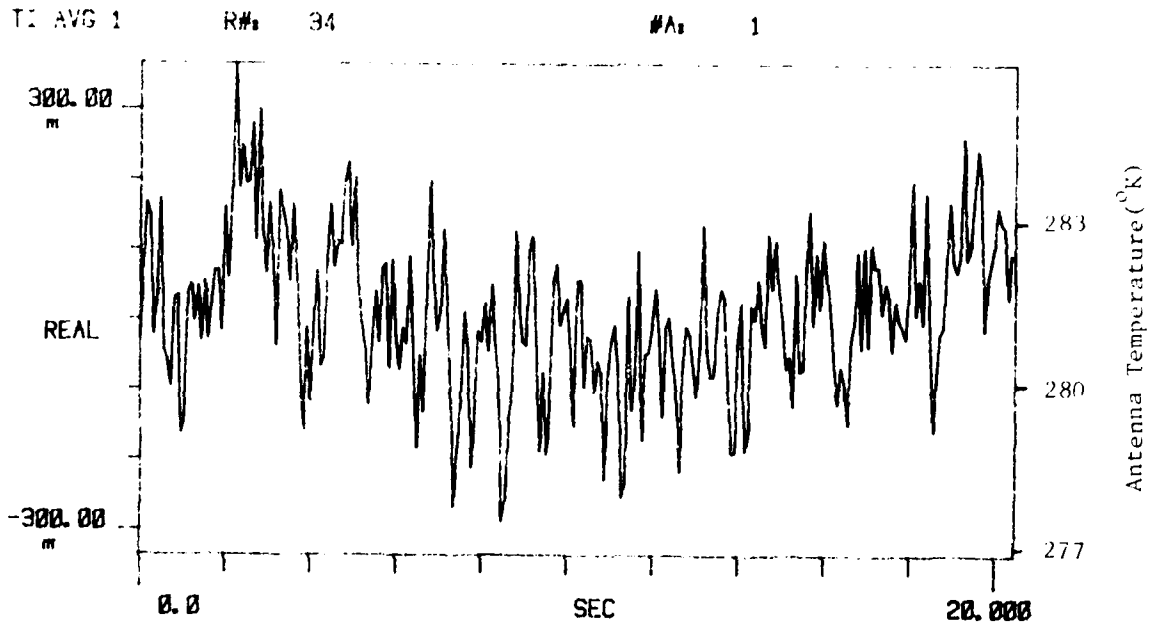
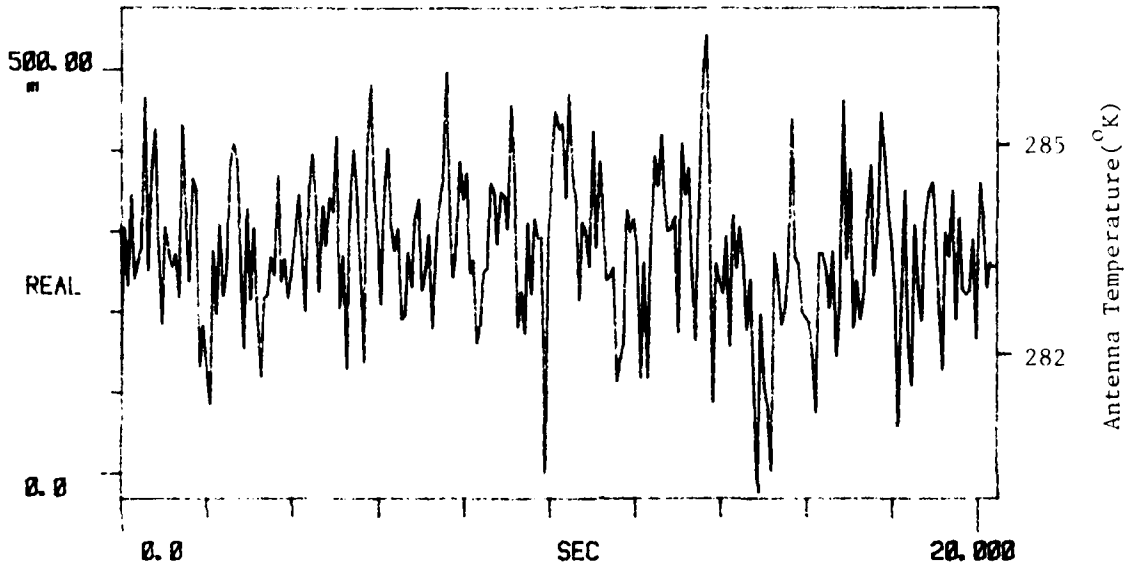


Figure C-3. Ambient Load Measurement. 2 Mar 80

TI AVG 1

R# 44

#A 1



TI AVG
-10.000

R# 44

#A 1

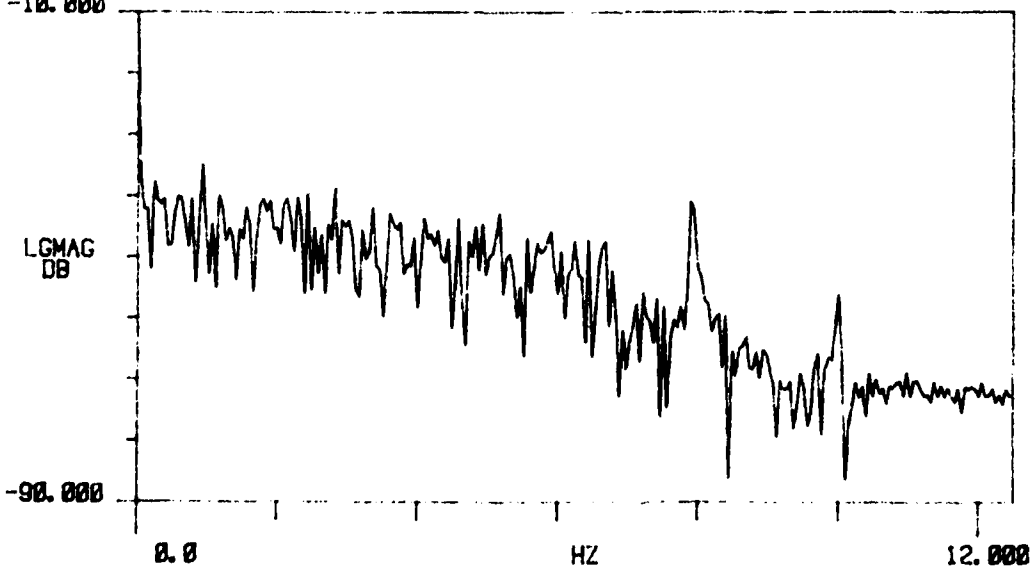
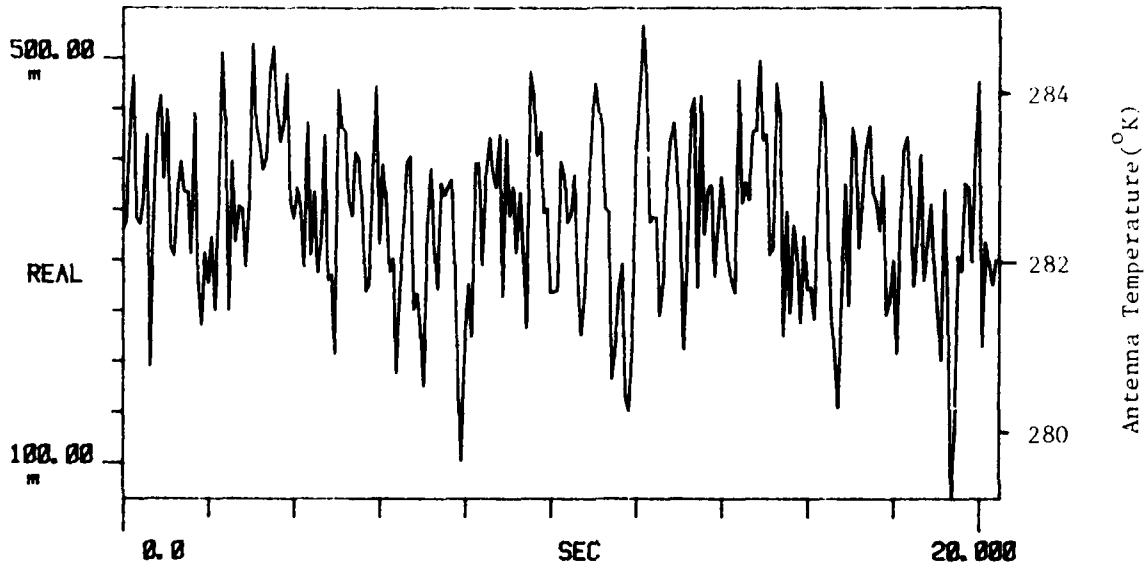


Figure C-3. Ambient Load Measurement. 2 Mar 80
79

TI AVG 1

R# 58

#A 1



TI AVG

R# 58

#A 1

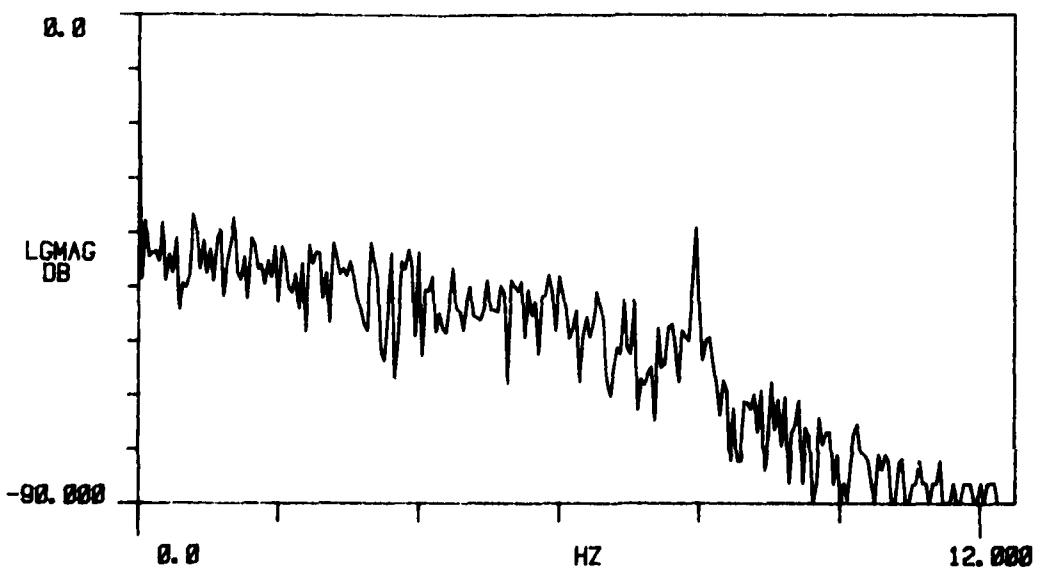


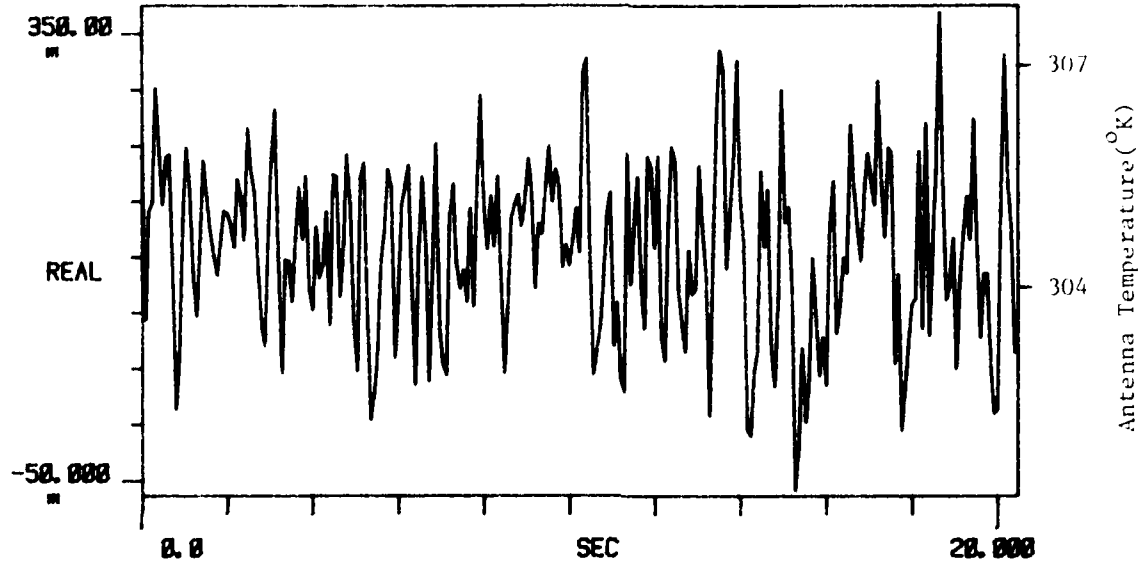
Figure C-3. Ambient Load Measurement. 2 Mar 80

C-4. 8 March 1980
Ambient Load Measurements

TI AVG 1

R# 19

#As 1



TI AVG 1

R# 19

#As 1

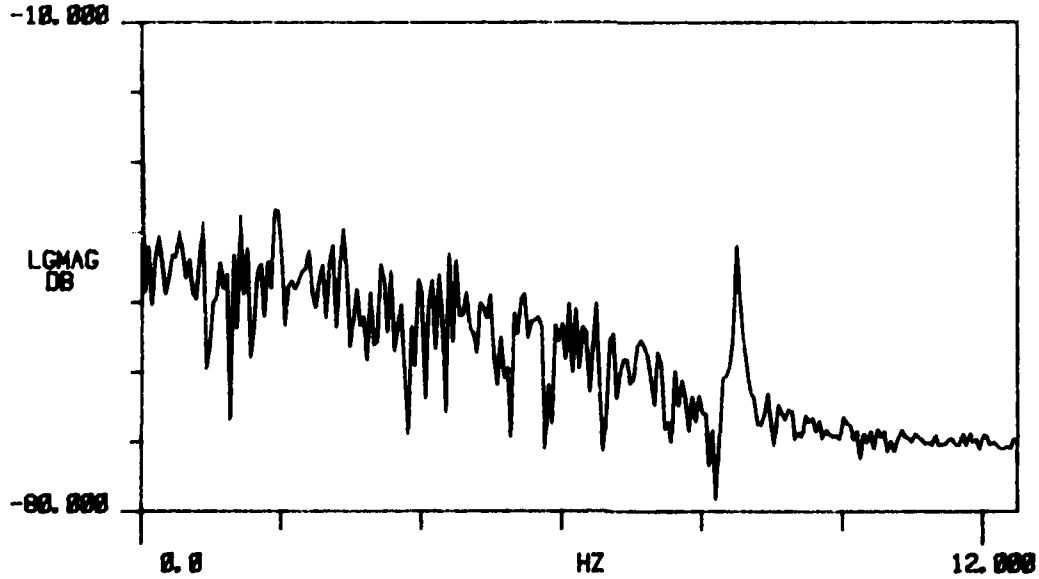
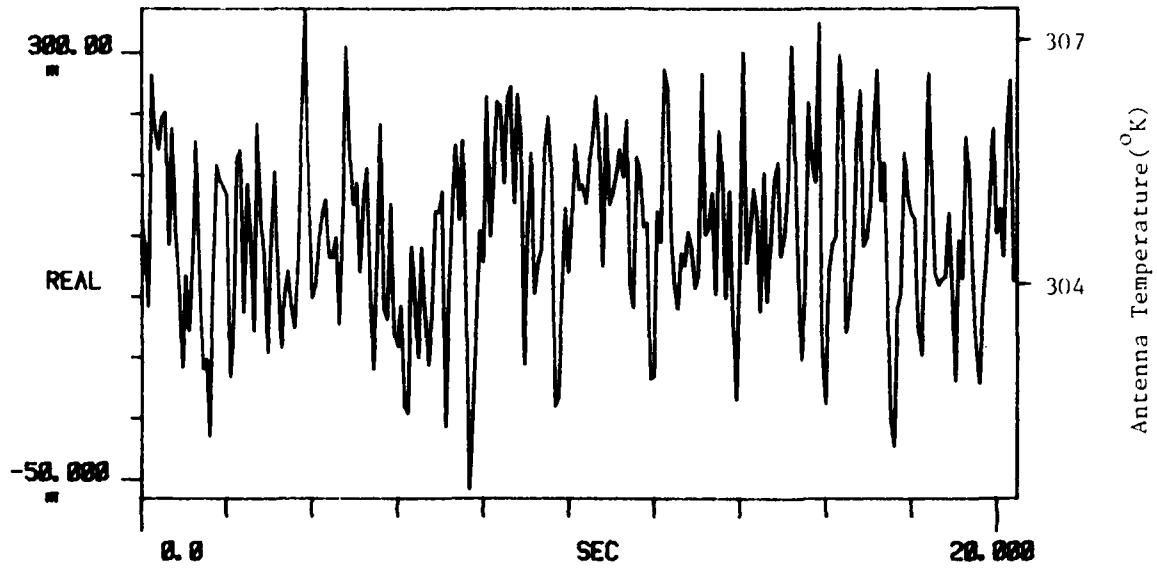


Figure C-4. Ambient Load Measurement. 8 Mar 80

TI AVG 1

R# 8

#A 1



TI AVG
-10.000

R# 8

#A 1

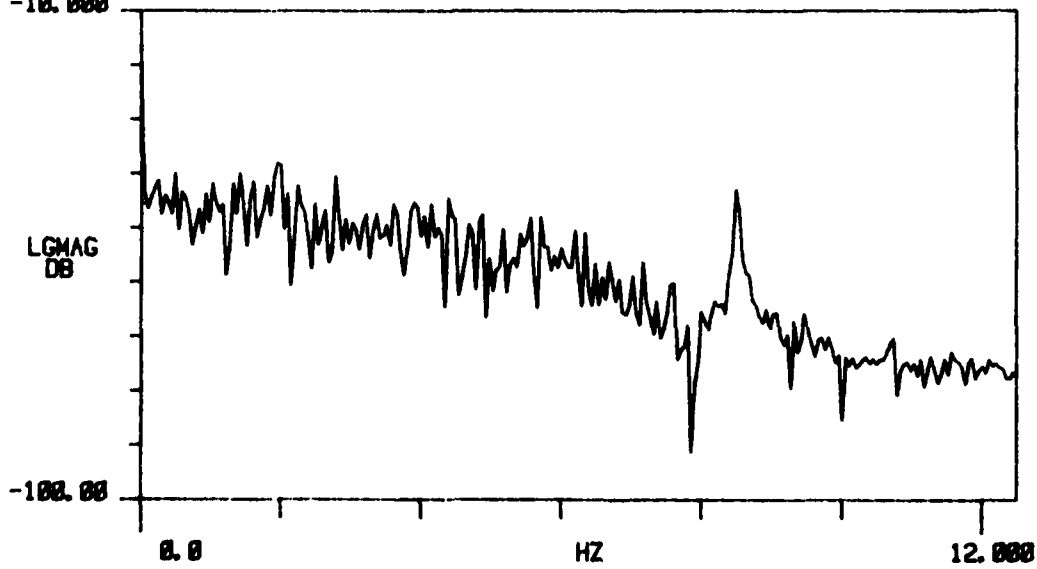


Figure C-4. Ambient Load Measurement. 8 Mar 80

C-5 11 March 1980
Ambient Load Measurements

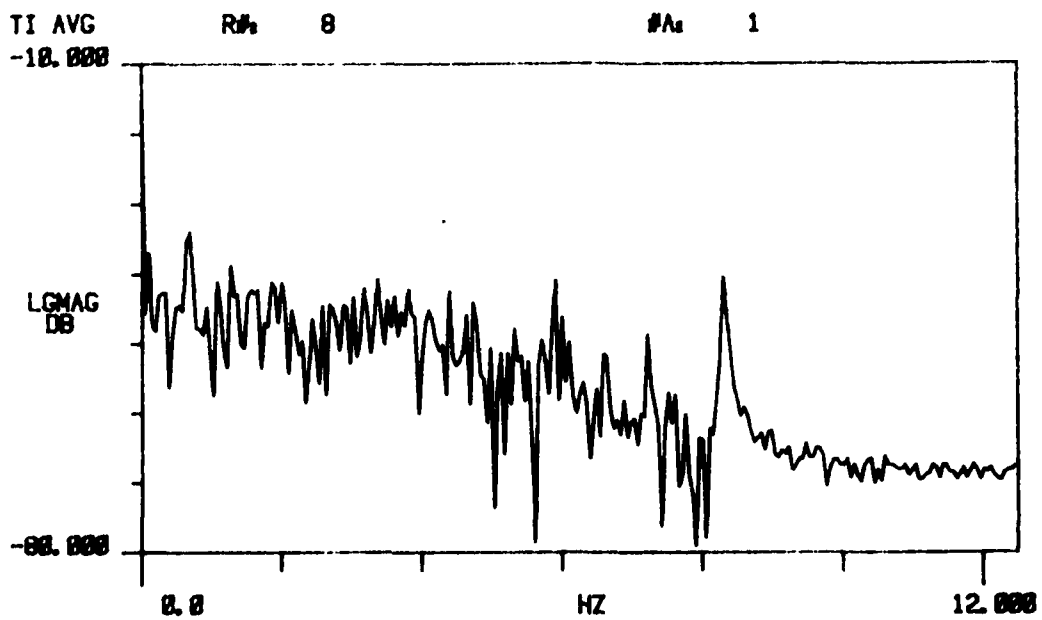
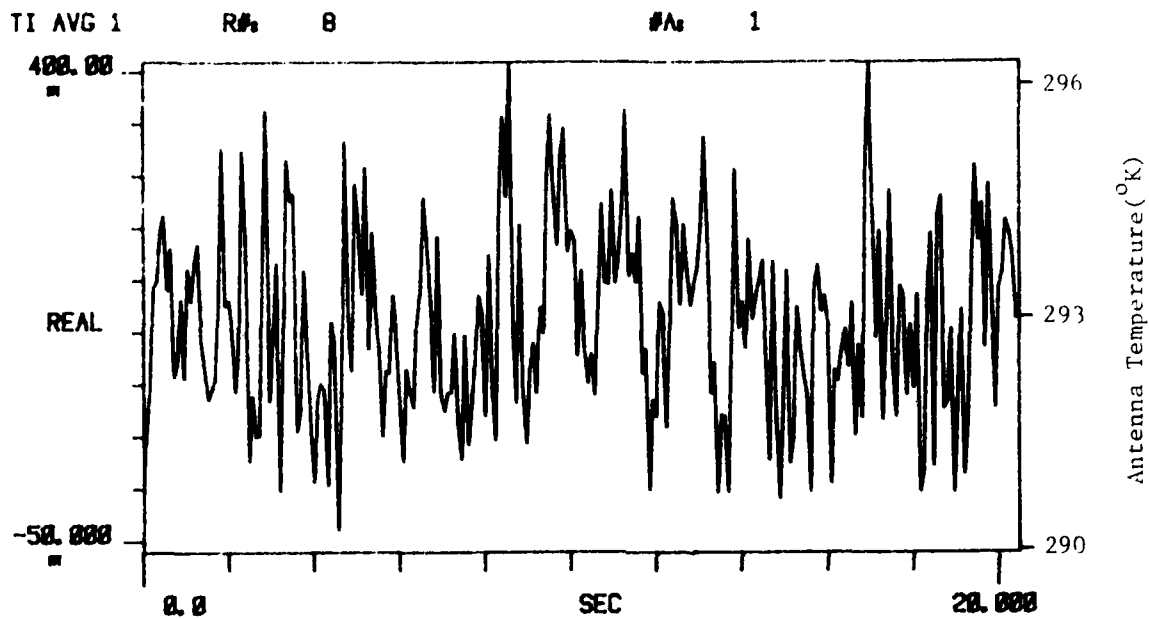


Figure C-5. Ambient Load Measurement. 11 Mar 80

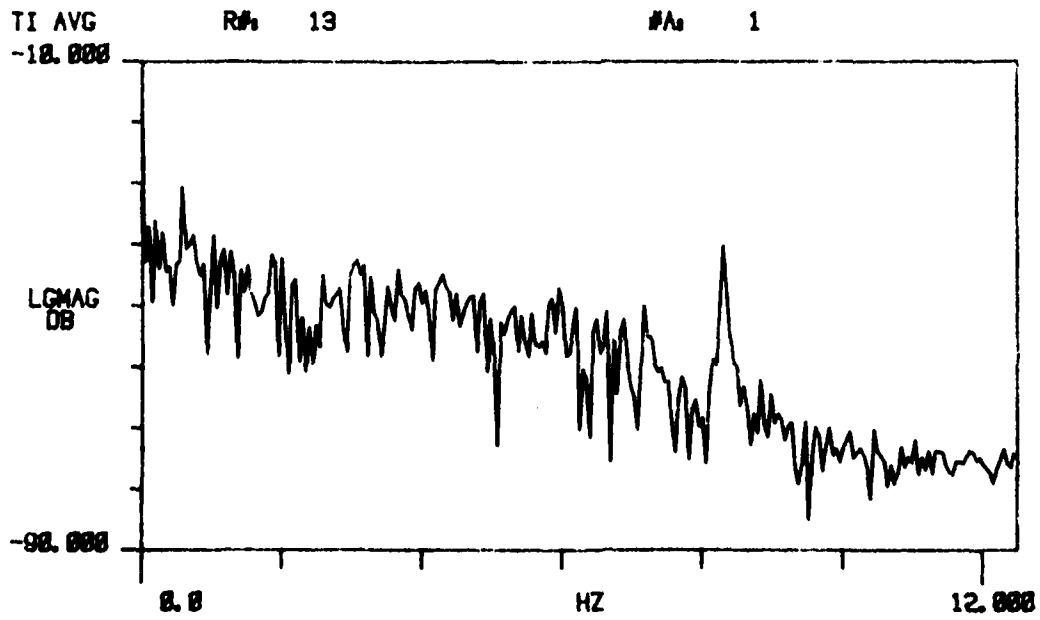
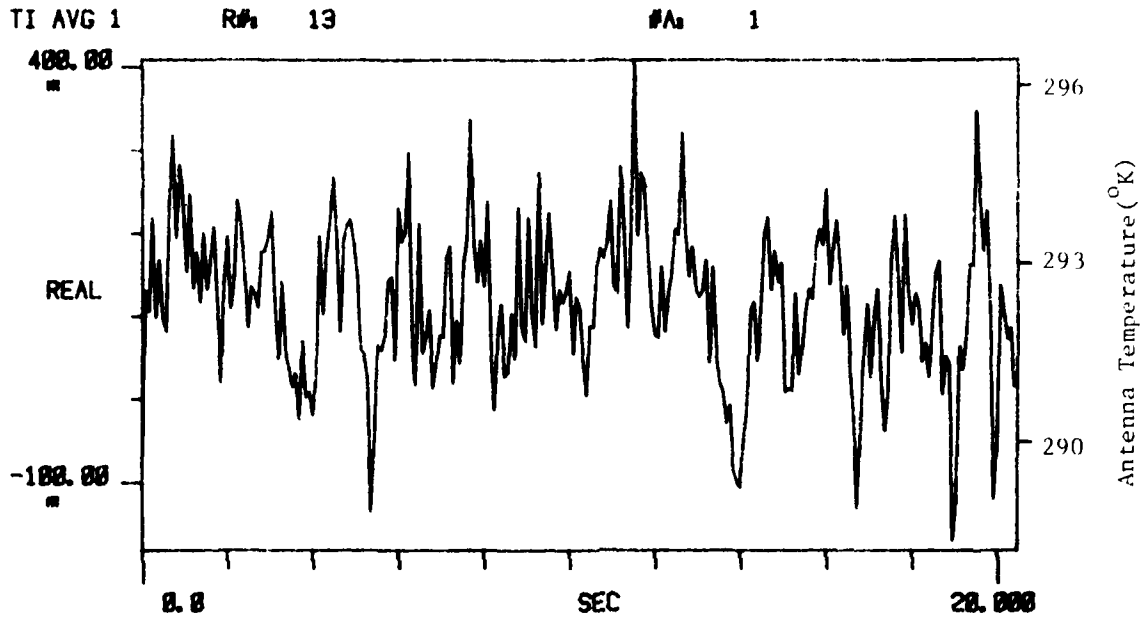
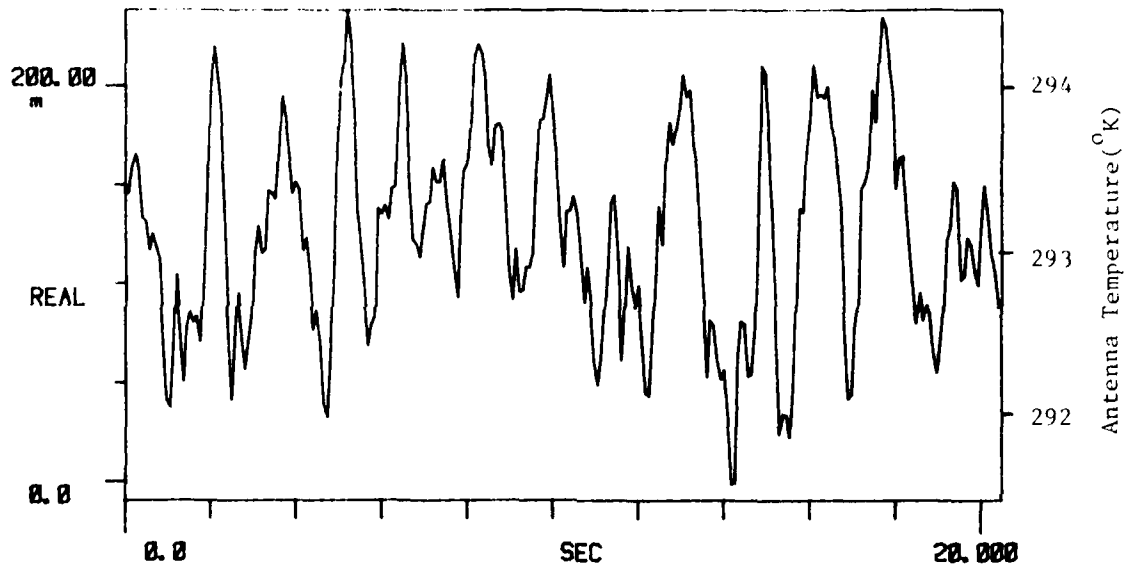


Figure C-5. Ambient Load Measurement. 11 Mar 80

TI AVG 1

R# 25

#A 1



TI AVG
-10.000

R# 25

#A 1

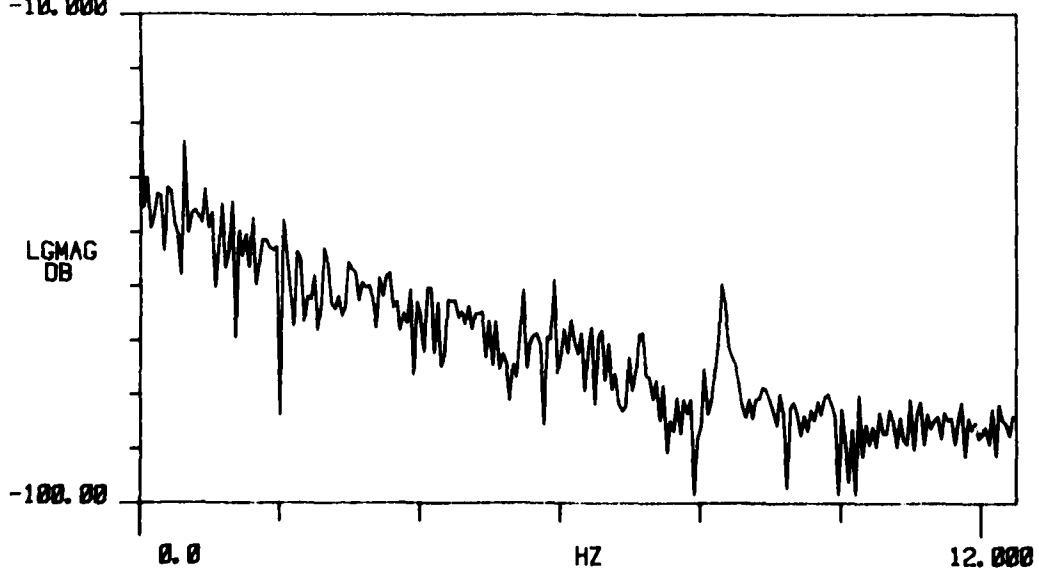
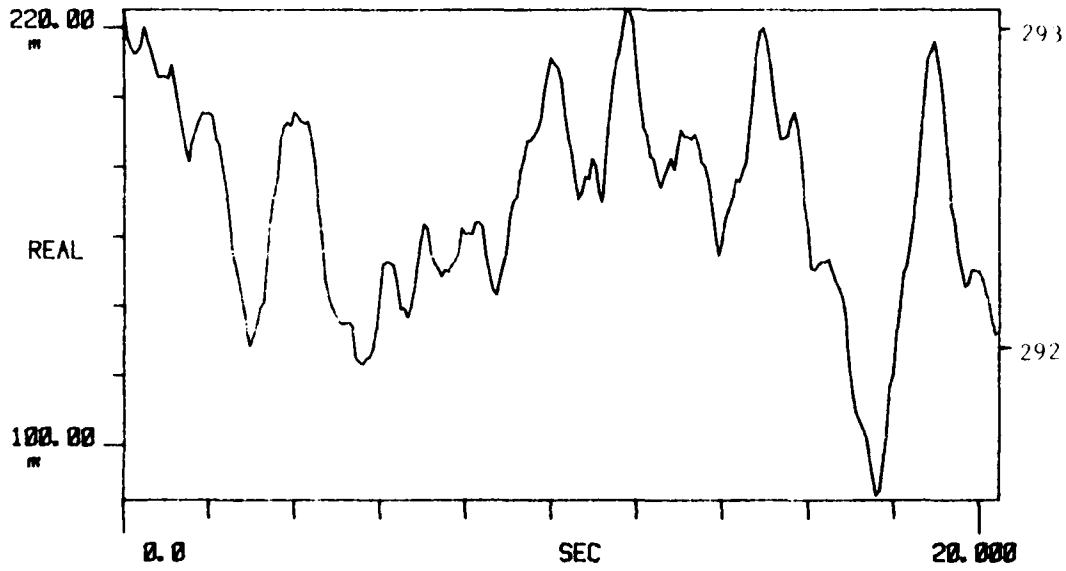


Figure C-5. Ambient Load Measurement. 11 Mar 80

TI AVG 1

R# 29

#A 1



TI AVG
-10.000

R# 29

#A 1

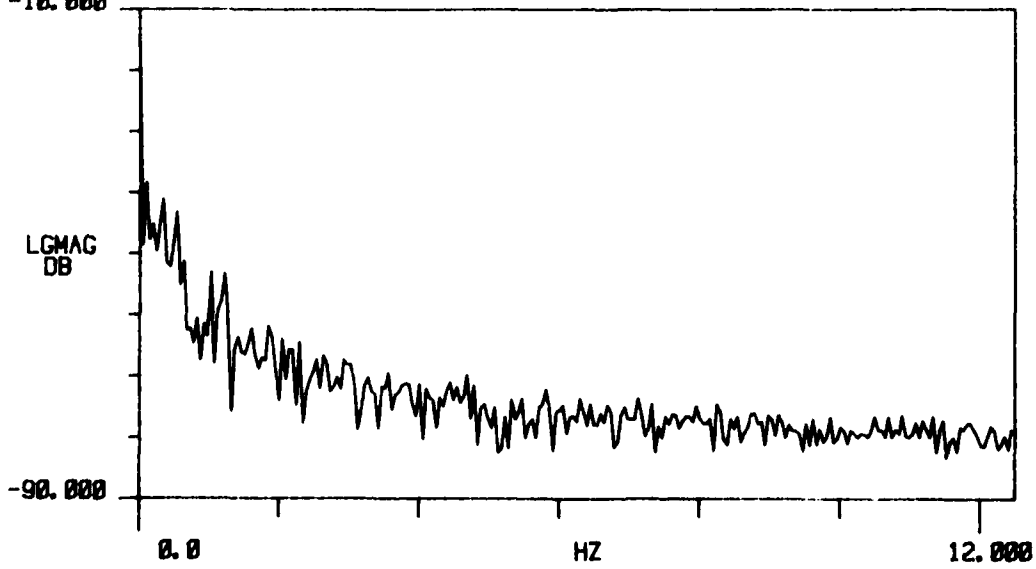
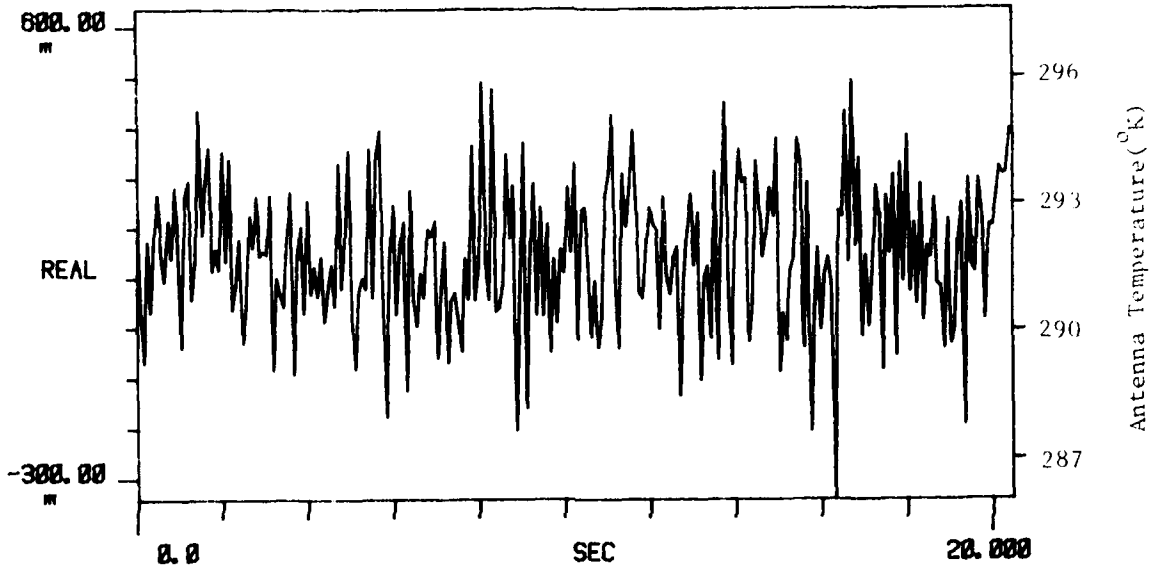


Figure C-5. Ambient Load Measurement. 11 Mar 80

TI AVG 1

R#s 42

#As 1



TI AVG 1

R#s 42

#As 1

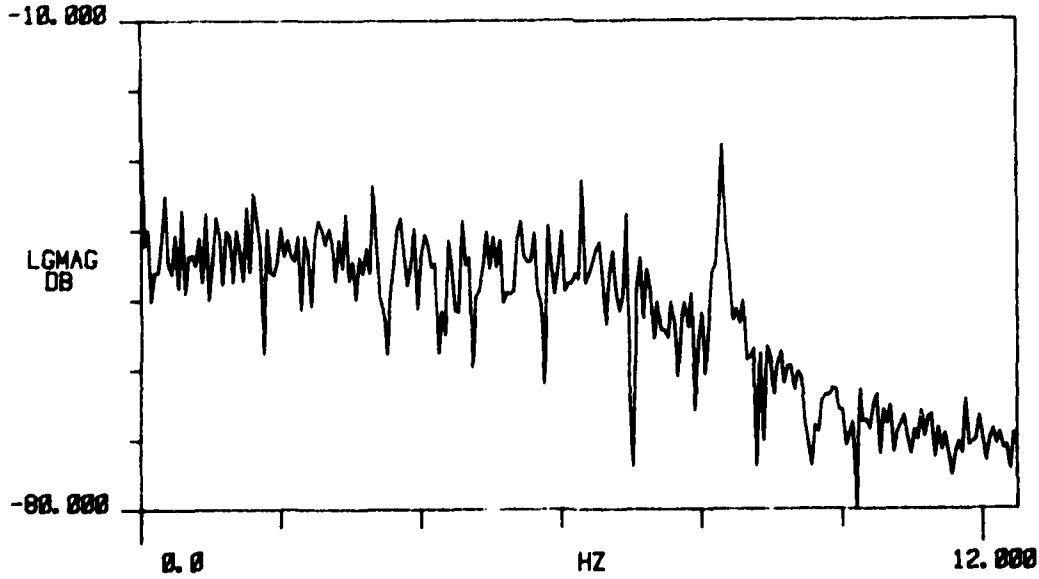


Figure C-5. Ambient Load Measurement. 11 Mar 80

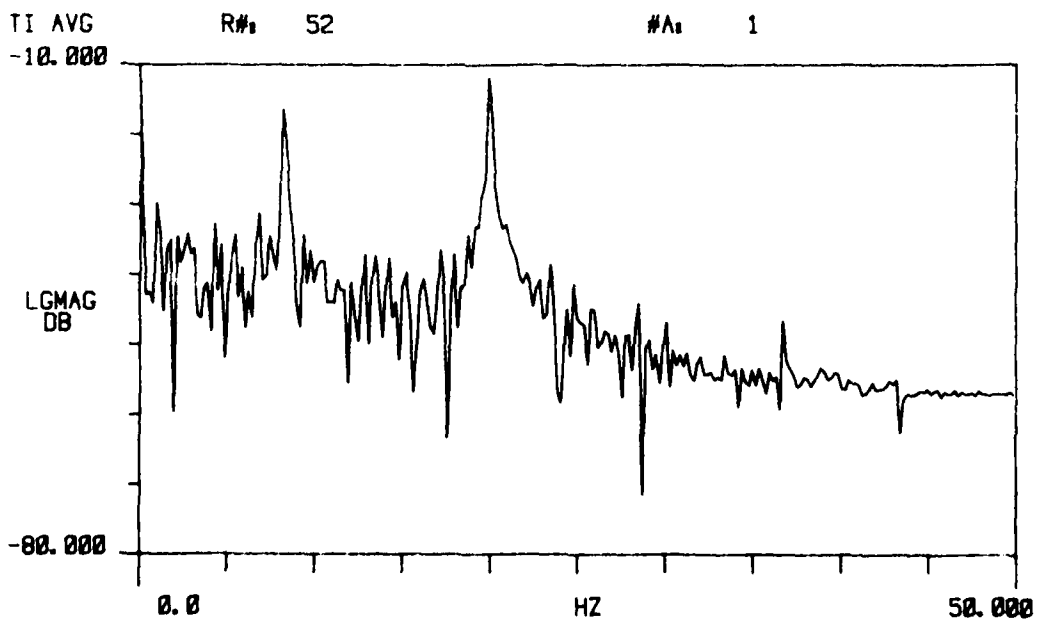
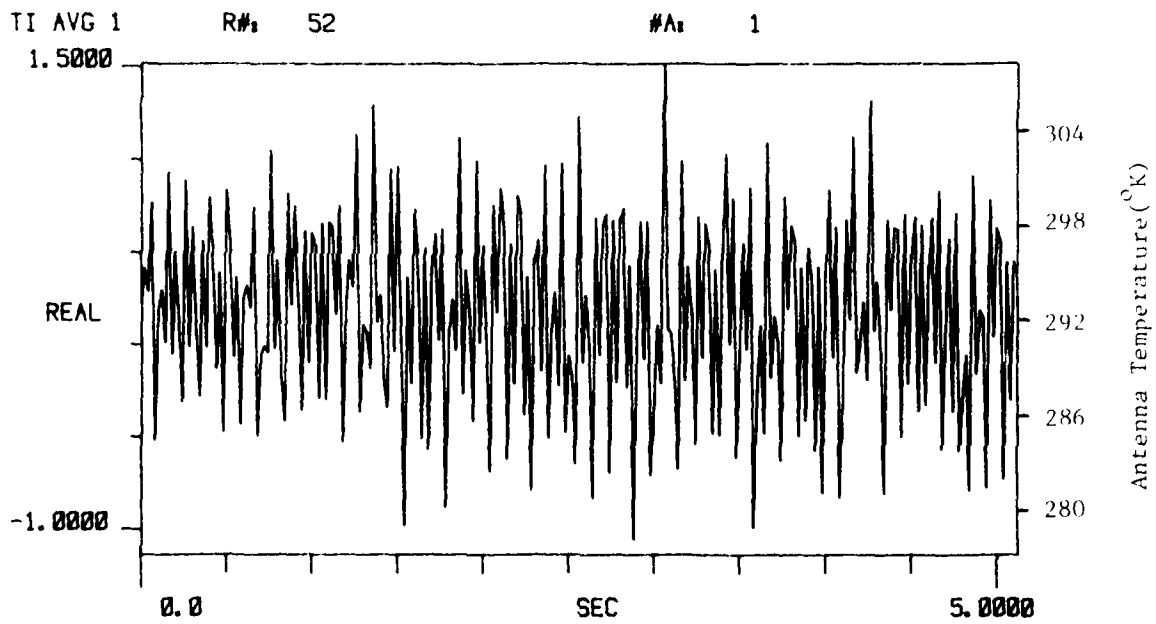
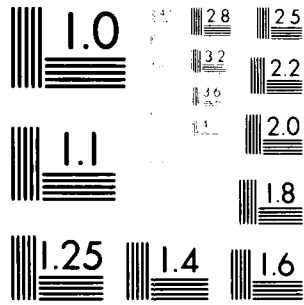


Figure C-5. Ambient Load Measurement, 11 Mar 80

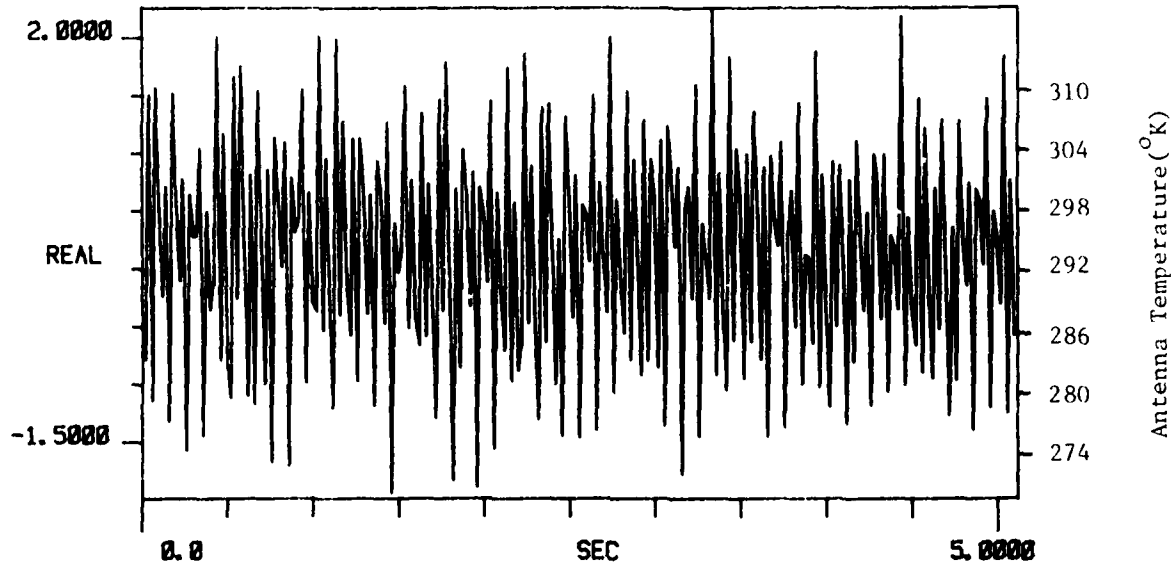


MICROCOPY RESOLUTION TEST CHART
NBS 1963-A

TI AVG 1

R# 60

#A 1



TI AVG

R# 60

#A 1

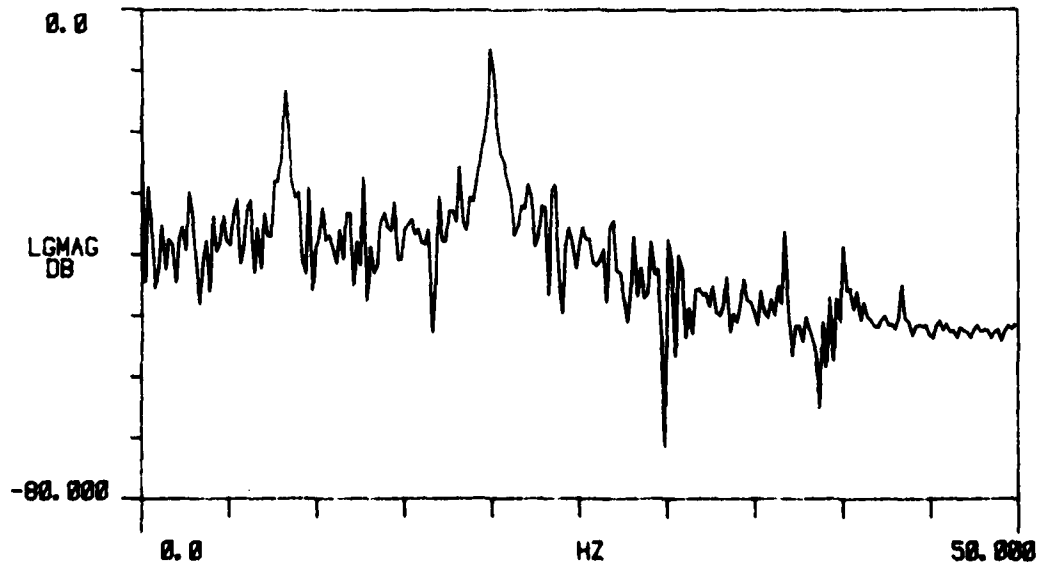


Figure C-5. Ambient Load Measurement. 11 Mar 80

C-6. 16 March 1980
Ambient Load Measurements

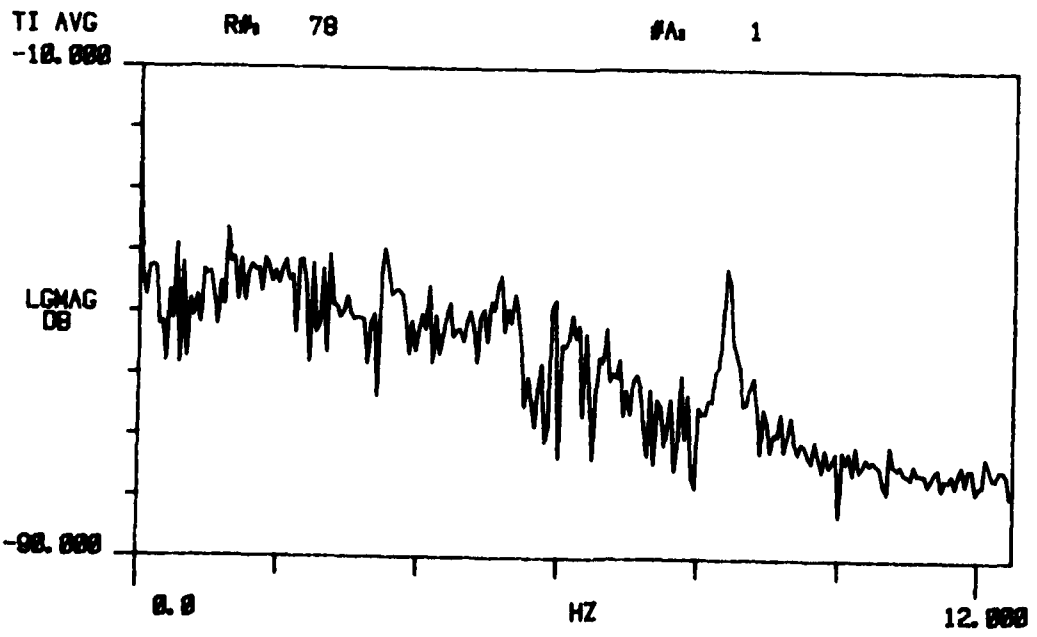
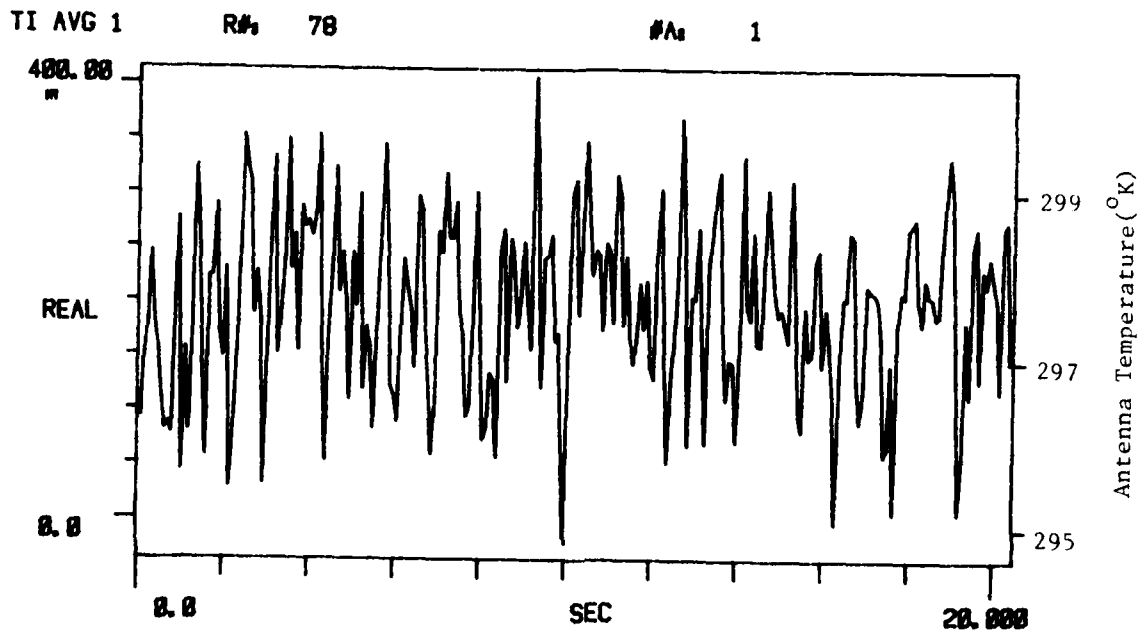
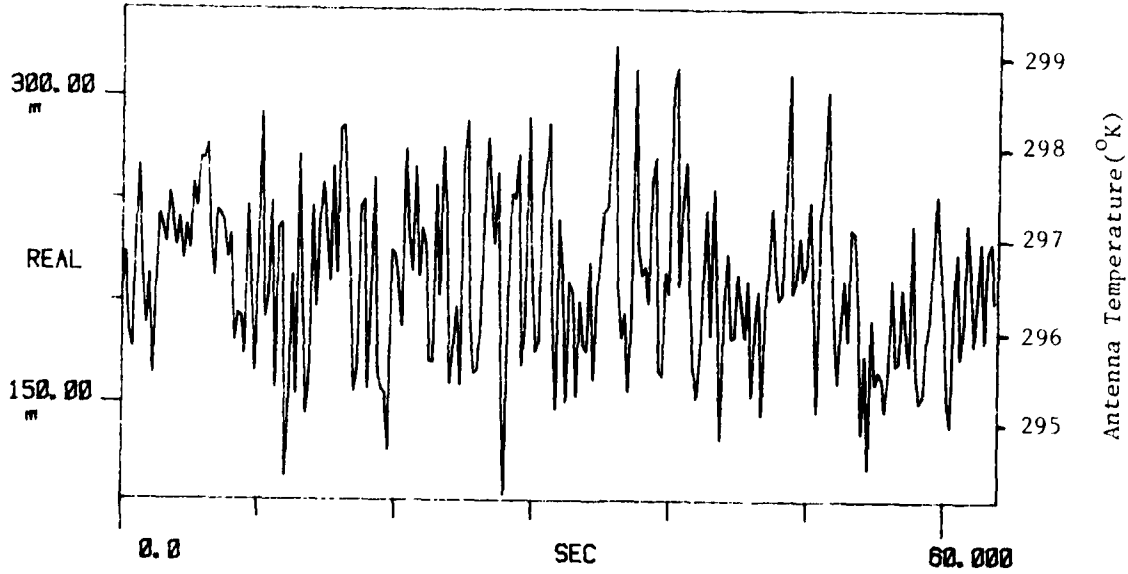


Figure C-6. Ambient Load Measurement. 16 Mar 80

TI AVG 1

R# 99

#A 1



TI AVG
-10.000

R# 99

#A 1

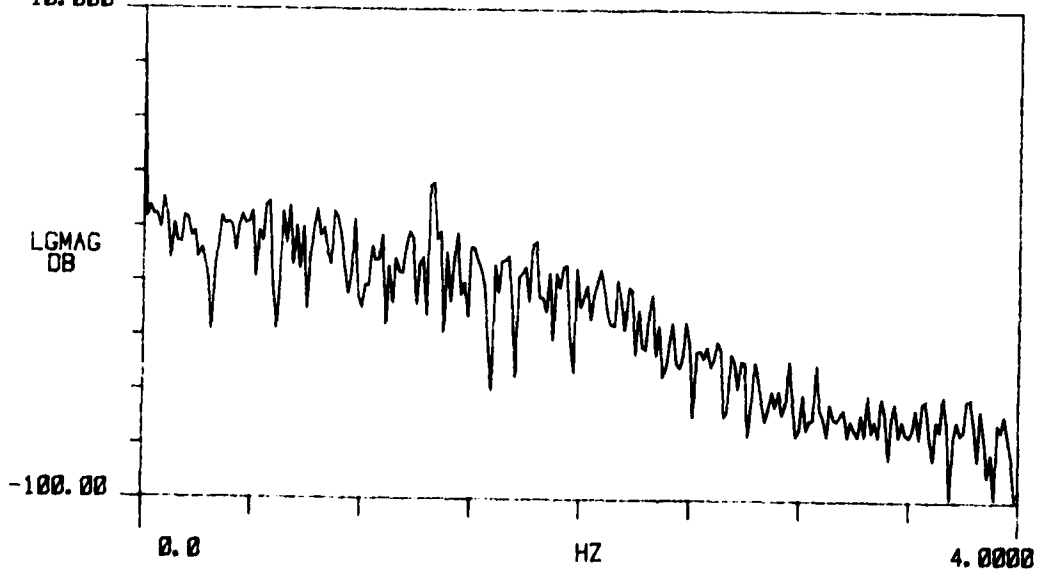
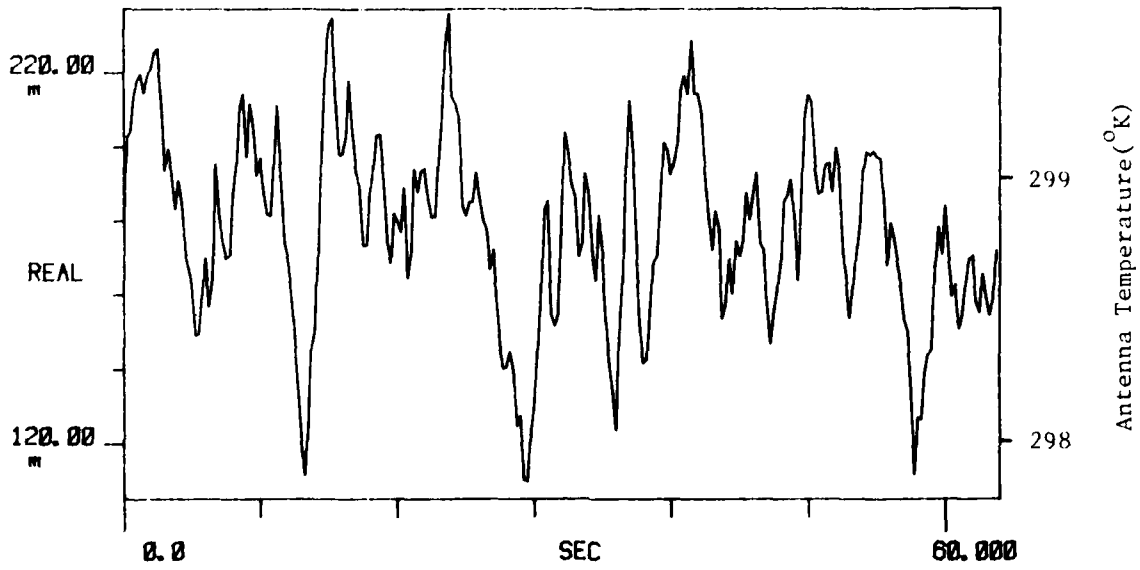


Figure C-6. Ambient Load Measurement. 16 Mar 80

TI AVG 1

R#s 115

#As 1



TI AVG
-10.000

R#s 115

#As 1

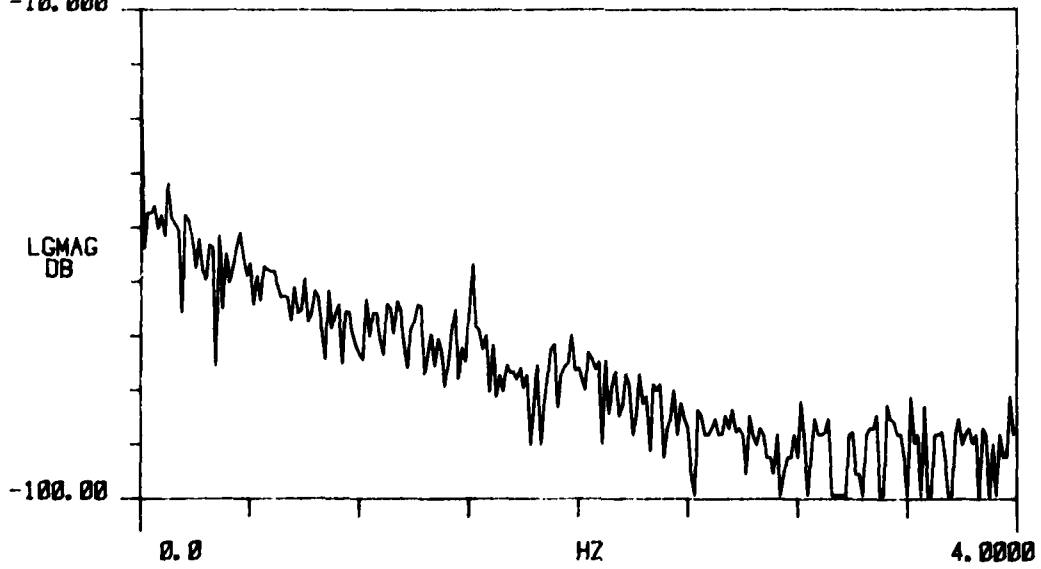


Figure C-6. Ambient Load Measurement. 16 Mar 80

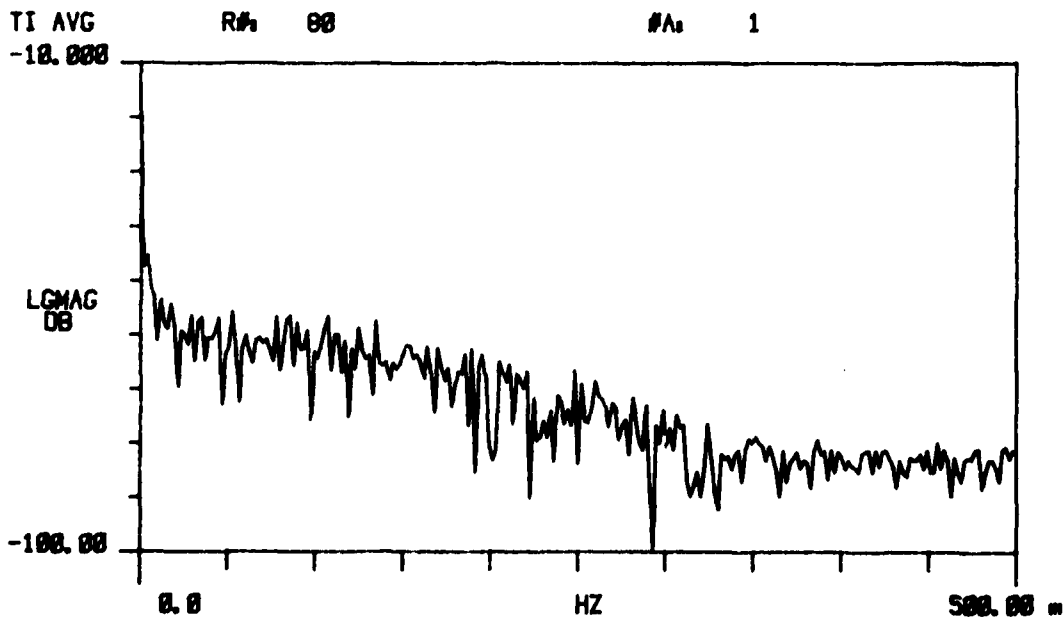
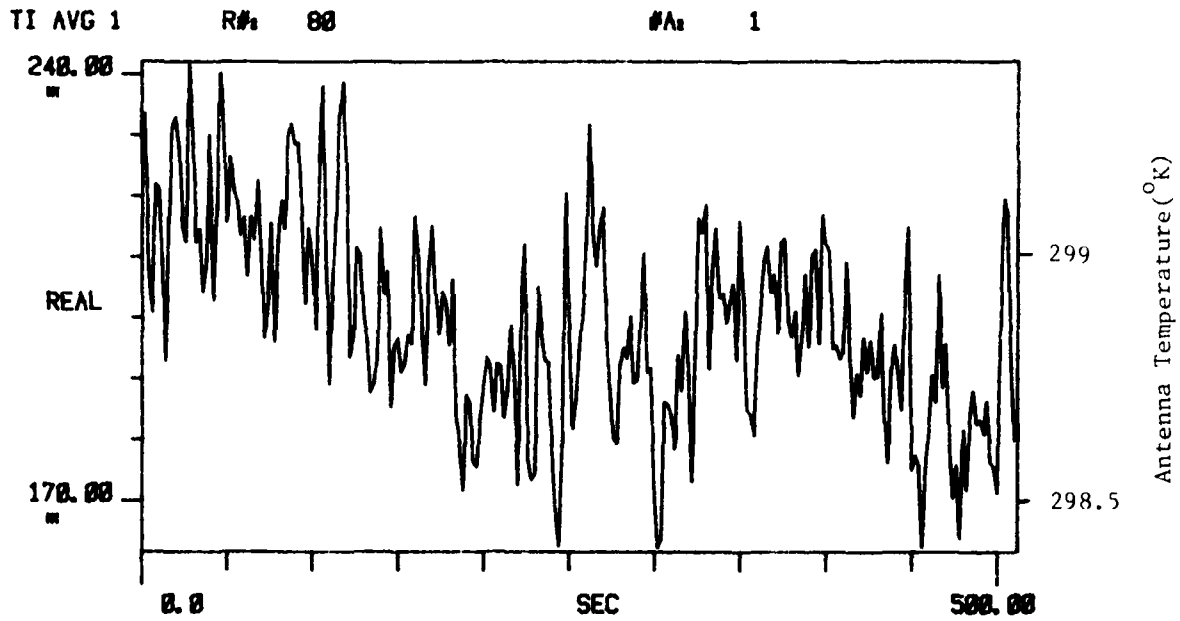
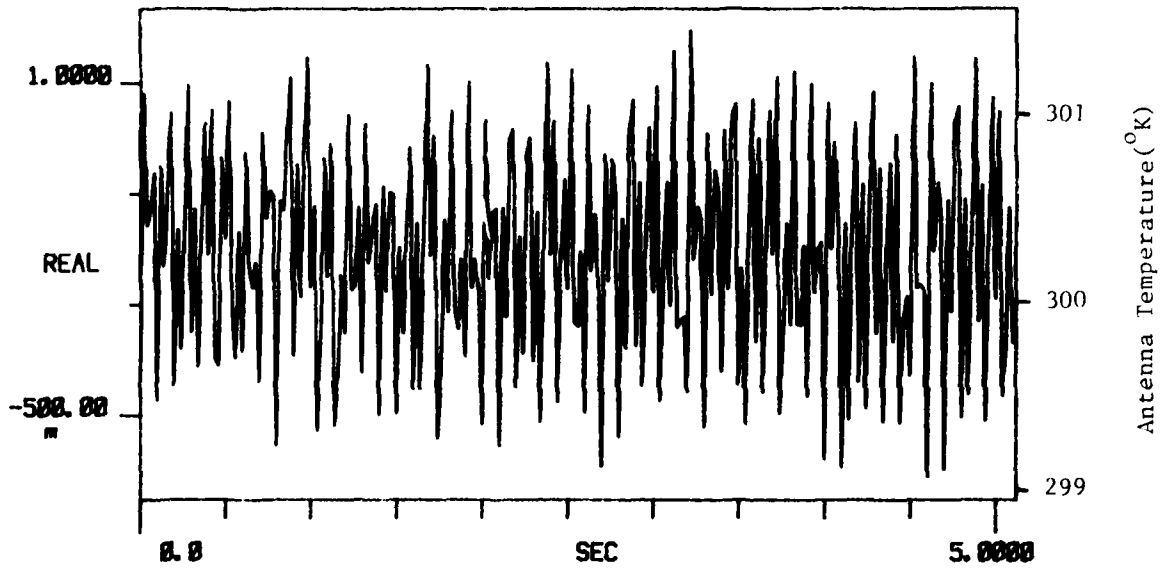


Figure C-6. Ambient Load Measurement. 16 Mar 80

TI AVG 1 R# 89 #A 1



TI AVG 1 R# 89 #A 1
-10.000

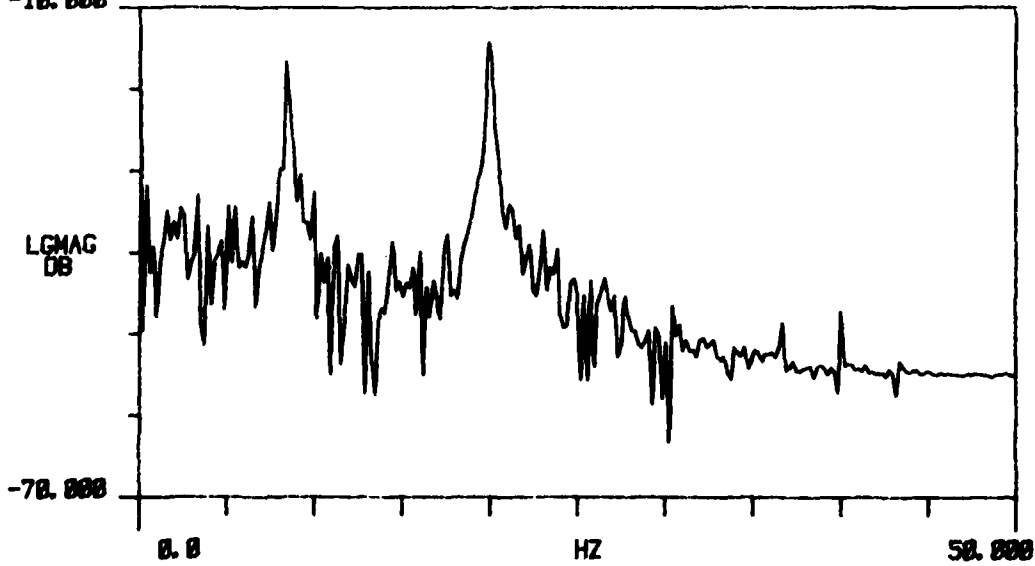
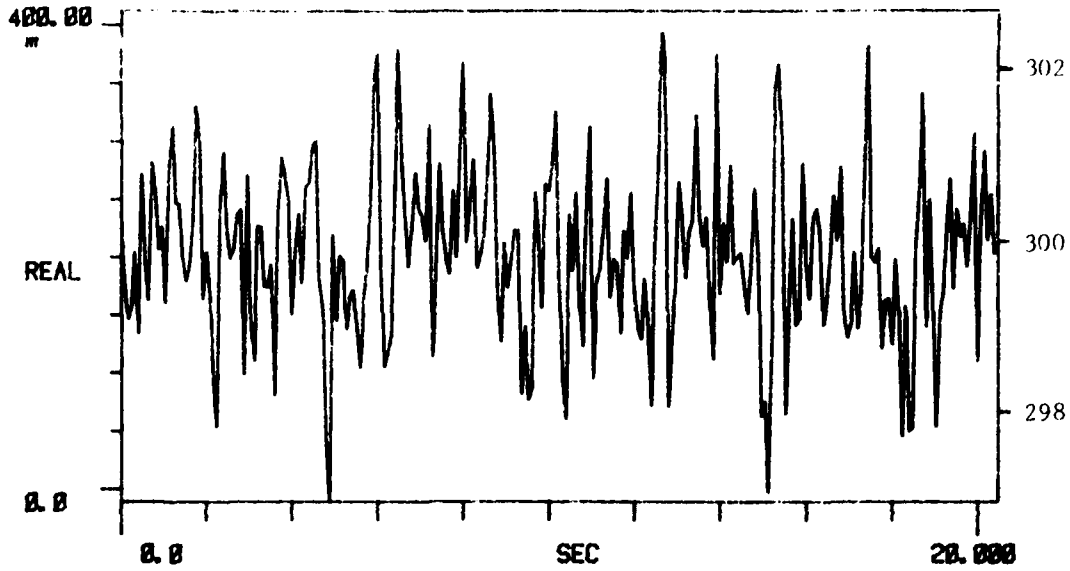


Figure C-6. Ambient Load Measurement. 16 Mar 80

TI AVG 1

R# 99

#A 1



TI AVG

R# 99

#A 1

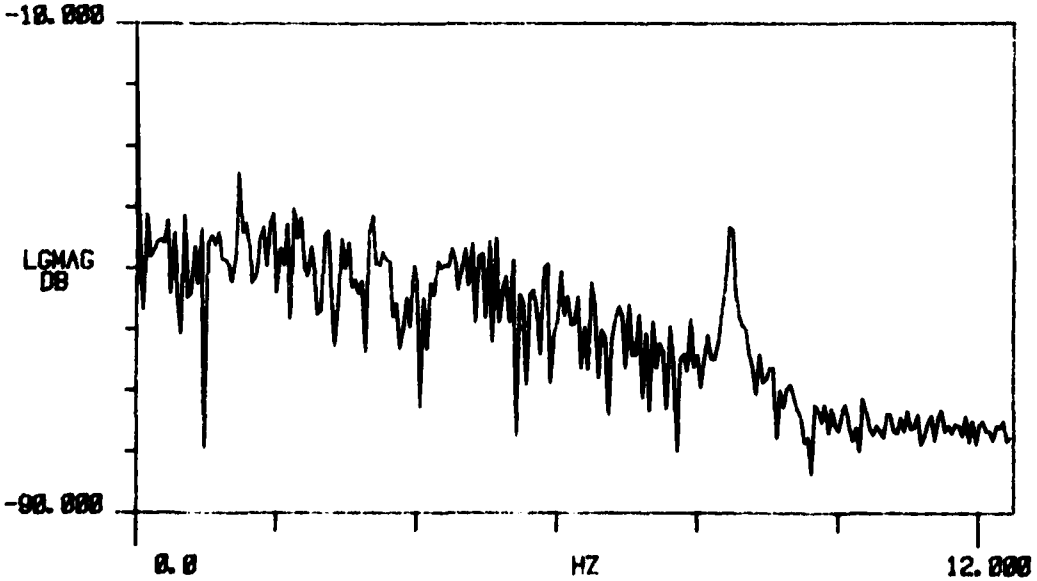


Figure C-6. Ambient Load Measurement. 16 Mar 80

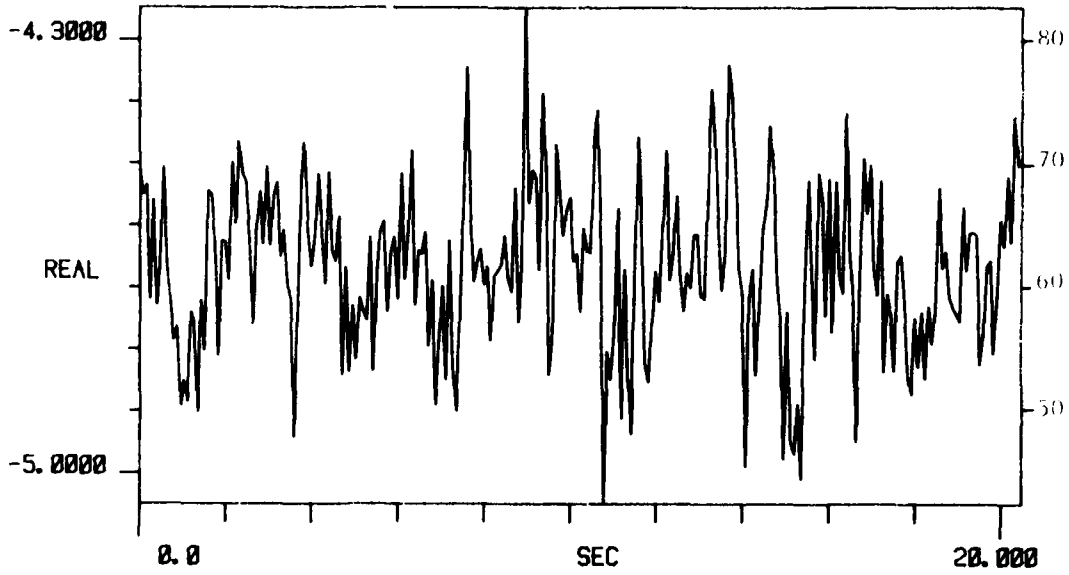
APPENDIX D
ZENITH SKY DATA

D-1. 28 February 1980
Zenith Sky Measurements

TI AVG 1

R# 9

#A 1



TI AVG 1

R# 9

#A 1

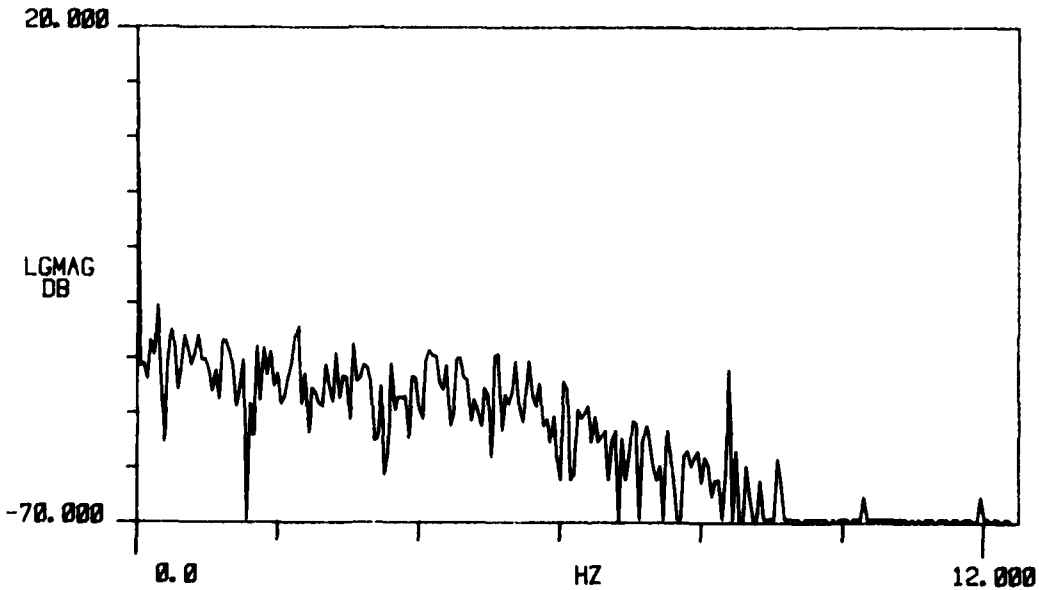
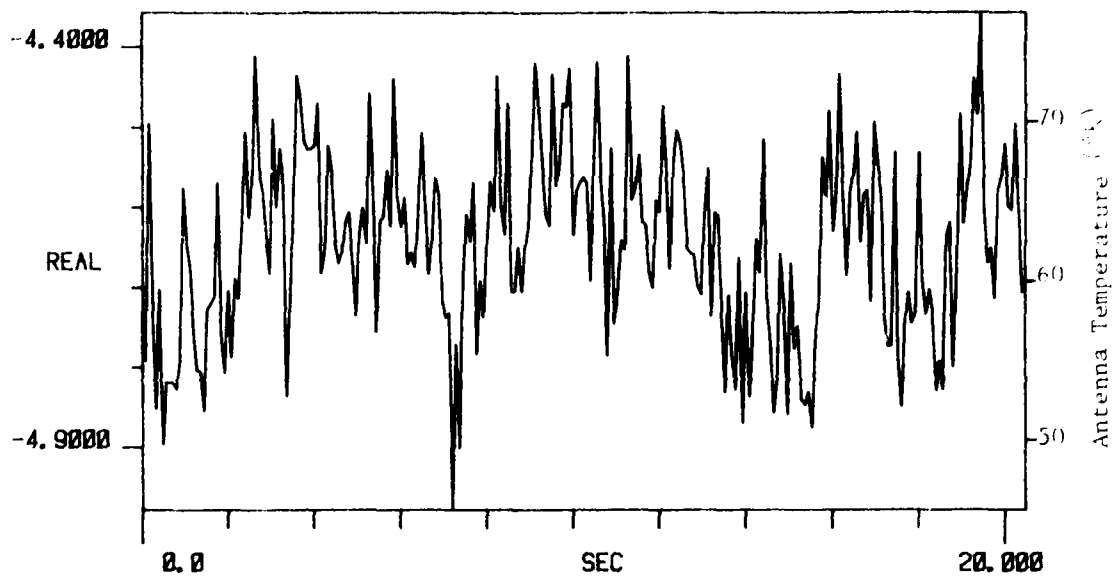


Figure D-1. Zenith Sky Measurement 28 Feb 80

TI AVG 1 R#s 10

#As 1



TI AVG 1 R#s 10
20.000

#As 1

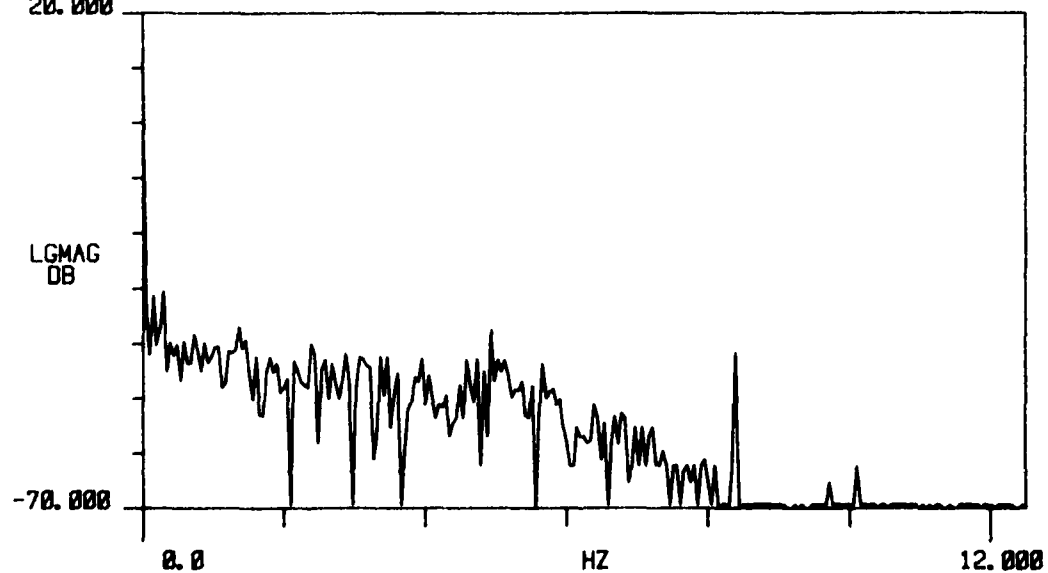


Figure D-1. Zenith Sky Measurement. 28 Feb 80

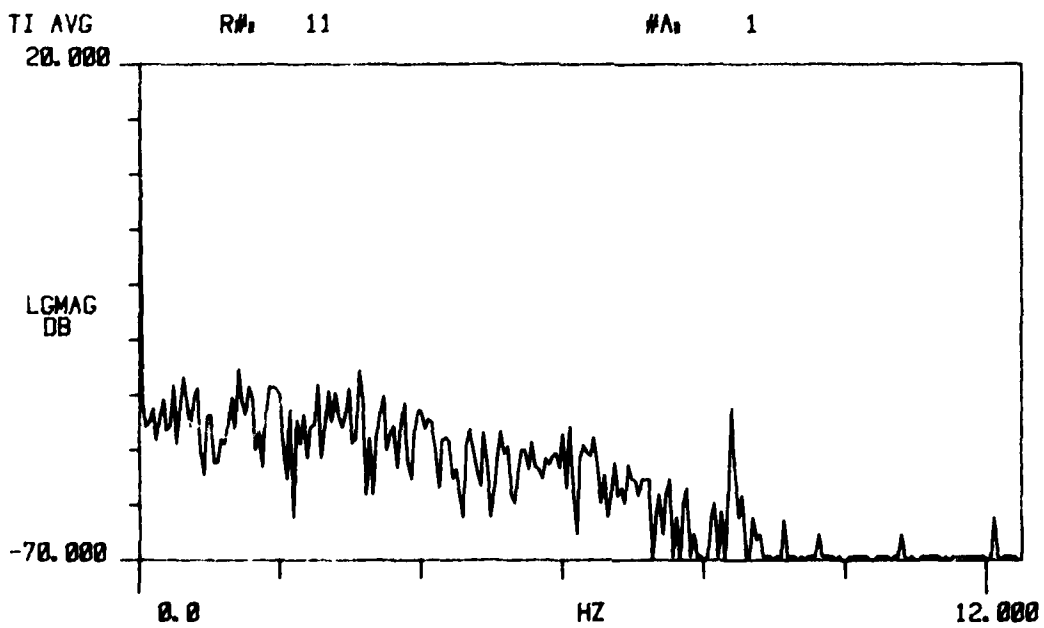
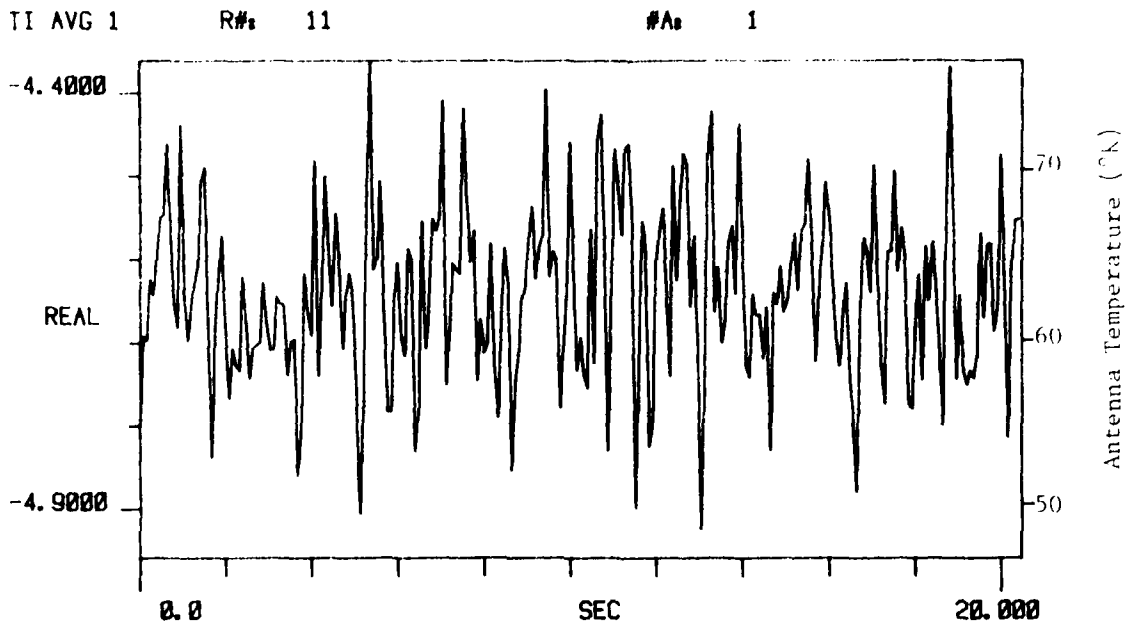


Figure D-1. Zenith Sky Measurement 28 Feb 80

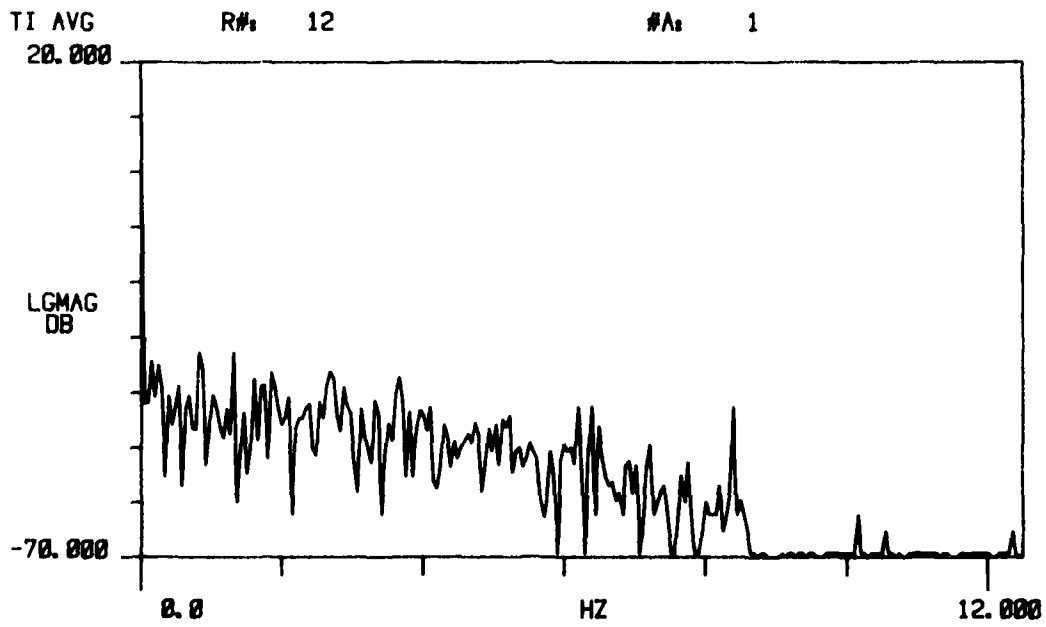
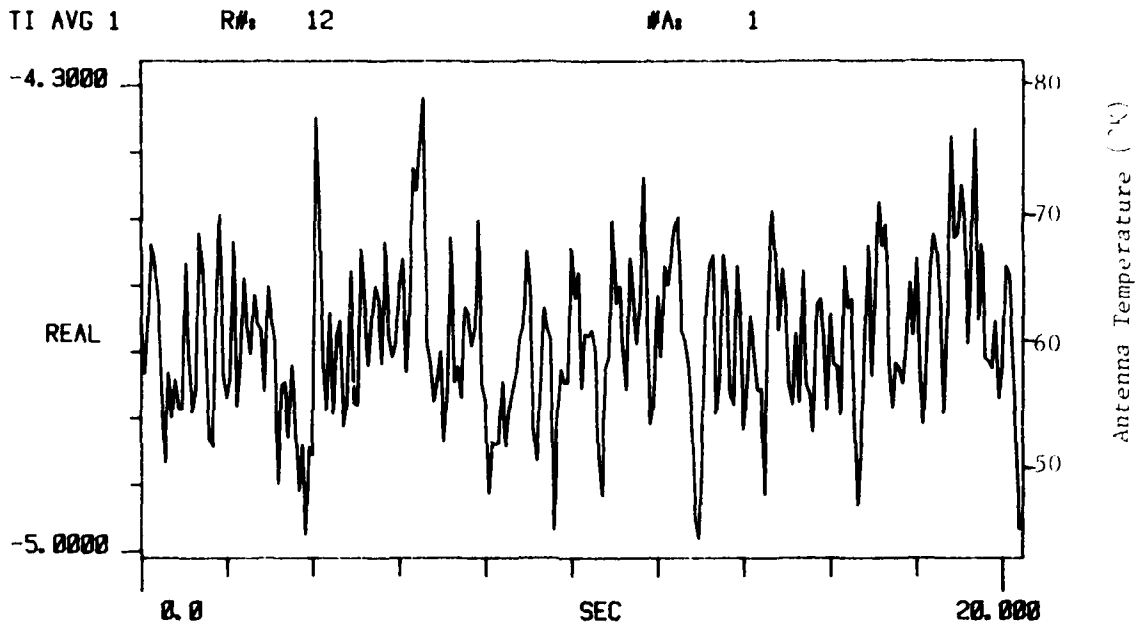


Figure D-1. Zenith Sky Measurement. 28 Feb 80

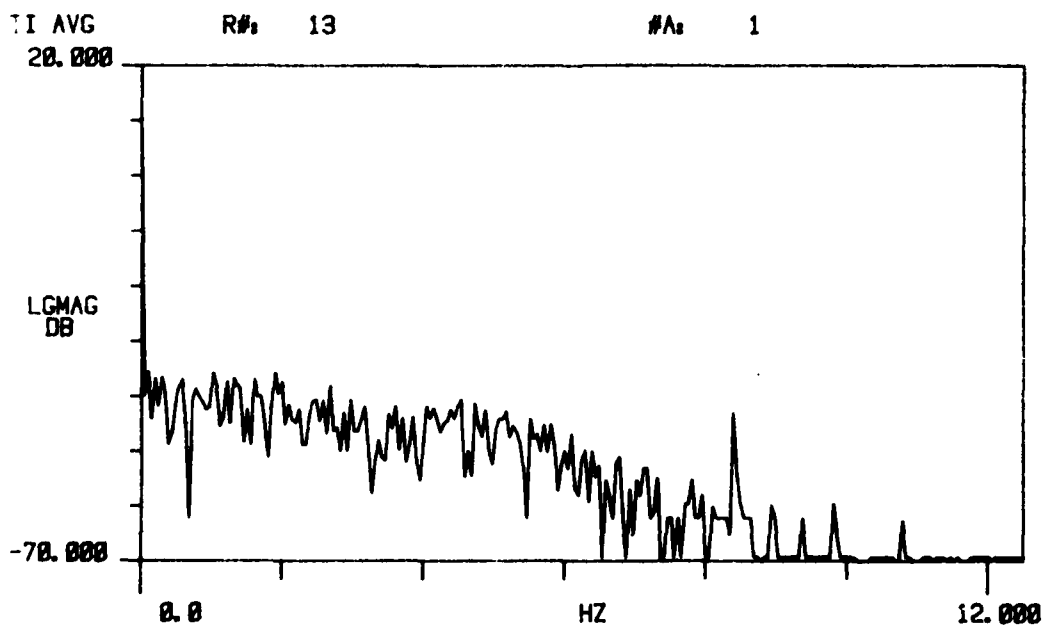
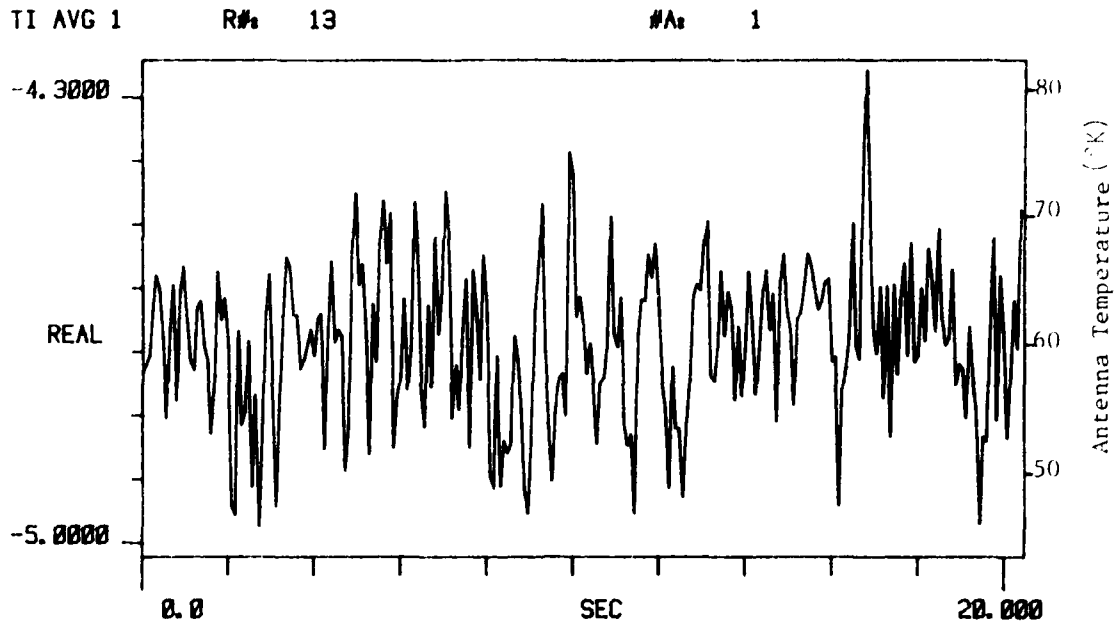
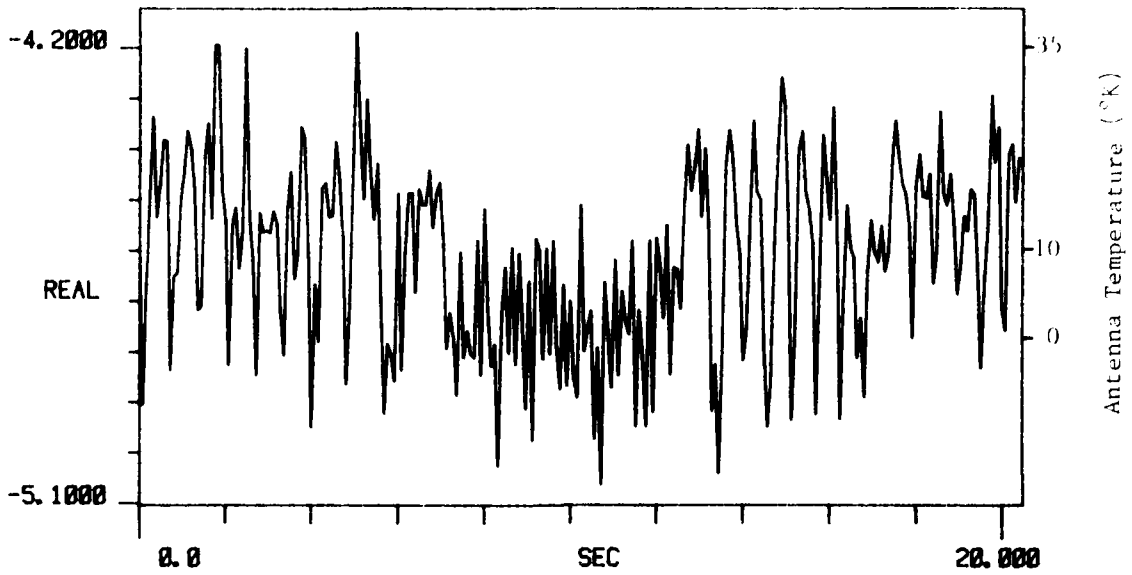


Figure D-1. Zenith Sky Measurement. 28 Feb 80

TI AVG 1

R# 18

#As 1



TI AVG
20.000

R# 18

#As 1

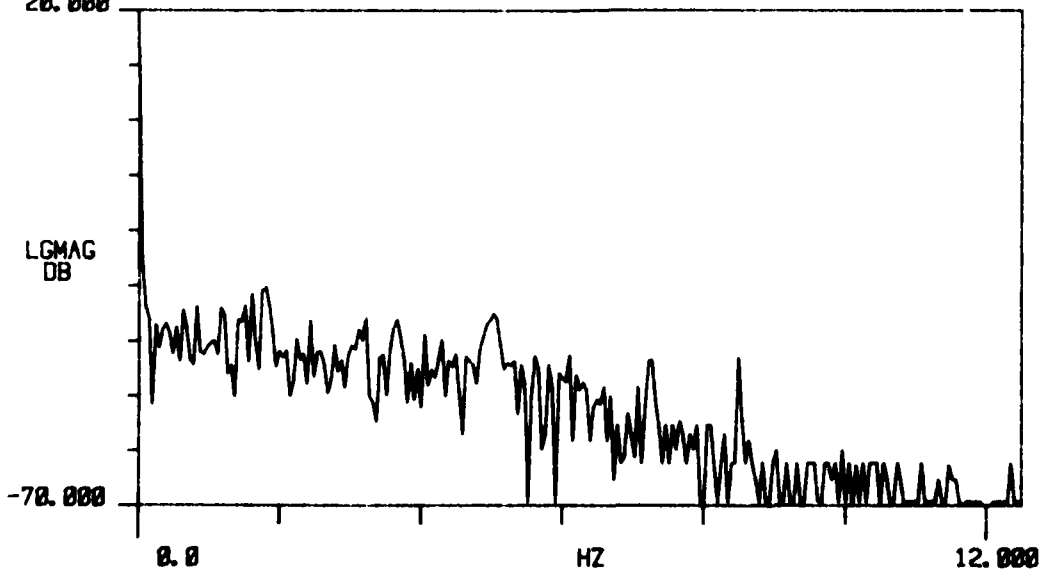


Figure D-1. Zenith Sky Measurement. 28 Feb 80

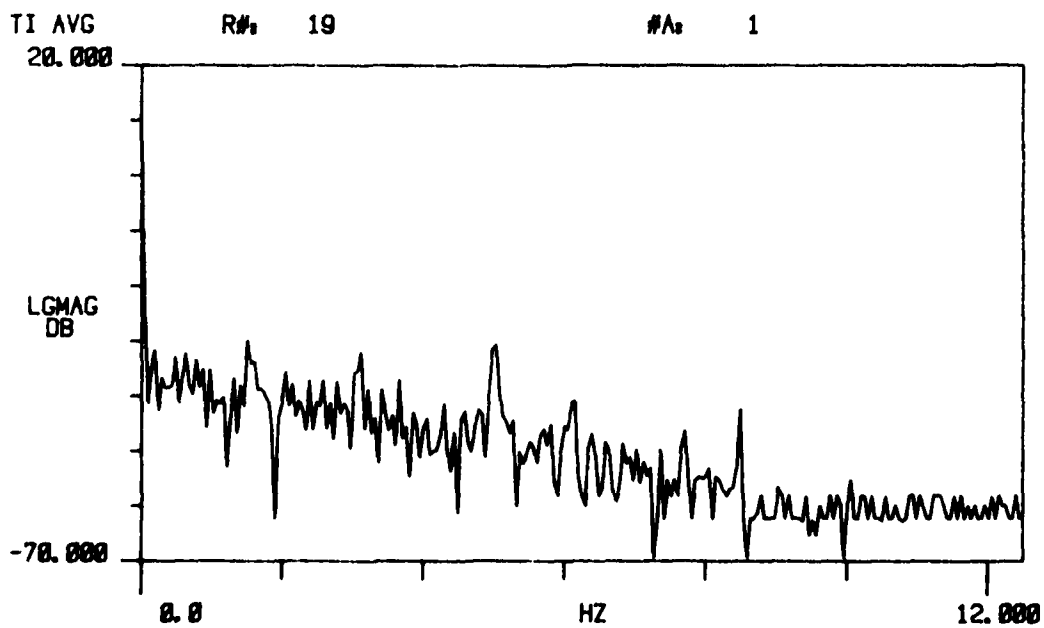
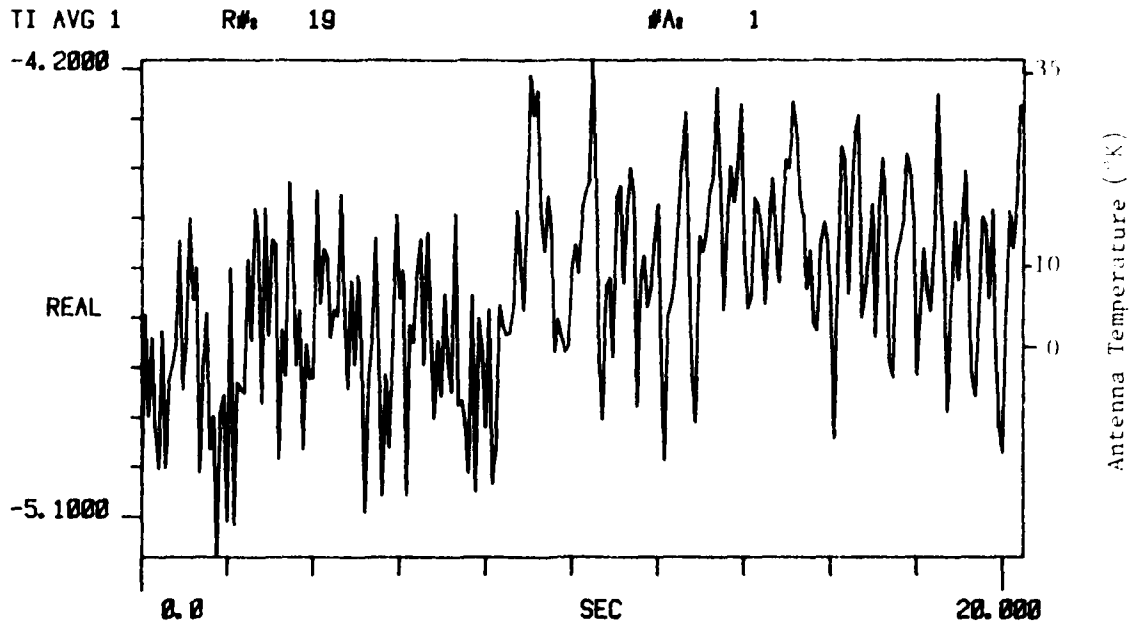


Figure D-1. Zenith Sky Measurement. 28 Feb 80

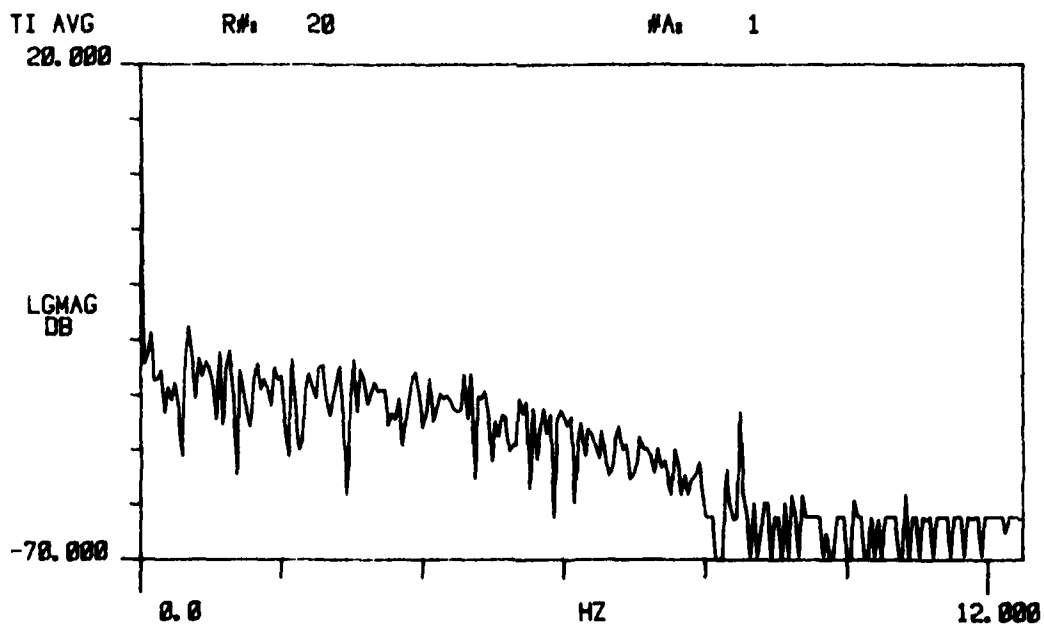
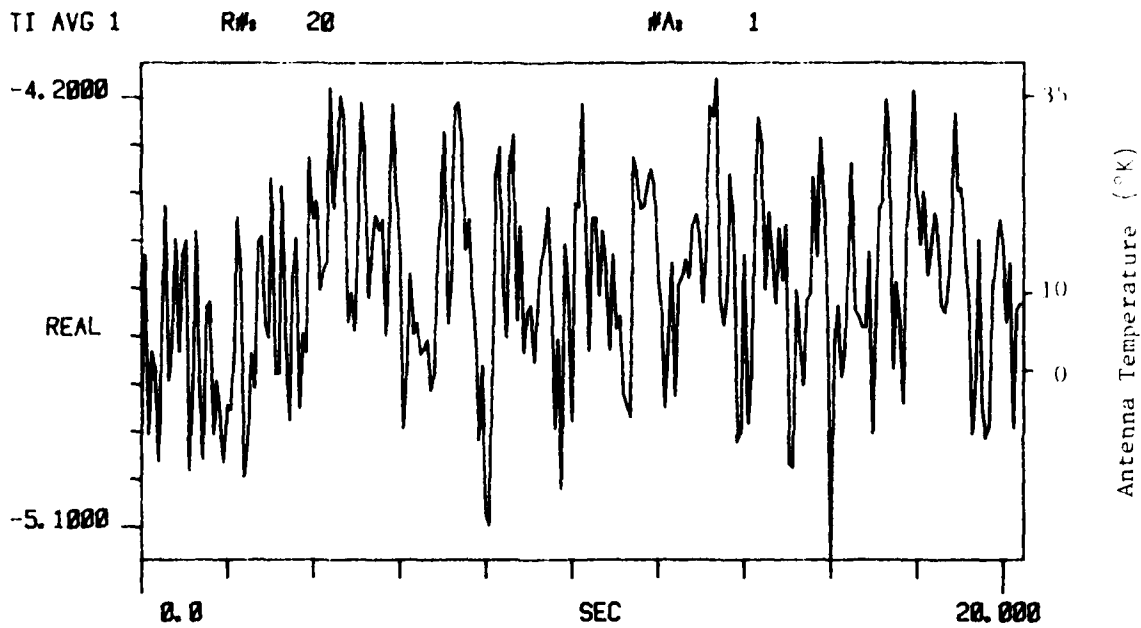
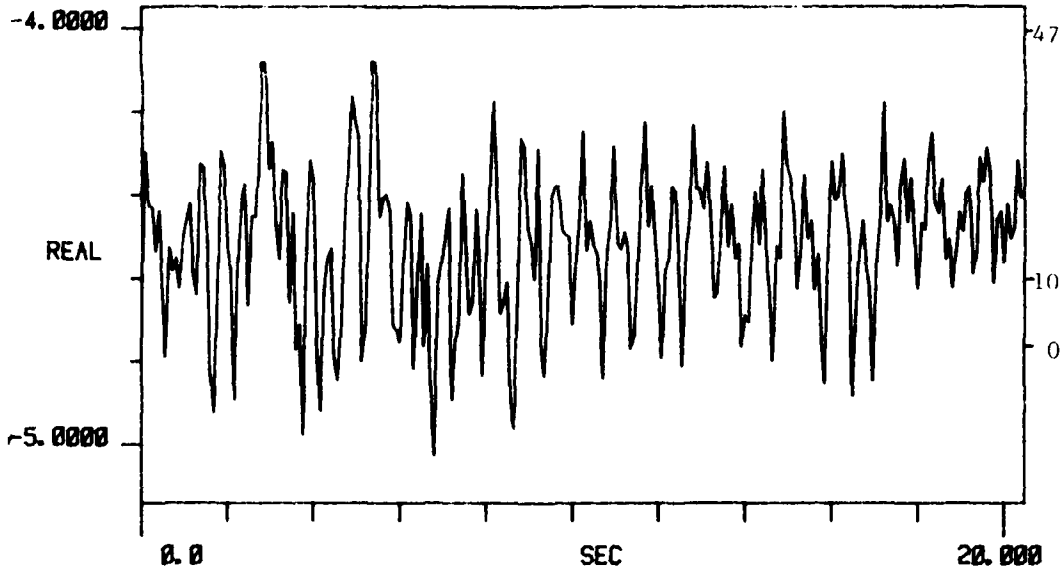


Figure D-1. Zenith Sky Measurement. 28 Feb 80

TI AVG 1

R# 21

#A 1



TI AVG
20.000

R# 21

#A 1

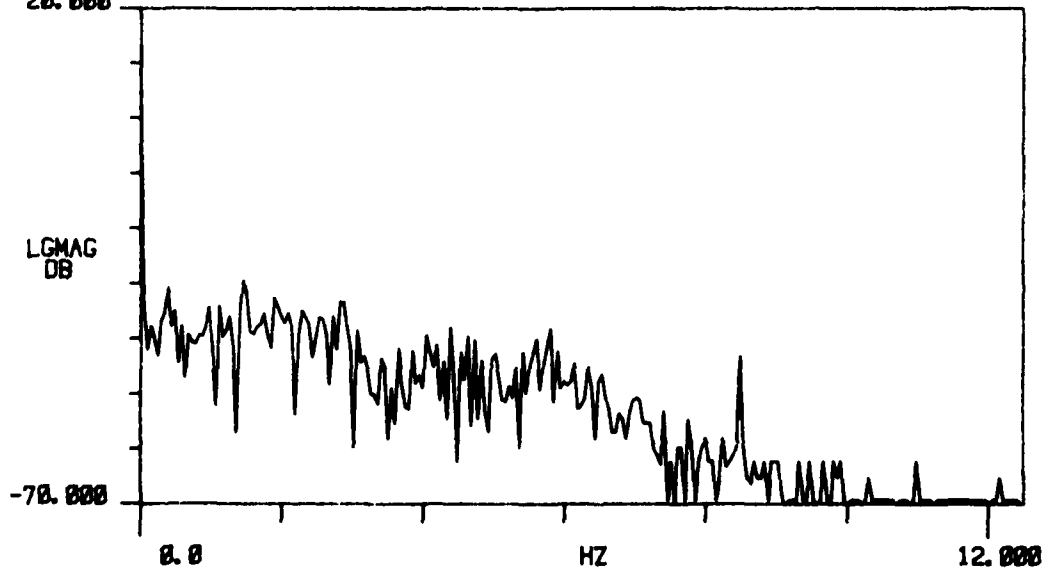
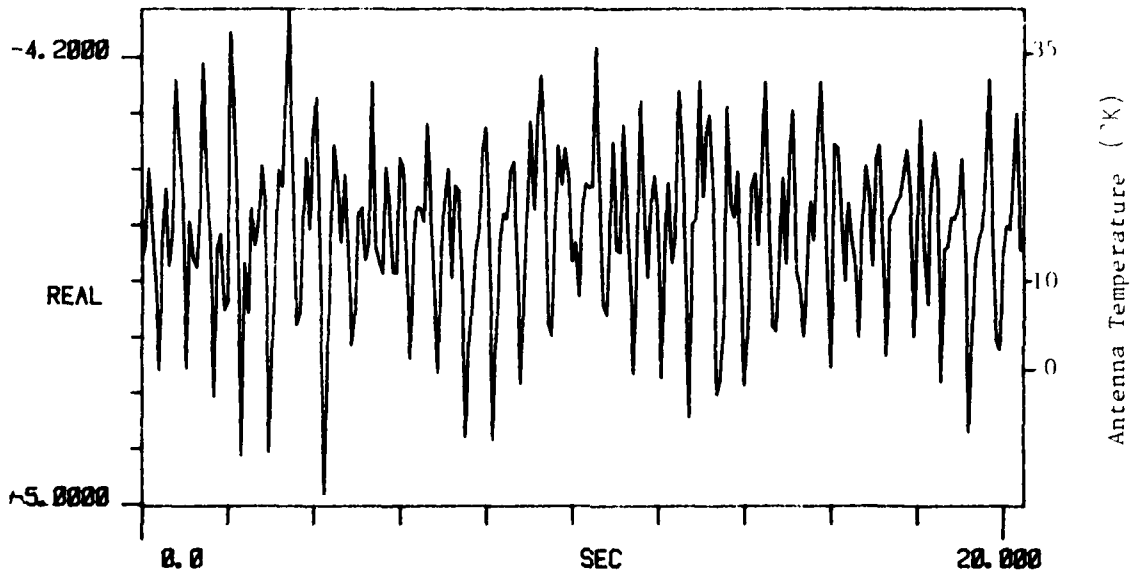


Figure D-1. Zenith Sky Measurement. 28 Feb 80

TI AVG 1

R# 23

#A 1



TI AVG
20.000

R# 23

#A 1

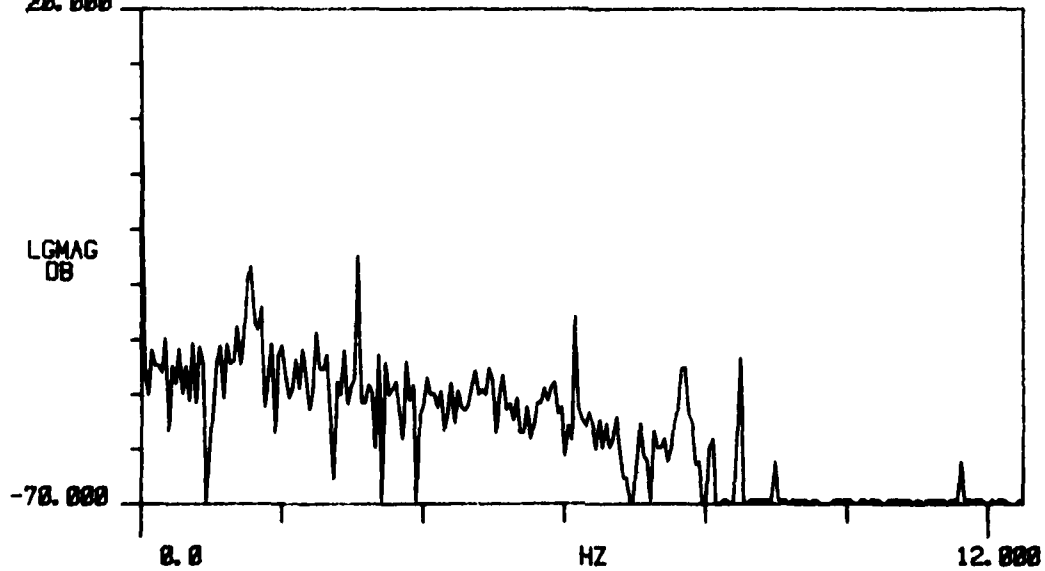
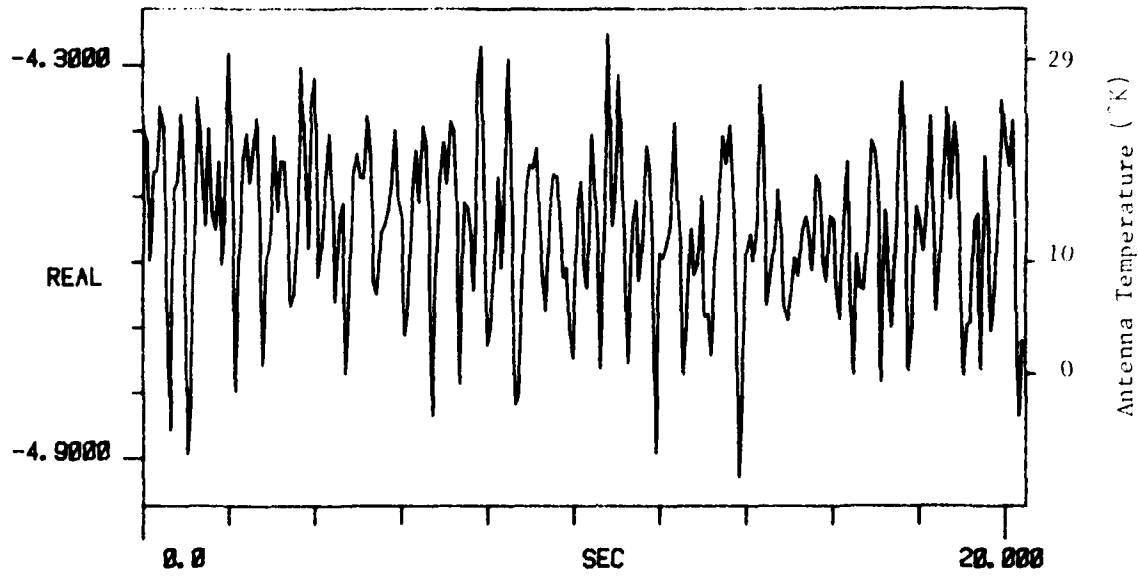


Figure D-1. Zenith Sky Measurement. 28 Feb 80

TI AVG 1

R# 24

#A 1



TI AVG
20.000

R# 24

#A 1

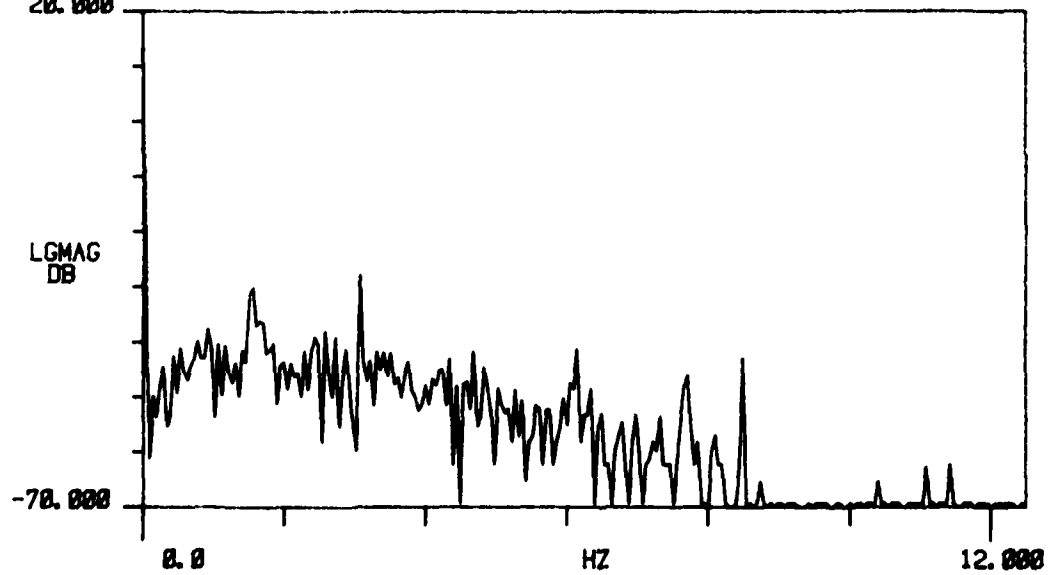
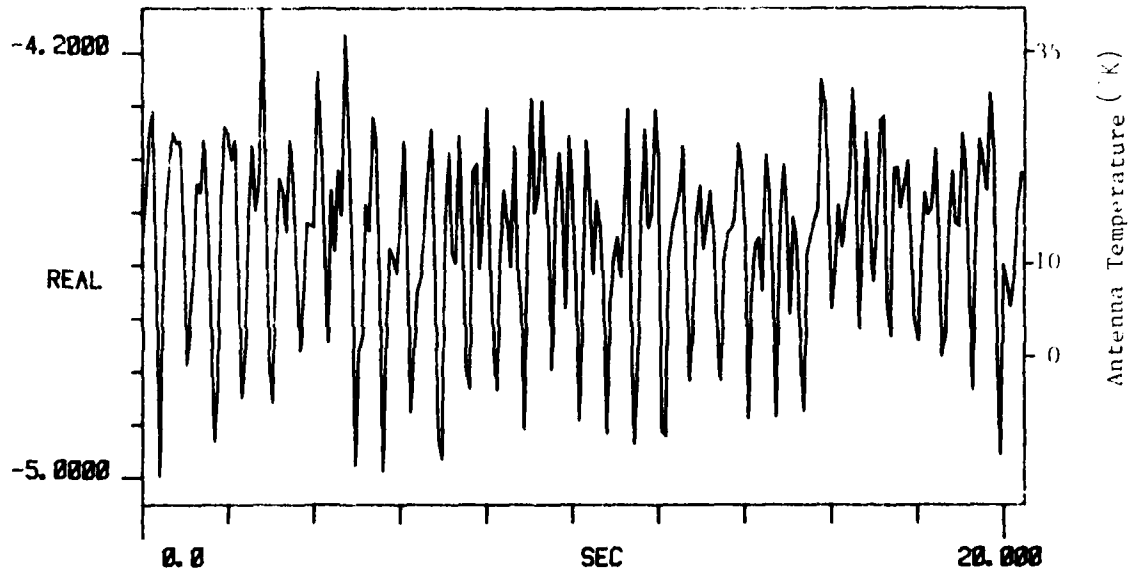


Figure D-1. Zenith Sky Measurement. 28 Feb 80

TI AVG 1

R# 25

#A 1



TI AVG
20.000

R# 25

#A 1

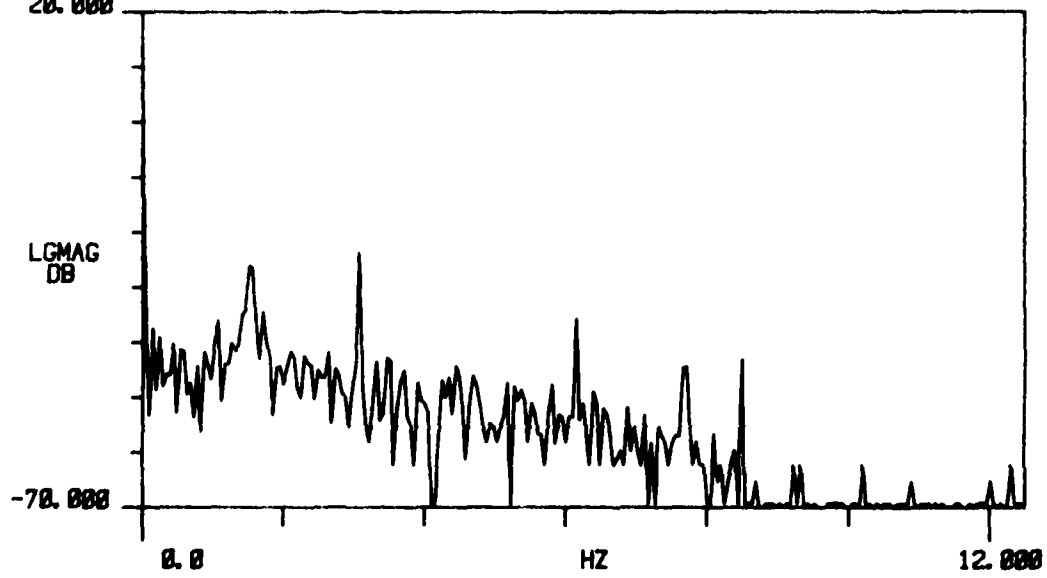
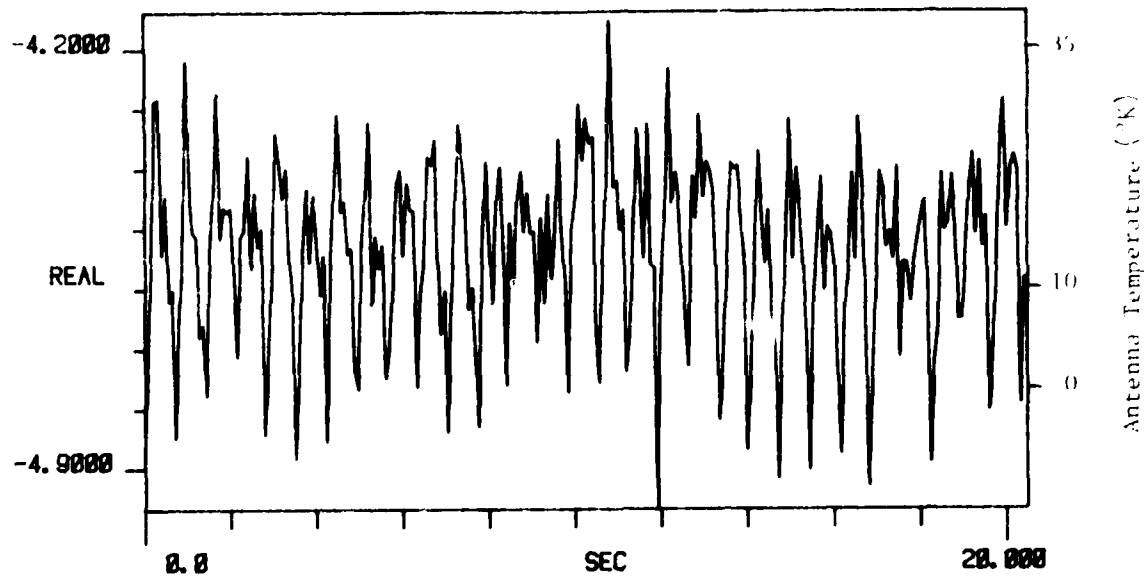


Figure D-1. Zenith Sky Measurement. 28 Feb 80

TI AVG 1

R# 26

#A 1



TI AVG 1
20.000

R# 26

#A 1

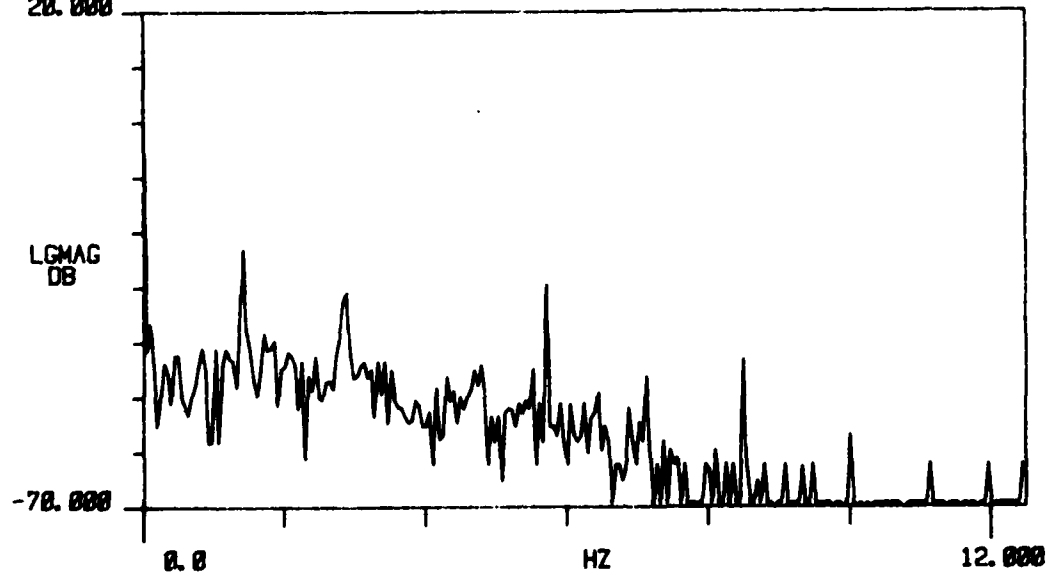
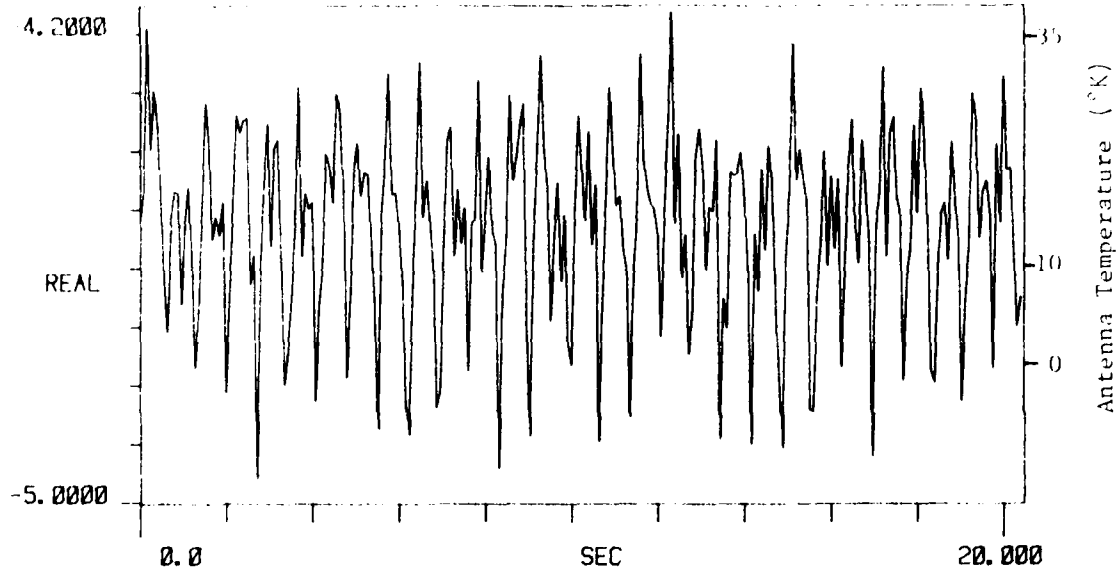


Figure D-1. Zenith Sky Measurement. 28 Feb 80

TI AVG 1

R#: 27

#A: 1



TI AVG
20.000

R#: 27

#A: 1

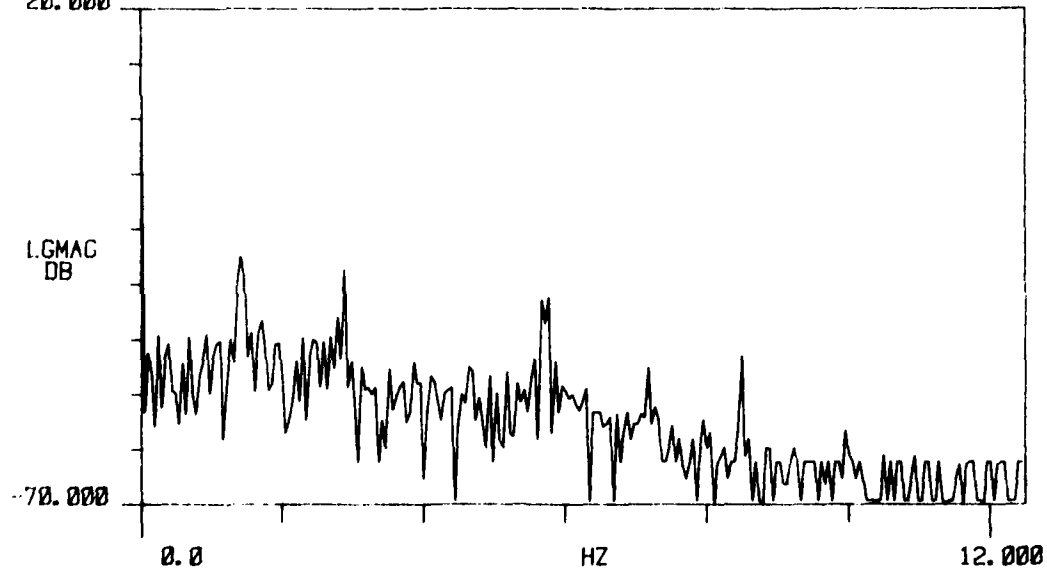


Figure D-1. Zenith Sky Measurement. 28 Feb 80

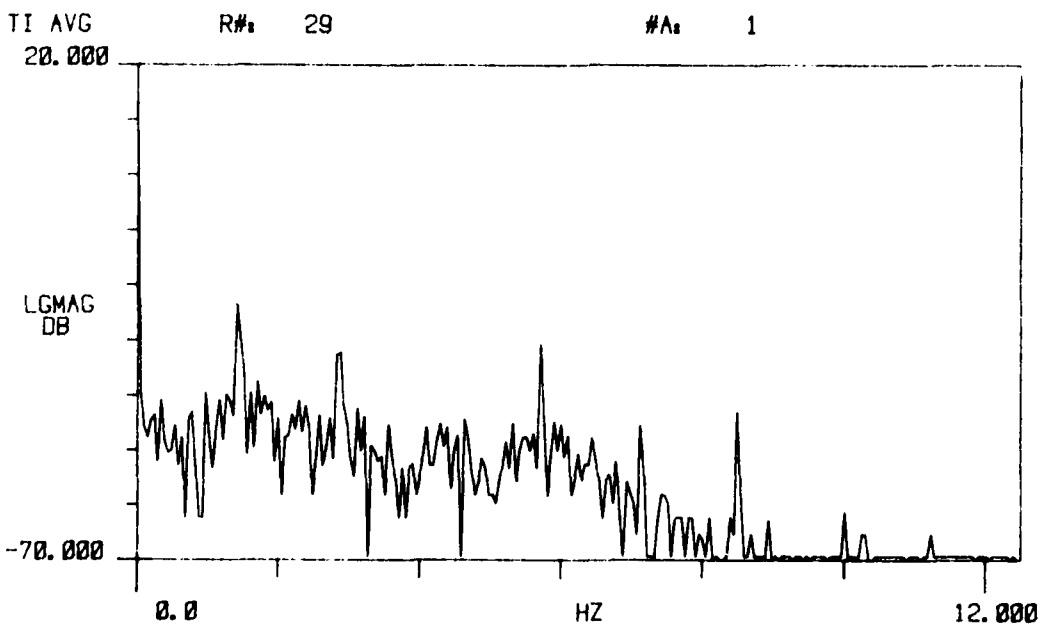
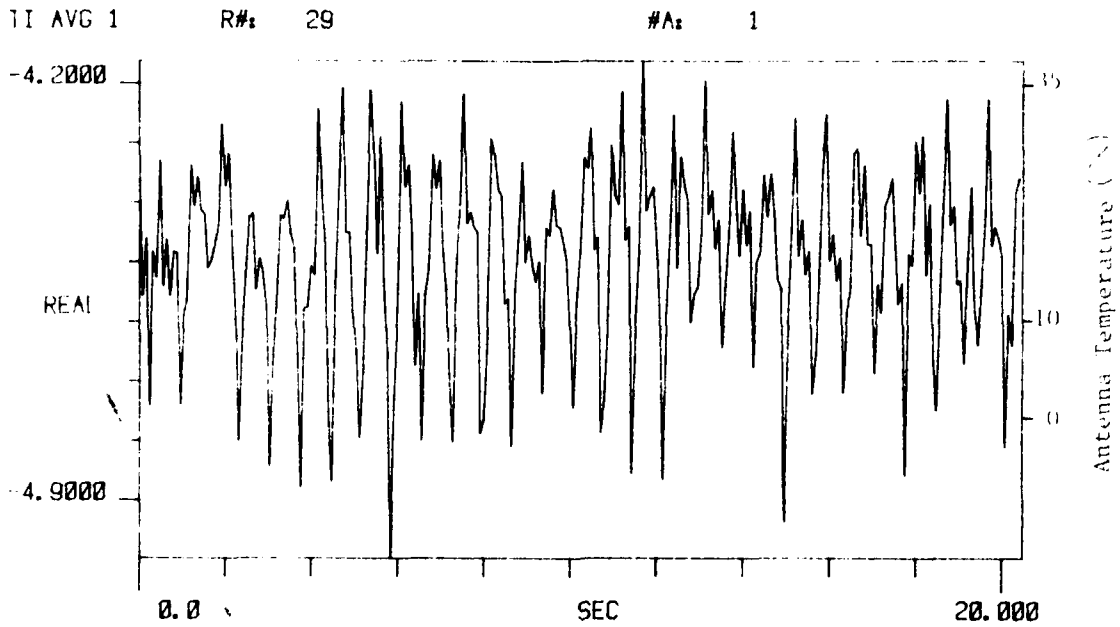
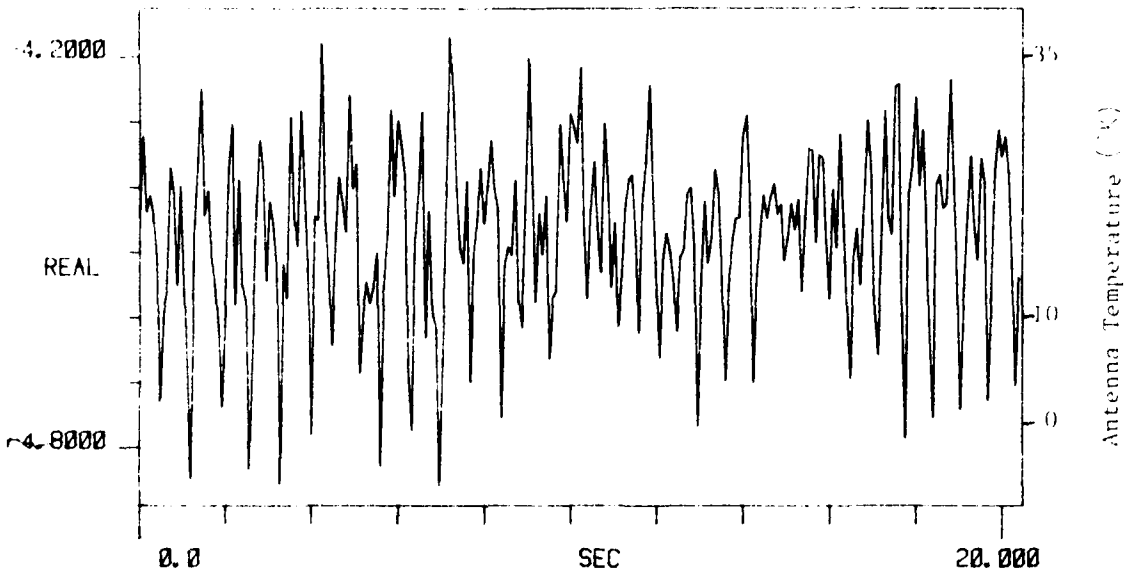


Figure D-1. Zenith Sky Measurement. 28 Feb 80

TI AVG 1

R# 30

#A 1



TI AVG
20.000

R# 30

#A 1

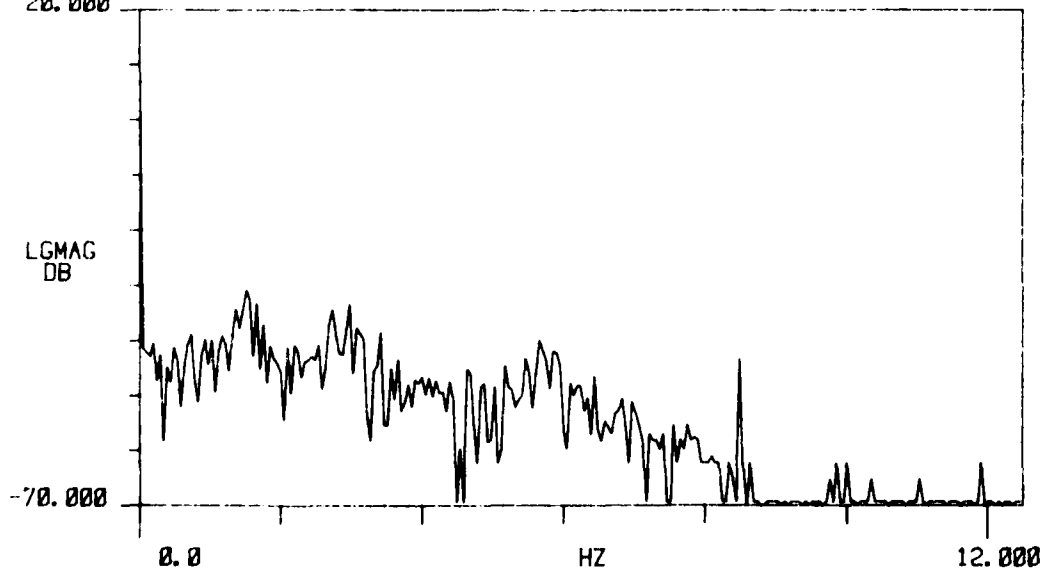
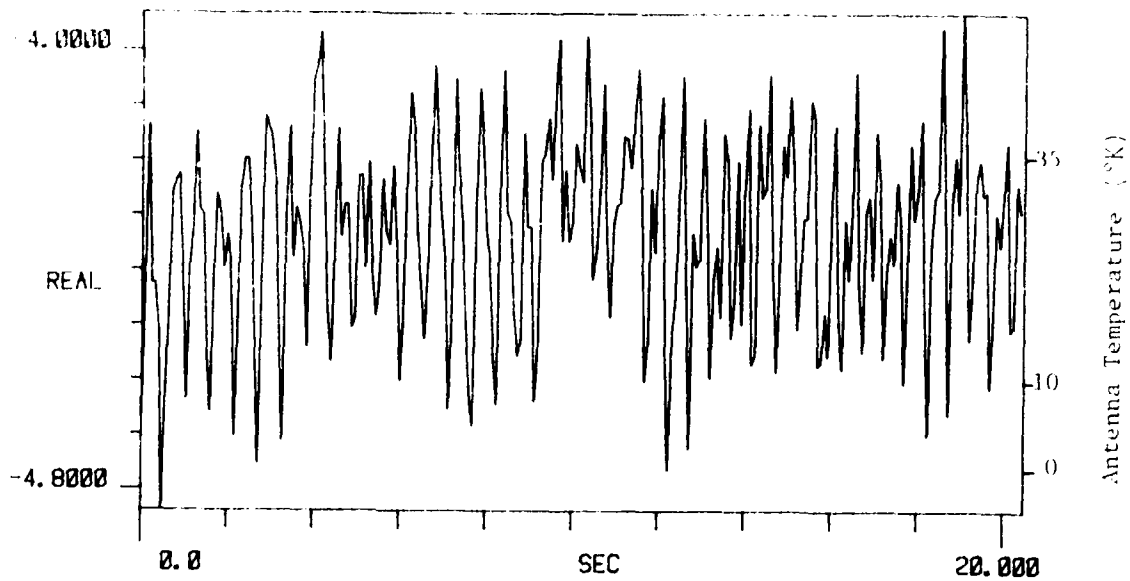


Figure D-1. Zenith Sky Measurement. 28 Feb 80

TI AVG 1

R# 34

#A 1



TI AVG

R# 34

#A 1

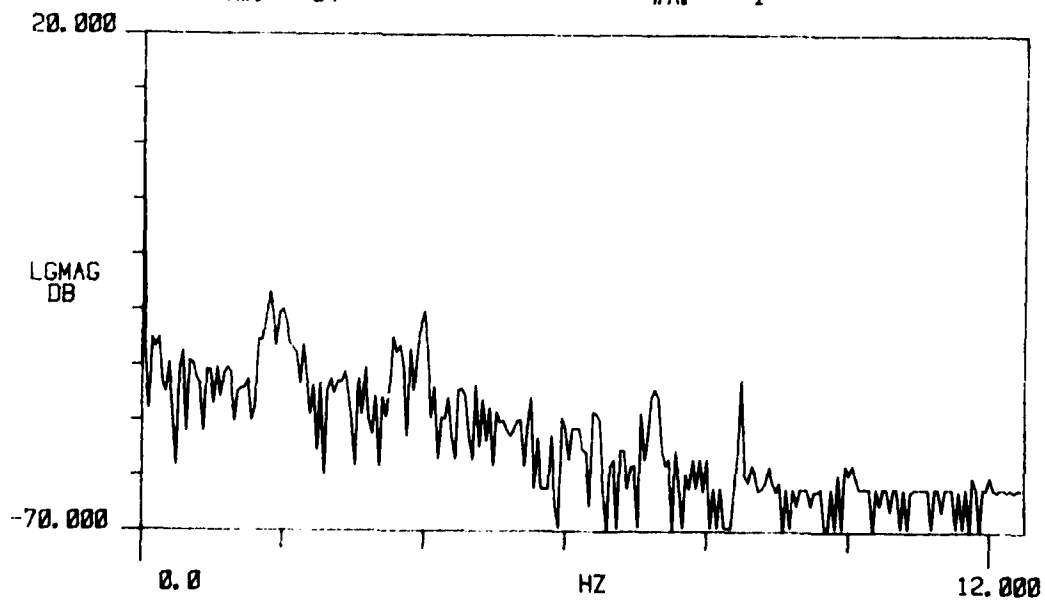


Figure D-1. Zenith Sky Measurement. 28 Feb 80

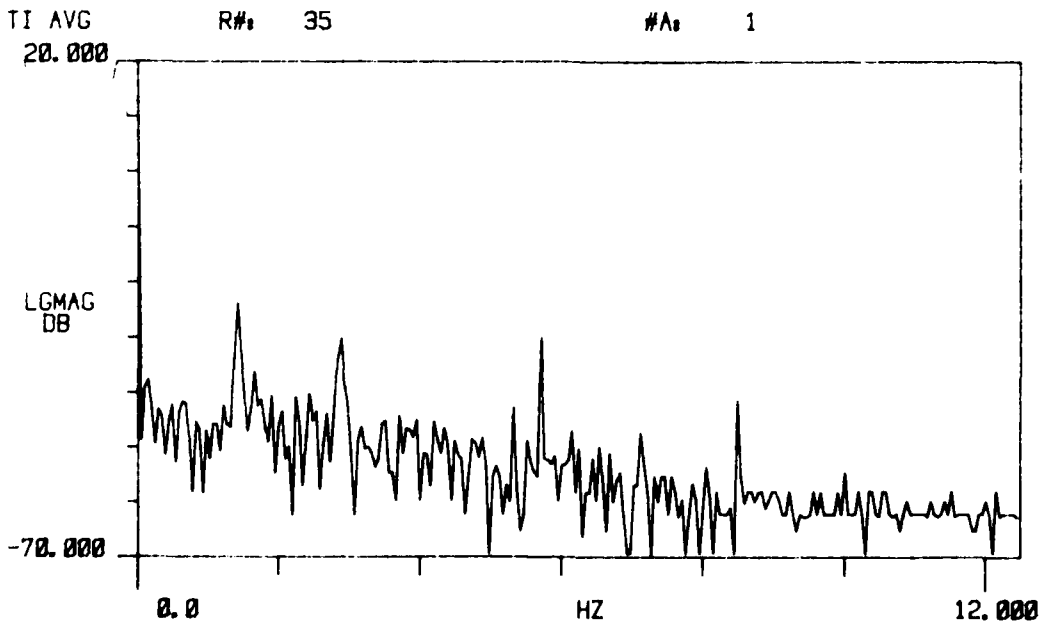
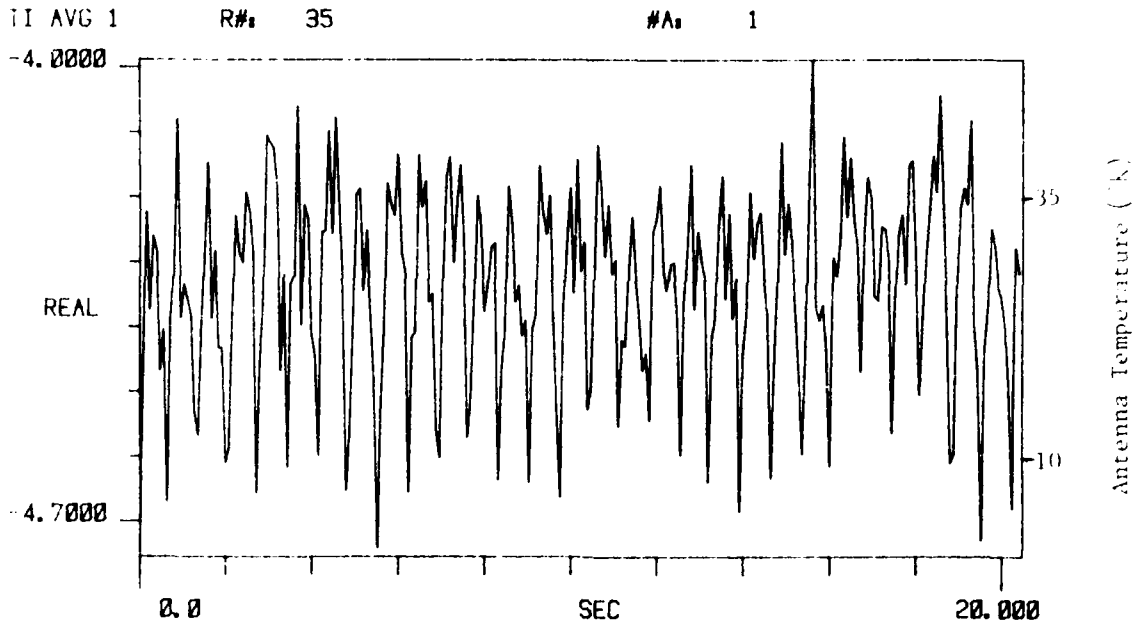


Figure D-1. Zenith Sky Measurement. 28 Feb 80

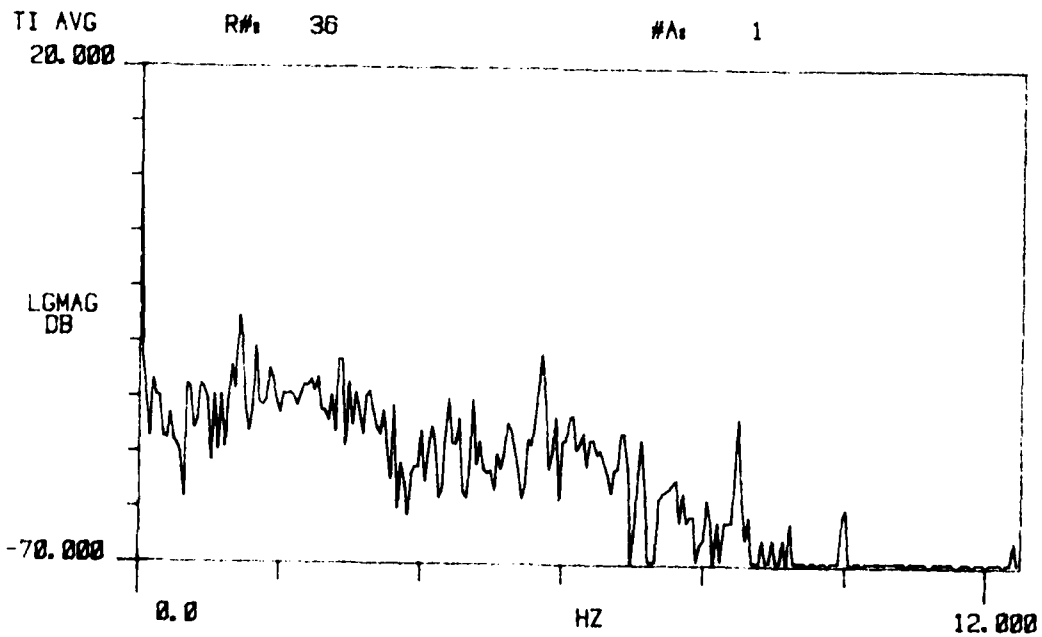
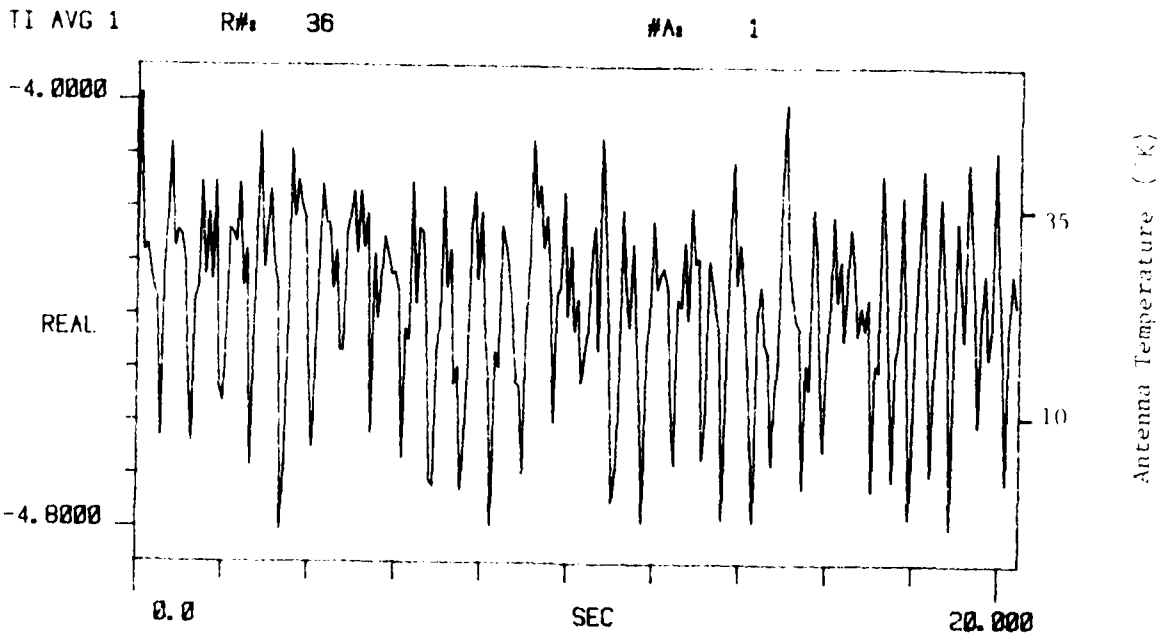


Figure D-1. Zenith Sky Measurement. 28 Feb 80

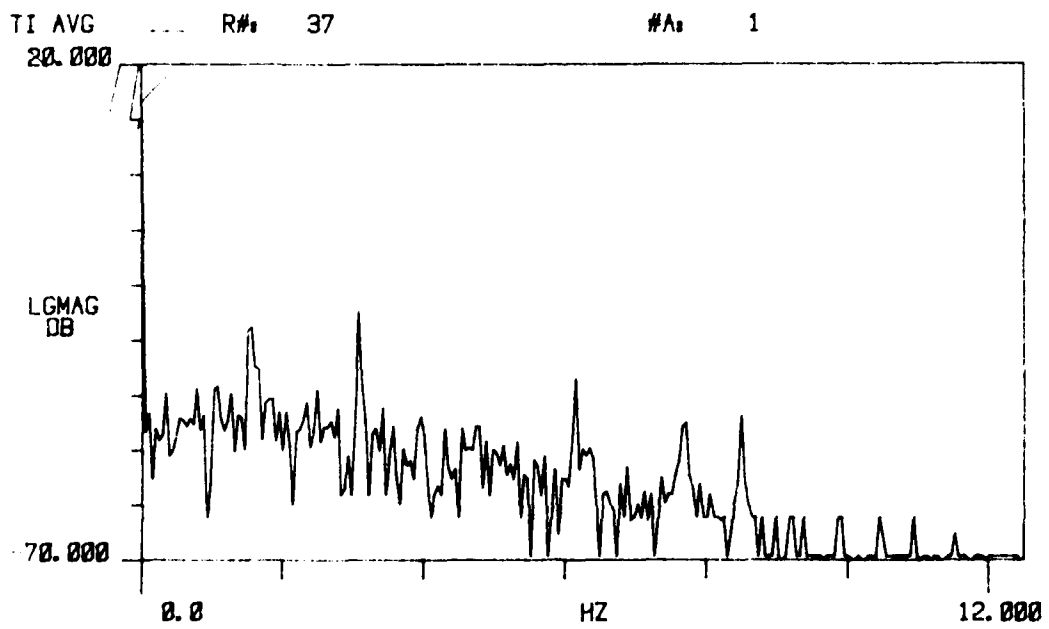
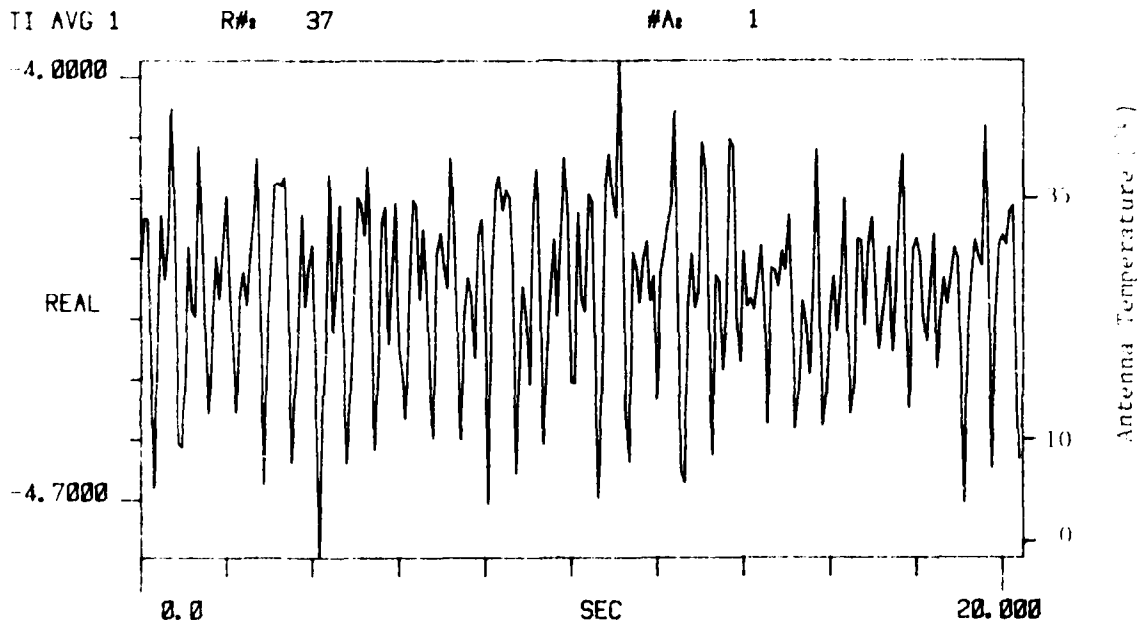


Figure D-1. Zenith Sky Measurement. 28 Feb 80

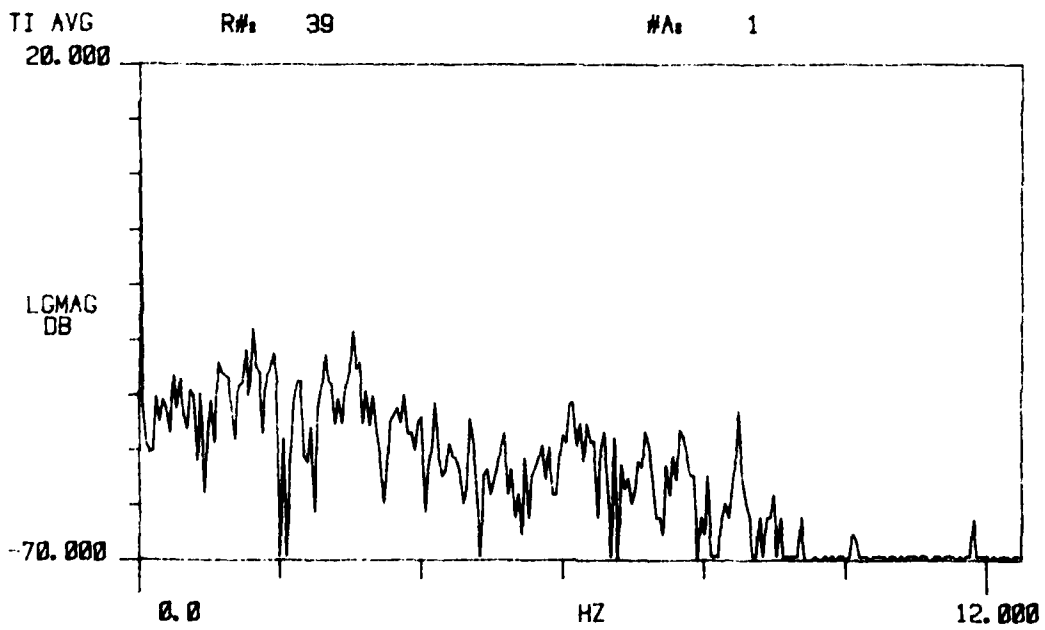
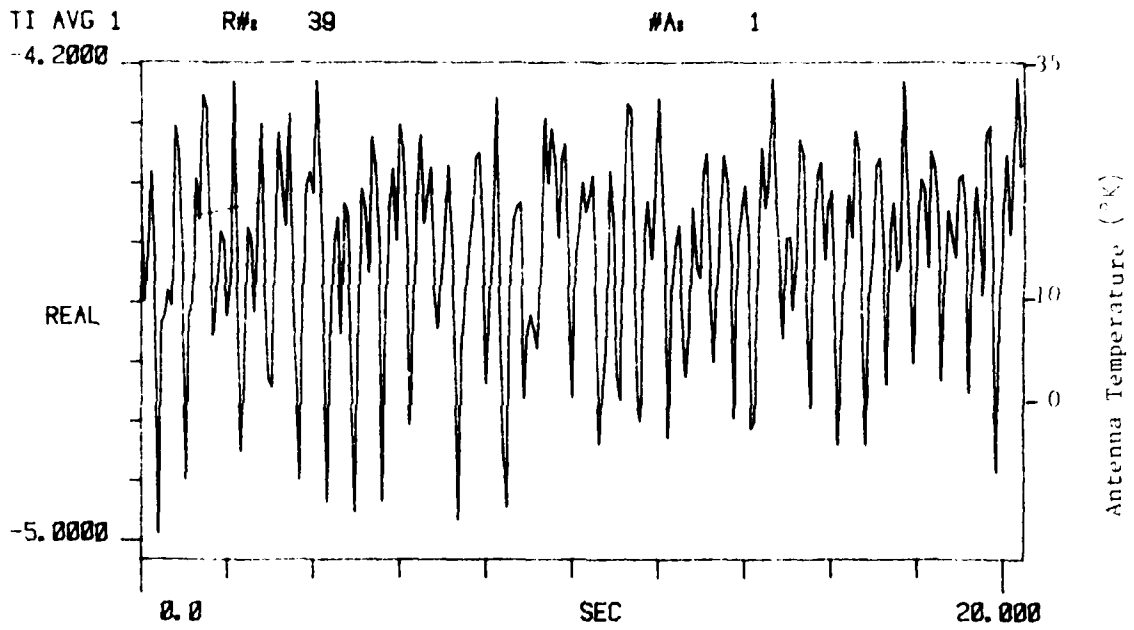
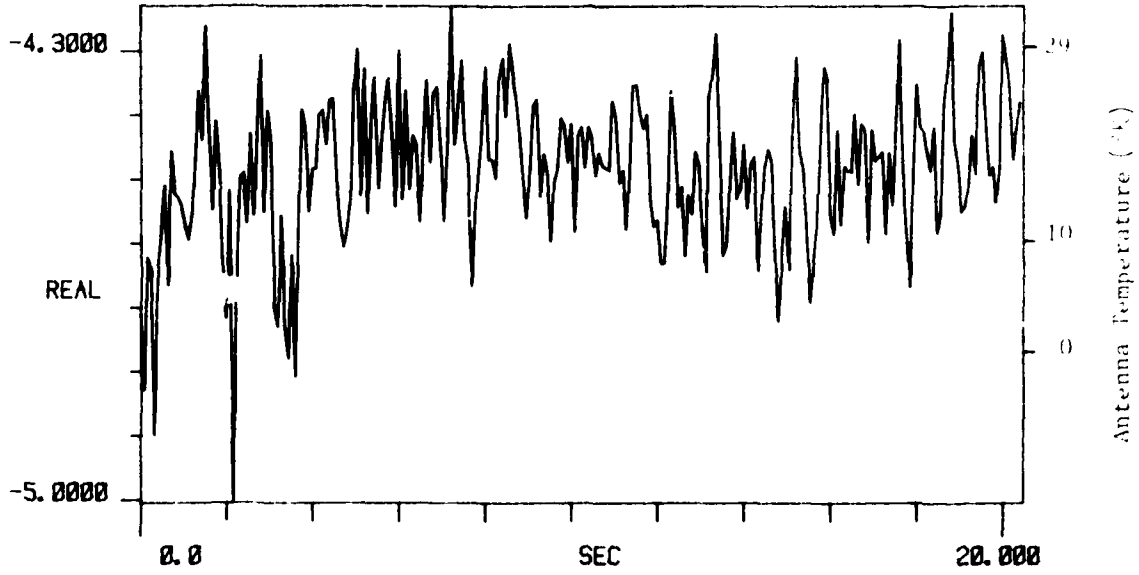


Figure D-1. Zenith Sky Measurement. 28 Feb 80

TI AVG 1

R# 40

#A 1



II AVG 1

R# 40

#A 1

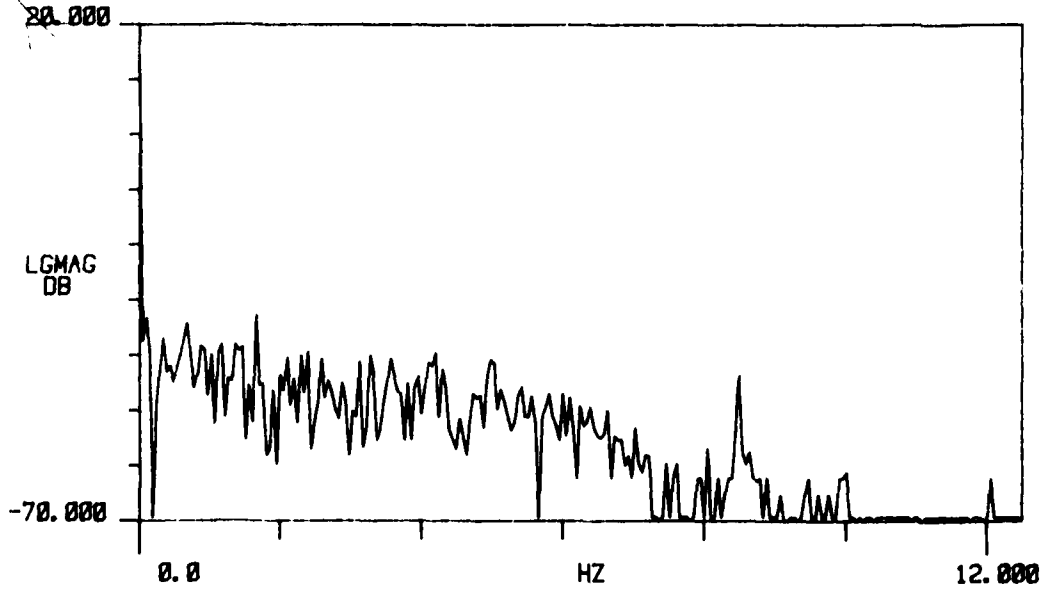


Figure D-1. Zenith Sky Measurement. 28 Feb 80

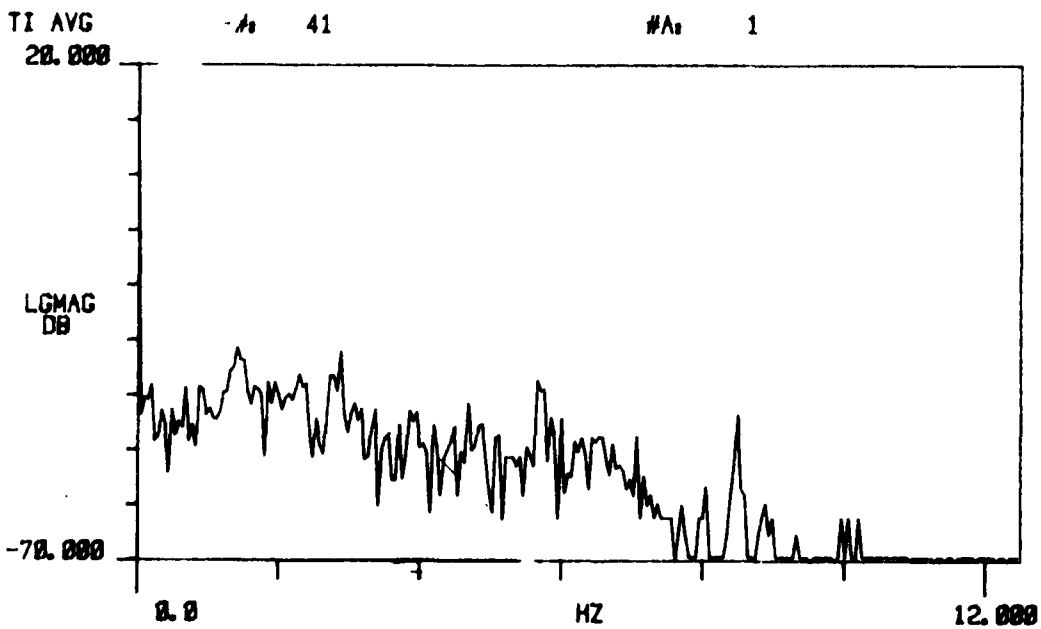
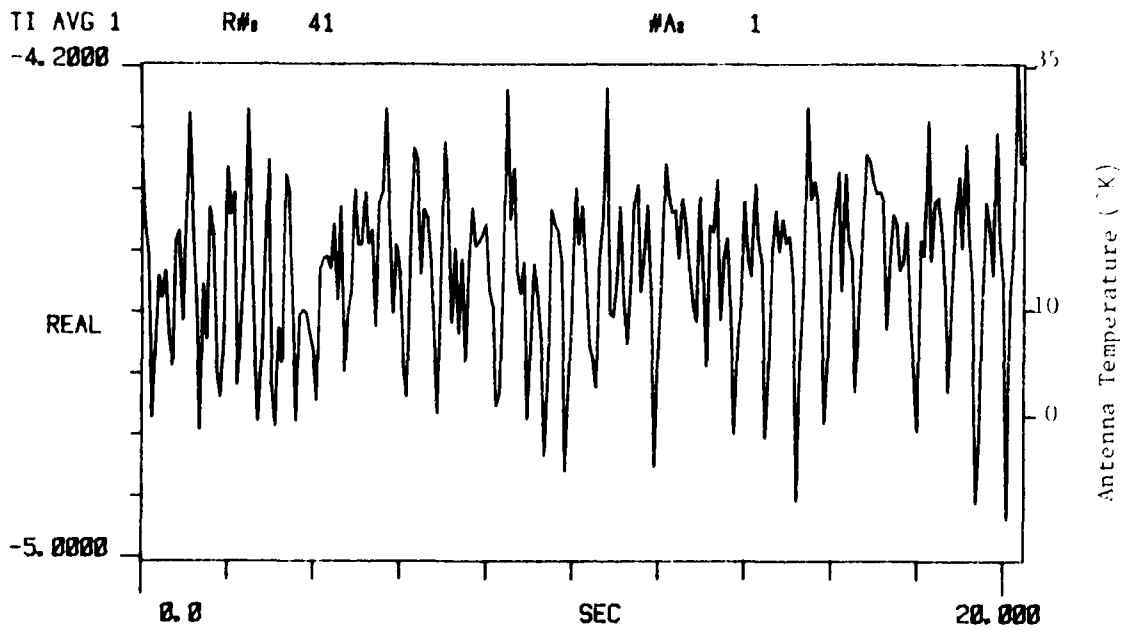
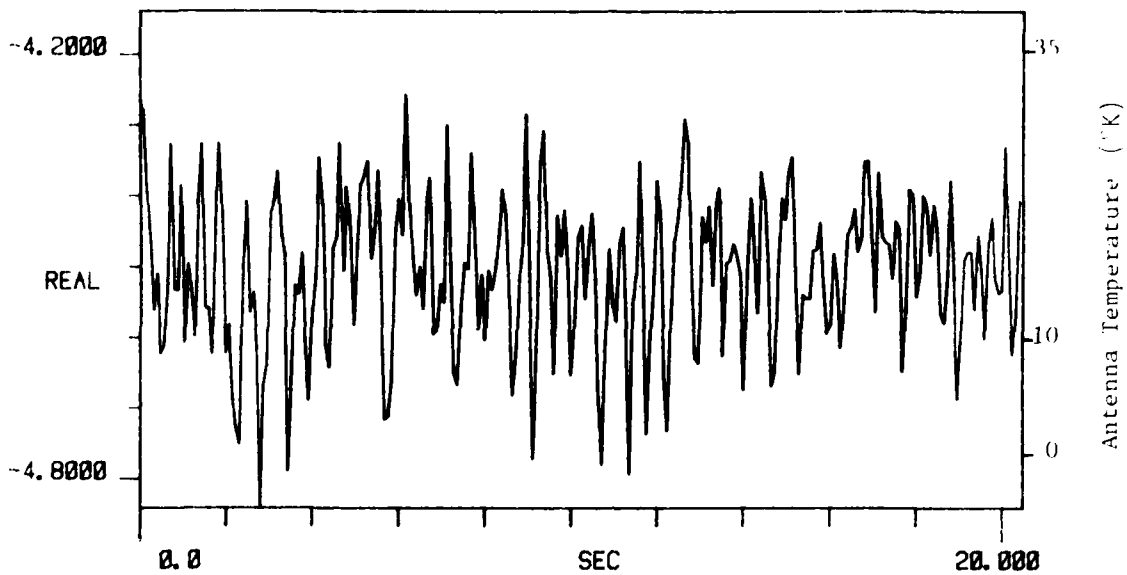


Figure D-1. Zenith Sky Measurement. 28 Feb 80

TI AVG 1

R# 42

#A 1



TI AVG 1

R# 42

#A 1

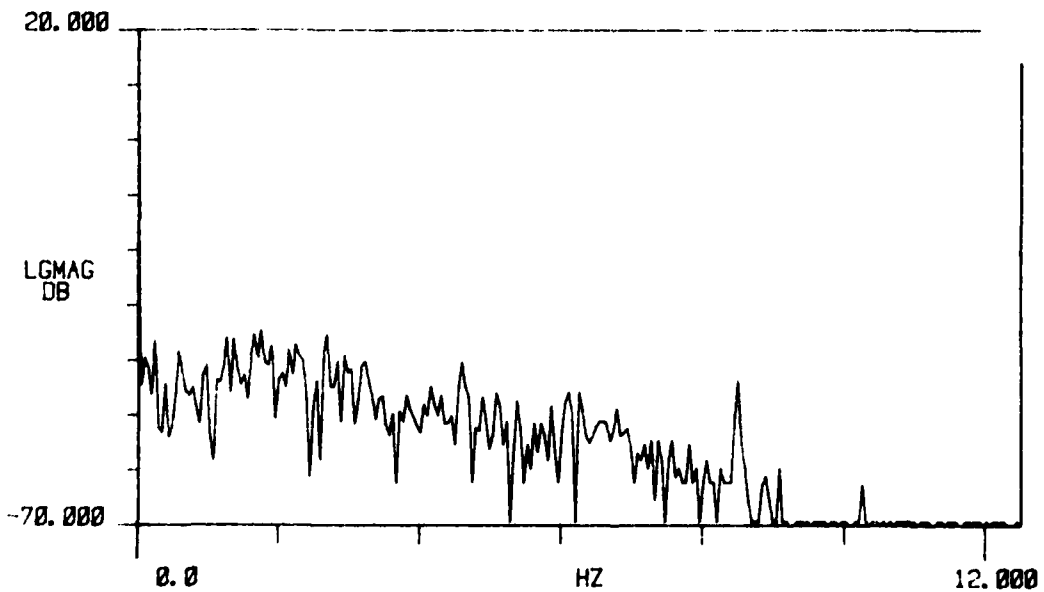
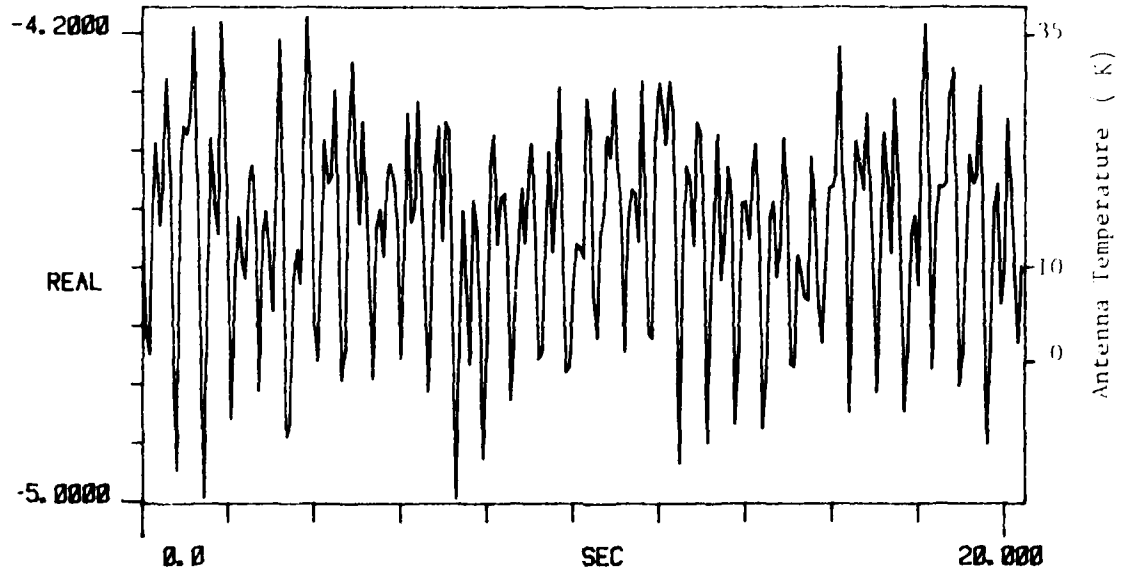


Figure D-1. Zenith Sky Measurement. 28 Feb 80

TI AVG 1

R# 43

#A 1



TI AVG

R# 43

#A 1

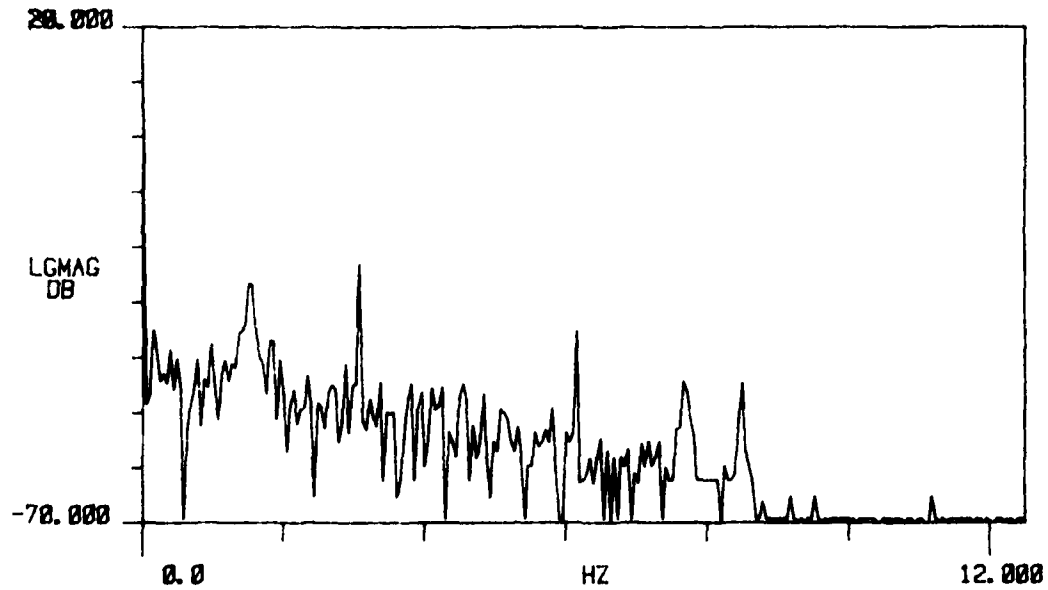


Figure D-1. Zenith Sky Measurement 28 Feb 80

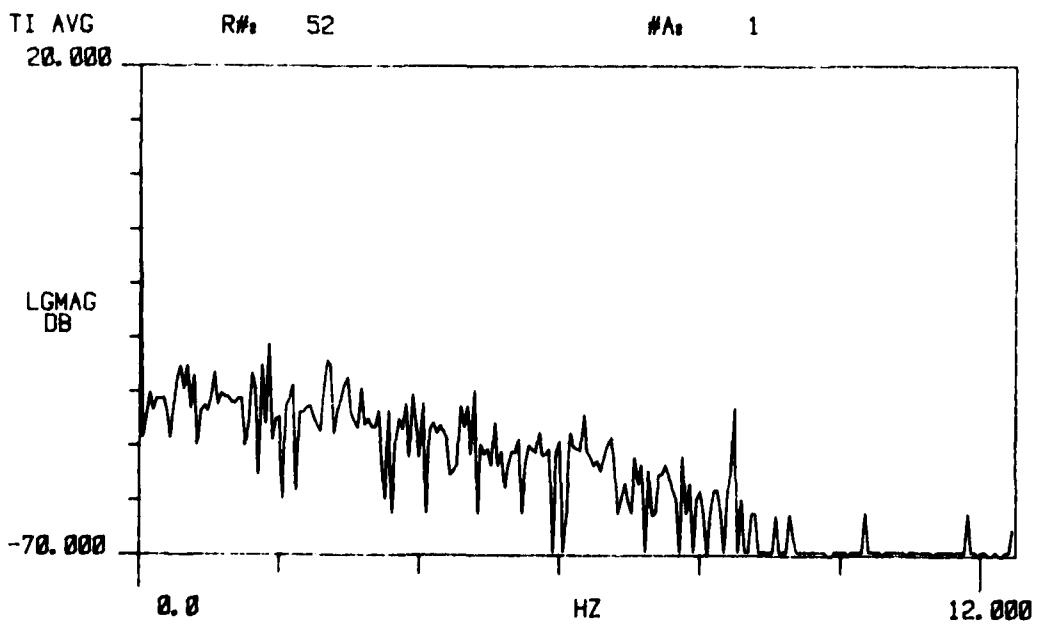
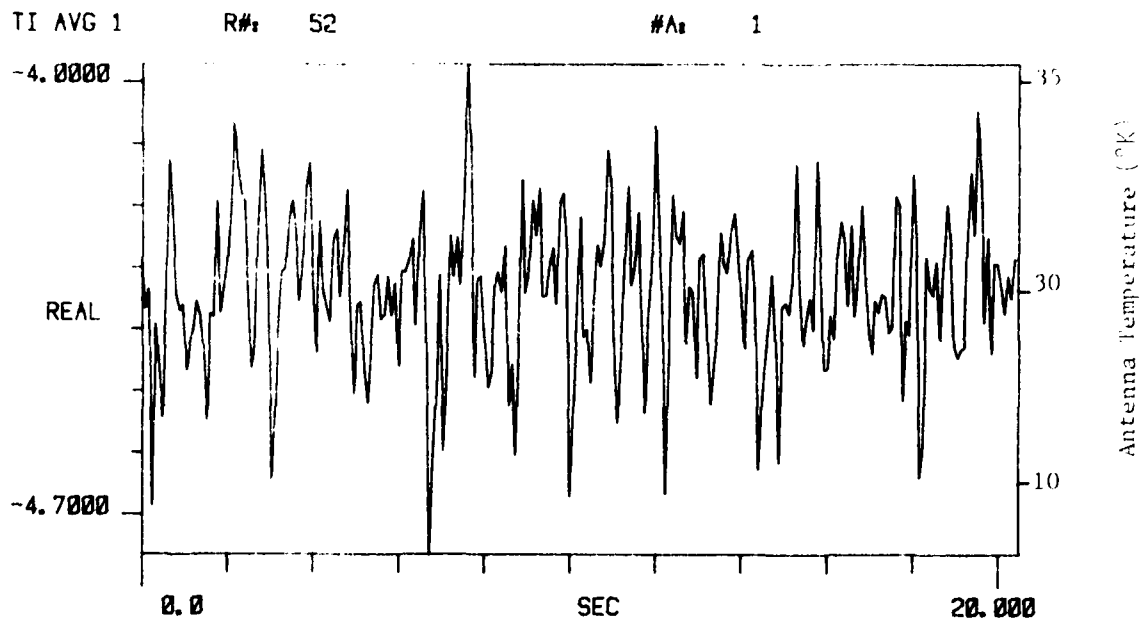
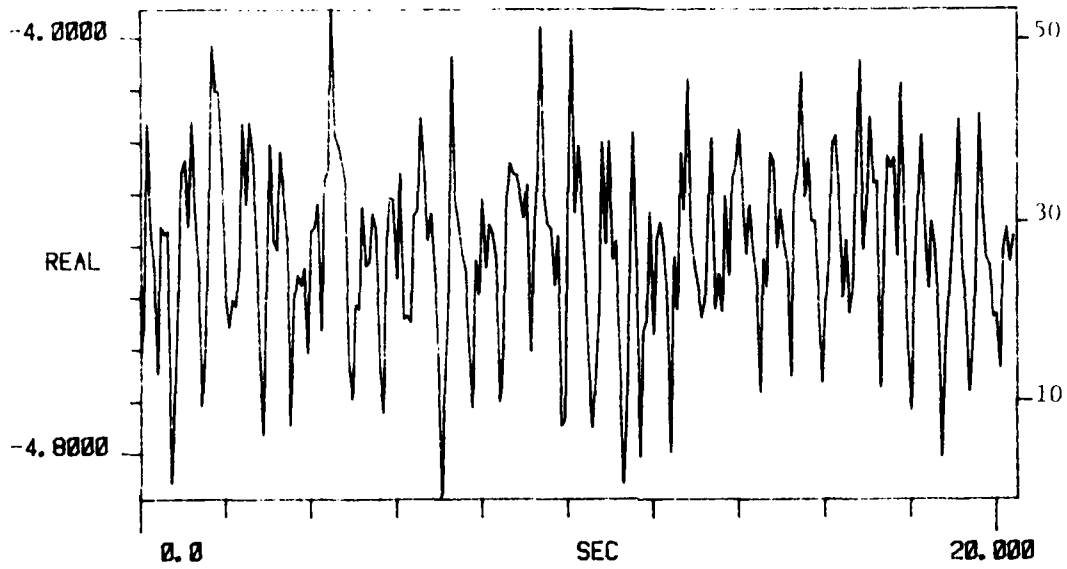


Figure D-1. Zenith Sky Measurement. 28 Feb 80
126

TI AVG 1

R# 53

#A 1



TI AVG 1
20.000

R# 53

#A 1

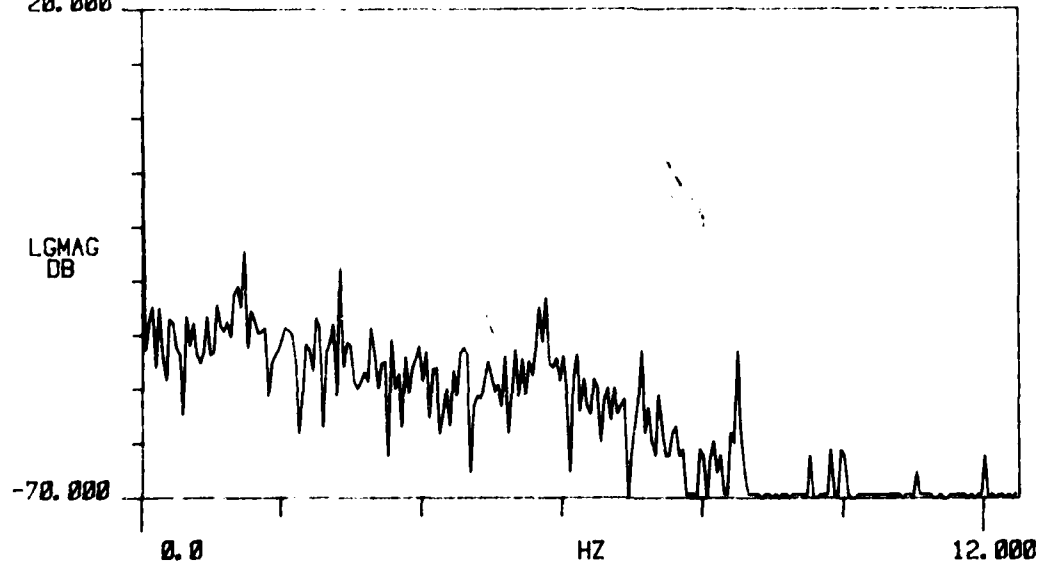
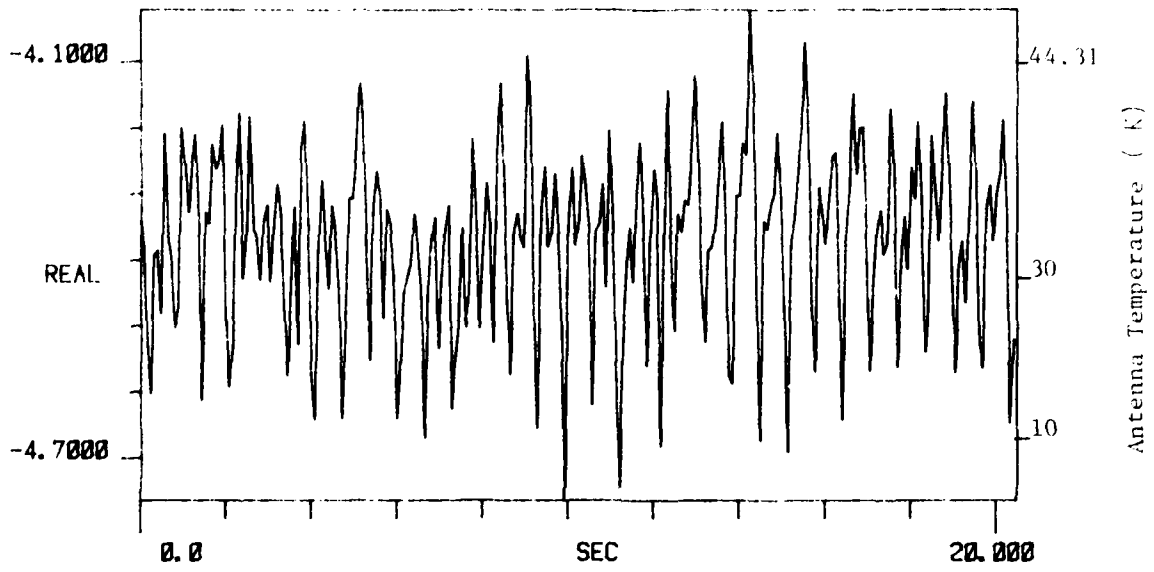


Figure D-1. Zenith Sky Measurement. 28 Feb 80

TI AVG 1

R# 54

#A 1



TI AVG
20.000

R# 54

#A 1

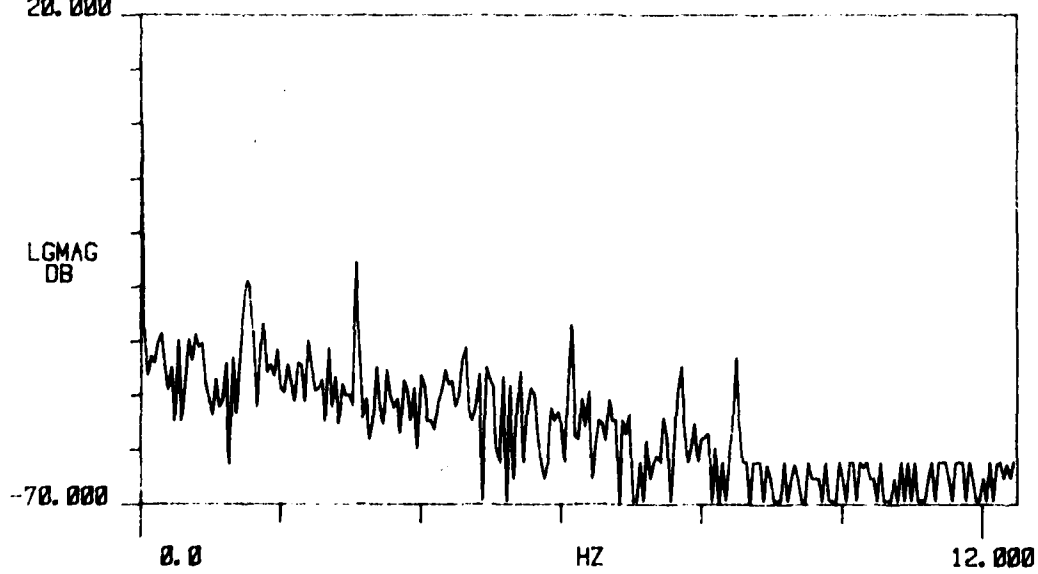
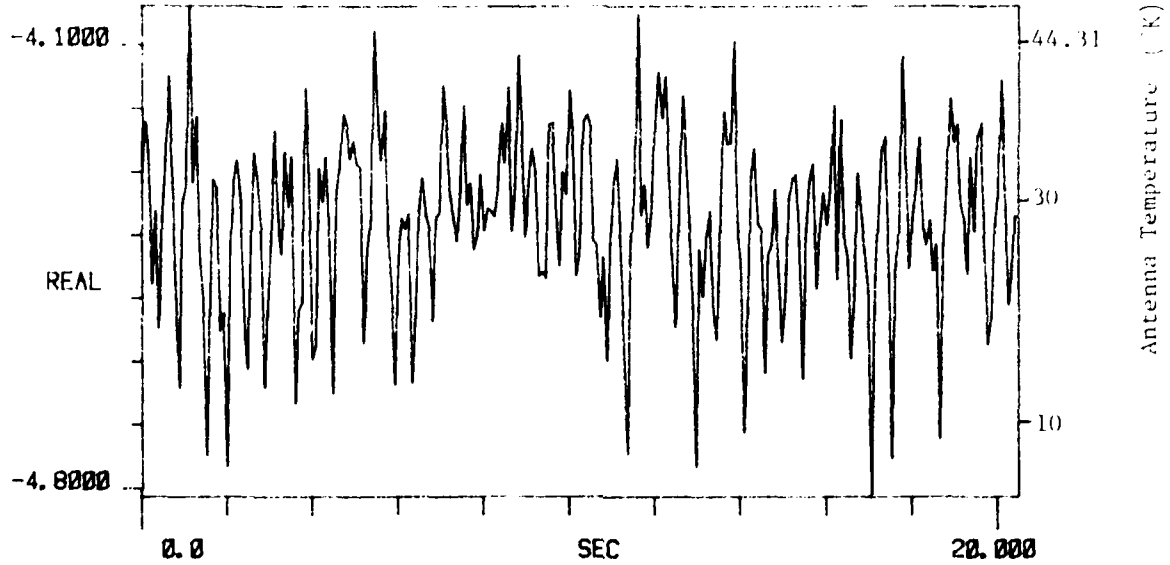


Figure D-1. Zenith Sky Measurement. 28 Feb 80
128

TI AVG 1

R# 55

#A 1



TI AVG
20.000

R# 55

#A 1

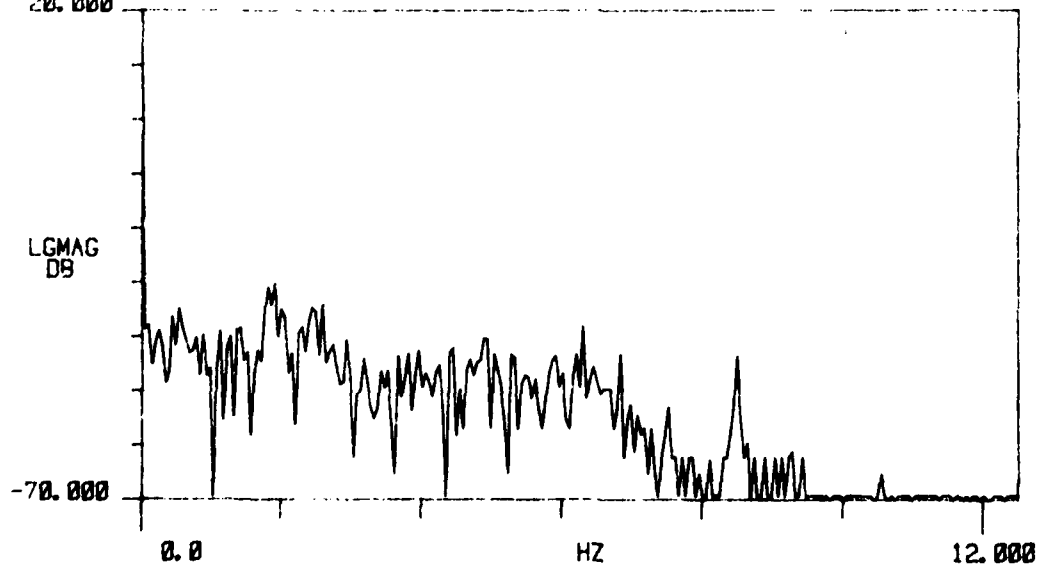


Figure D-1. Zenith Sky Measurement, 28 Feb 80
129

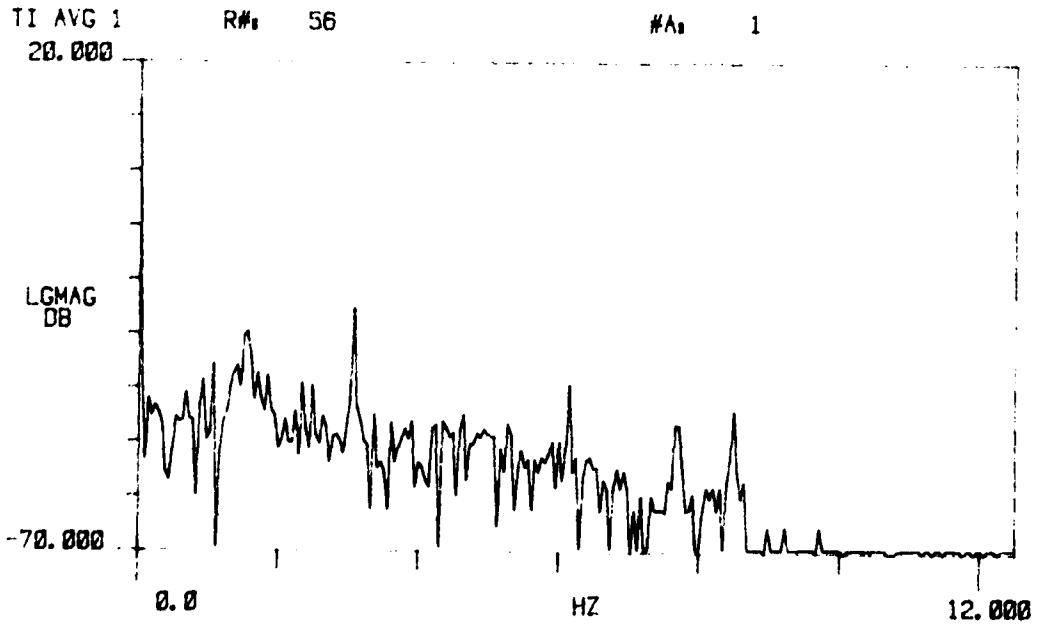
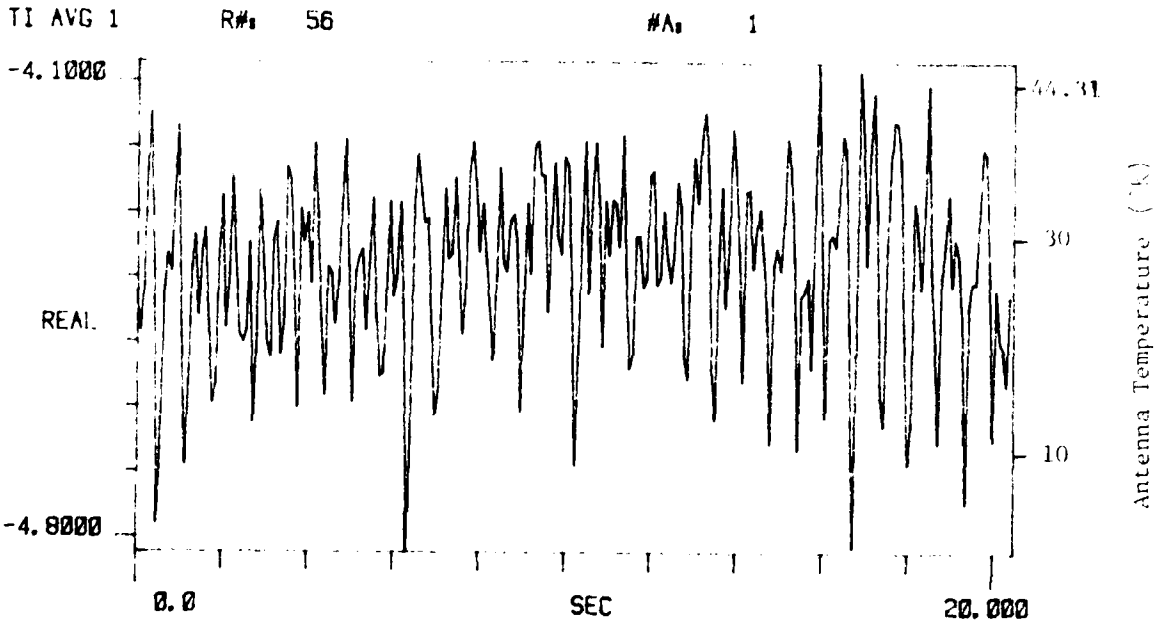
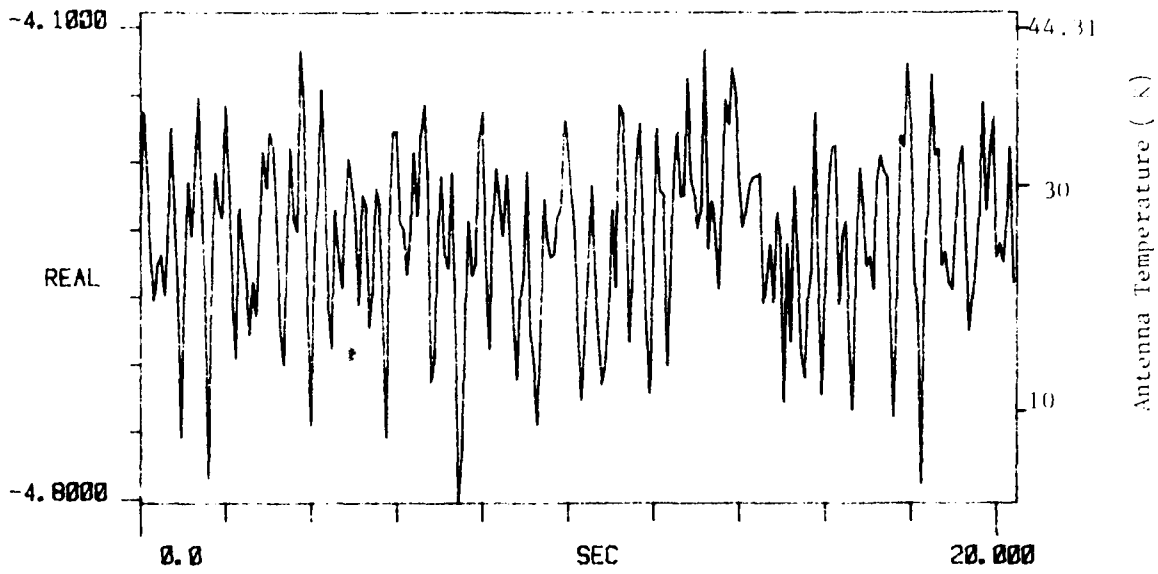


Figure D-1. Zenith Sky Measurement. 28 Feb 80
130

TI AVG 1

R# 58

#A 1



TI AVG

R# 58

#A 1

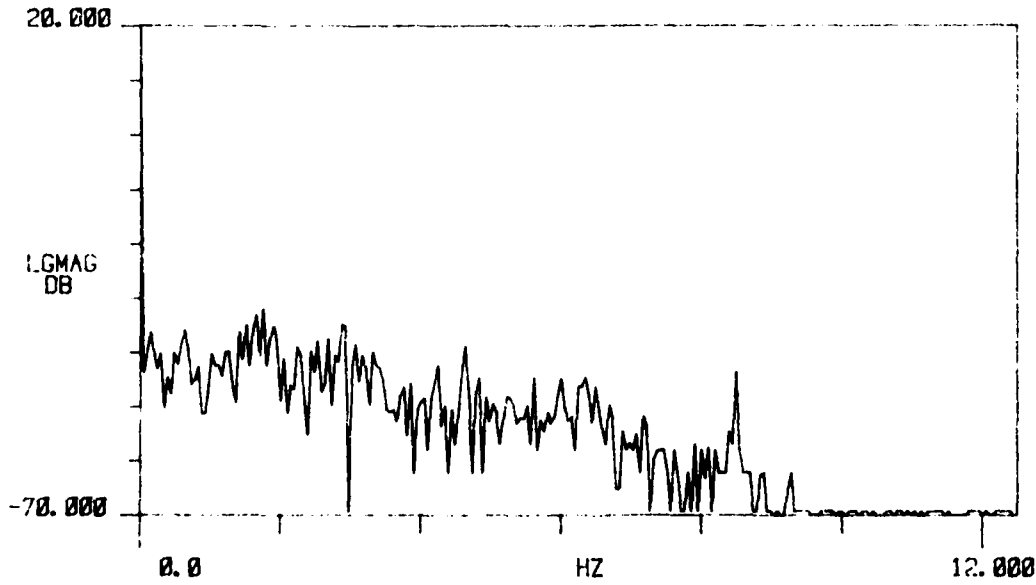
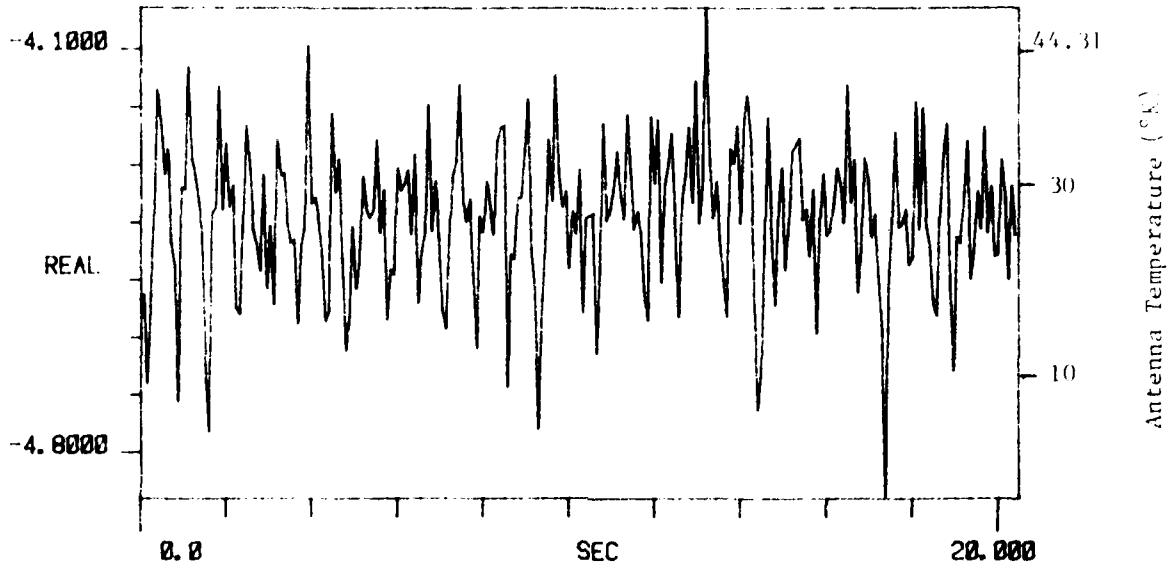


Figure D-1. Zenith Sky Measurement. 28 Feb 80
131

TI AVG 1

R# 59

#A 1



TI AVG
20.000

R# 59

#A 1

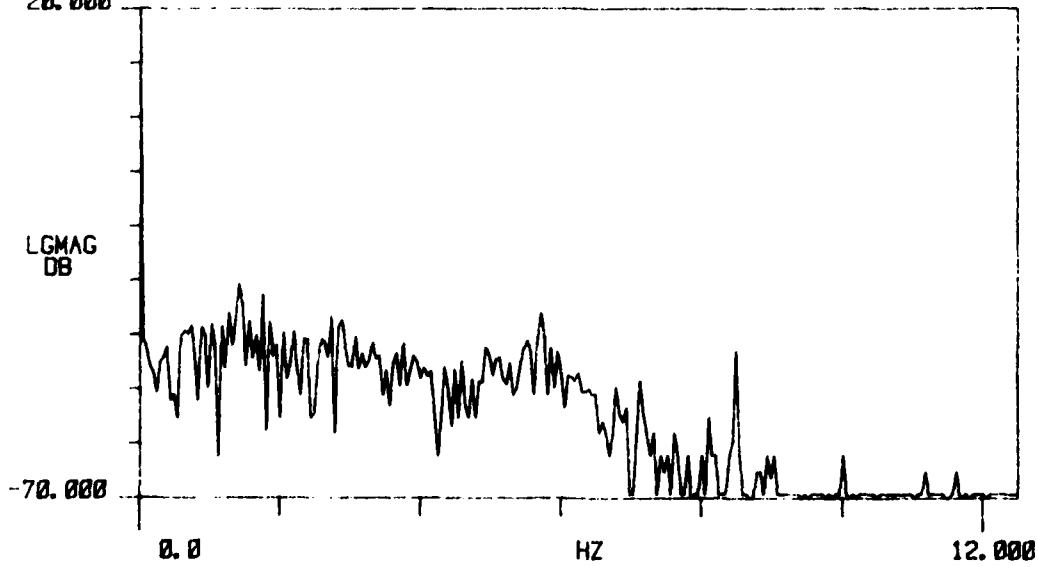


Figure D-1. Zenith Sky Measurement. 28 Feb 80

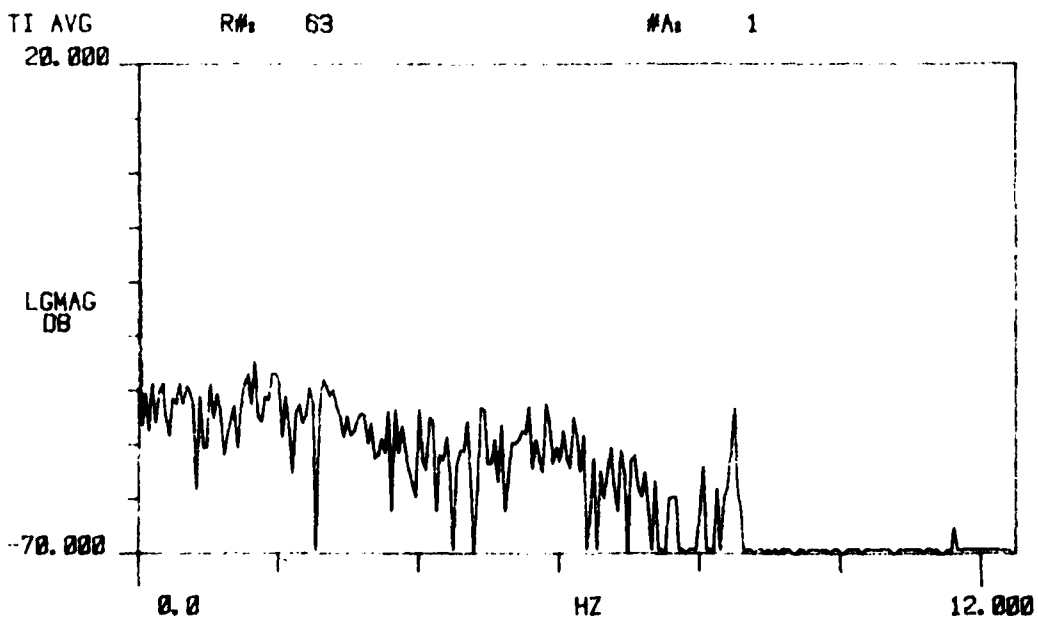
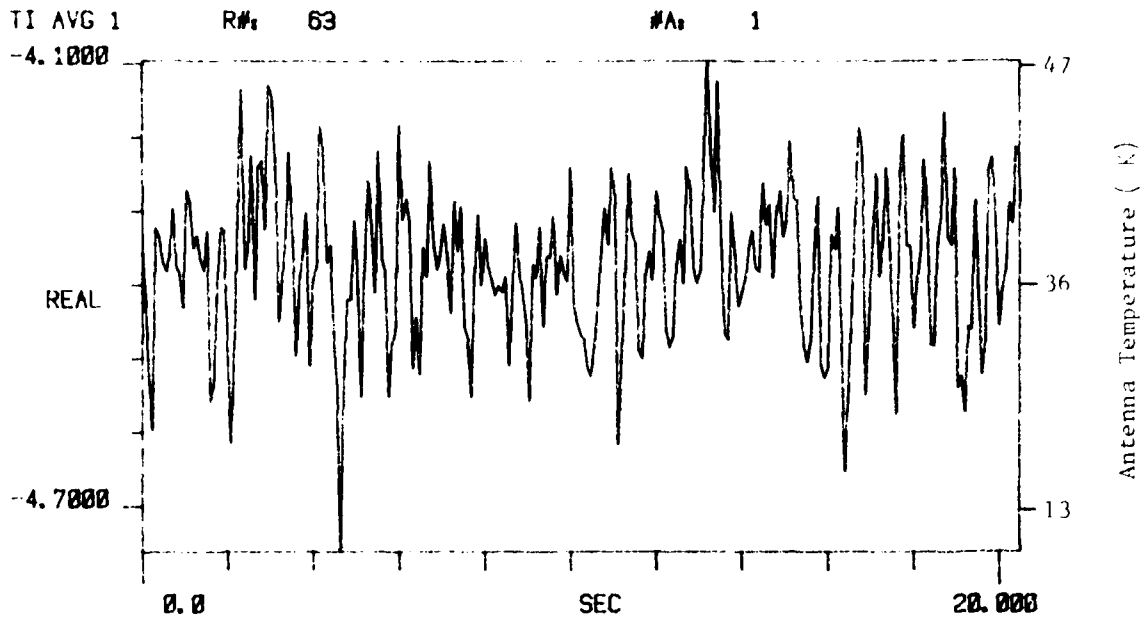


Figure D-1. Zenith Sky Measurement. 28 Feb 80

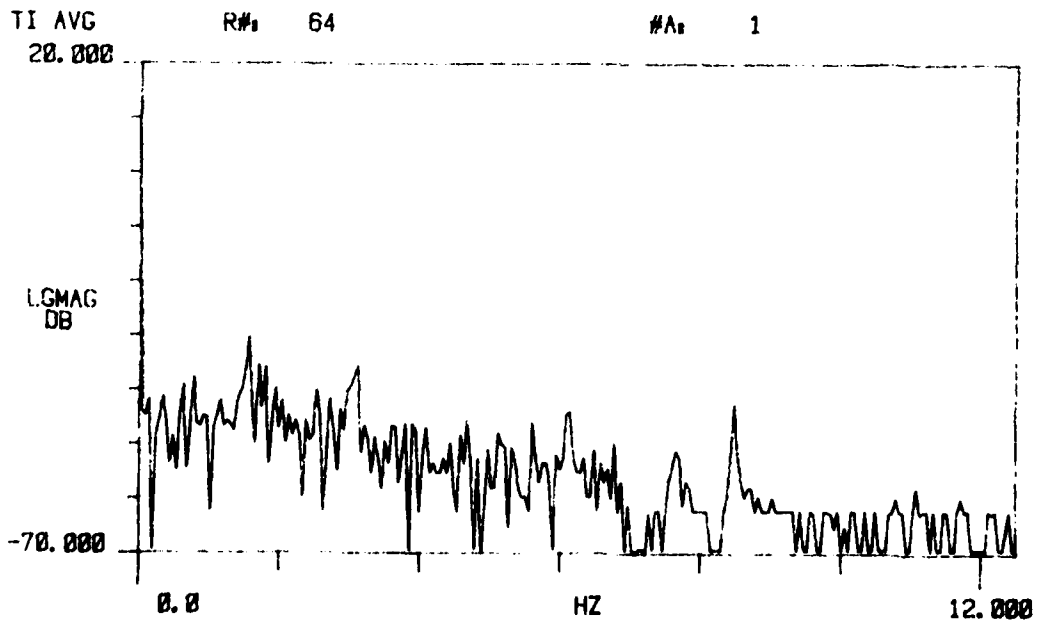
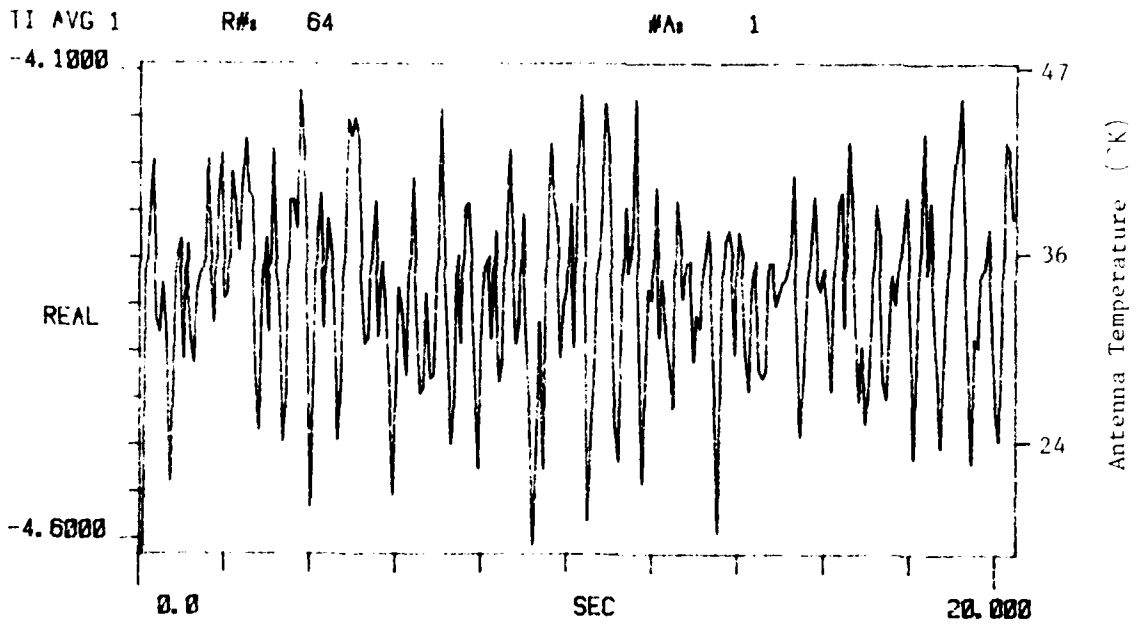


Figure D-1. Zenith Sky Measurement. 28 Feb 80

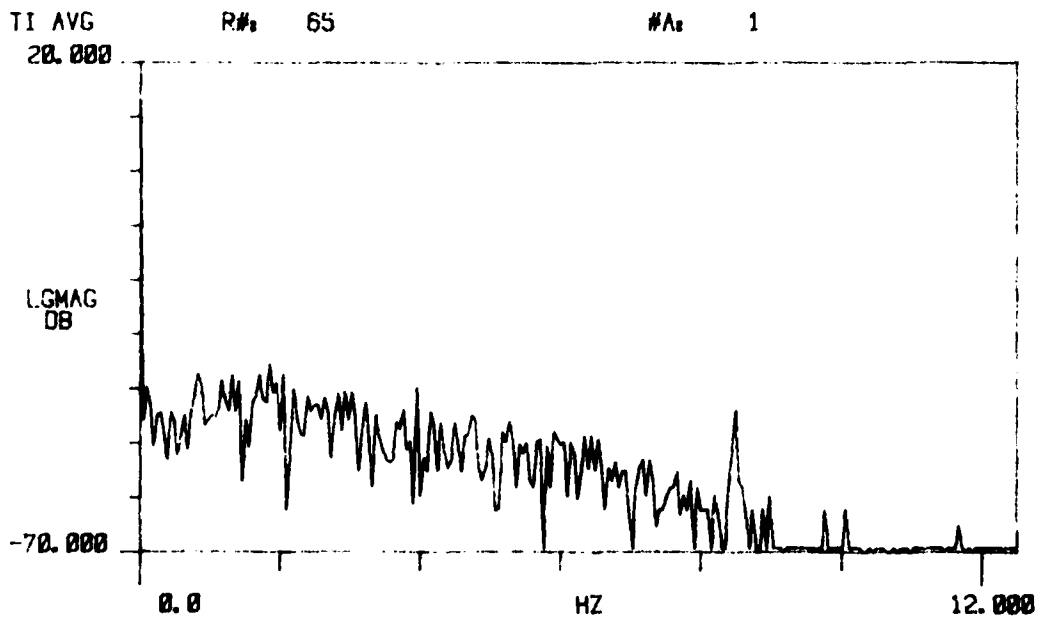
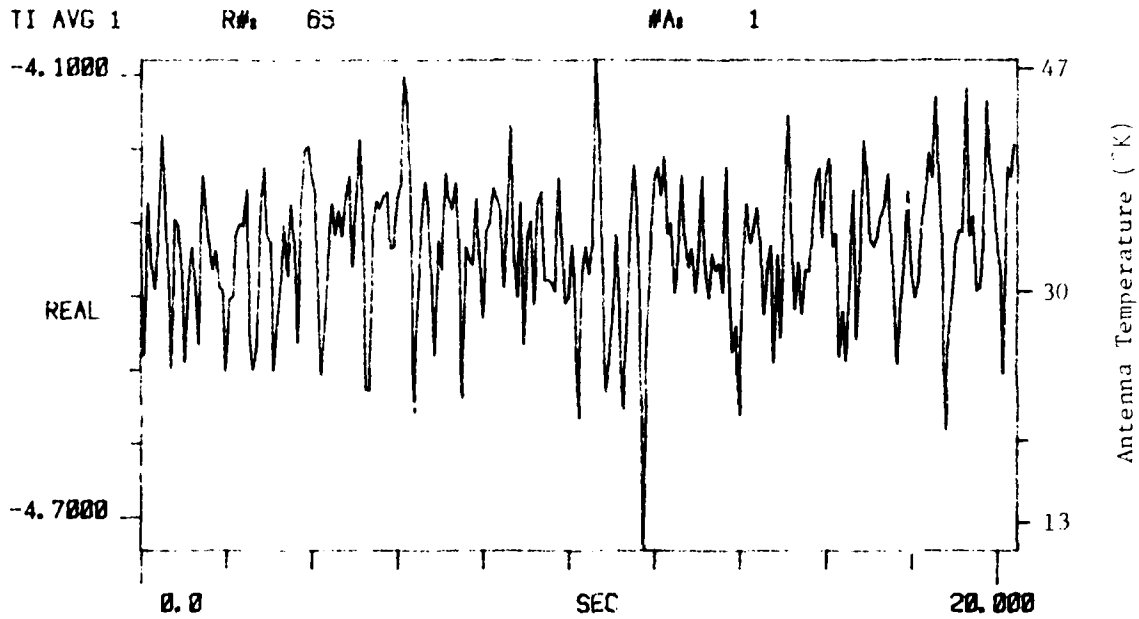
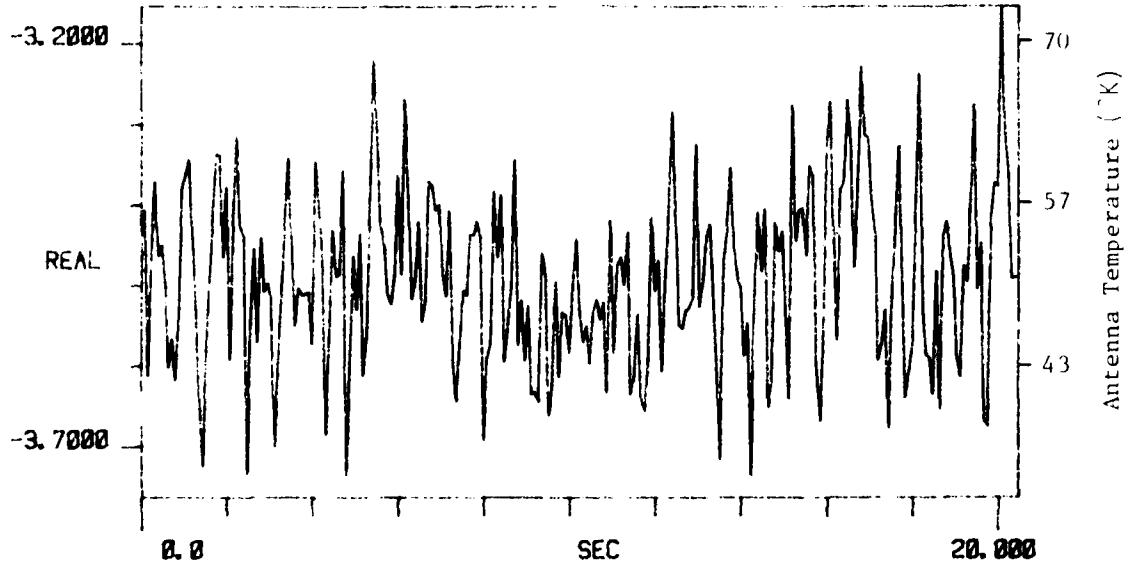


Figure D-1. Zenith Sky Measurement. 28 Feb 80

TI AVG 1

R# 71

#A 1



TI AVG
20.000

R# 71

#A 1

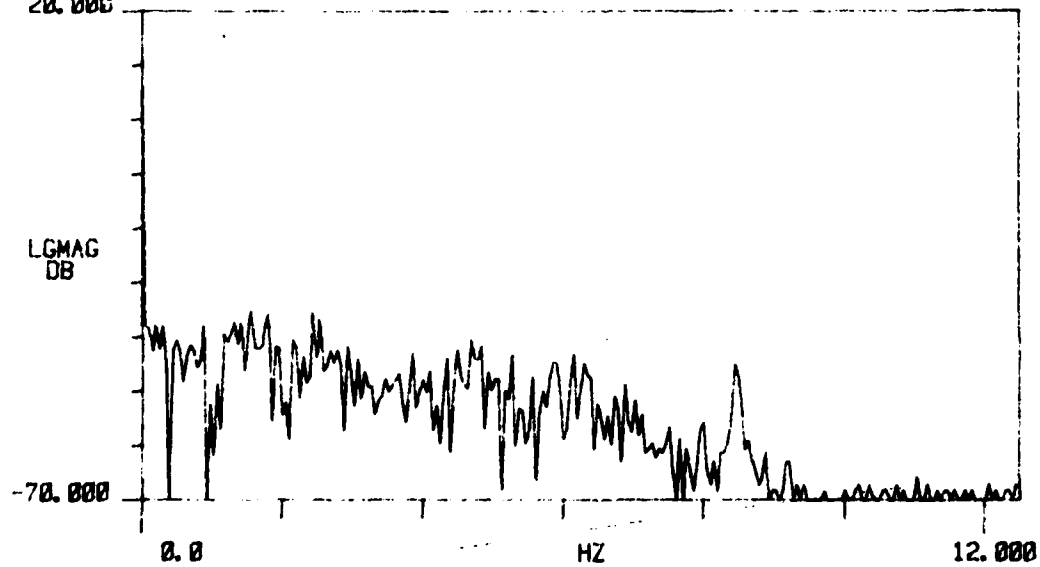
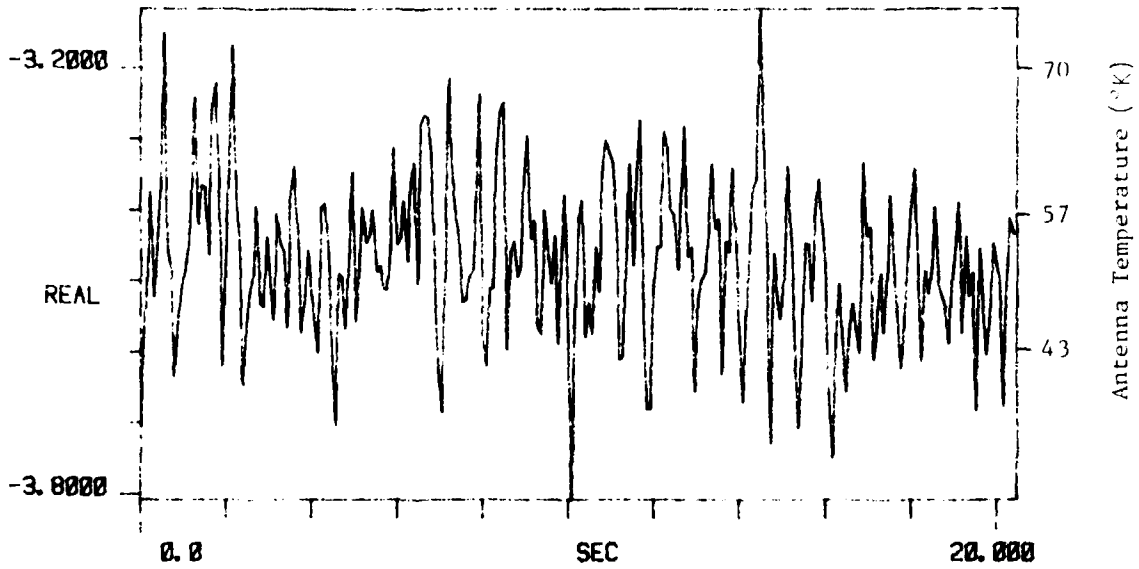


Figure D-1. Zenith Sky Measurement. 28 Feb 80

TI AVG 1

R#s 72

#As 1



TI AVG
20.000

R#s 72

#As 1

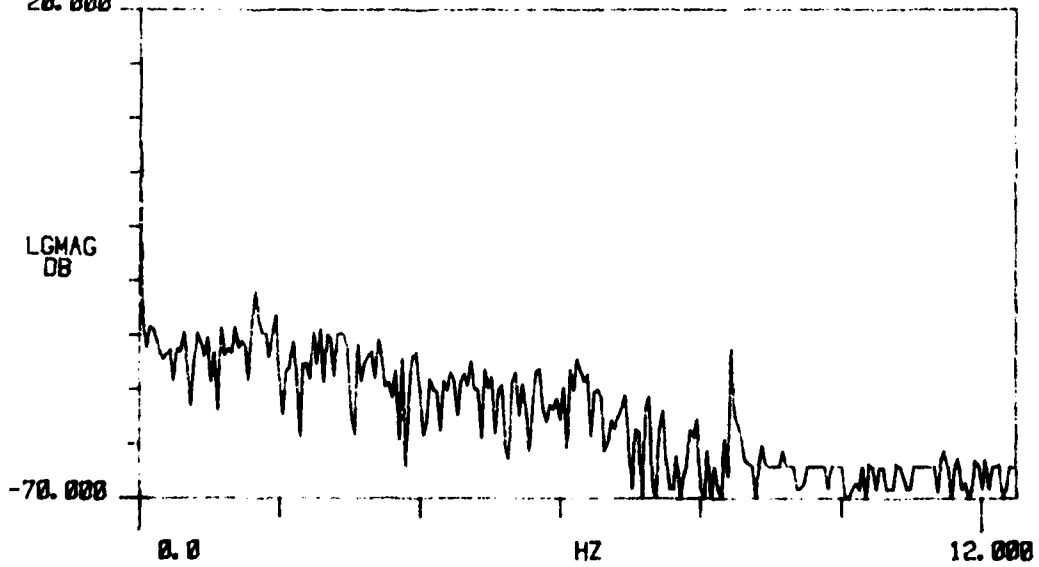


Figure D-1. Zenith Sky Measurement. 28 Feb 80

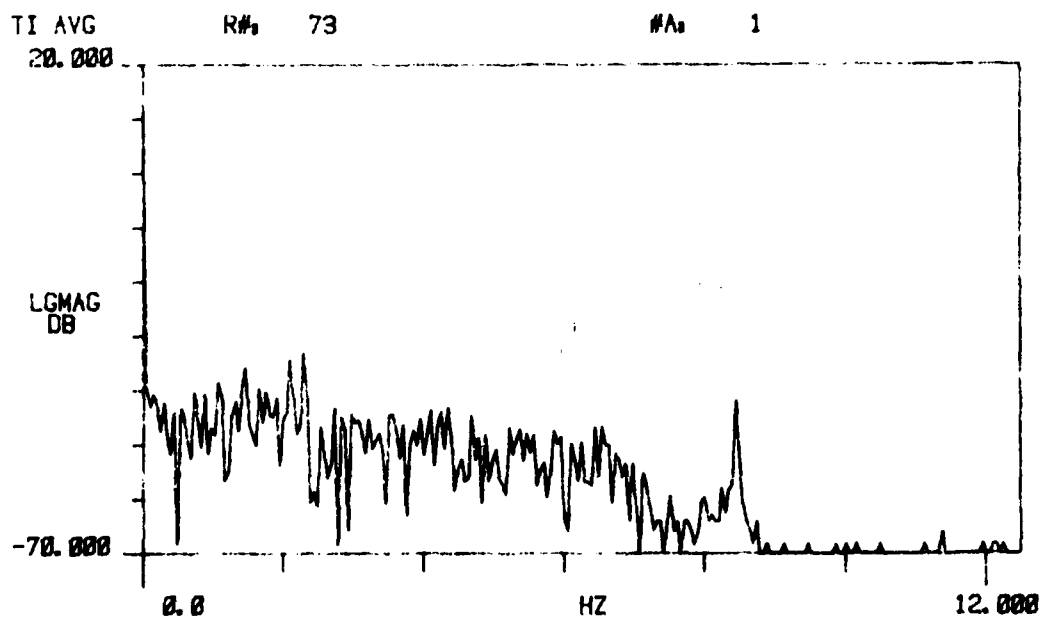
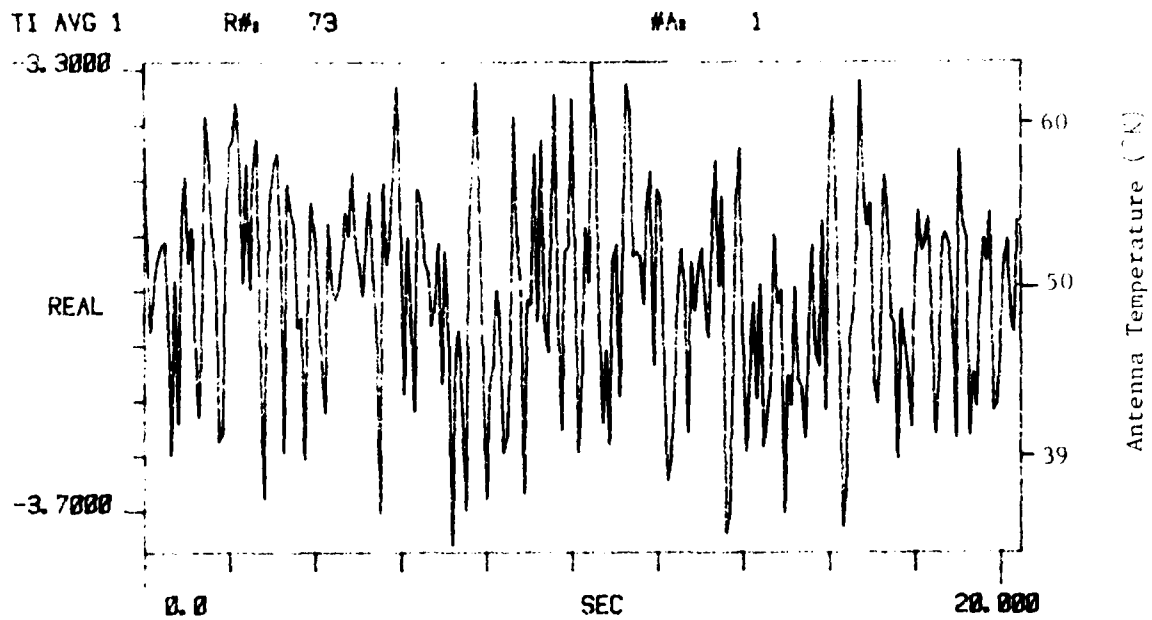


Figure D-1. Zenith Sky Measurement. 28 Feb 80

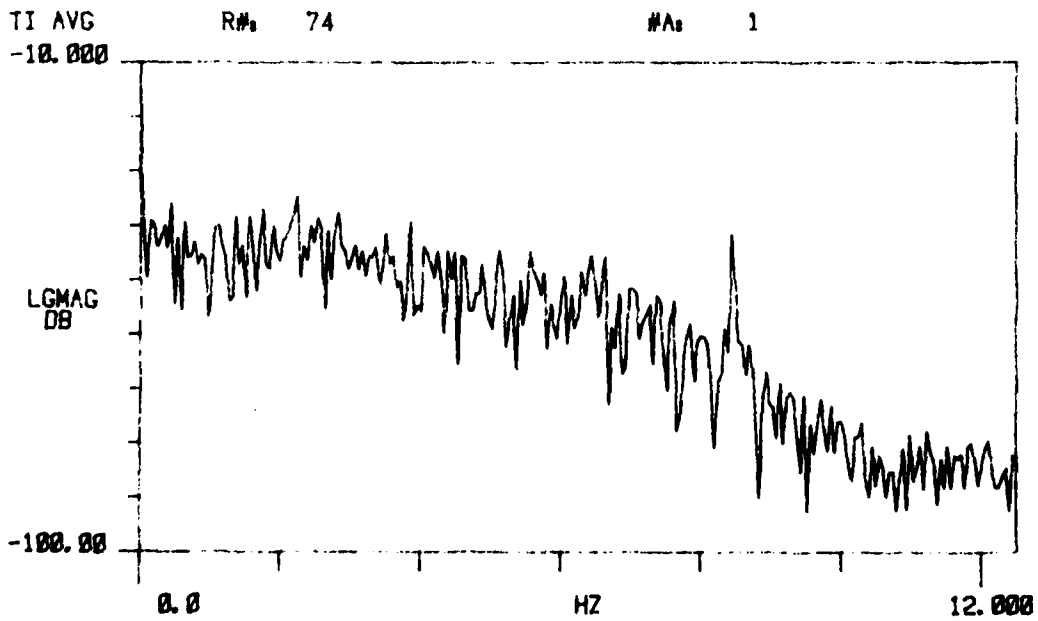
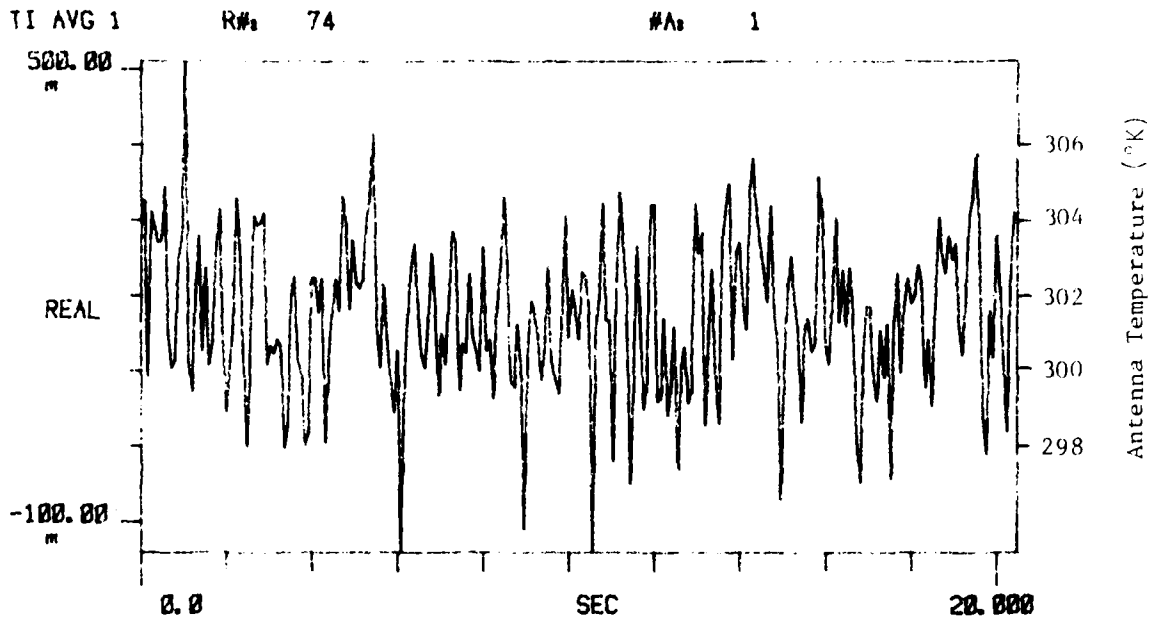


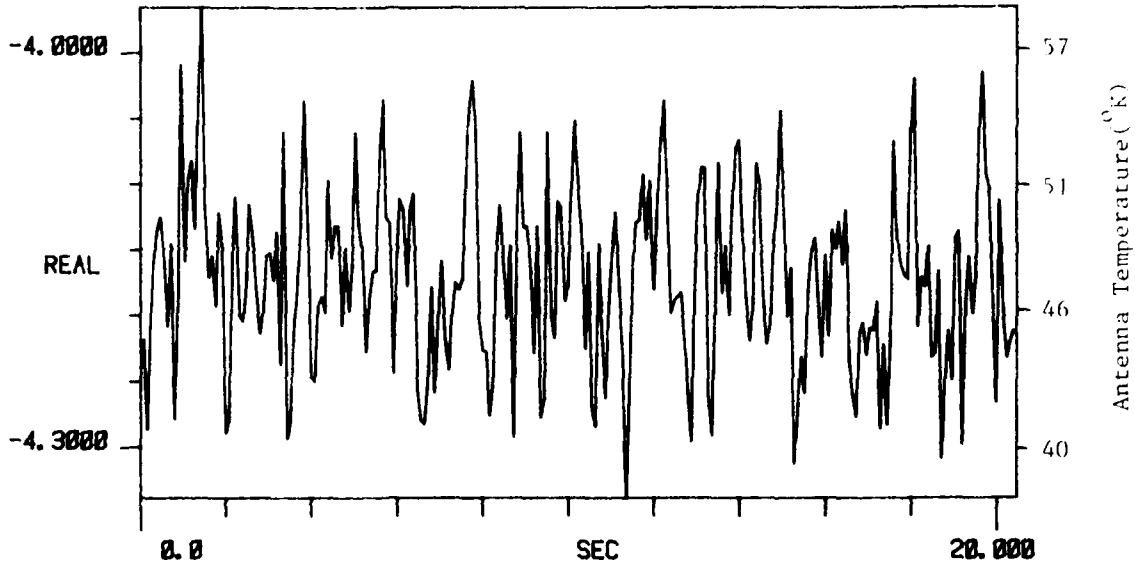
Figure D-1. Zenith Sky Measurement. 28 Feb 80

D-2. 29 February 1980
Zenith Sky Measurements

TI AVG 1

R# 78

#A 1



TI AVG
20.000

R# 78

#A 1

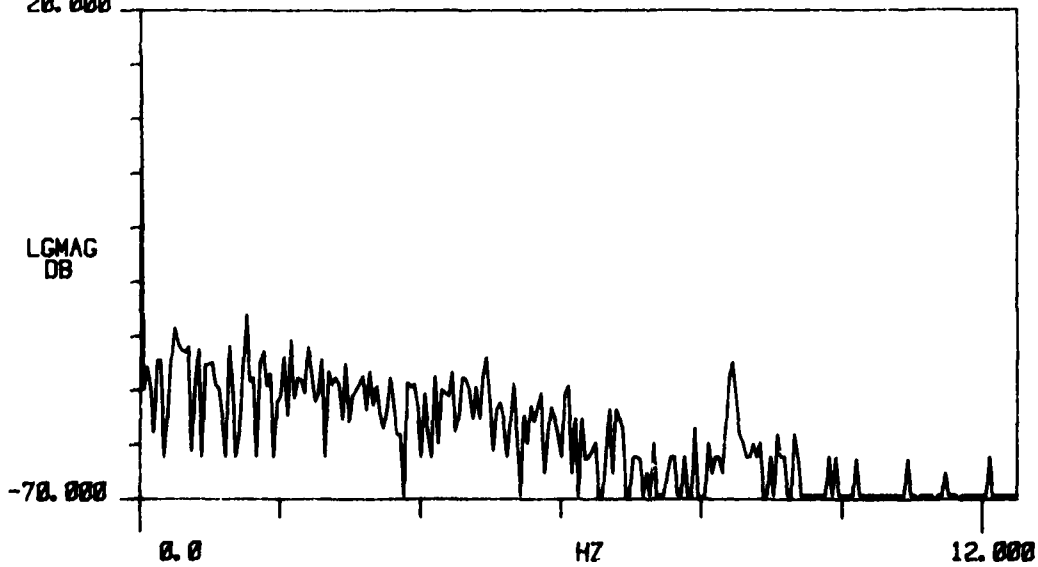


Figure D-2. Zenith Sky Measurement. 29 Feb 80

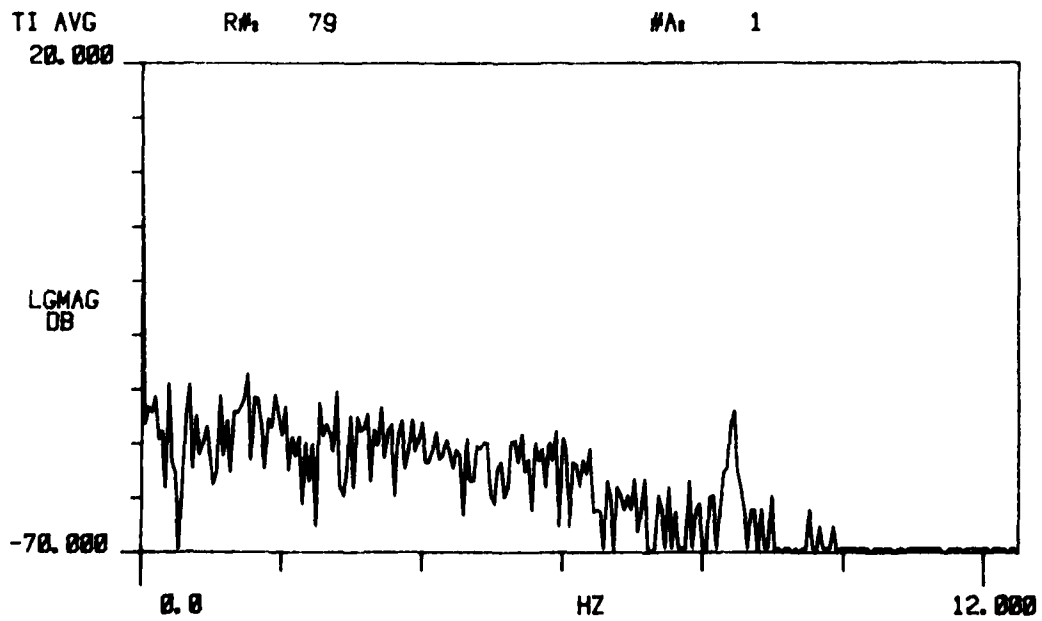
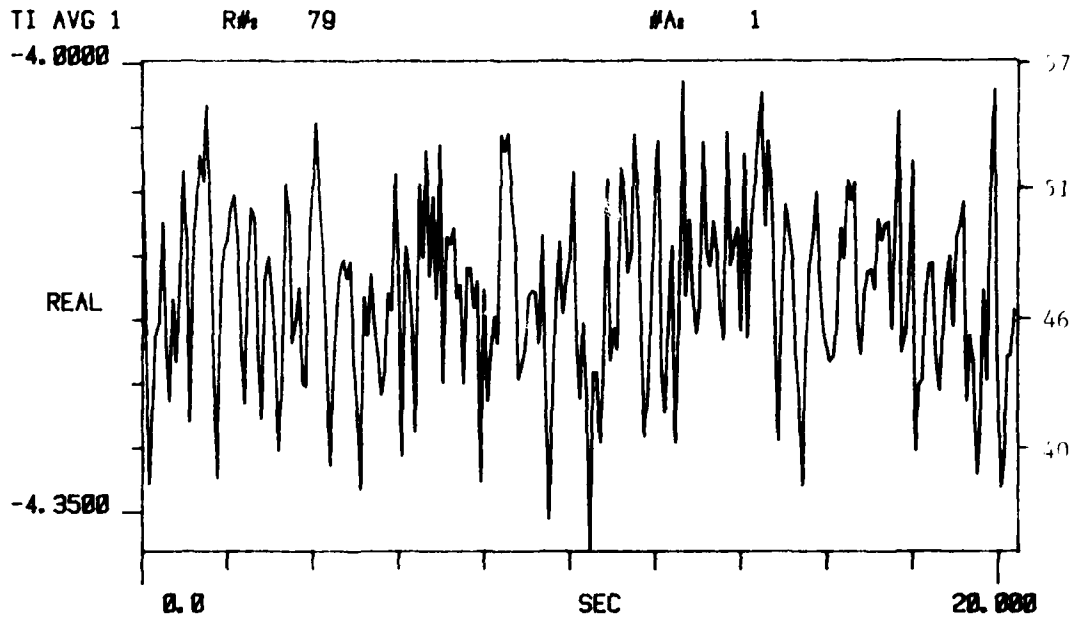


Figure D-2. Zenith Sky Measurement. 29 Feb 80

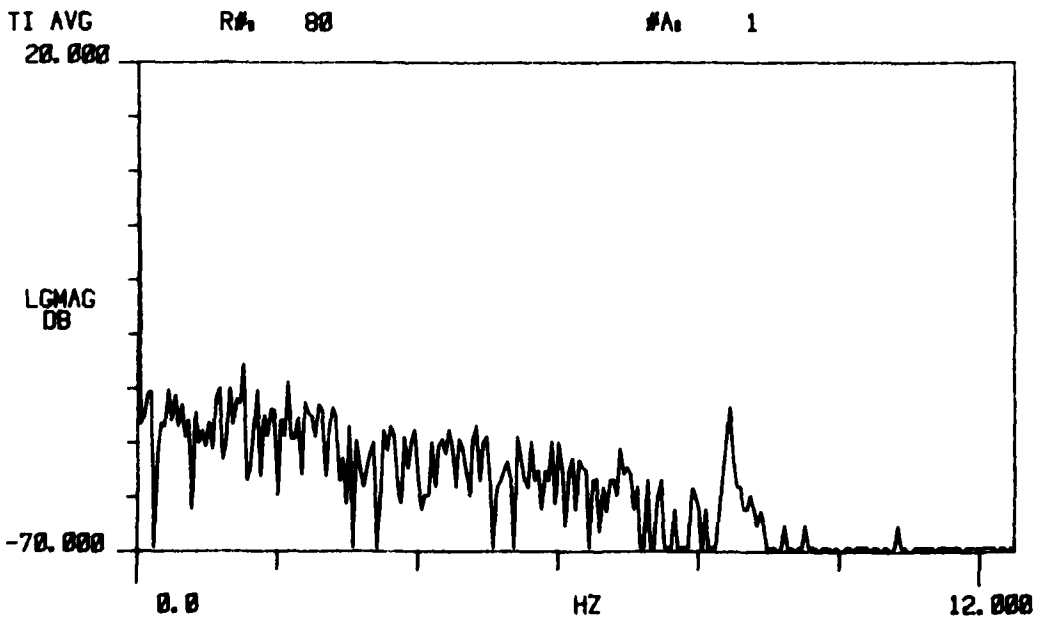
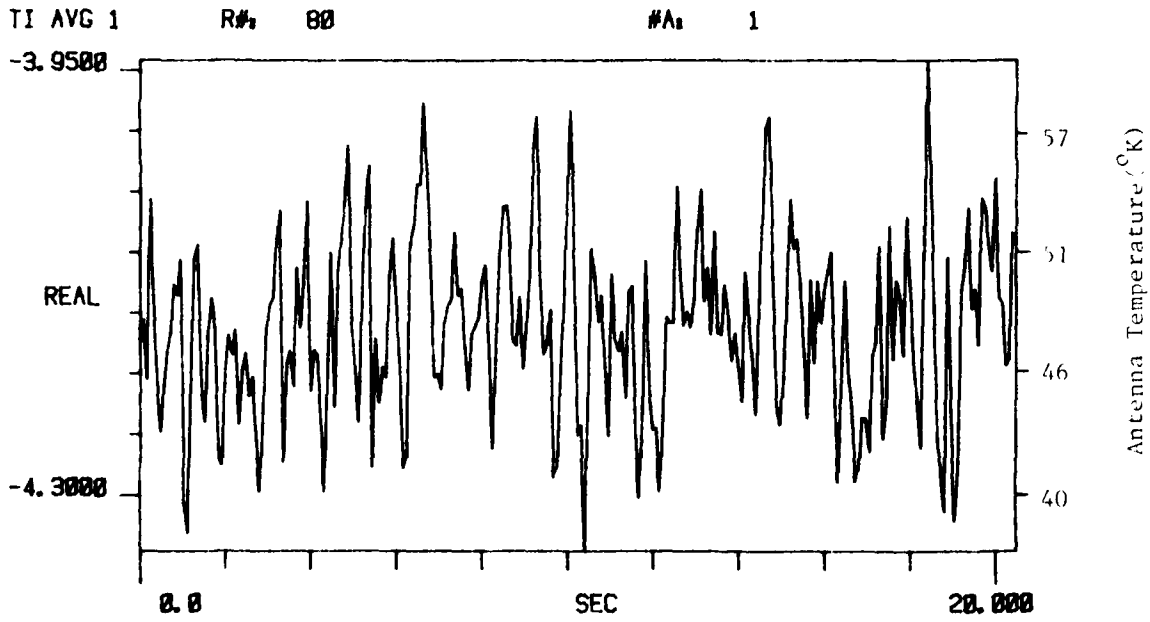
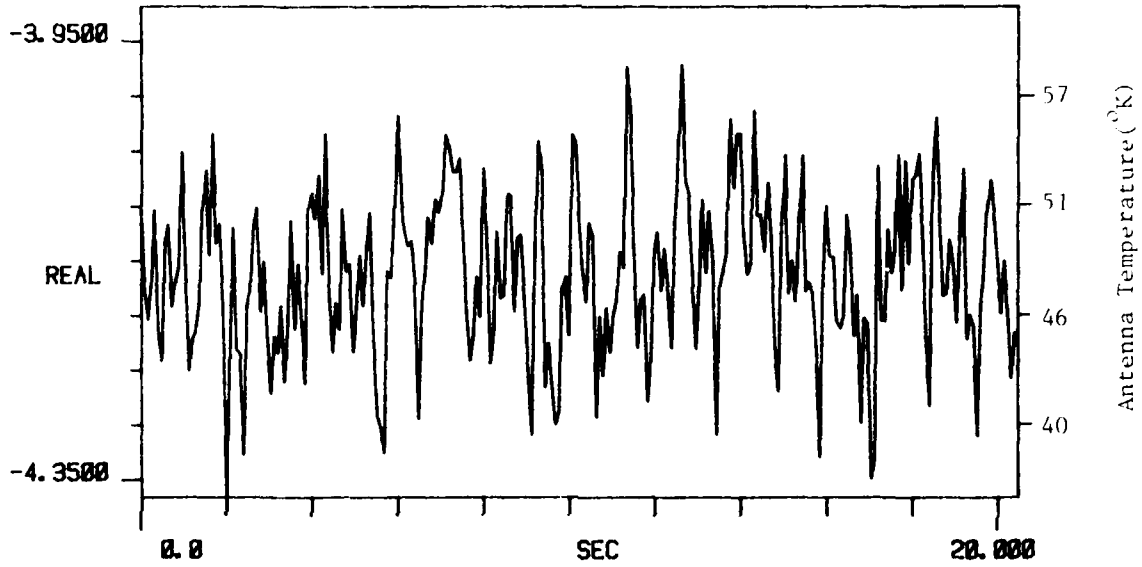


Figure D-2. Zenith Sky Measurement. 29 Feb 80

TI AVG 1

R# 81

#A 1



TI AVG
20.000

R# 81

#A 1

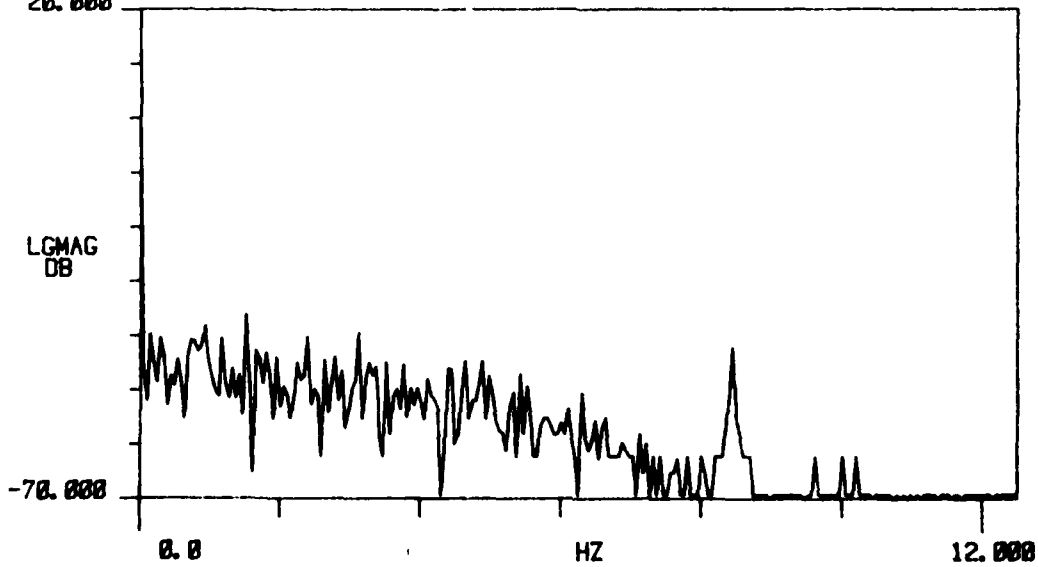
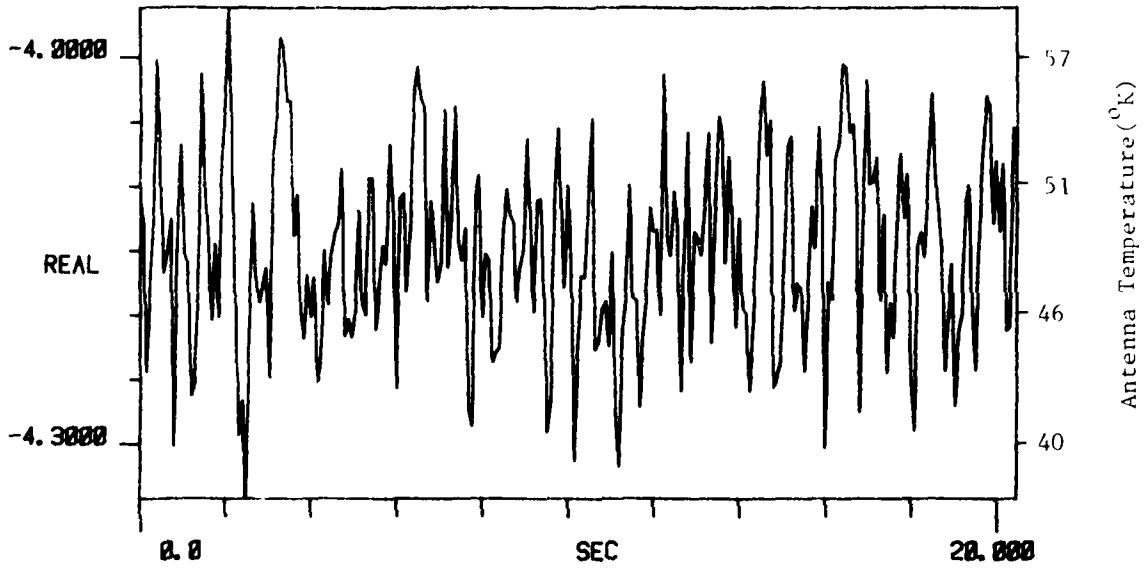


Figure D-2. Zenith Sky Measurement. 29 Feb 80

TI AVG 1

R# 82

#A 1



TI AVG 1

R# 82

#A 1

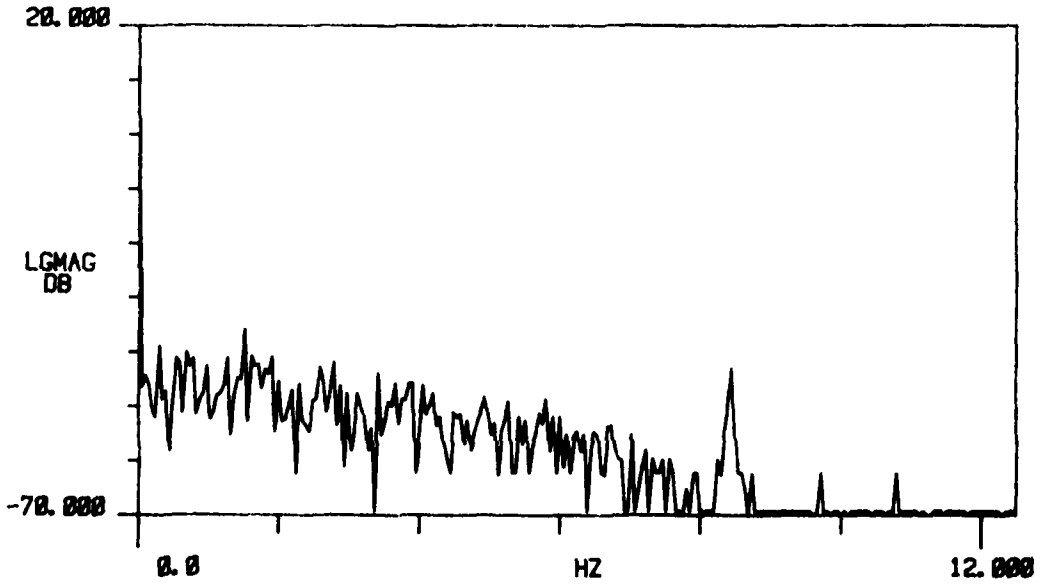


Figure D-2. Zenith Sky Measurement. 29 Feb 80

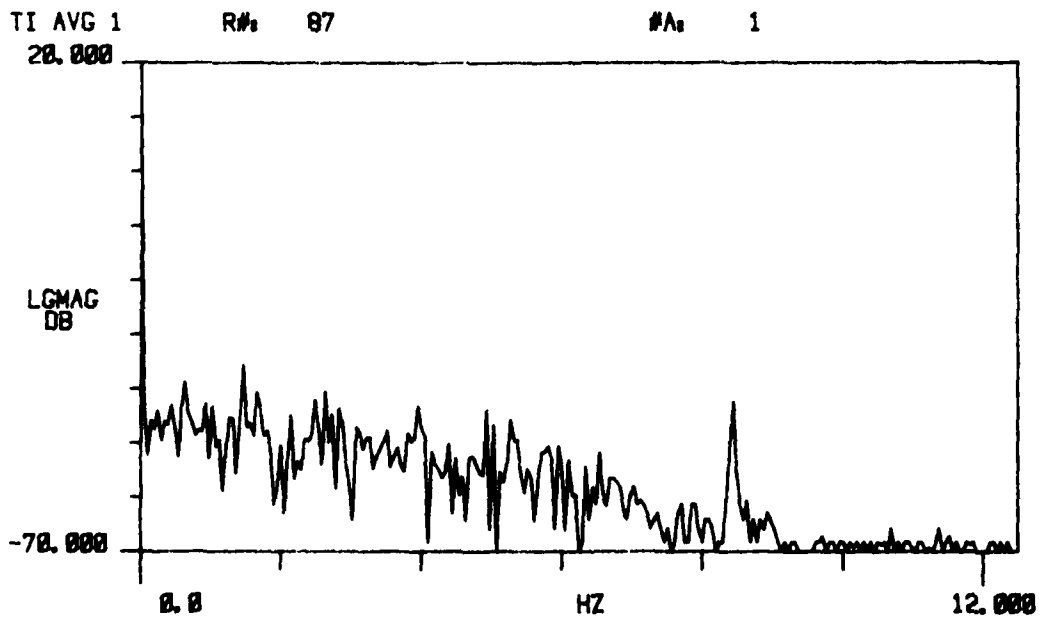
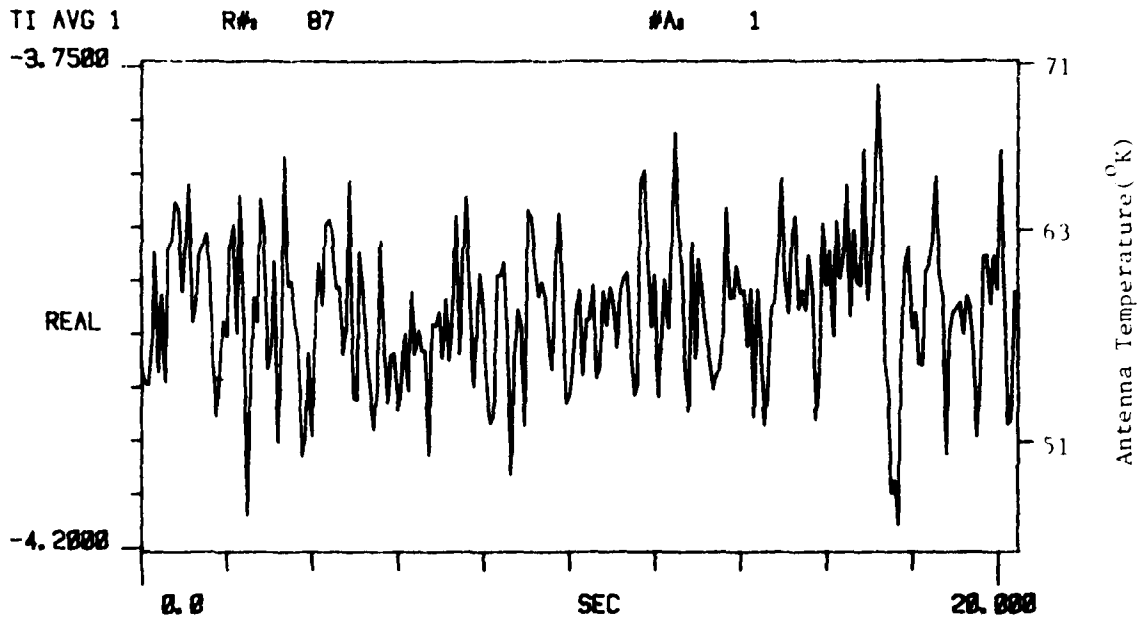
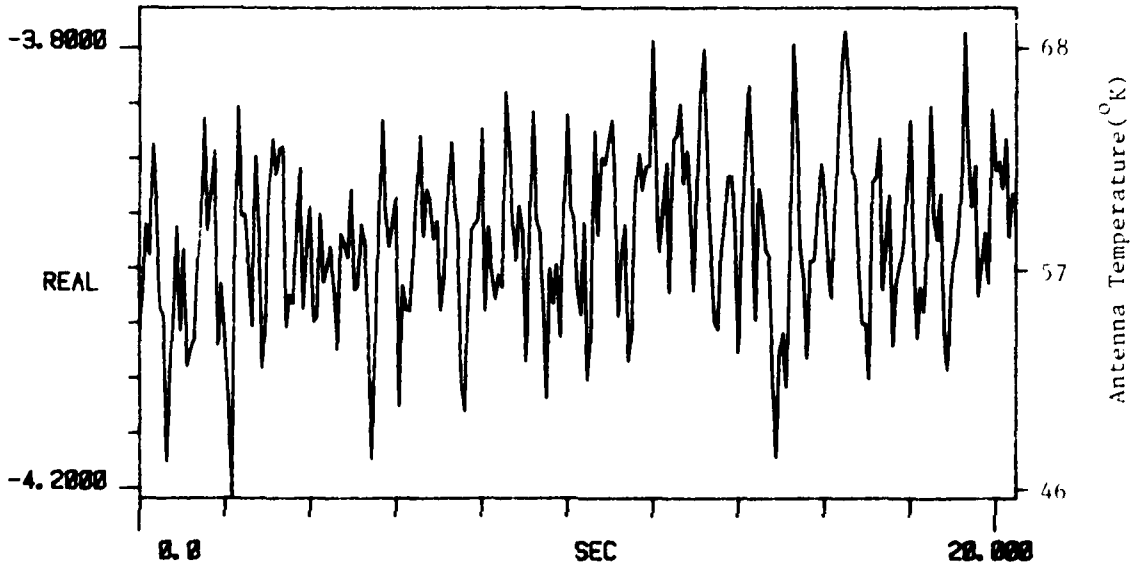


Figure D-2. Zenith Sky Measurement. 29 Feb 80

TI AVG 1

R# 88

#A₁ 1



TI AVG
20.000

R# 88

#A₁ 1

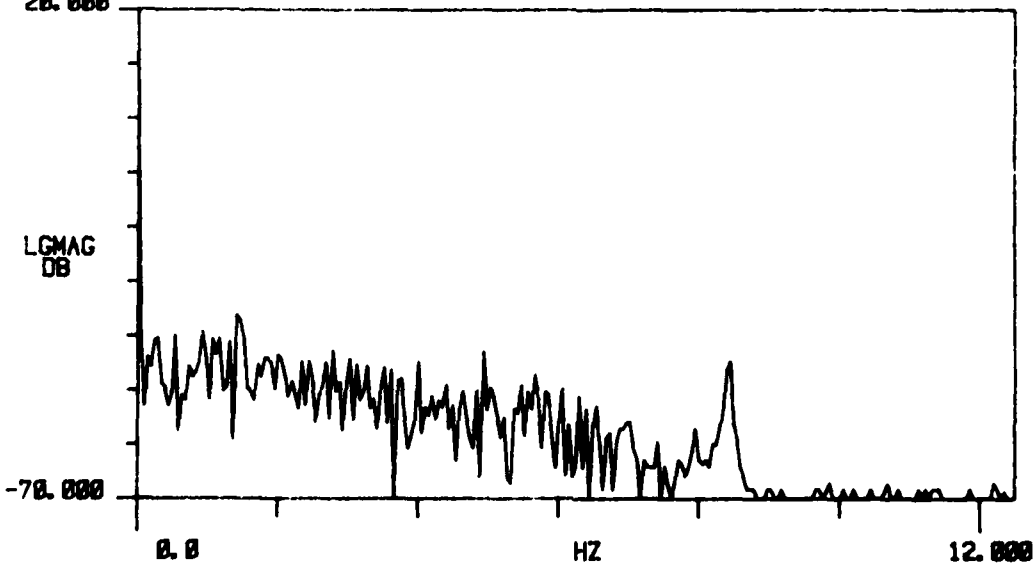
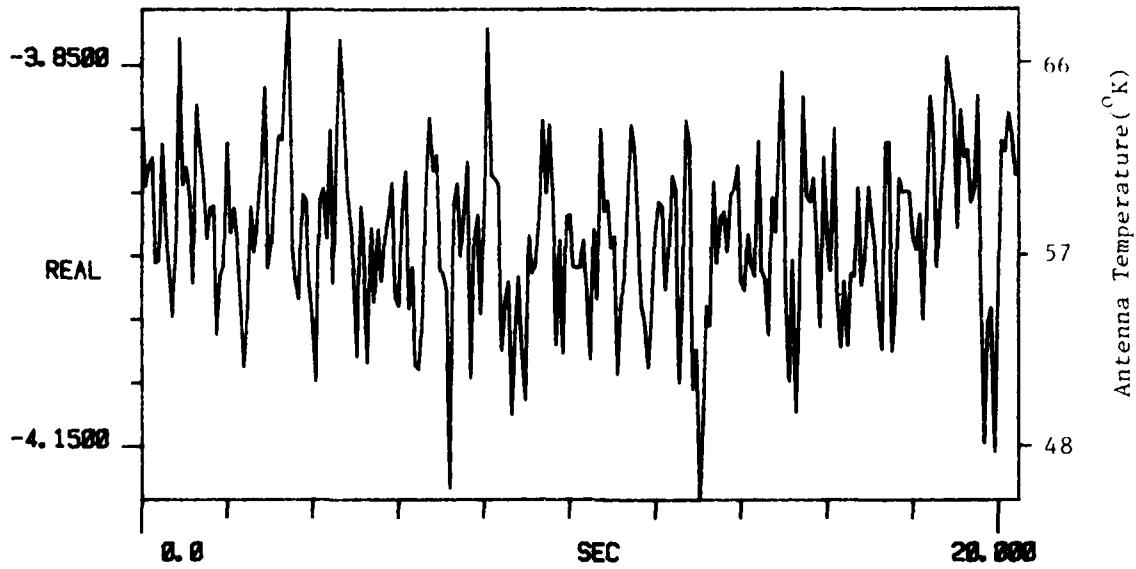


Figure D-2. Zenith Sky Measurement. 29 Feb 80

TI AVG 1

R# 89

#A 1



TI AVG
20.000

R# 89

#A 1

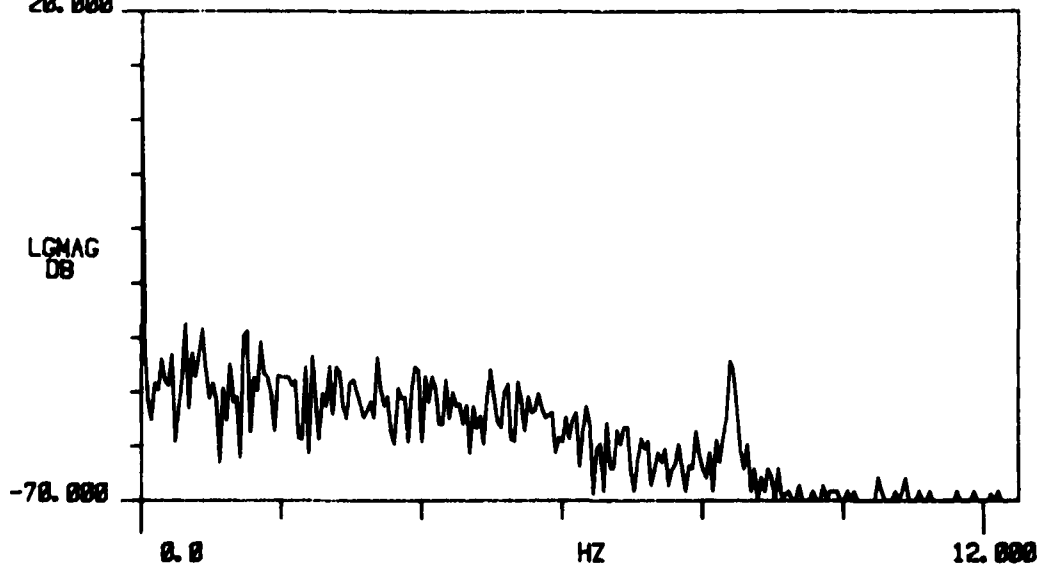
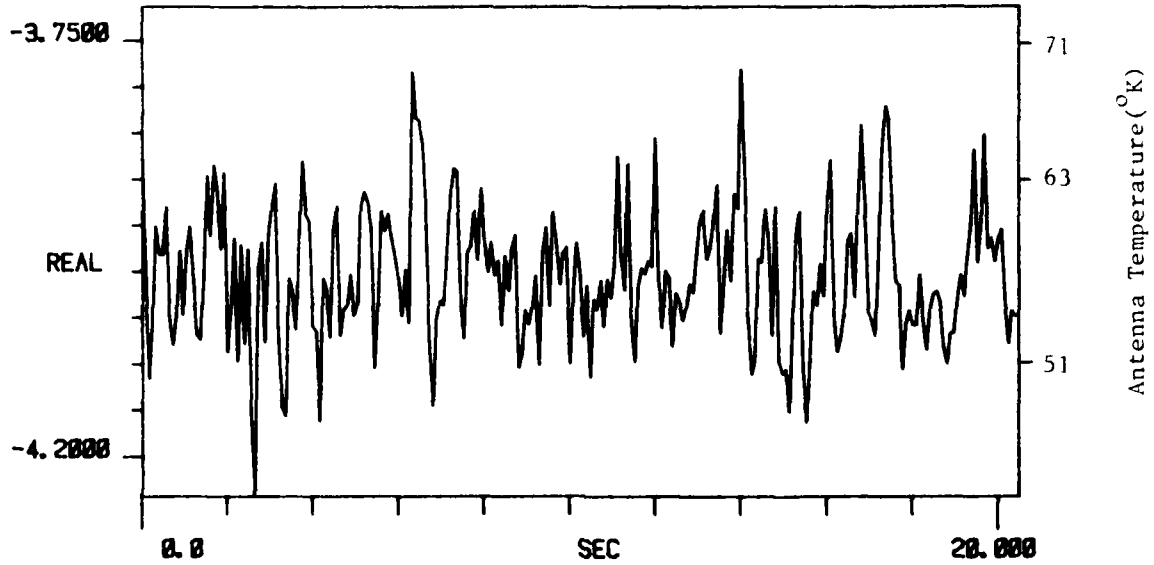


Figure D-2. Zenith Sky Measurement. 29 Feb 80

TI AVG 1

R# 98

#A 1



TI AVG
20.000

R# 98

#A 1

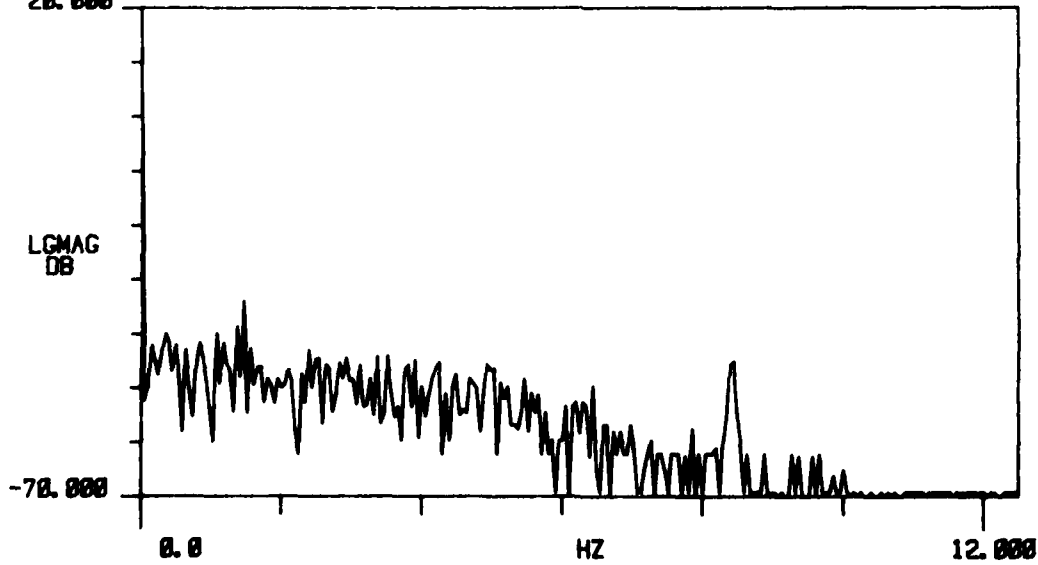


Figure D-2. Zenith Sky Measurement. 29 Feb 80

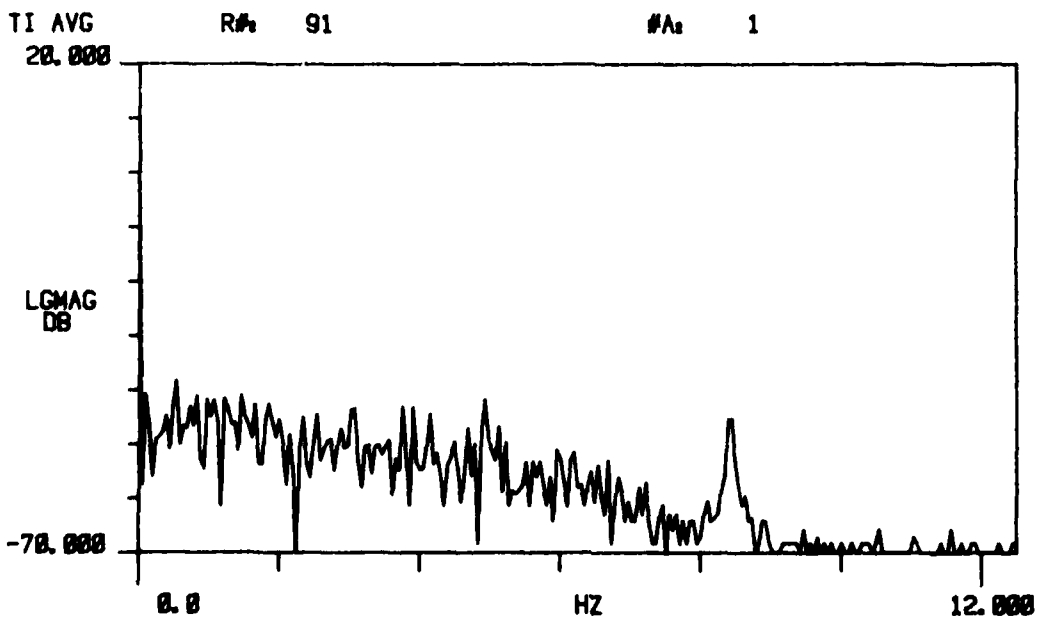
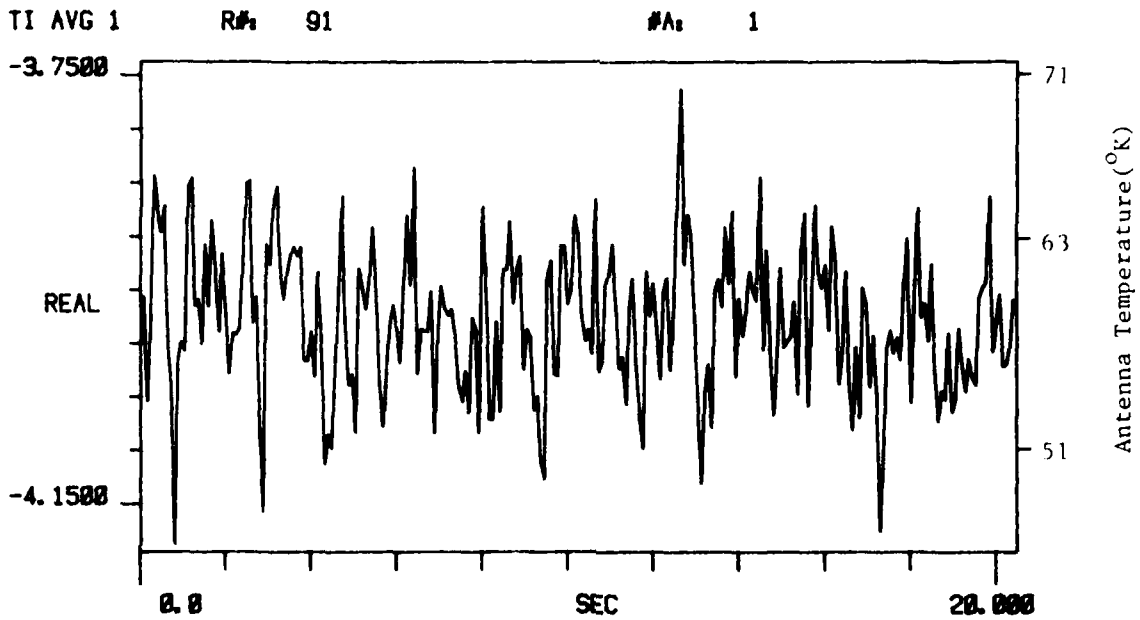


Figure D-2. Zenith Sky Measurement. 29 Feb 80

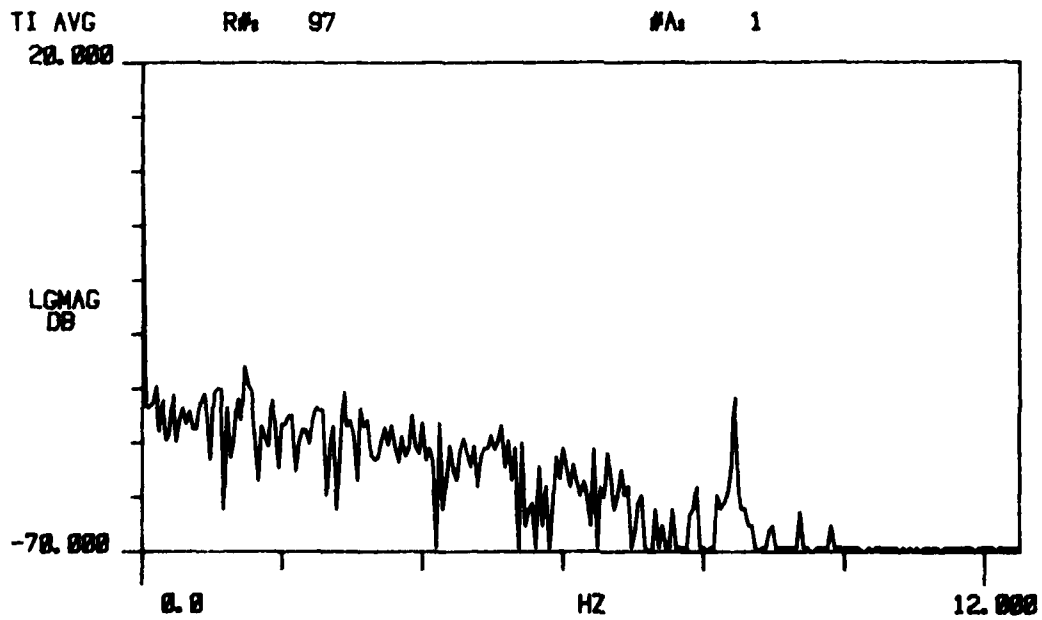
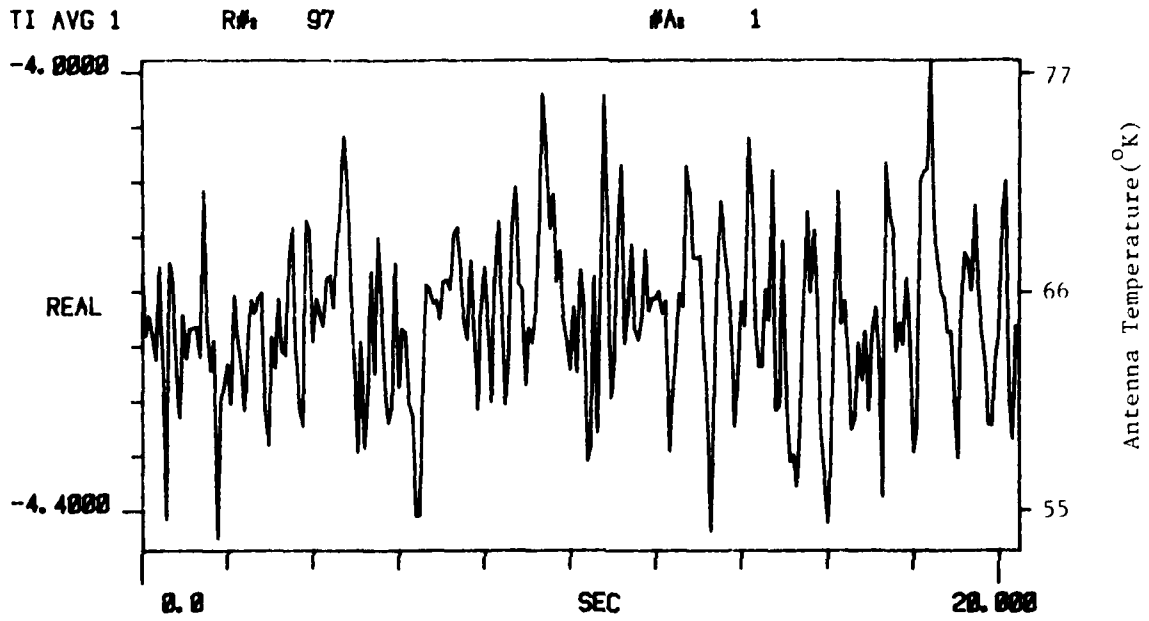
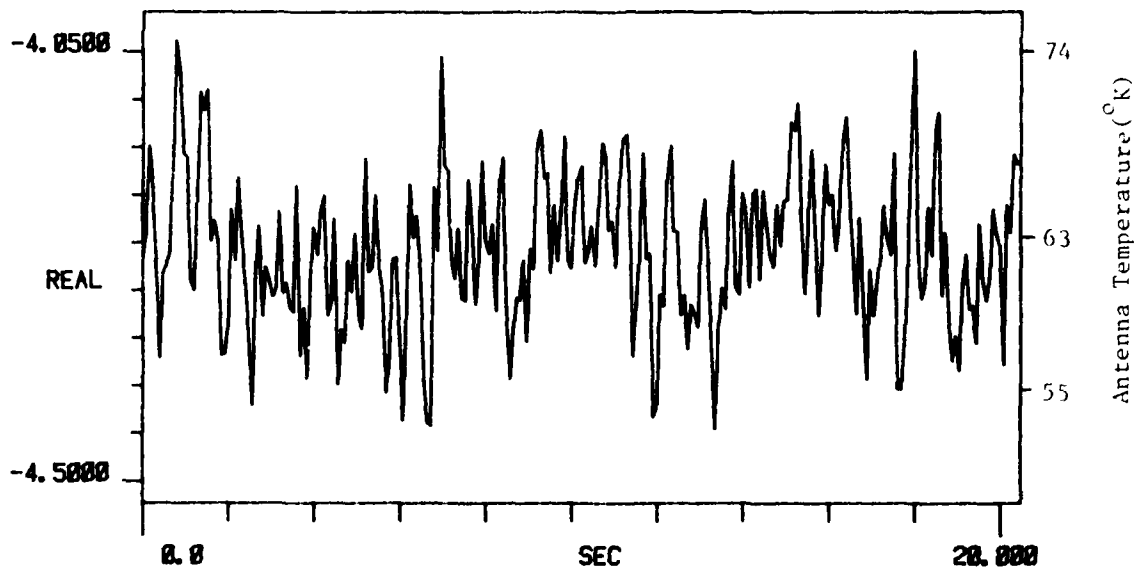


Figure D-2. Zenith Sky Measurement. 29 Feb 80

TI AVG 1 R# 98 #A 1



TI AVG 20.000 R# 98 #A 1

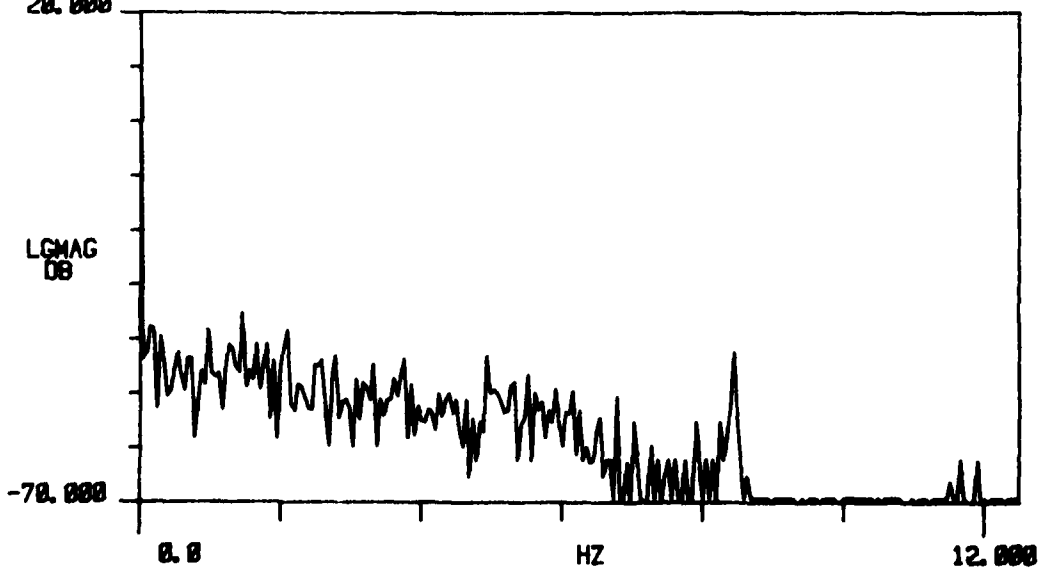
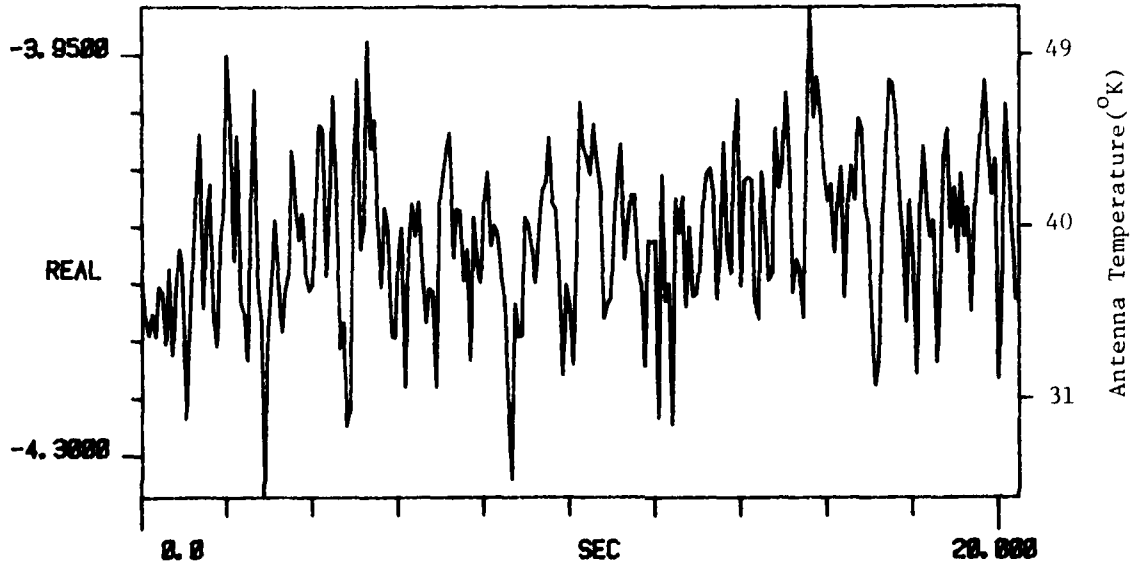


Figure D-2. Zenith Sky Measurement. 29 Feb 80

TI AVG 1

R# 186

#A_s 1



TI AVG
20.000

R# 186

#A_s 1

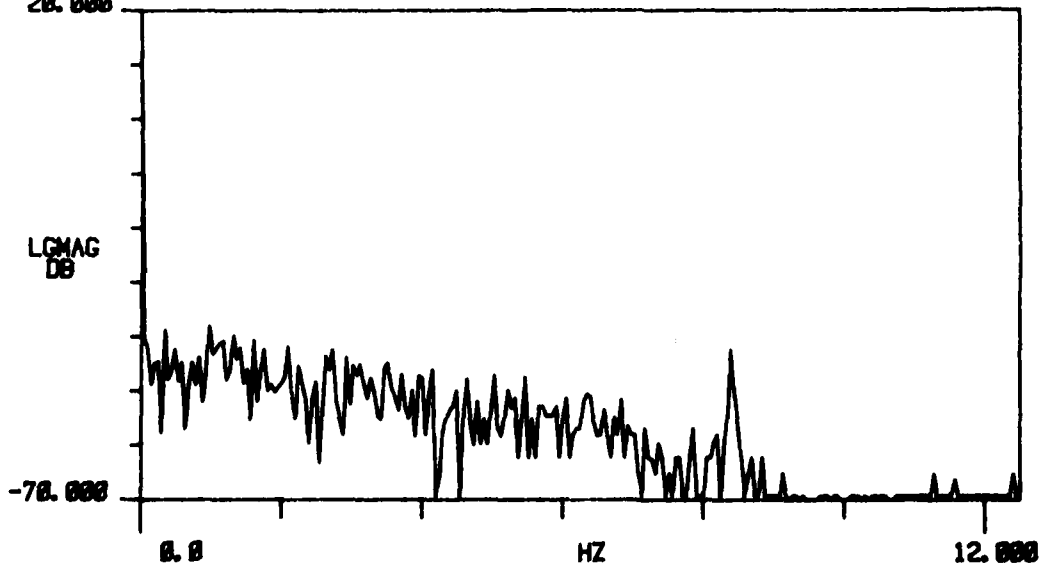
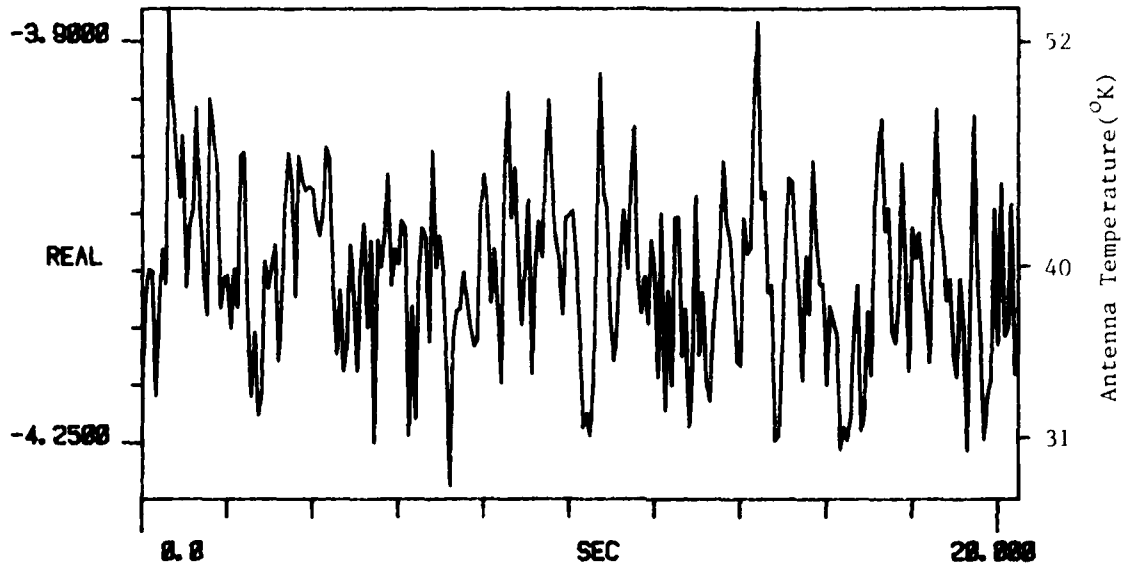


Figure D-2. Zenith Sky Measurement. 29 Feb 80
153

TI AVG 1

R# 187

#A_s 1



TI AVG
20.000

R# 187

#A_s 1

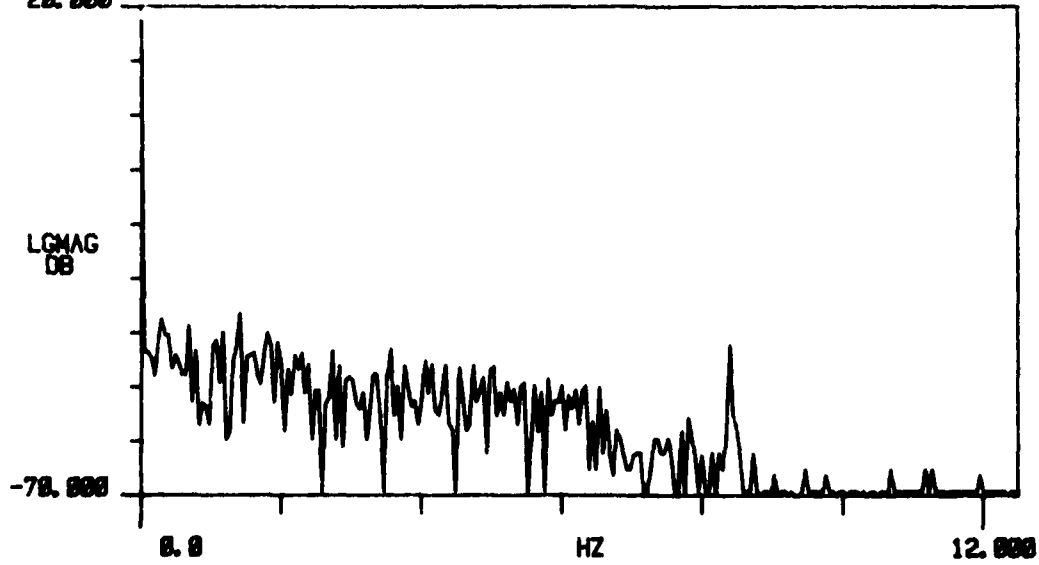
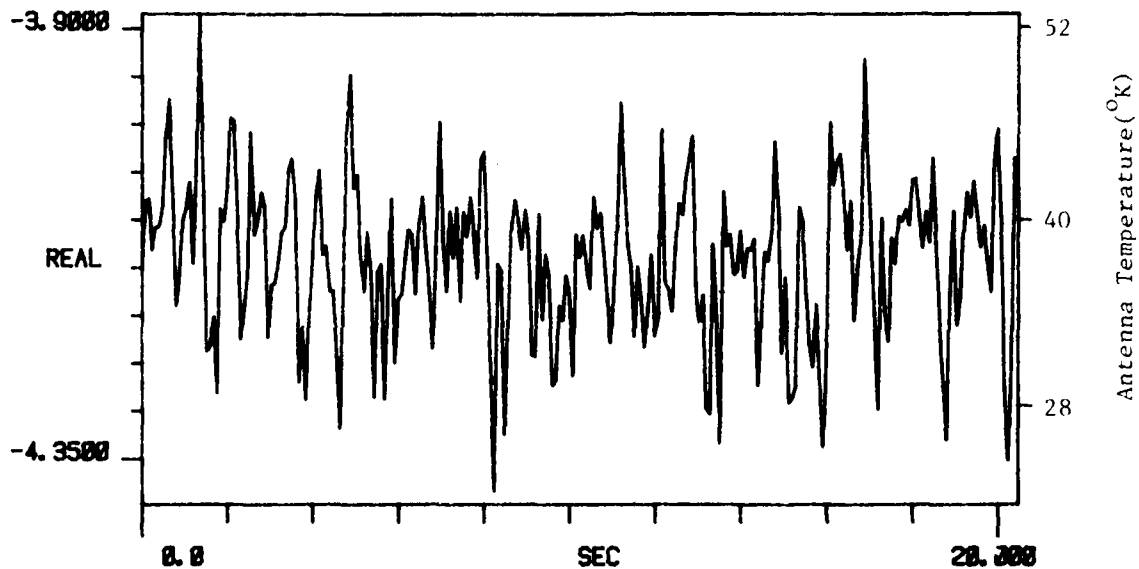


Figure D-2. Zenith Sky Measurement. 29 Feb 80

TI AVG 1

R# 100

#A 1



TI AVG

R# 100

#A 1

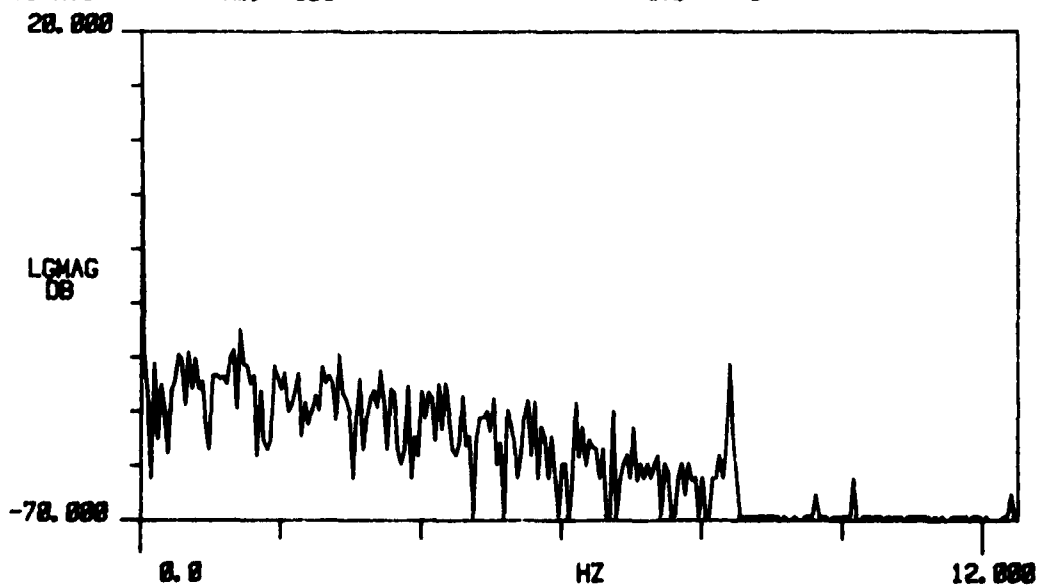


Figure D-2. Zenith Sky Measurement. 29 Feb 80

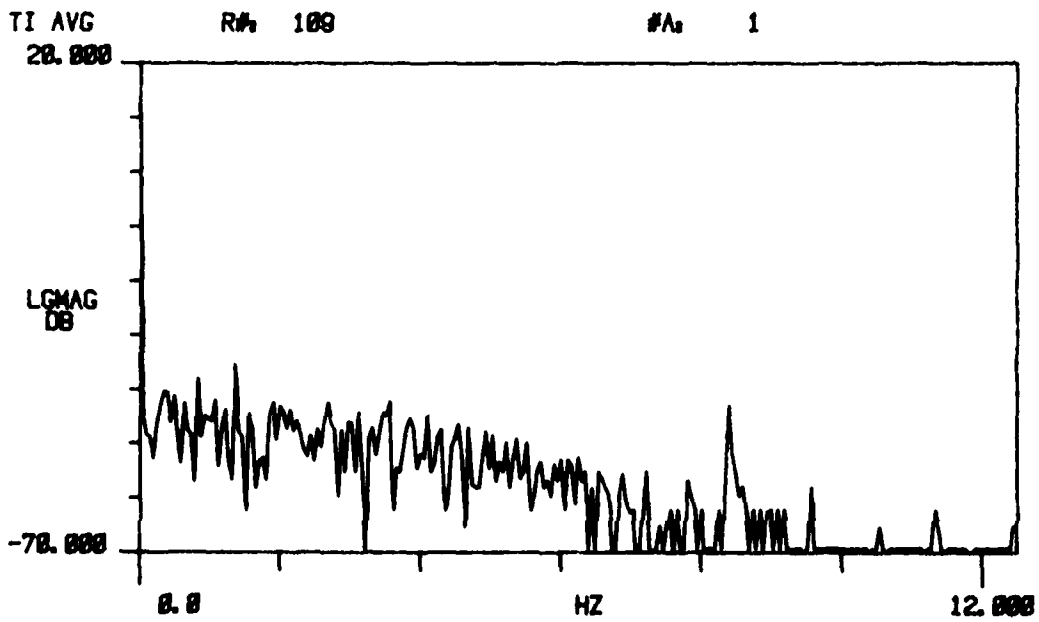
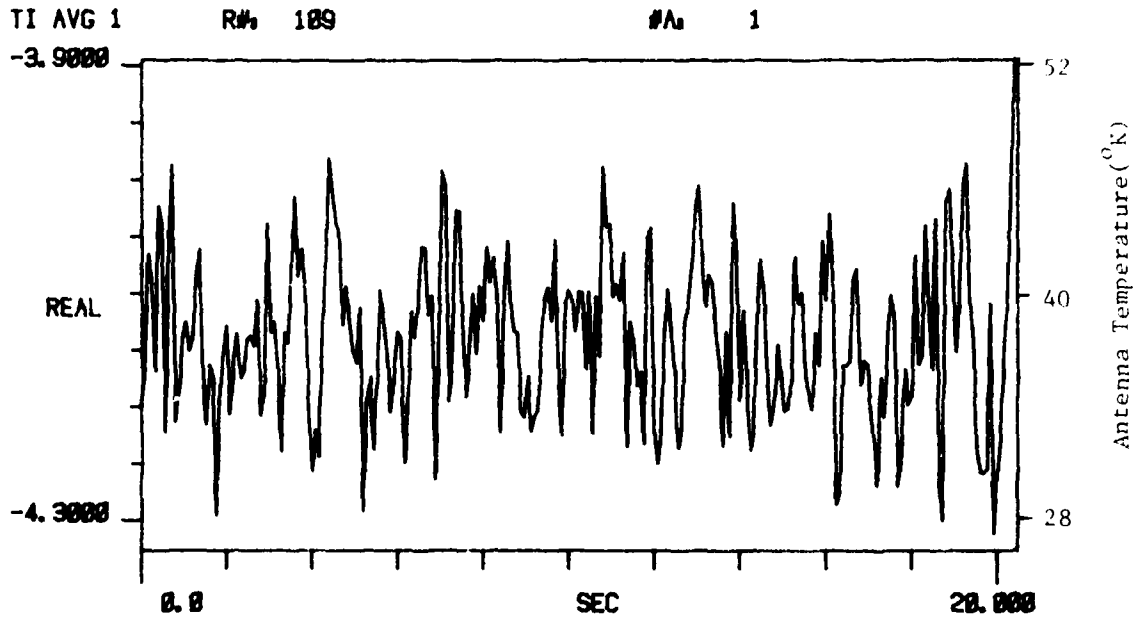
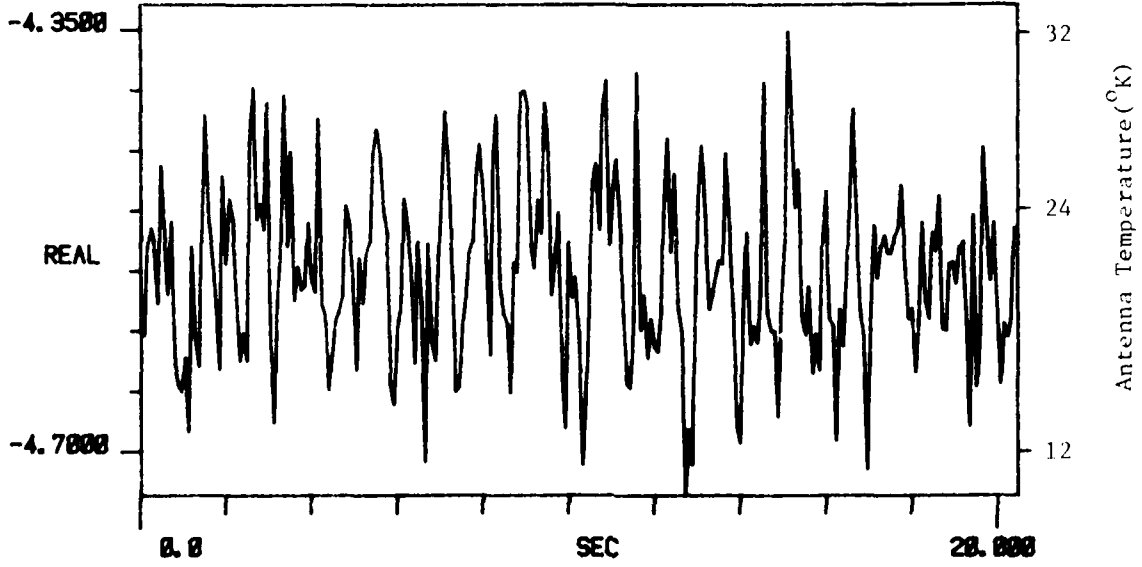


Figure D-2. Zenith Sky Measurement. 29 Feb 80

TI AVG 1

R# 116

#A 1



TI AVG
20.000

R# 116

#A 1

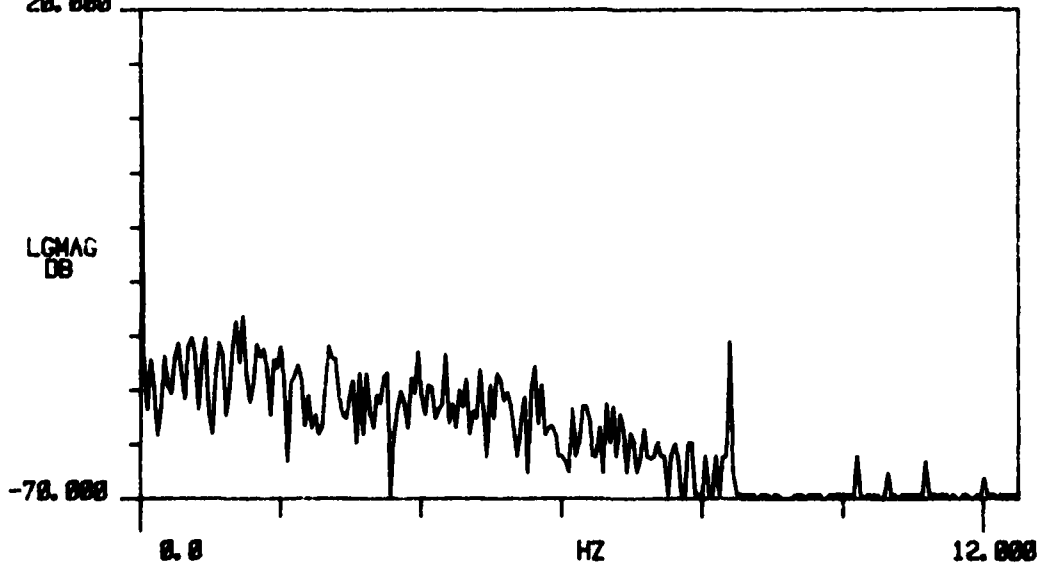
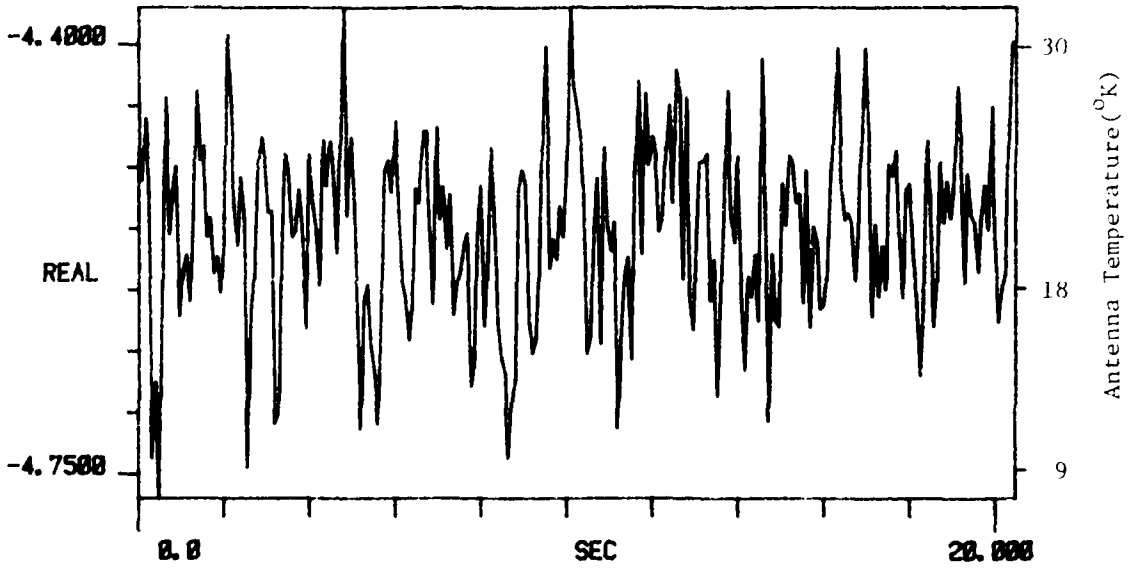


Figure D-2. Zenith Sky Measurement. 29 Feb 80

TI AVG 1

R# 117

#A 1



TI AVG
20.000

R# 117

#A 1

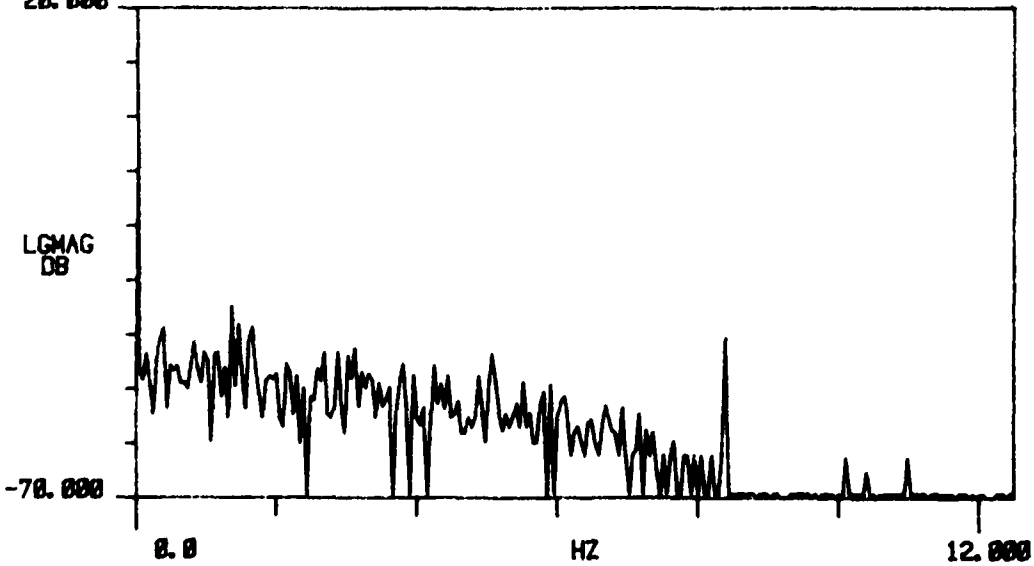


Figure D-2. Zenith Sky Measurement. 29 Feb 80

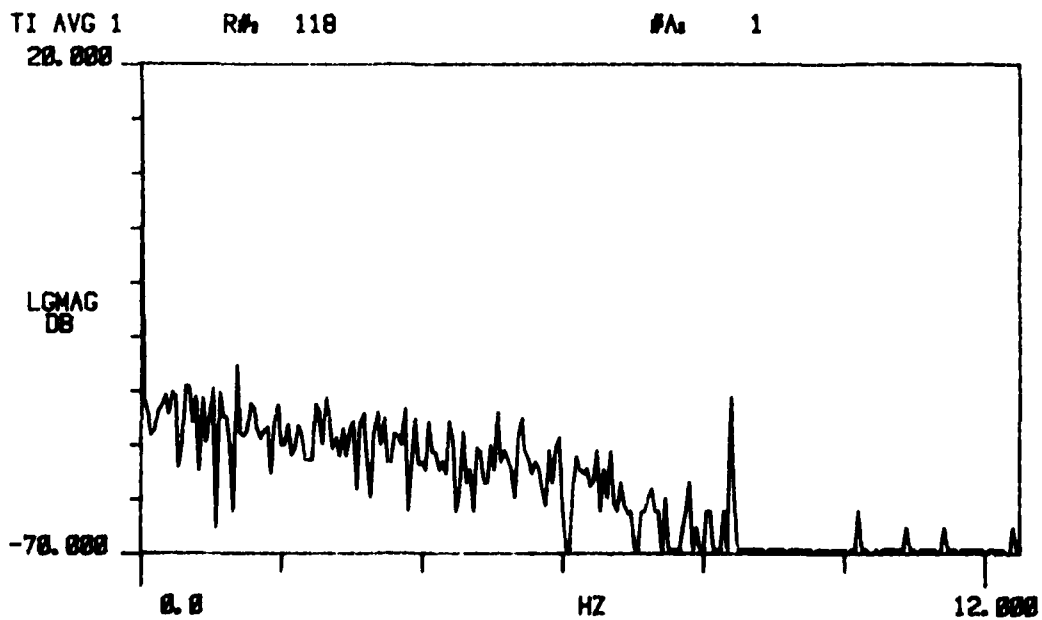
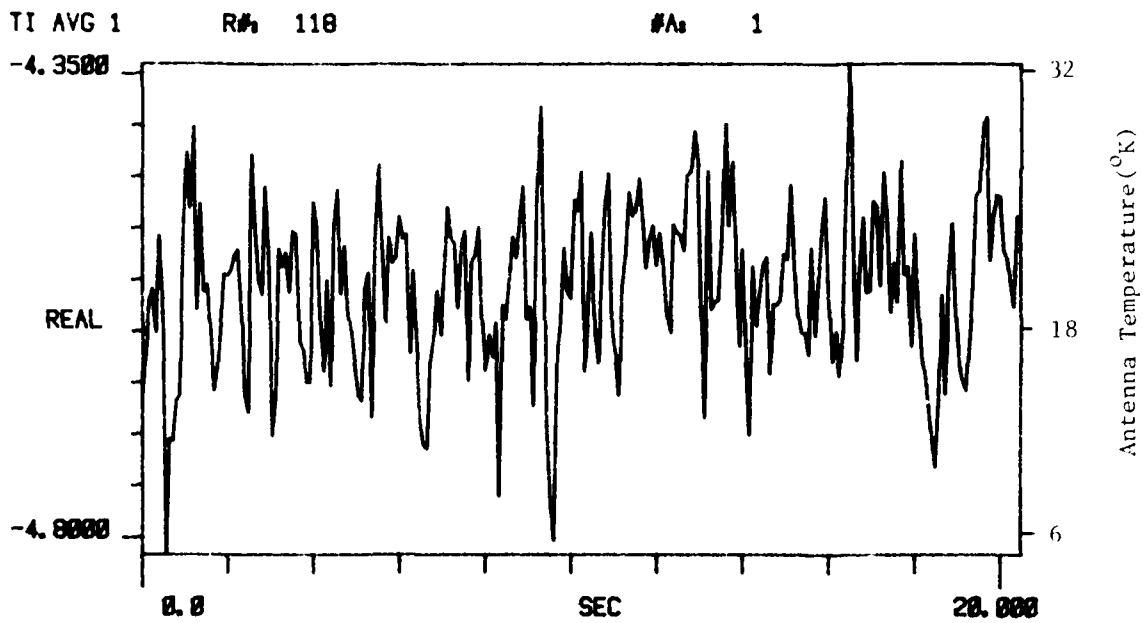
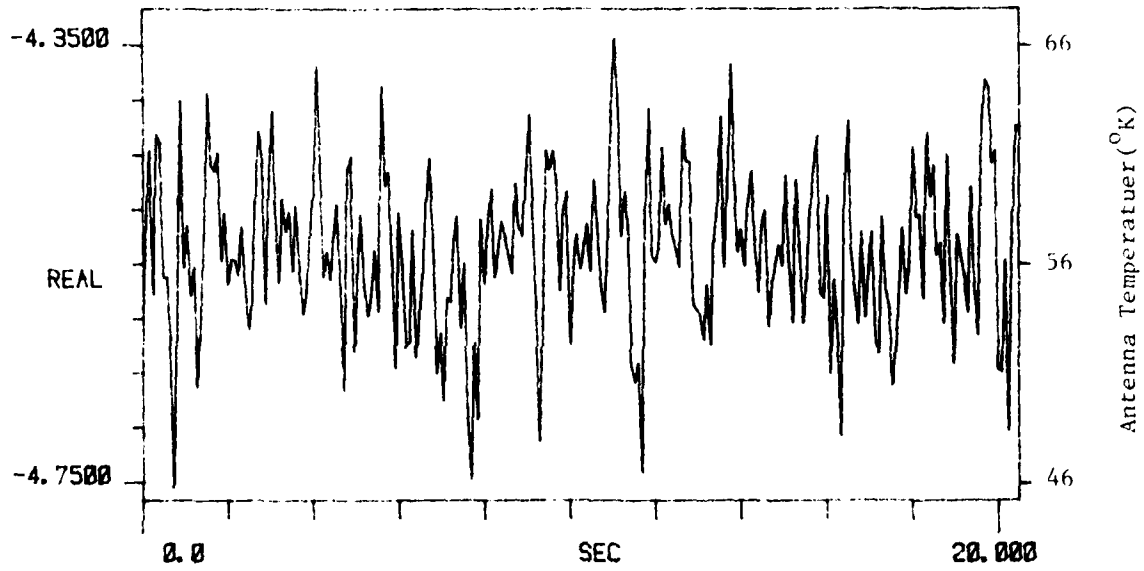


Figure D-2. Zenith Sky Measurement. 29 Feb 80

TI AVG 1

R# 12

#A 1



TI AVG
20.000

R# 12

#A 1

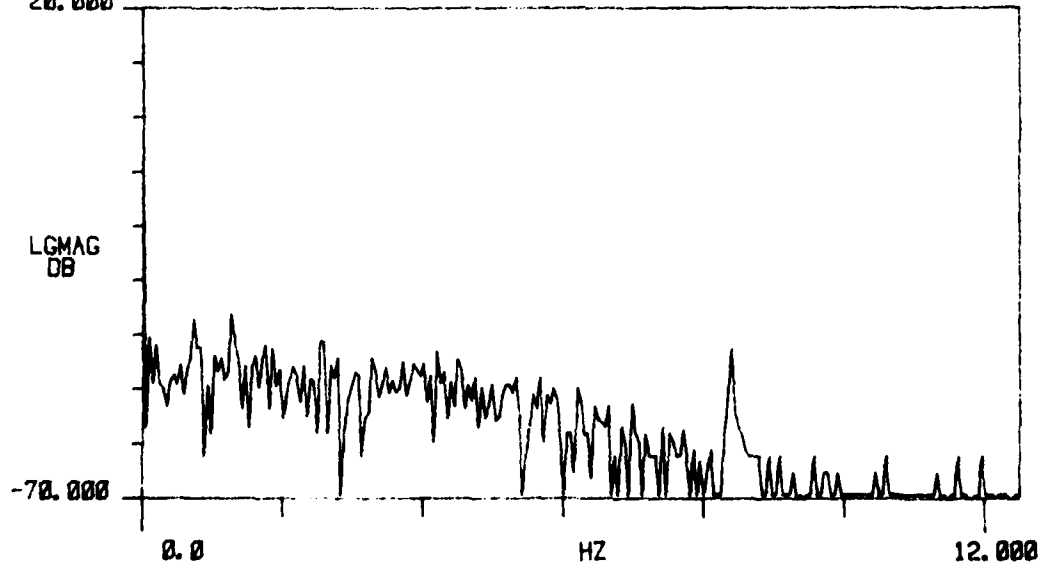
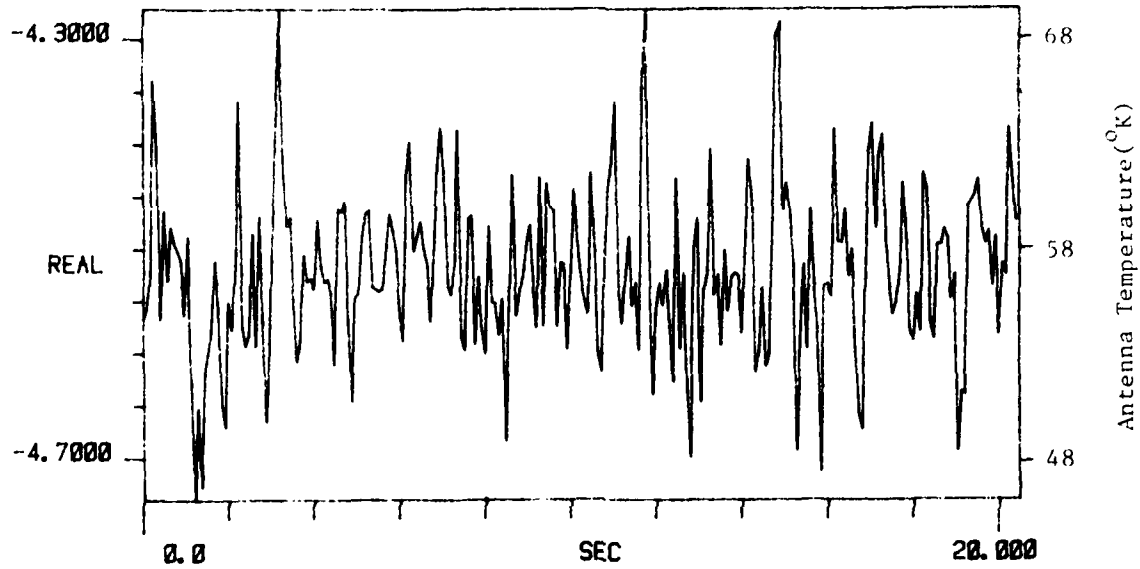


Figure D-2. Zenith Sky Measurement. 29 Feb 80

TI AVG 1

R# 13

#A 1



TI AVG
20.000

R# 13

#A 1

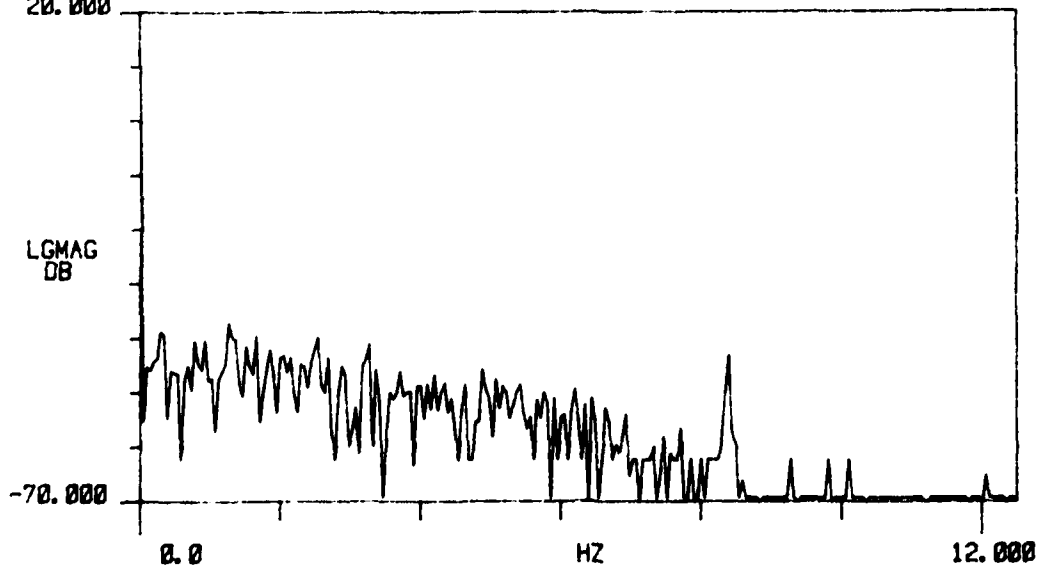
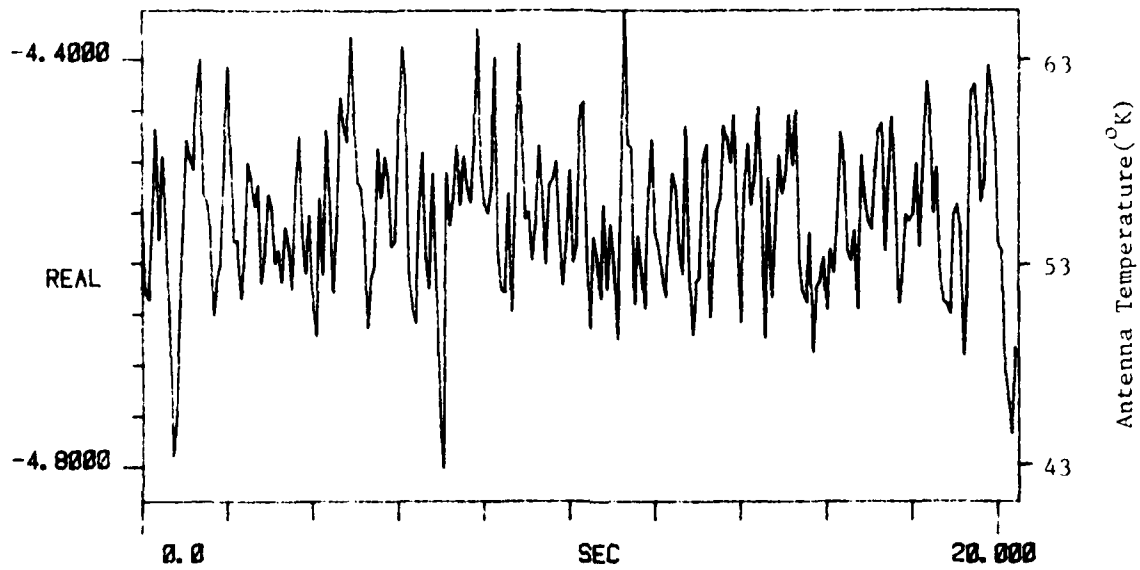


Figure D-2. Zenith Sky Measurement. 29 Feb 80

TI AVG 1

R# 14

#A 1



TI AVG 1
20.000

R# 14

#A 1

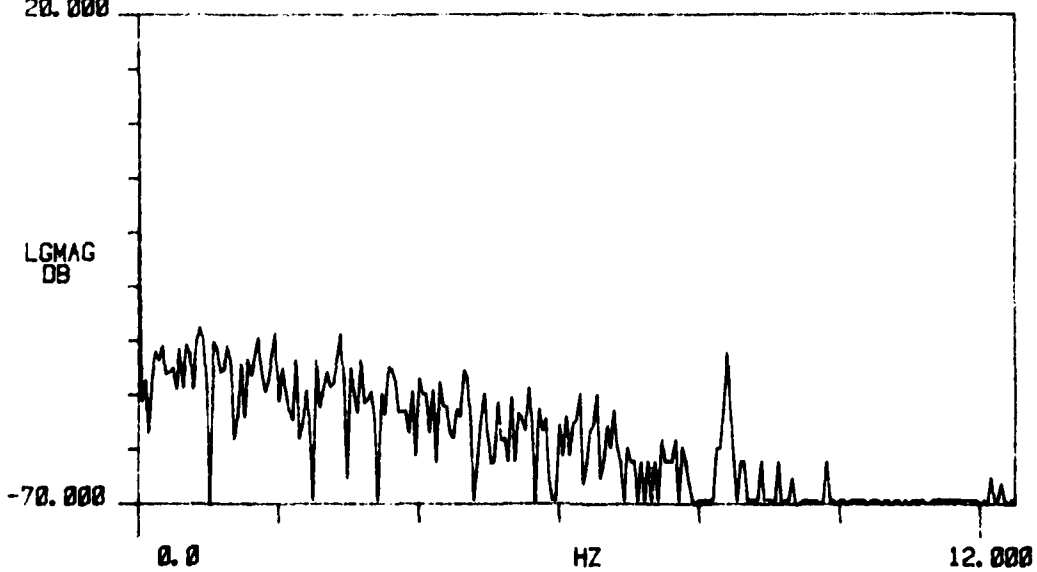


Figure D-2. Zenith Sky Measurement. 29 Feb 80

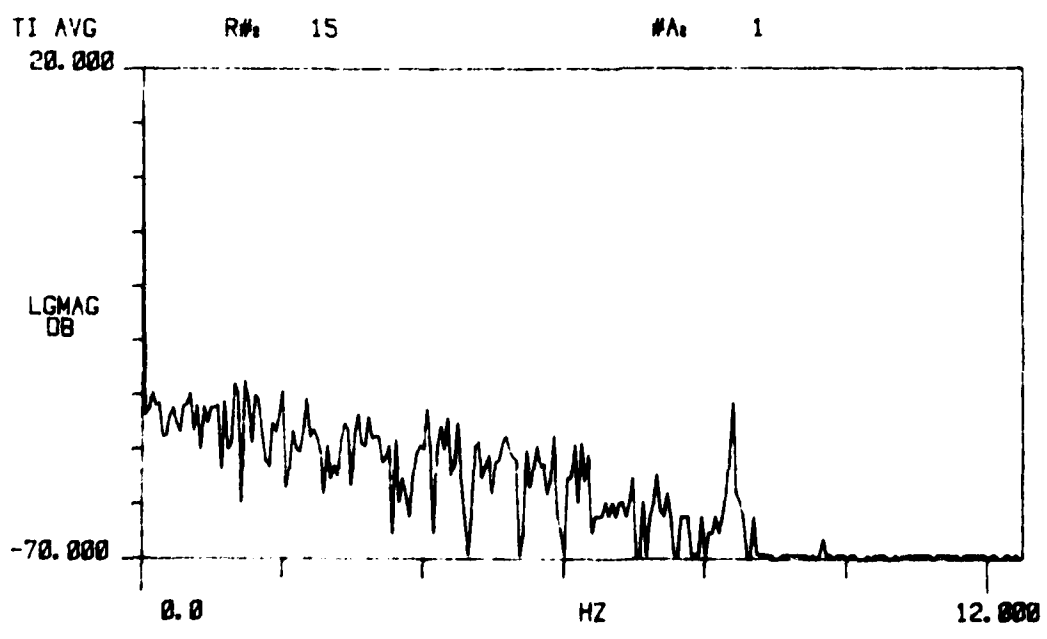
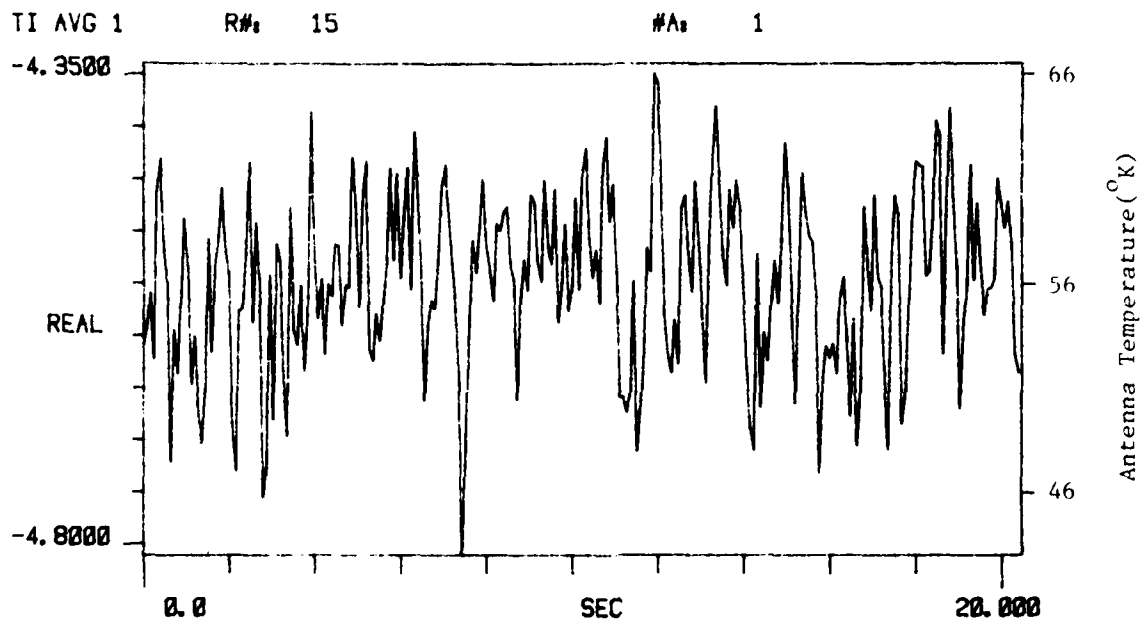


Figure D-2. Zenith Sky Measurement, 29 Feb 80

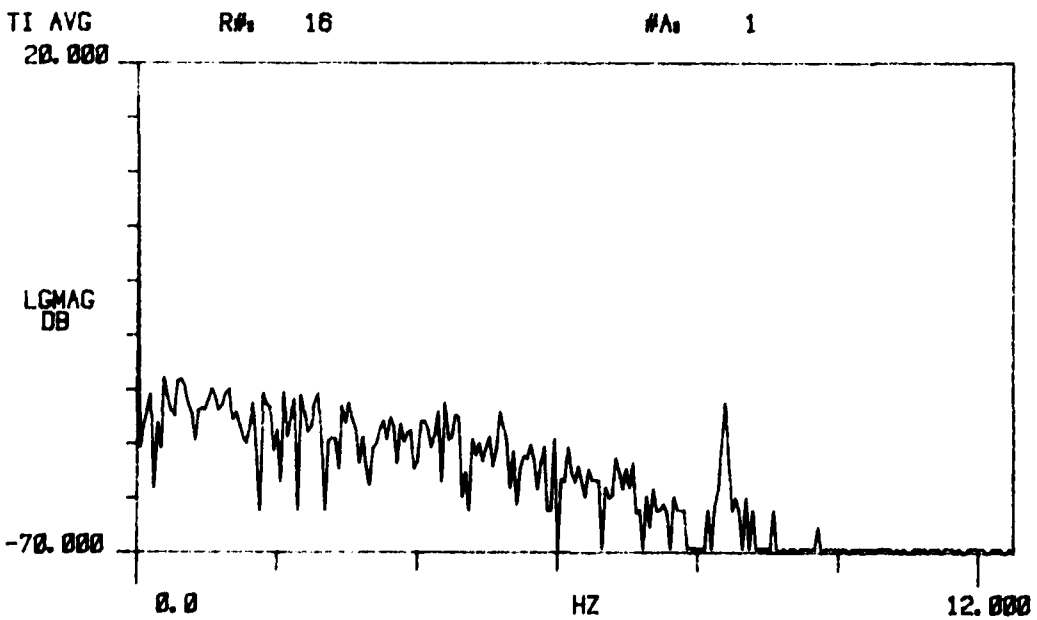
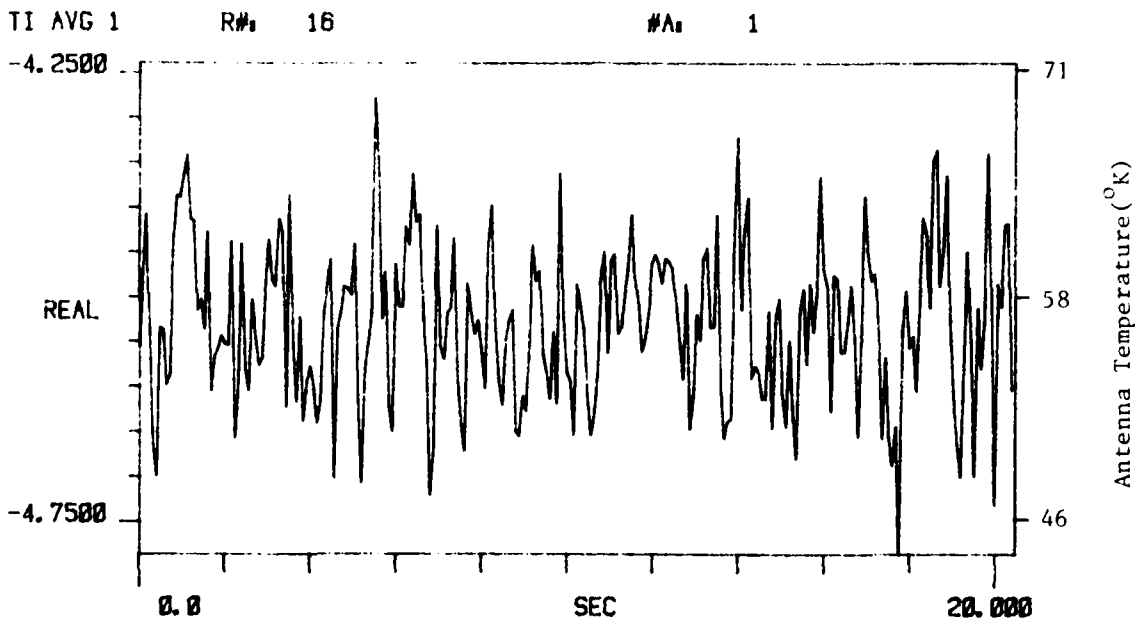


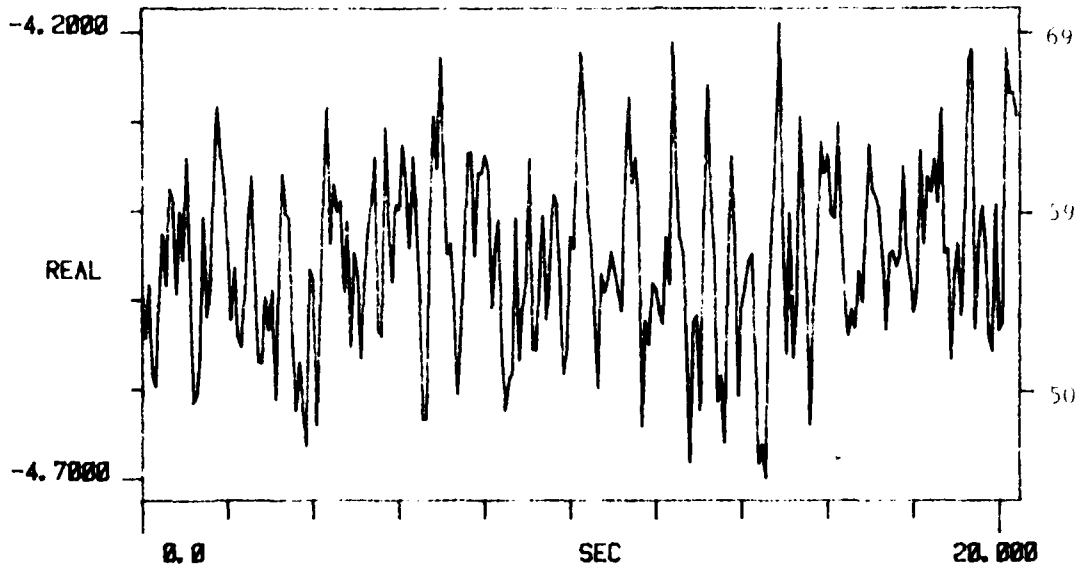
Figure D-2. Zenith Sky Measurement. 29 Feb 80

D-3. 2 March 1980
Zenith Sky Measurements

TI AVG 1

R# 36

#A 1



TI AVG
20.000

R# 36

#A 1

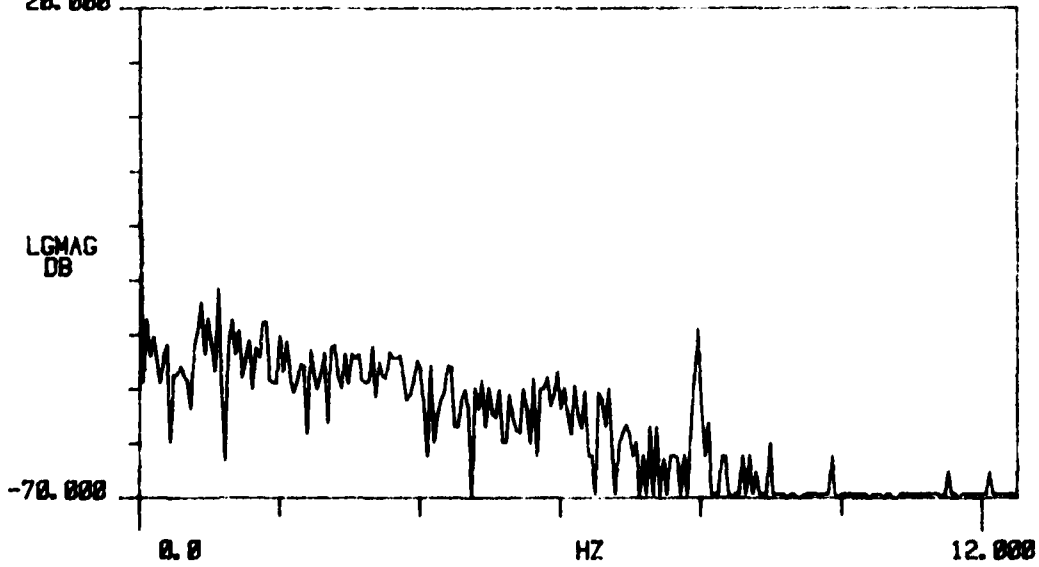
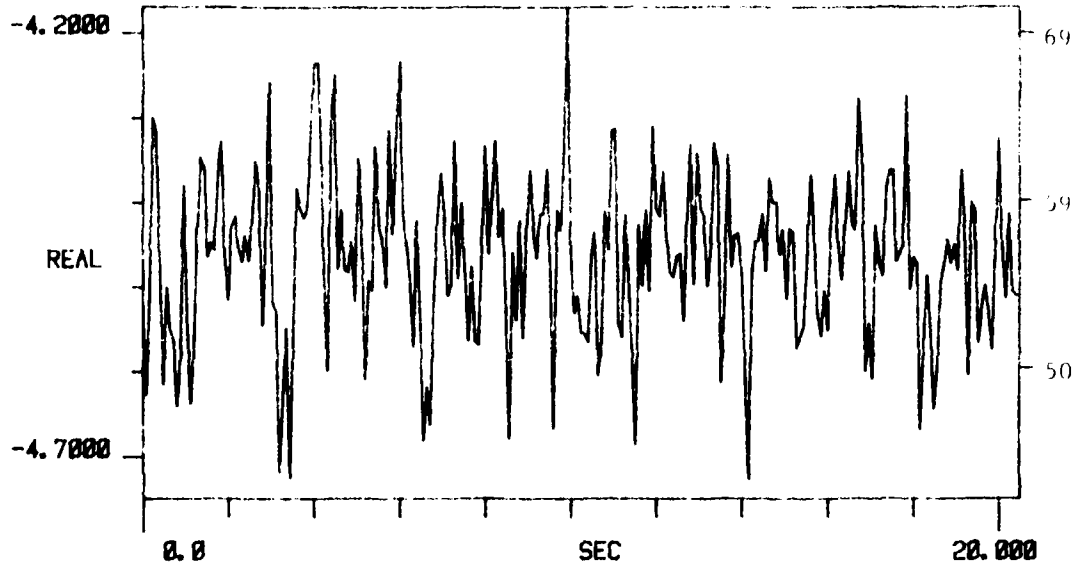


Figure D-3. Zenith Sky Measurement. 2 Mar 80

TI AVG 1

R# 37

#A 1



TI AVG
20.000

R# 37

#A 1

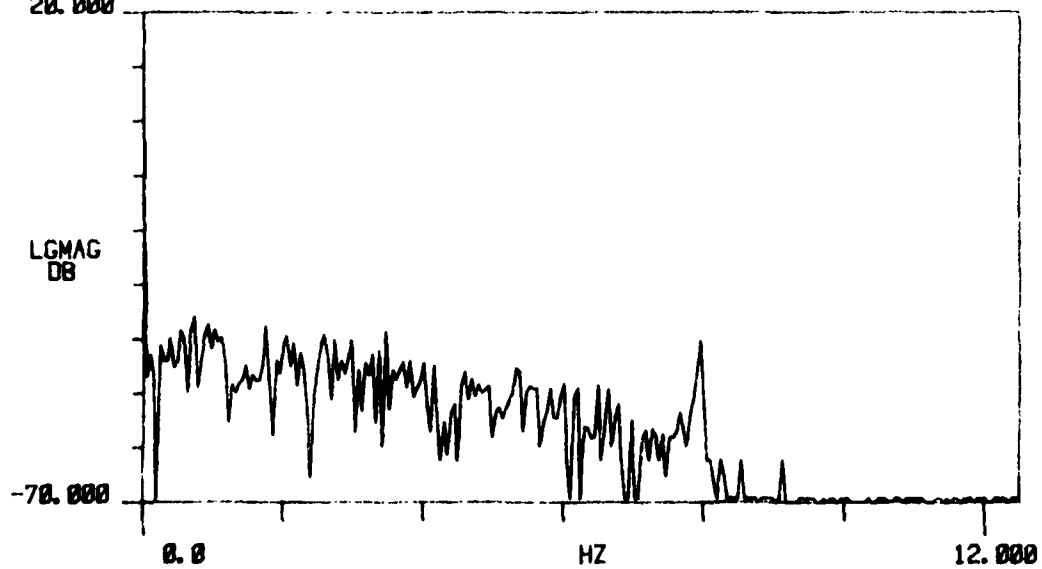
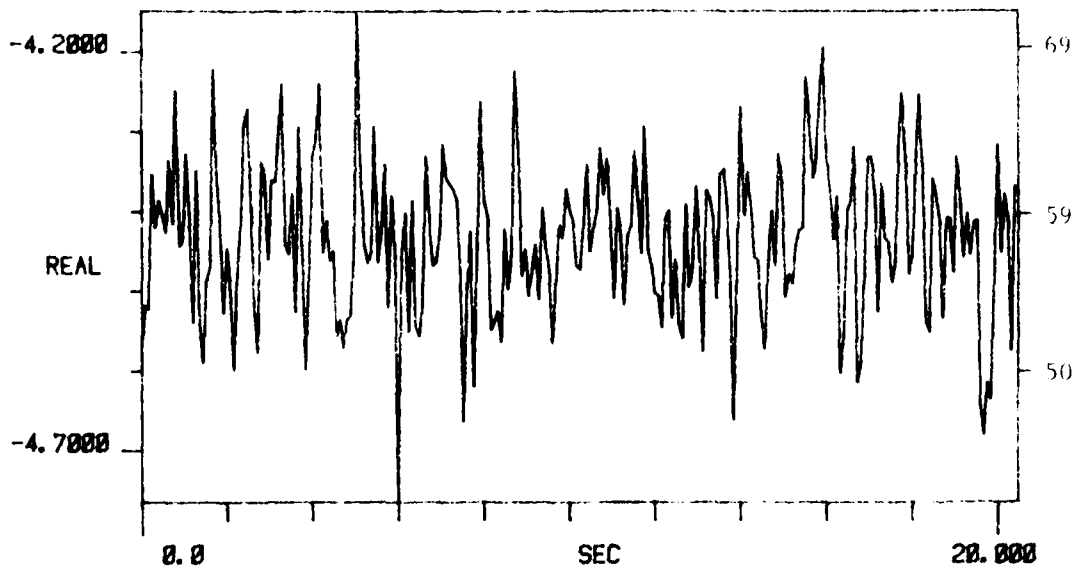


Figure D-3. Zenith Sky Measurement. 2 Mar 80

TI AVG 1

R# 38

#A 1



TI AVG
20.000

R# 38

#A 1

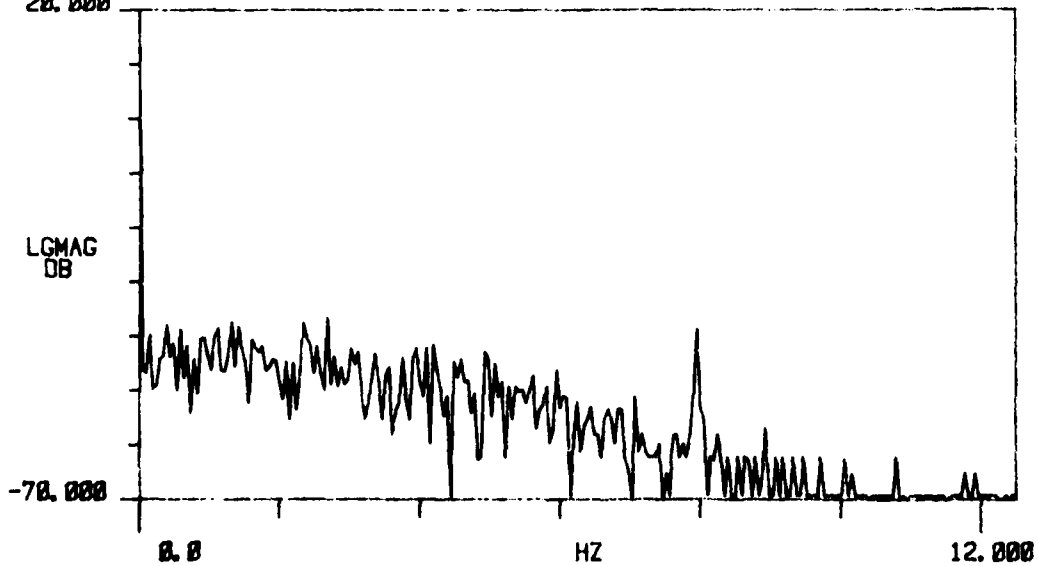
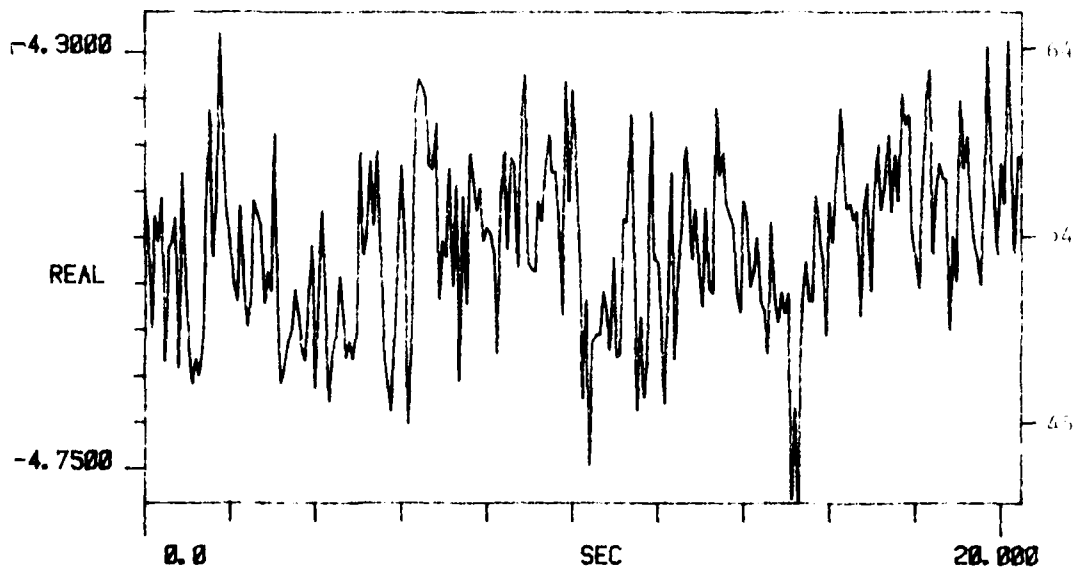


Figure D-3. Zenith Sky Measurement. 2 Mar 80

J1 AVG 1 R# 39 #A 1



TI AVG R# 39 #A 1

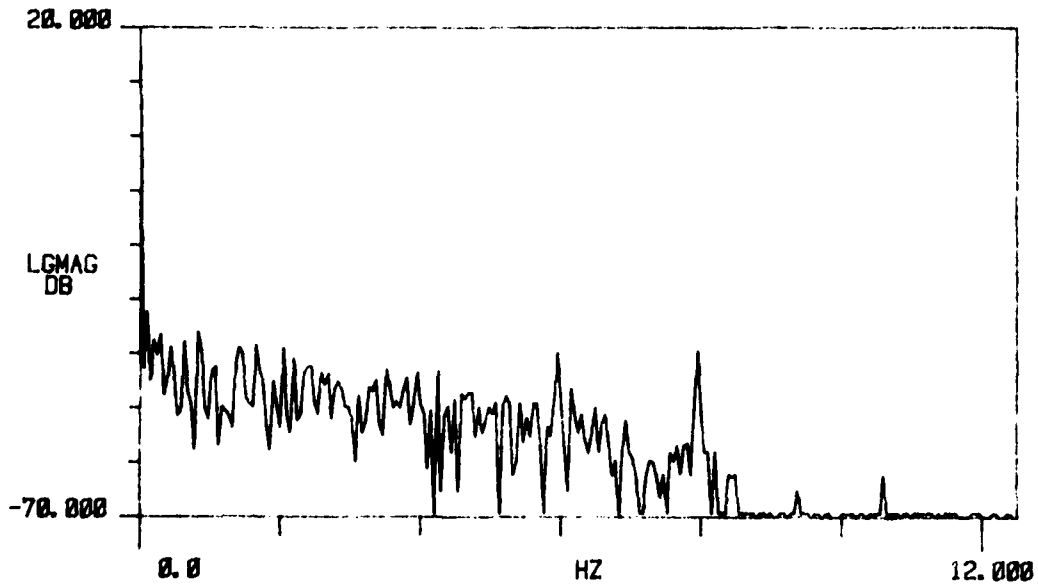
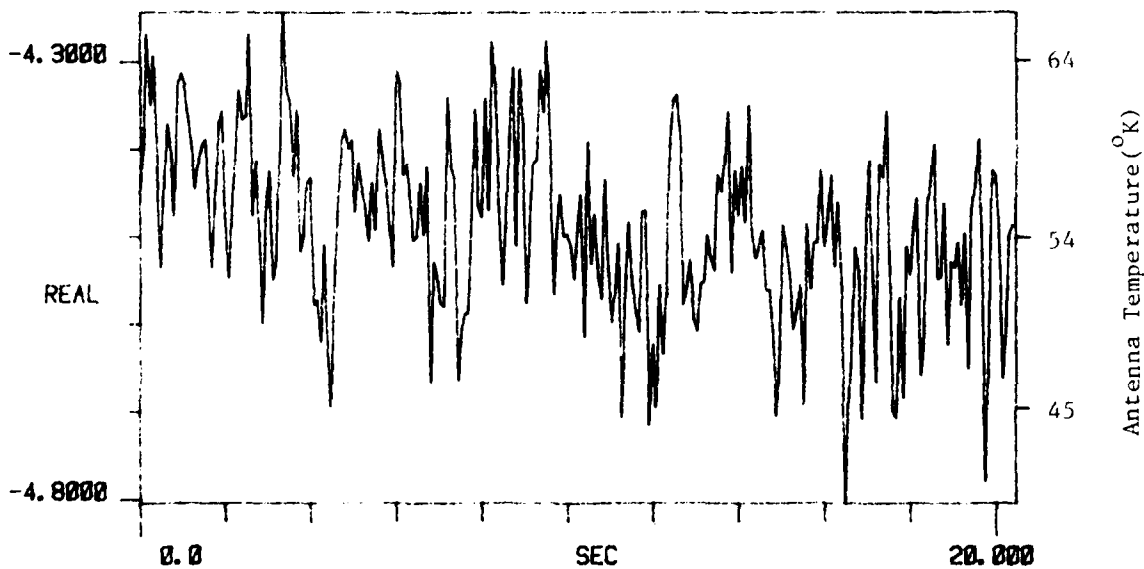


Figure D-3. Zenith Sky Measurement. 2 Mar 80

TI AVG 1

R# 40

#A 1



TI AVG
20.000

R# 40

#A 1

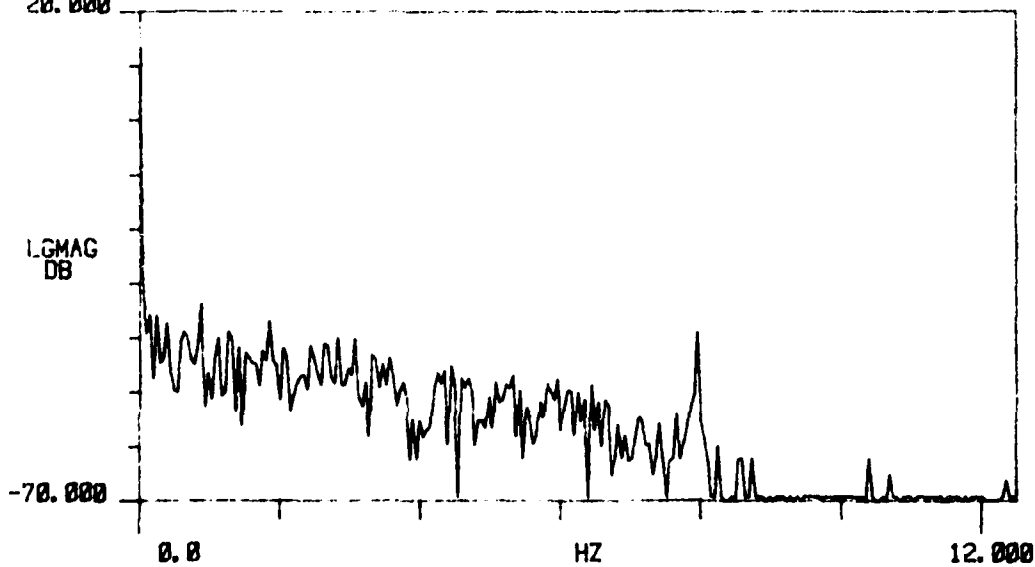
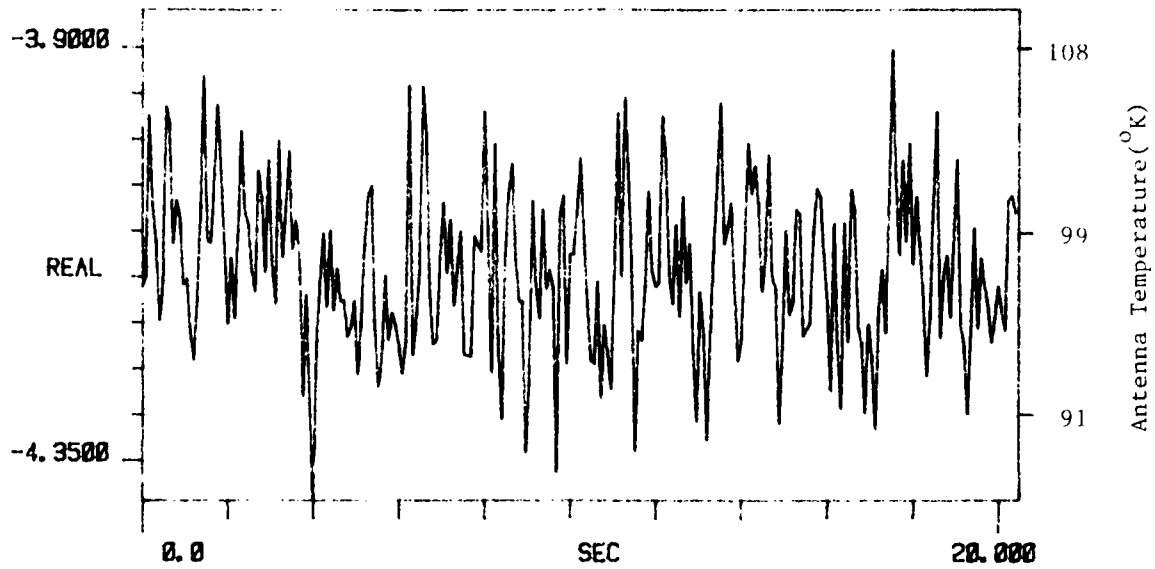


Figure D-3. Zenith Sky Measurement. 2 Mar 80

TI AVG 1

R# 45

#A 1



TI AVG
20.000

R# 45

#A 1

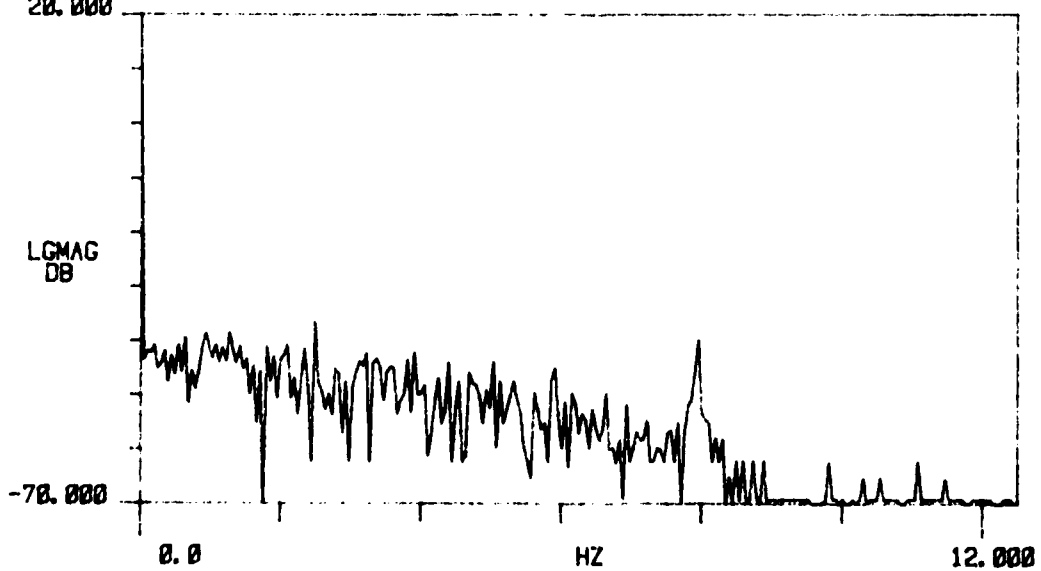


Figure D-3. Zenith Sky Measurement. 2 Mar 80

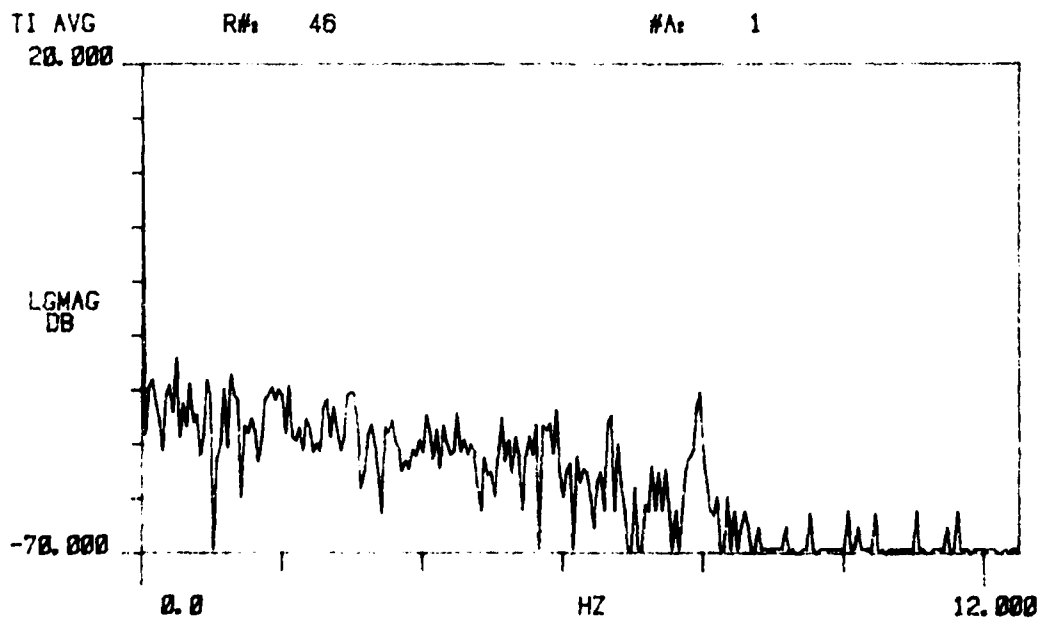
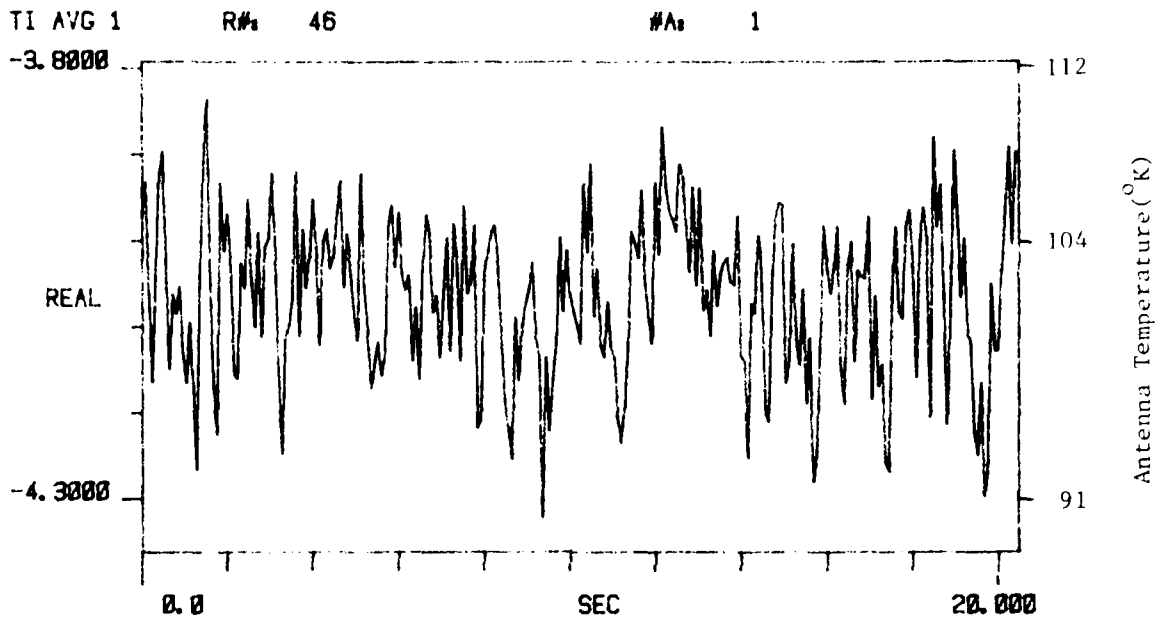
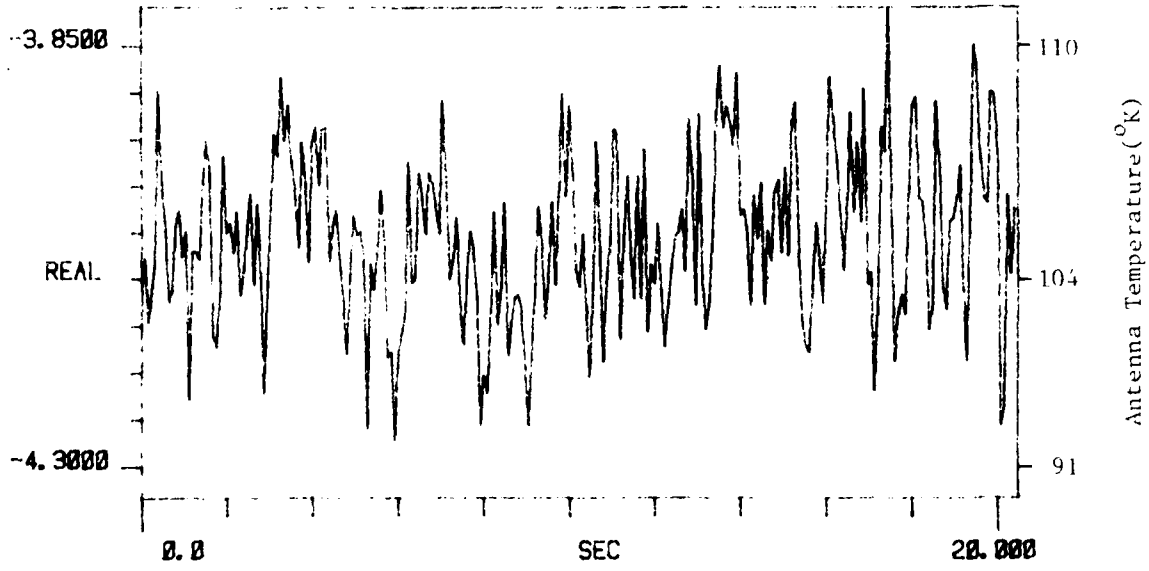


Figure D-3. Zenith Sky Measurement. 2 Mar 80

TI AVG 1

R# 47

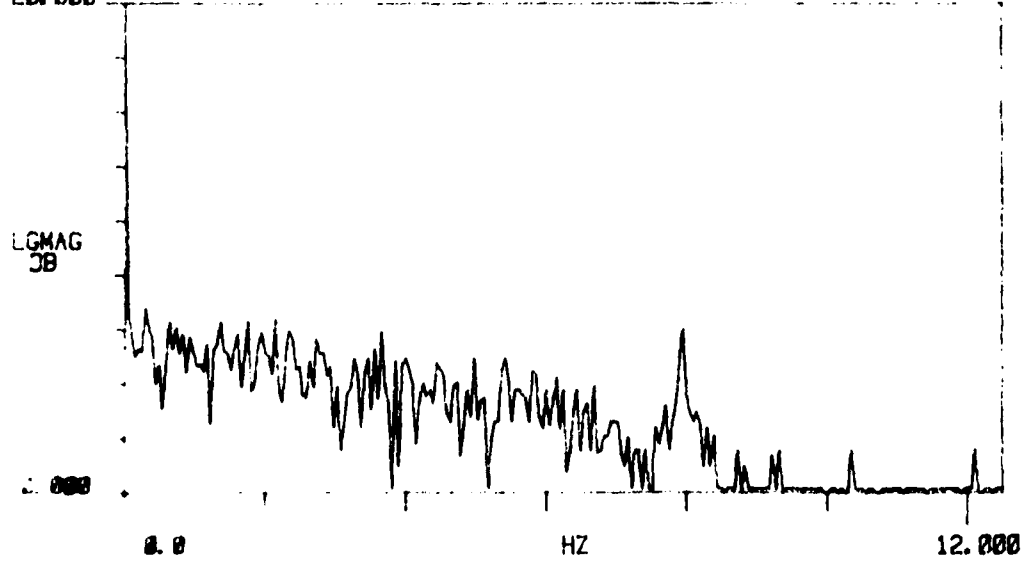
#A 1



TI AVG
20.000

R# 47

#A 1



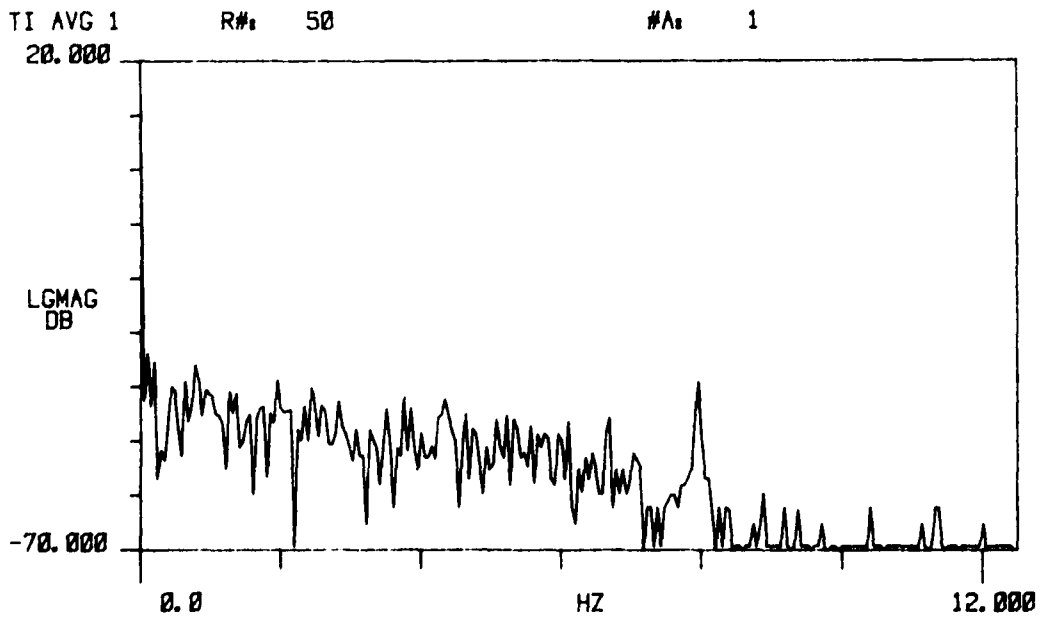
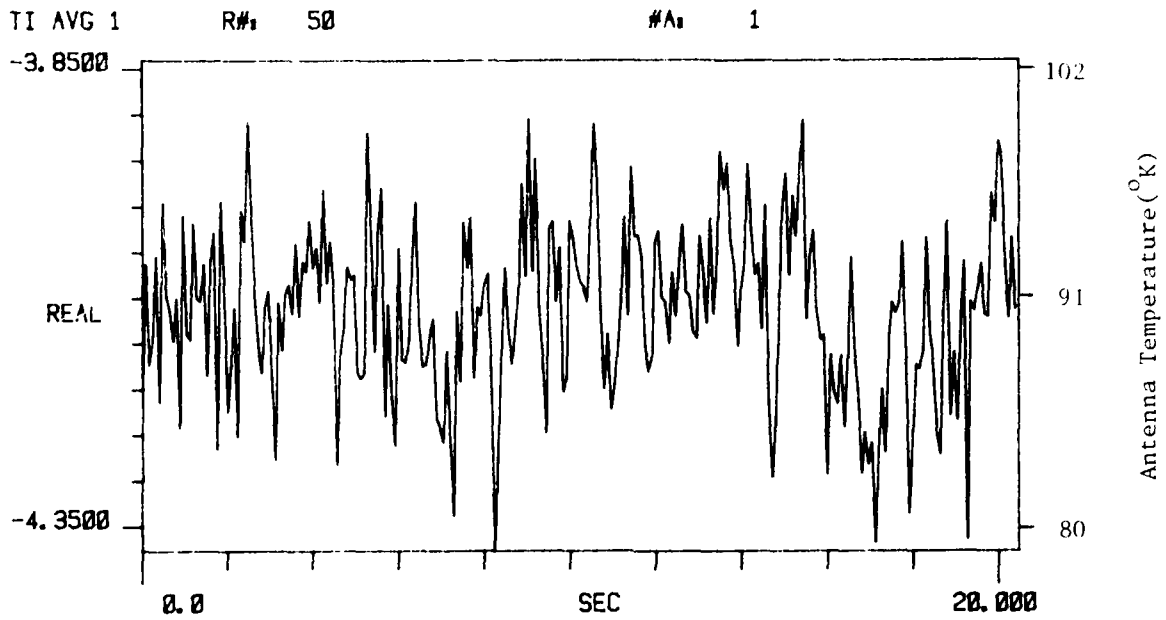
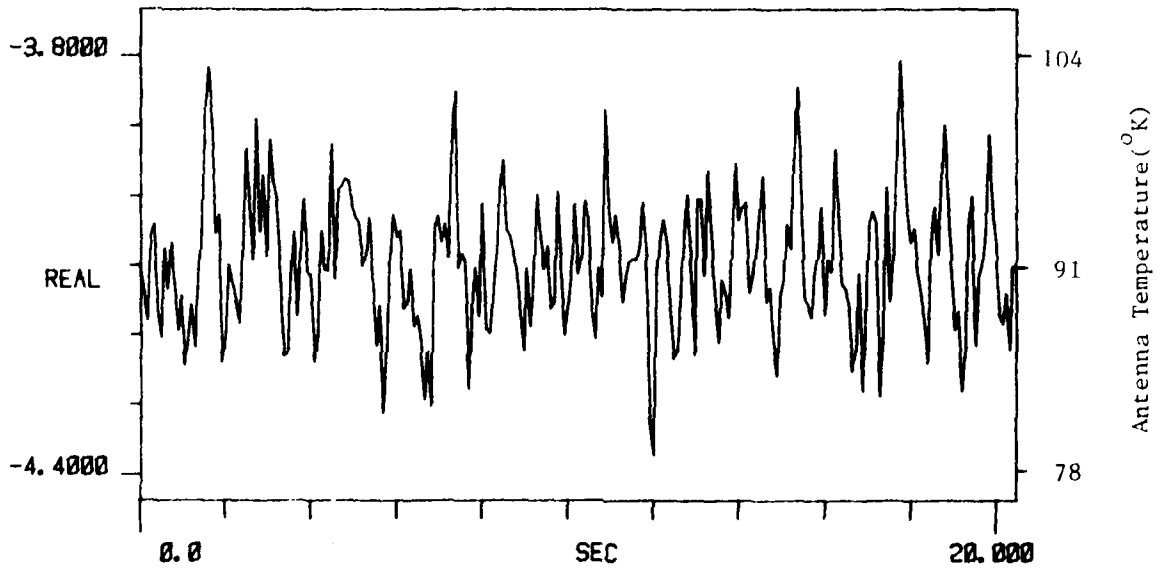


Figure D-3. Zenith Sky Measurement. 2 Mar 80

TI AVG 1

R# 51

#A 1



TI AVG
20.000

R# 51

#A 1

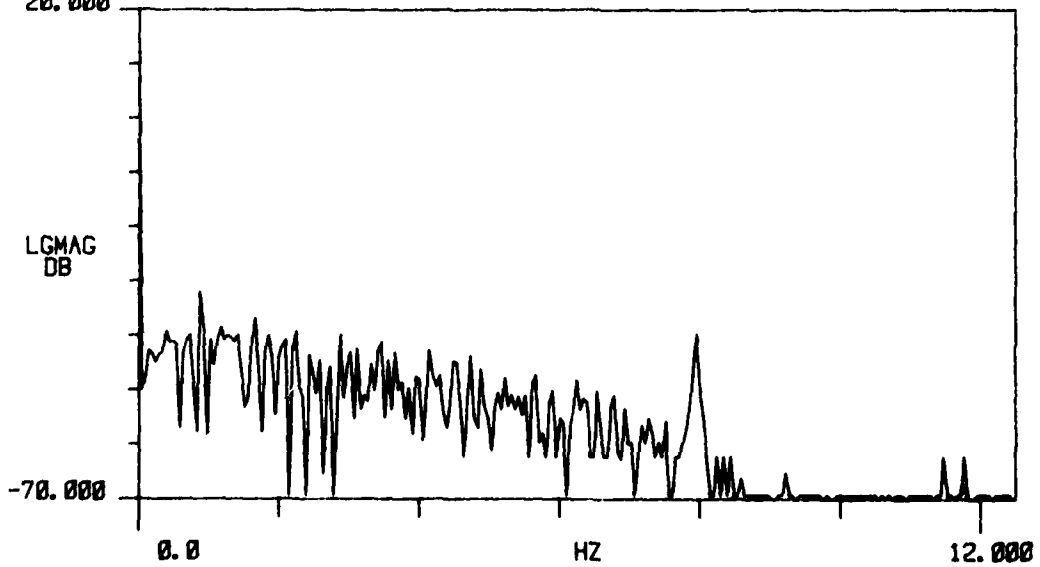
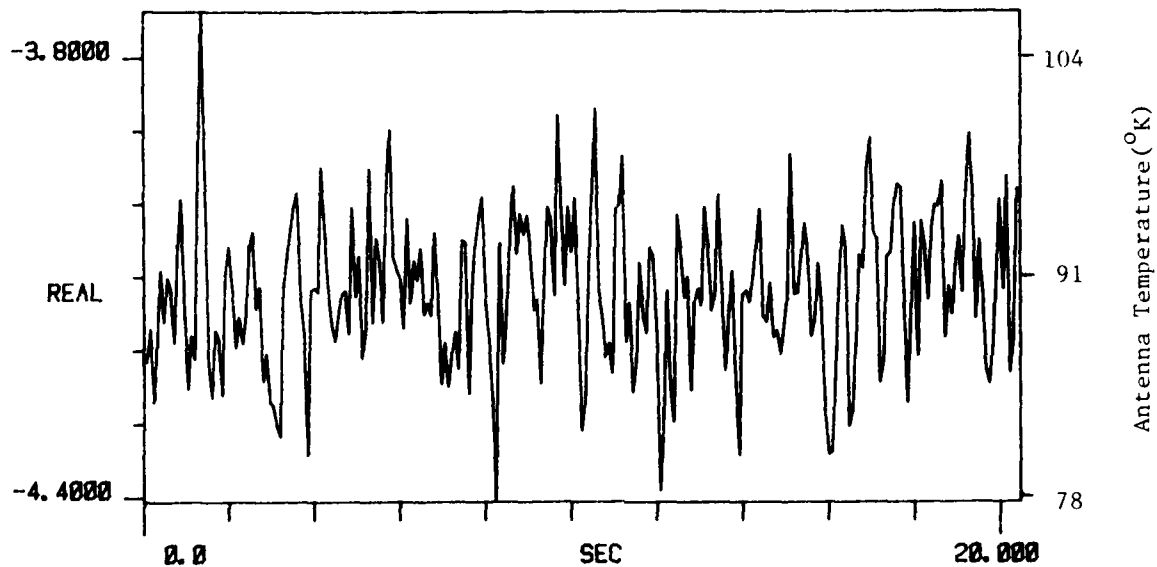


Figure D-3. Zenith Sky Measurement. 2 Mar 80

TI AVG 1

R# 52

#A 1



TI AVG

R# 52

#A 1

20.000

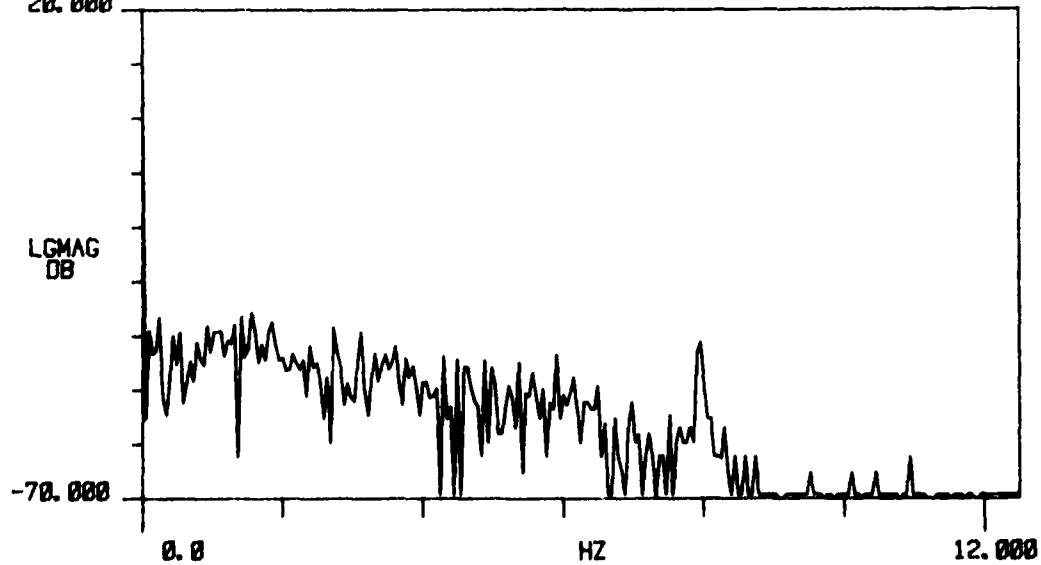


Figure D-3. Zenith Sky Measurement. 2 Mar 80

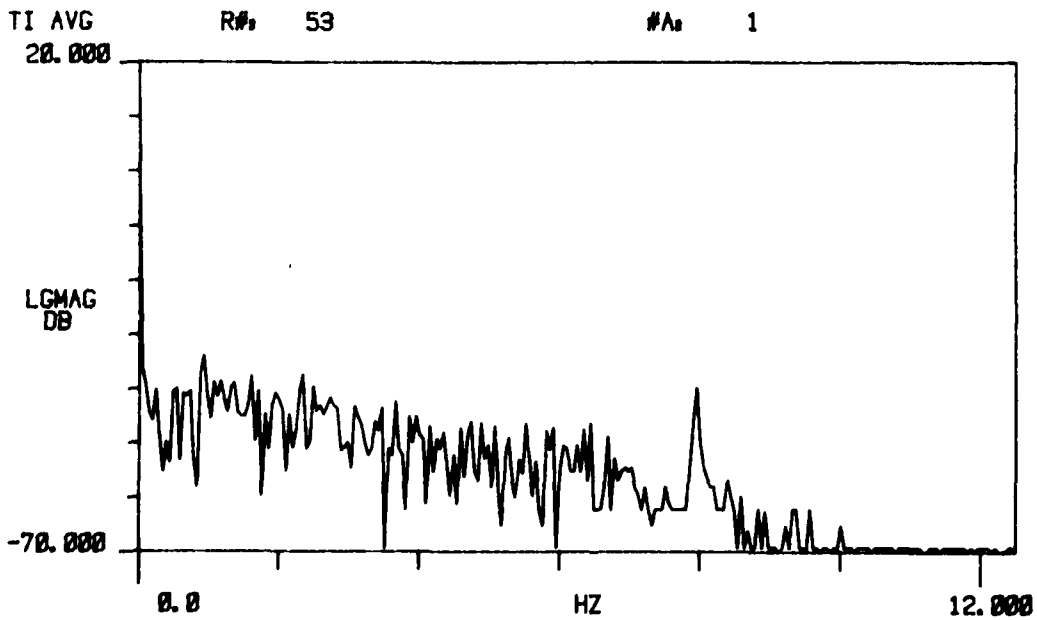
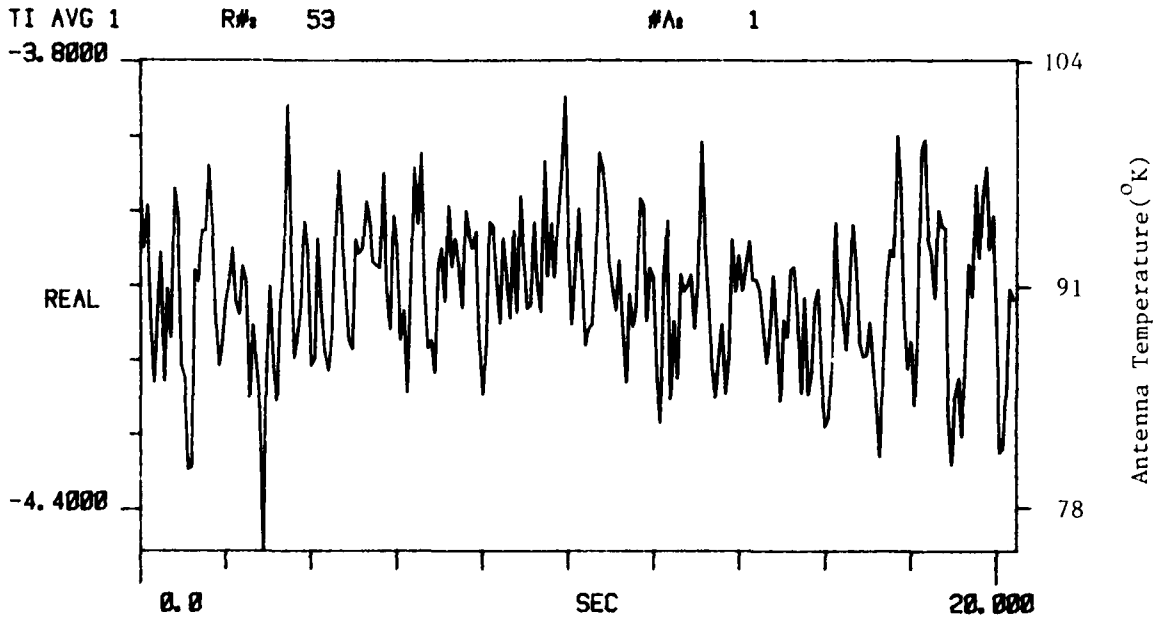


Figure D-3. Zenith Sky Measurement. 2 Mar 80

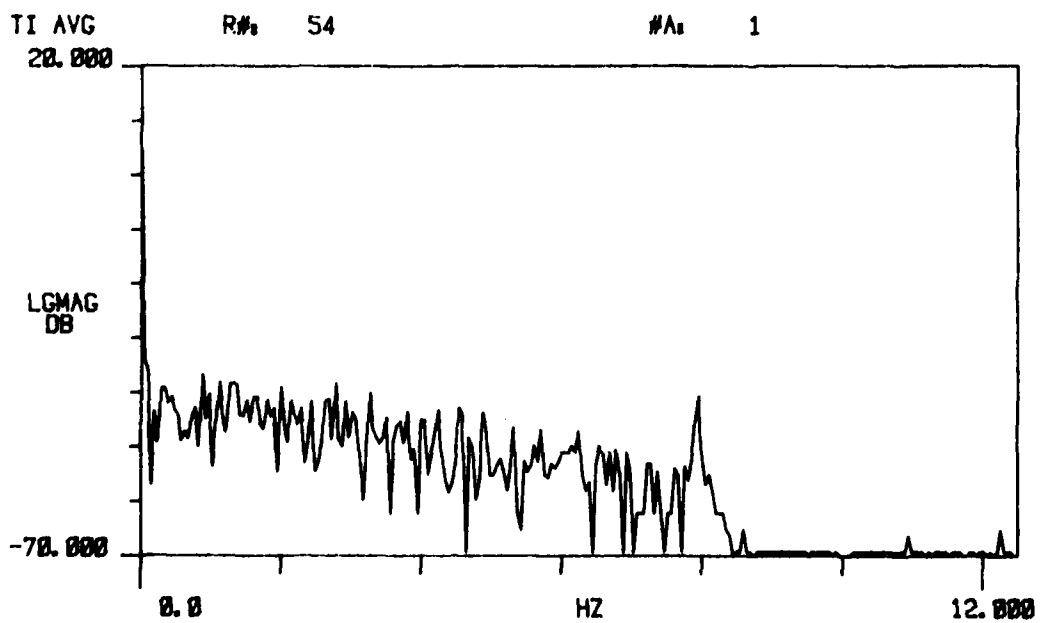
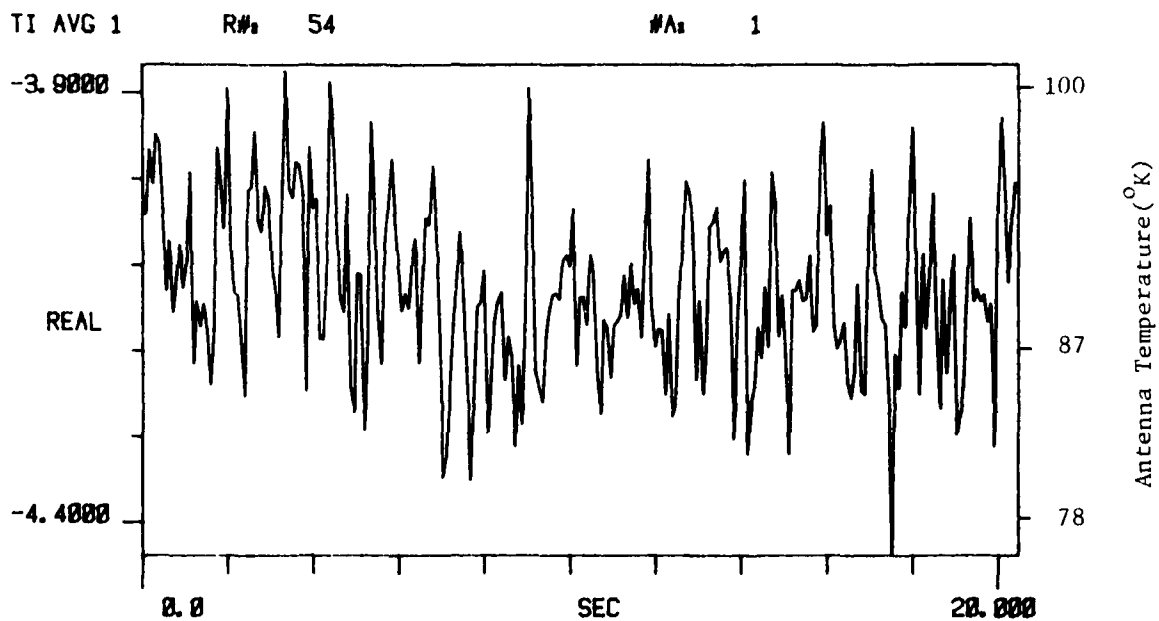
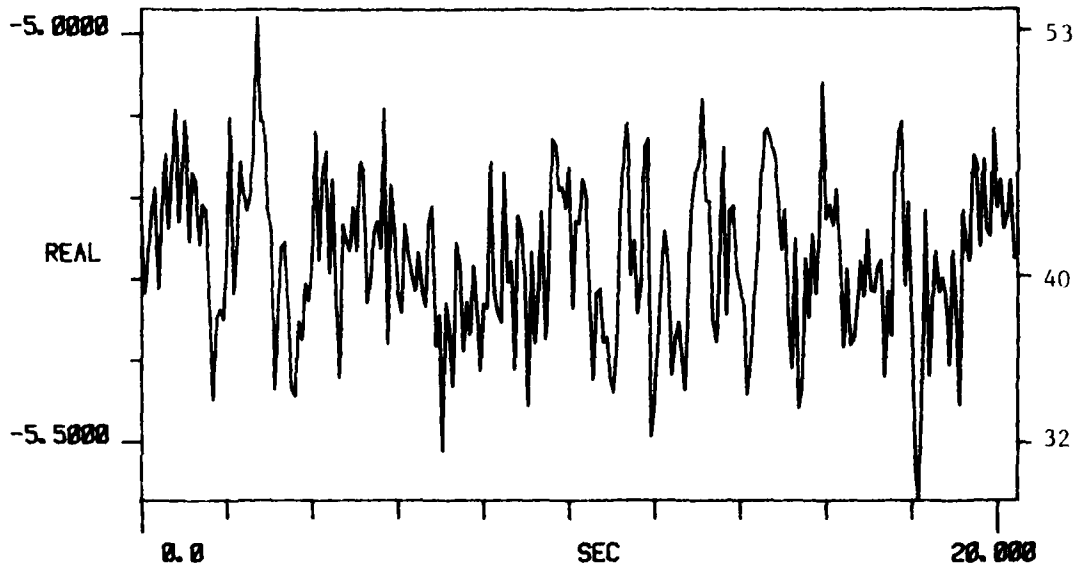


Figure D-3. Zenith Sky Measurement. 2 Mar 80

TI AVG 1

R# 60

#A 1



TI AVG 1
20.000

R# 60

#A 1

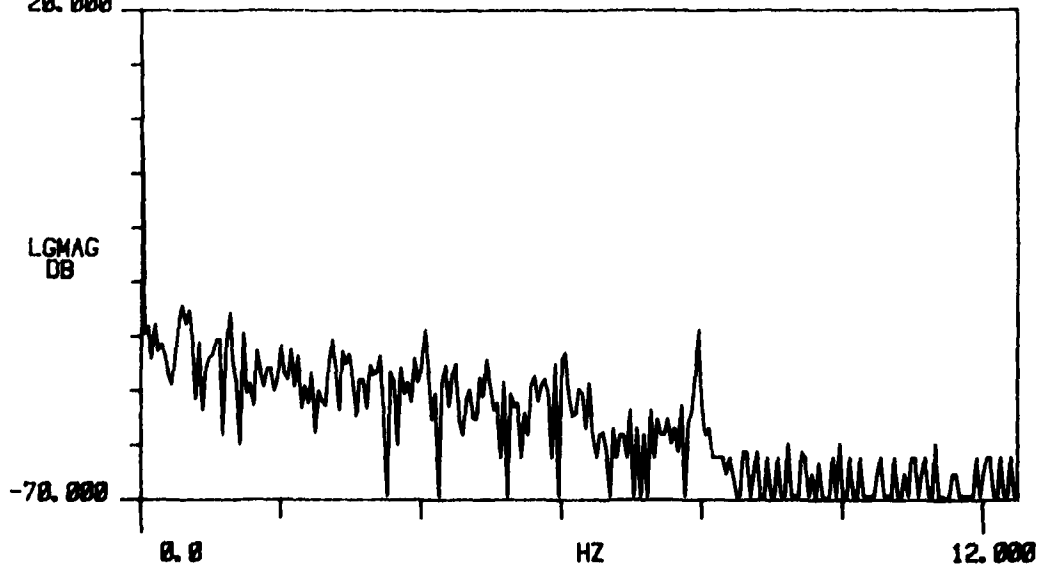
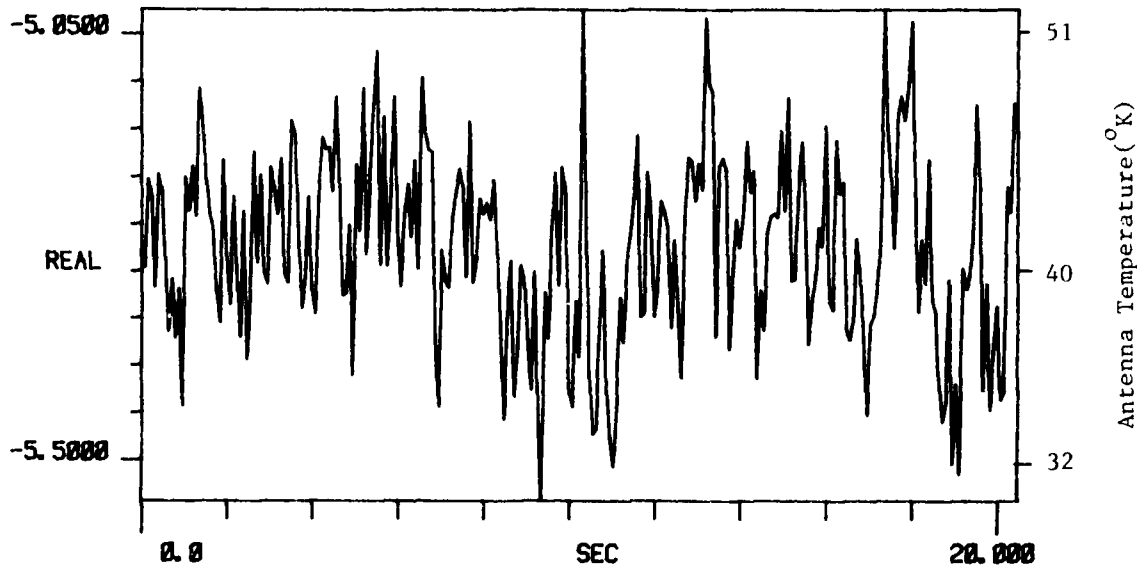


Figure D-3. Zenith Sky Measurement. 2 Mar 80

TI AVG 1

R# 61

#A 1



TI AVG
20.000

R# 61

#A 1

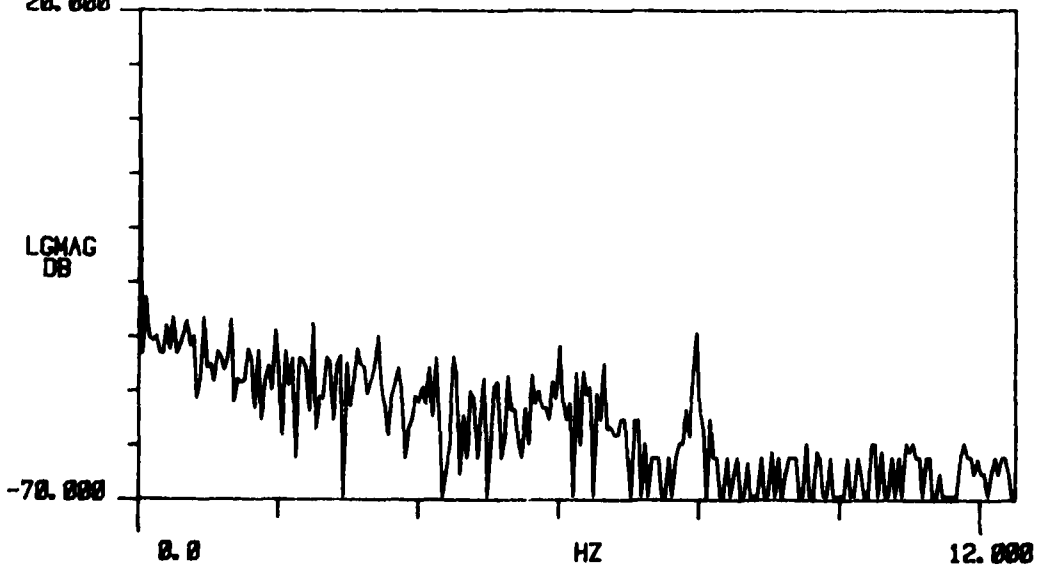
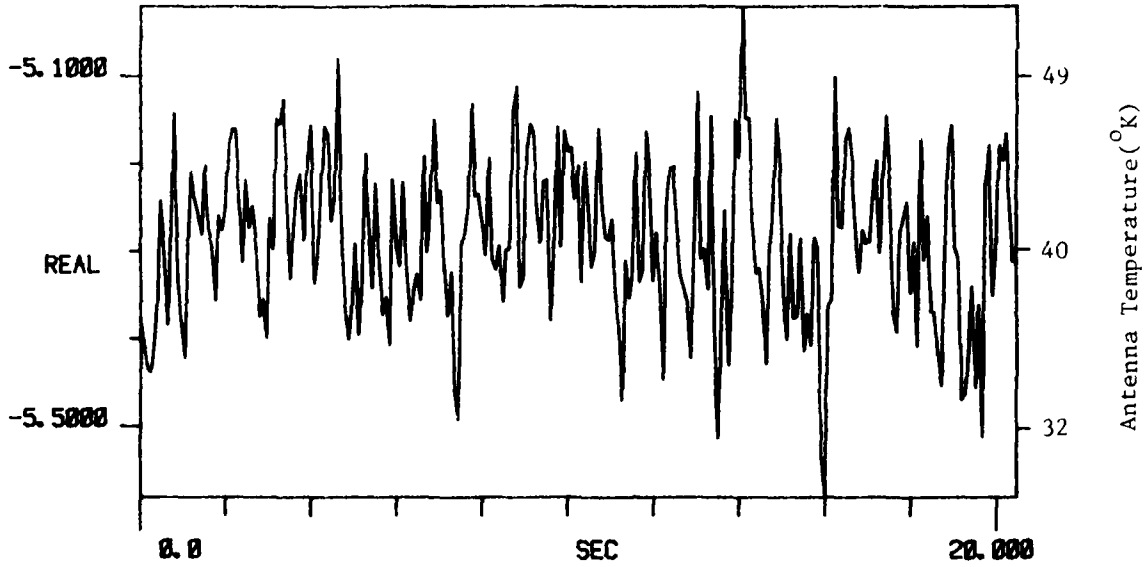


Figure D-3. Zenith Sky Measurement. 2 Mar 80
180

TI AVG 1

R# 62

#A 1



TI AVG
20.000

R# 62

#A 1

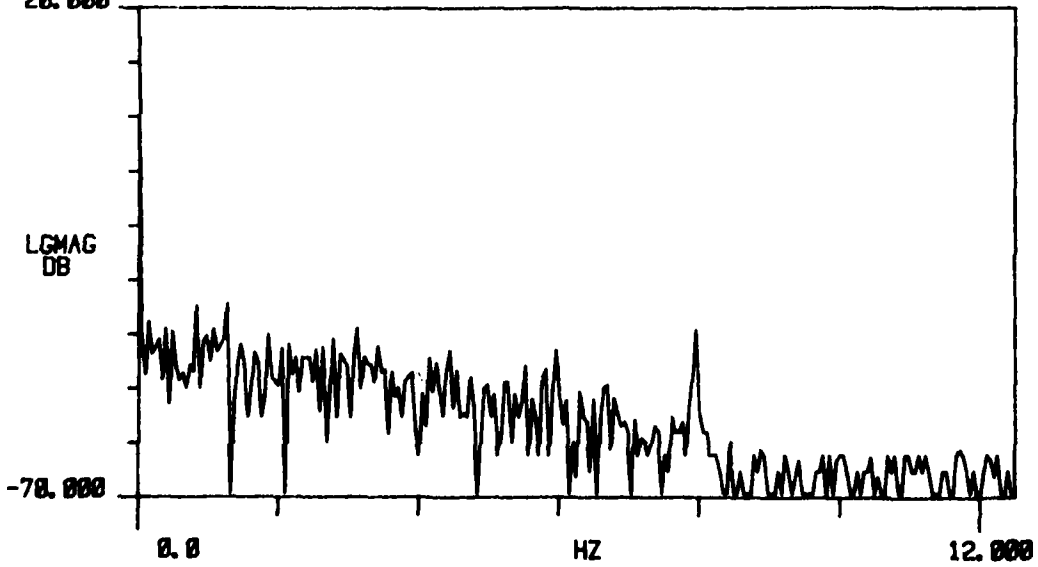
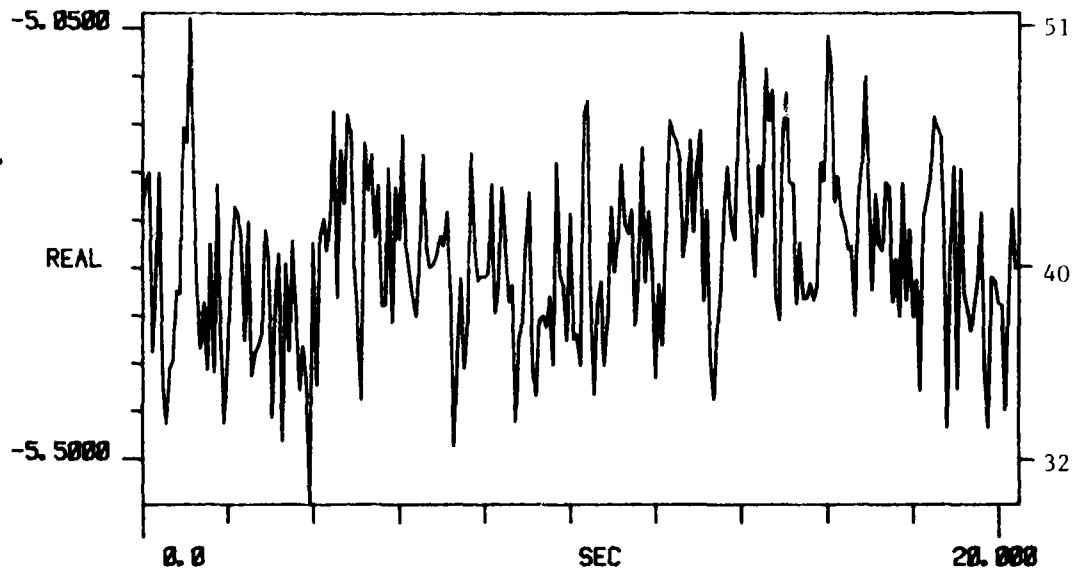


Figure D-3. Zenith Sky Measurement. 2 Mar 80

TI AVG 1

R# 63

#A 1



TI AVG

R# 63

#A 1

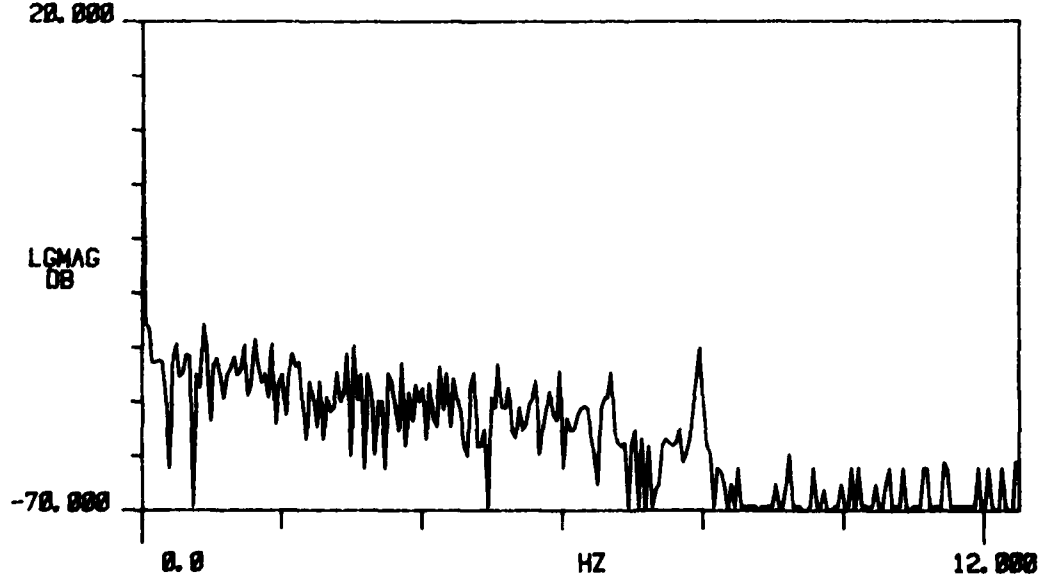
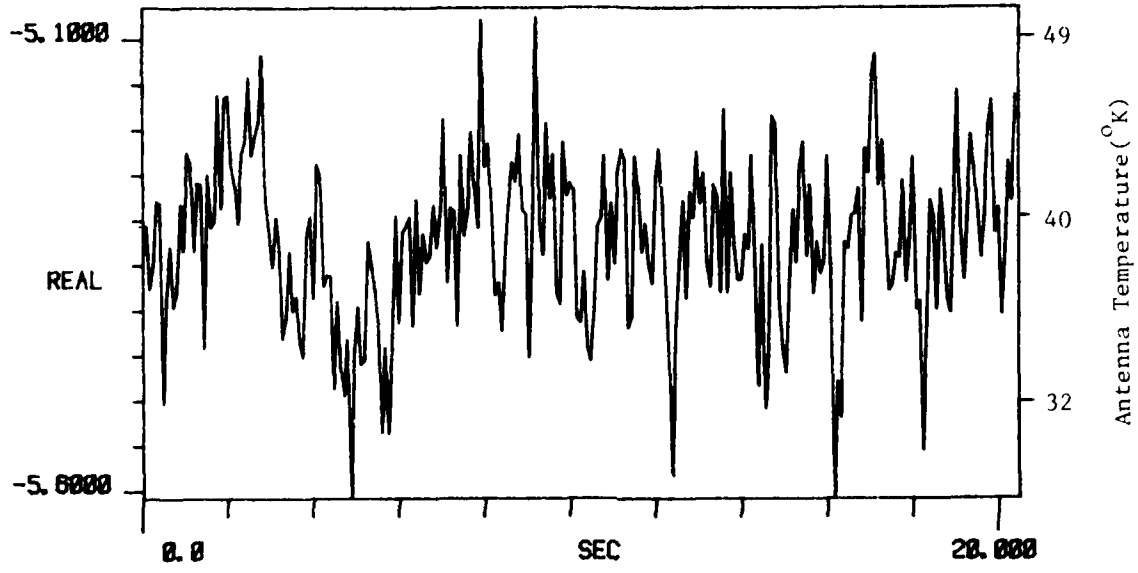


Figure D-3. Zenith Sky Measurement. 2 Mar 80

TI AVG 1

R# 64

#A 1



TI AVG
20.000

R# 64

#A 1

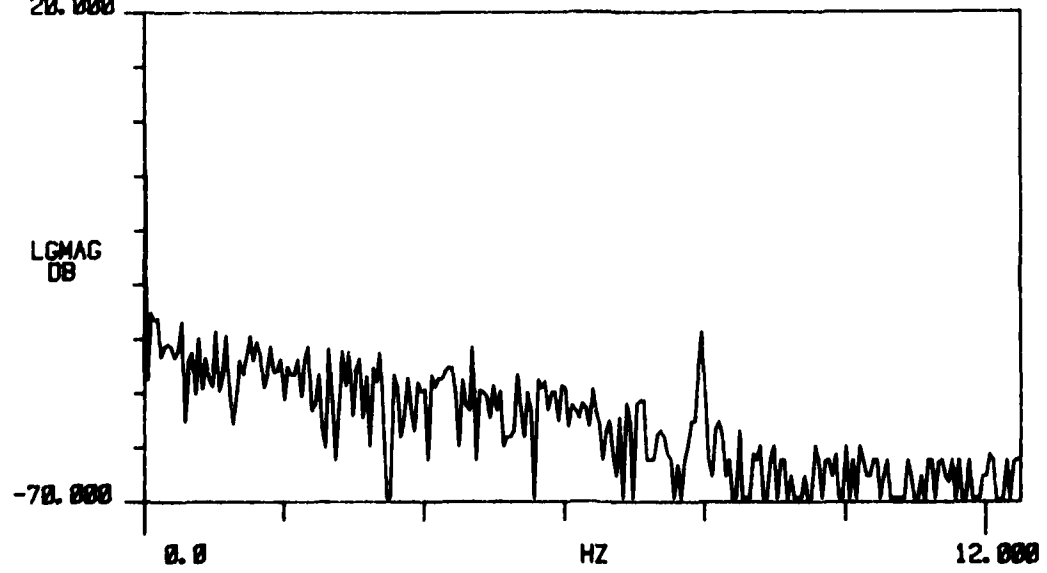
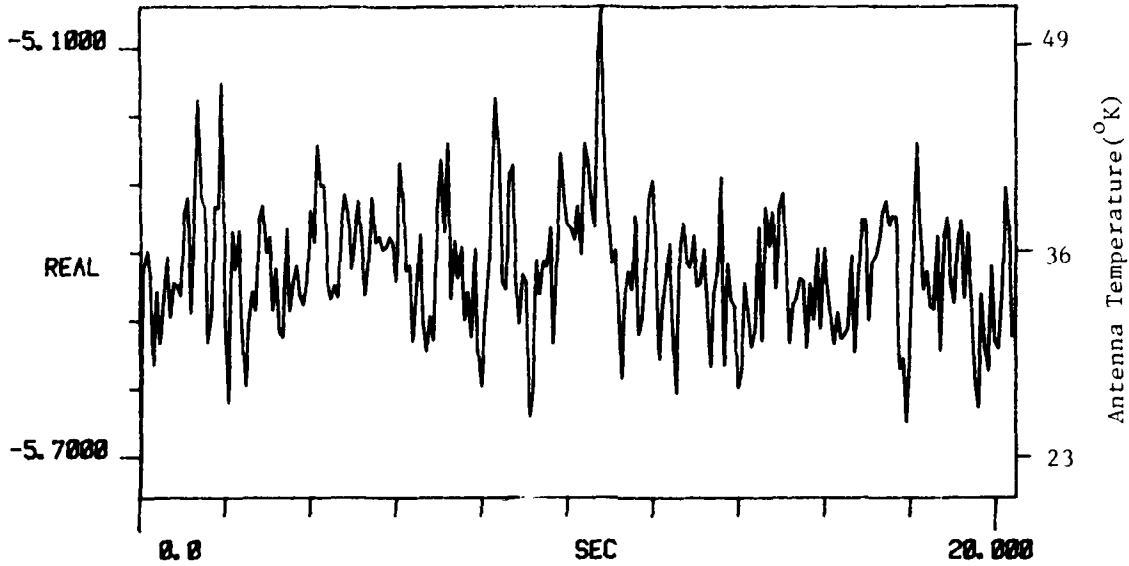


Figure D-3. Zenith Sky Measurement. 2 Mar 80

TI AVG 1

R# 65

#A 1



TI AVG
20.000

R# 65

#A 1

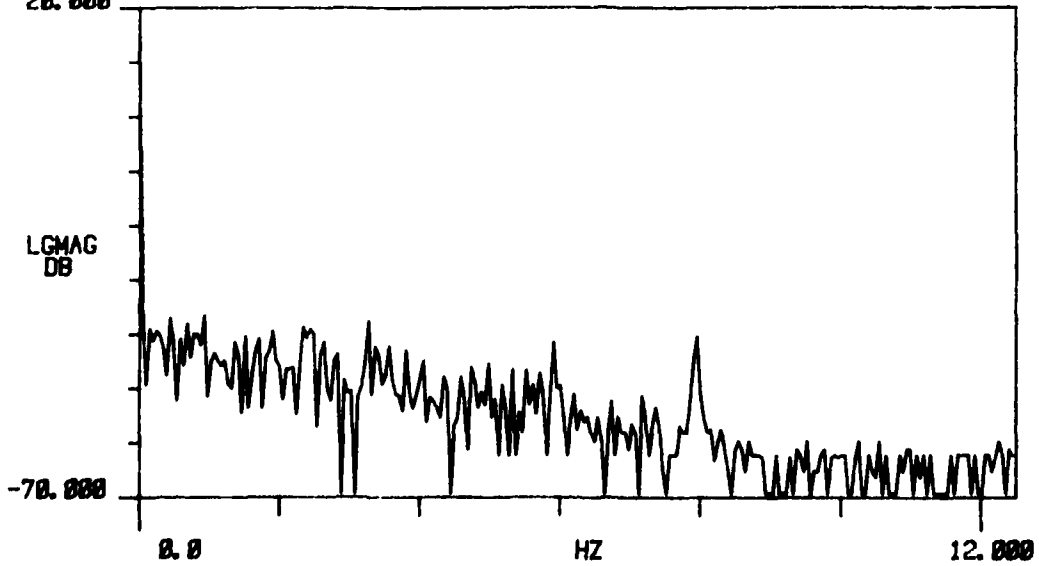
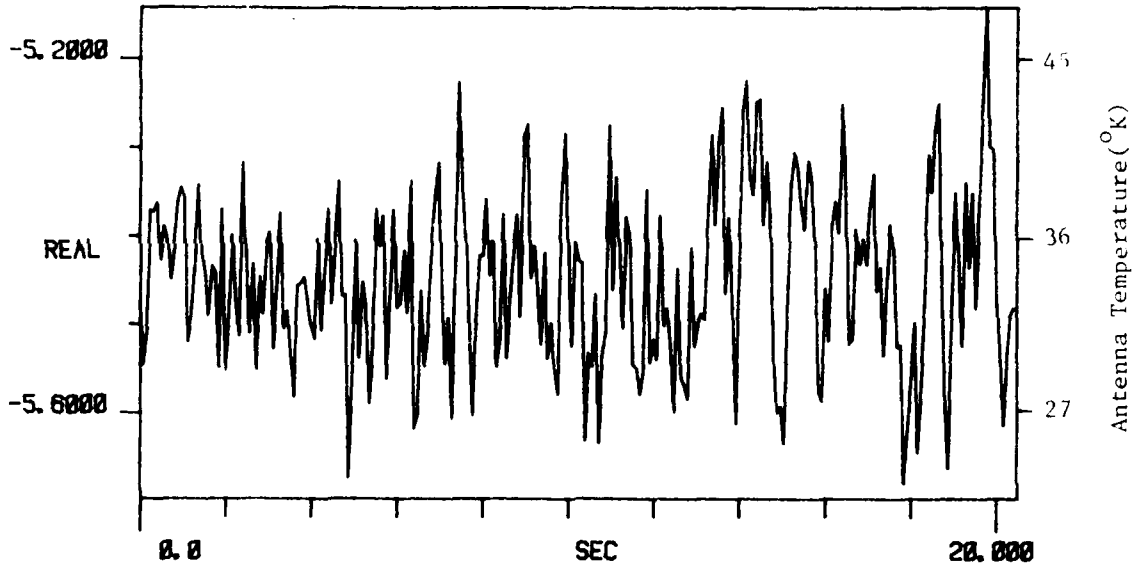


Figure D-3. Zenith Sky Measurement. 2 Mar 80
184

TI AVG 1

R# 71

#A 1



TI AVG
20.000

R# 71

#A 1

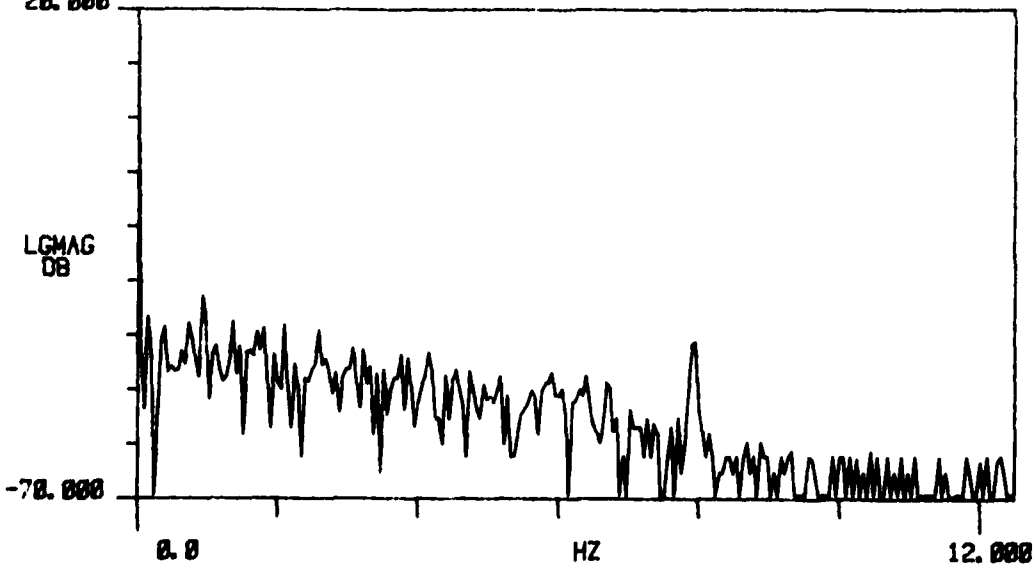
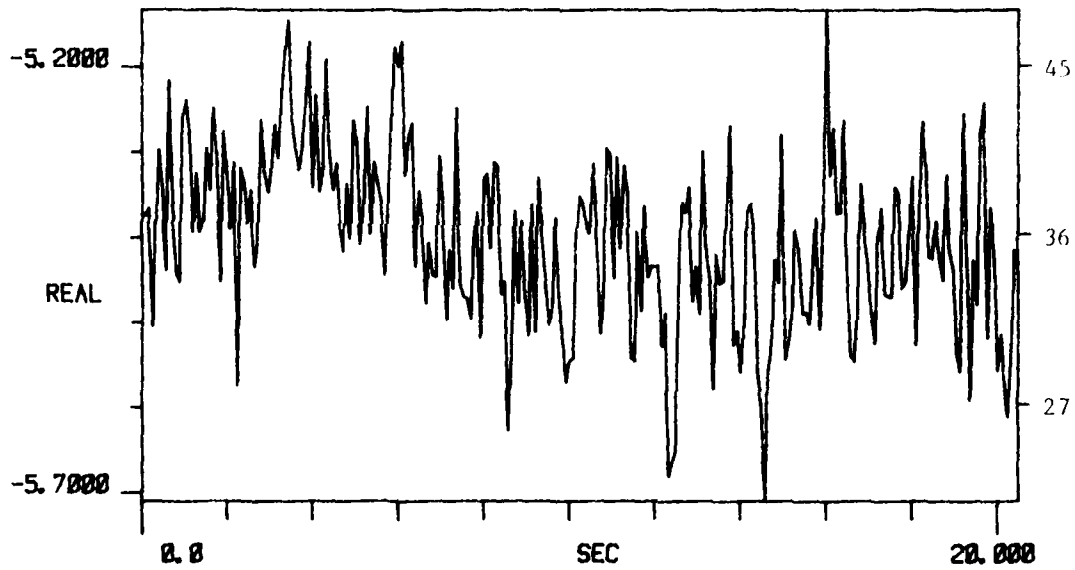


Figure D-3. Zenith Sky Measurement 2 Mar 80

TI AVG 1

R# 72

#A 1



TI AVG
20.000

R# 72

#A 1

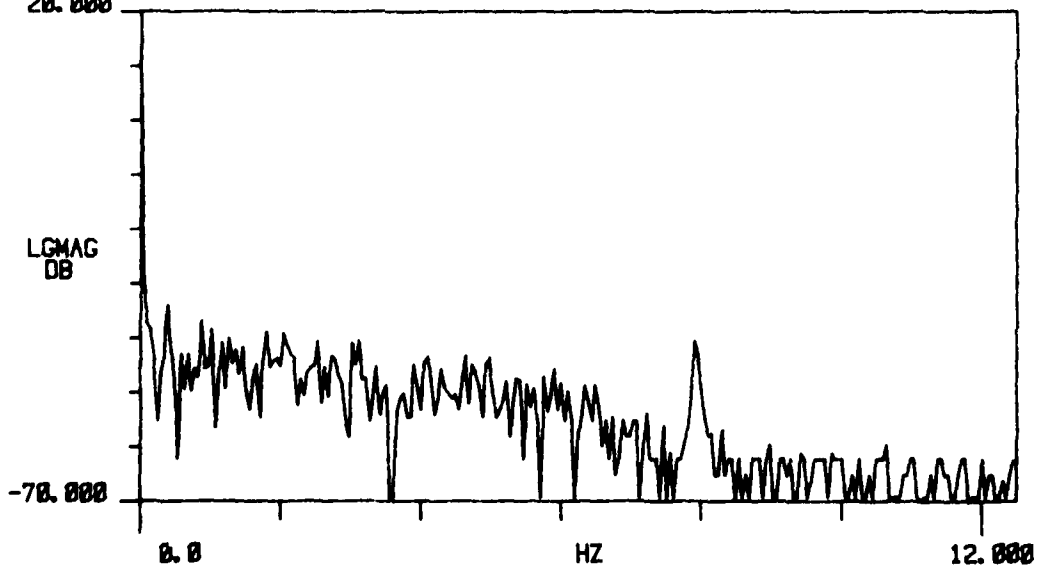


Figure D-3, Zenith Sky Measurement, 2 Mar 80
186

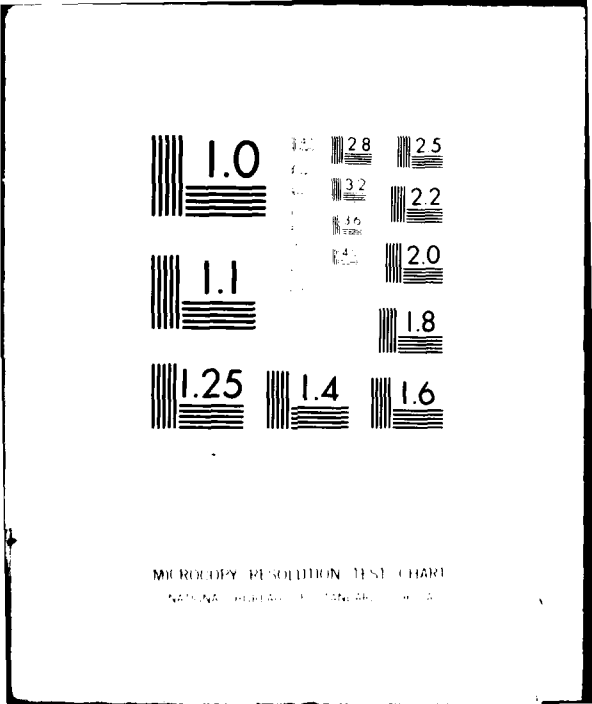
AD-A096 636 GEORGIA INST OF TECH ATLANTA ENGINEERING EXPERIMENT —ETC F/8 4/1
MILLIMETER WAVE ATMOSPHERIC RADIONOMETRY OBSERVATIONS. (U)
UNCLASSIFIED MAR 81 J H RAINWATER, J J GALLAGHER N80173-78-C-0165
GIT/EES-A-2173 NL

3 1/2 x 3

300000



END
DATE
FILMED
6 81
DTIC

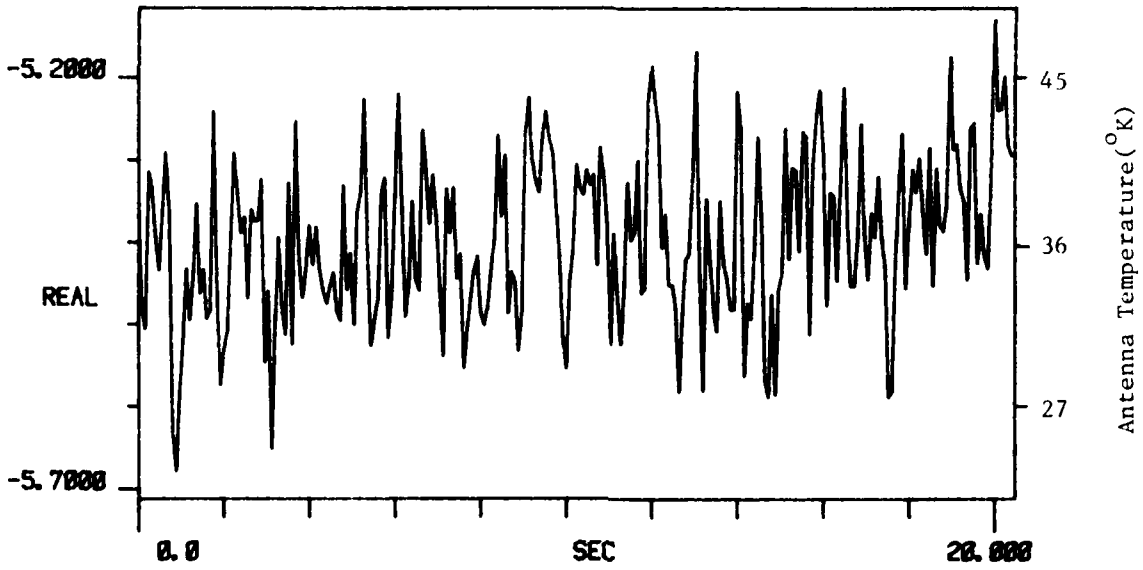


MICROCOPY RESOLUTION TEST CHART
NBS 1963-A

TI AVG 1

R# 73

#A 1



TI AVG
20.000

R# 73

#A 1

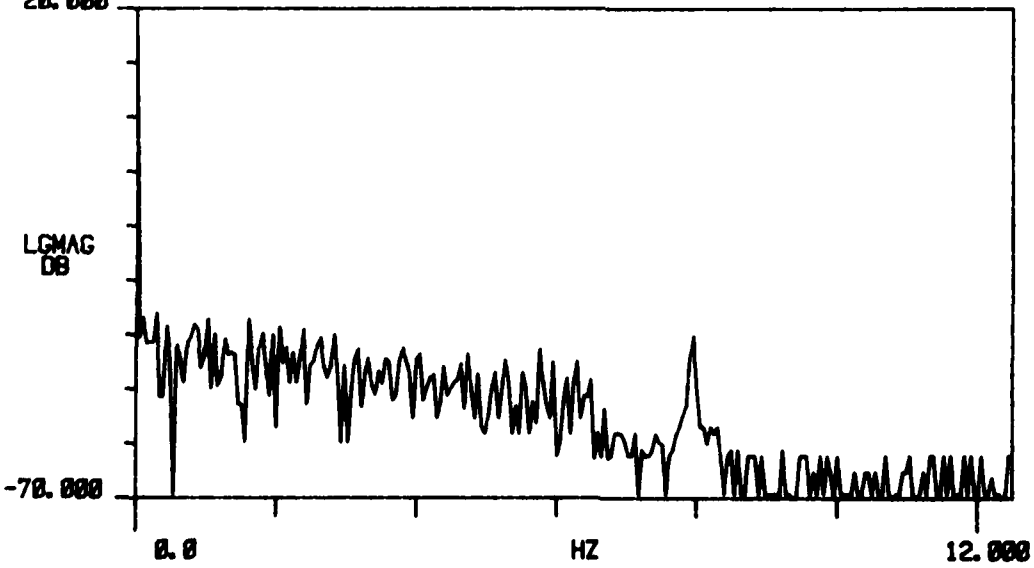
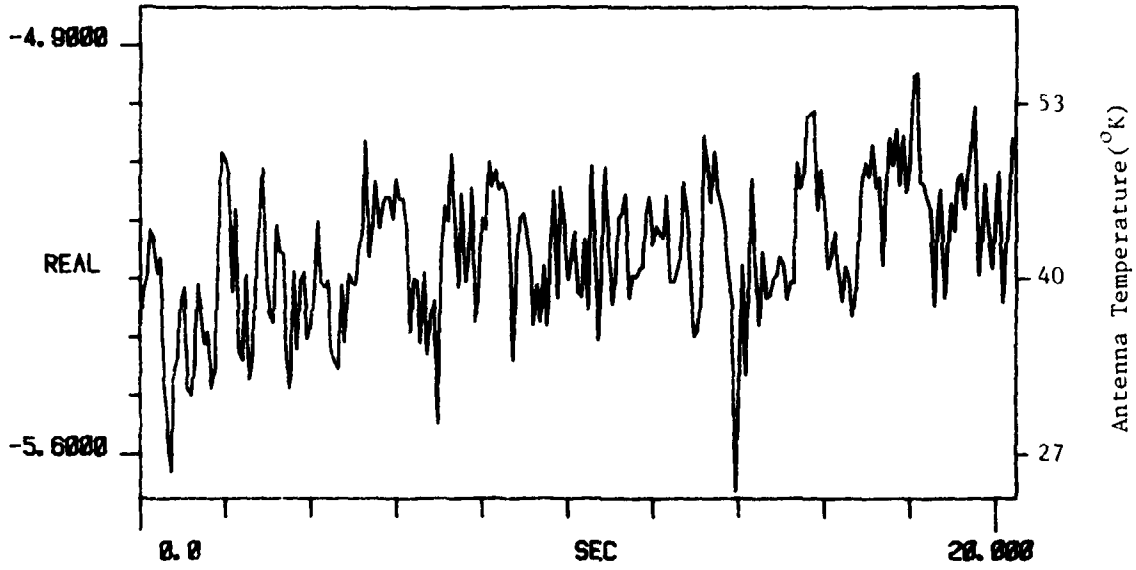


Figure D-3. Zenith Sky Measurement. 2 Mar 80

TI AVG 1

R# 74

#A 1



TI AVG

R# 74

#A 1

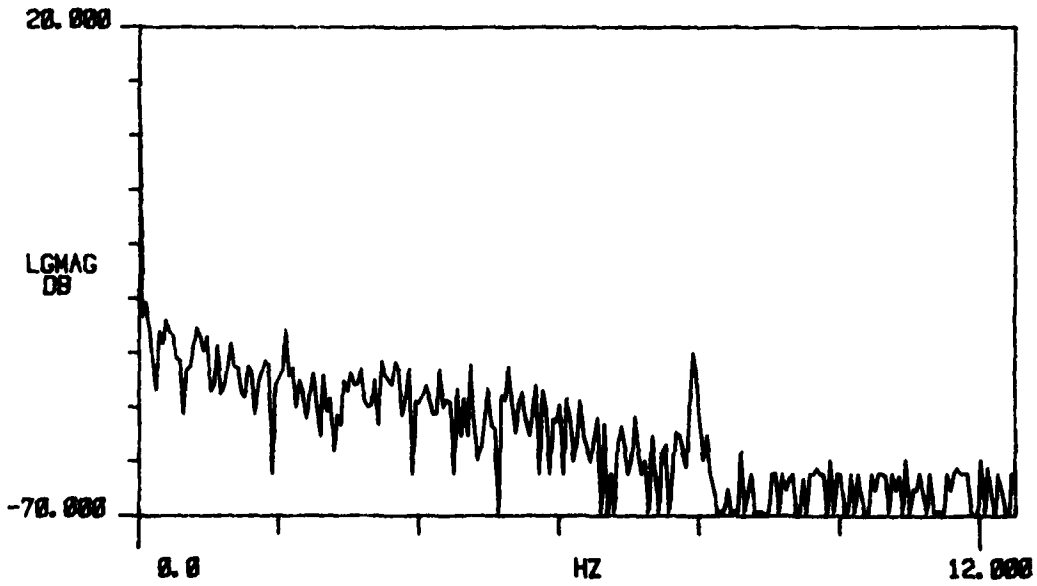
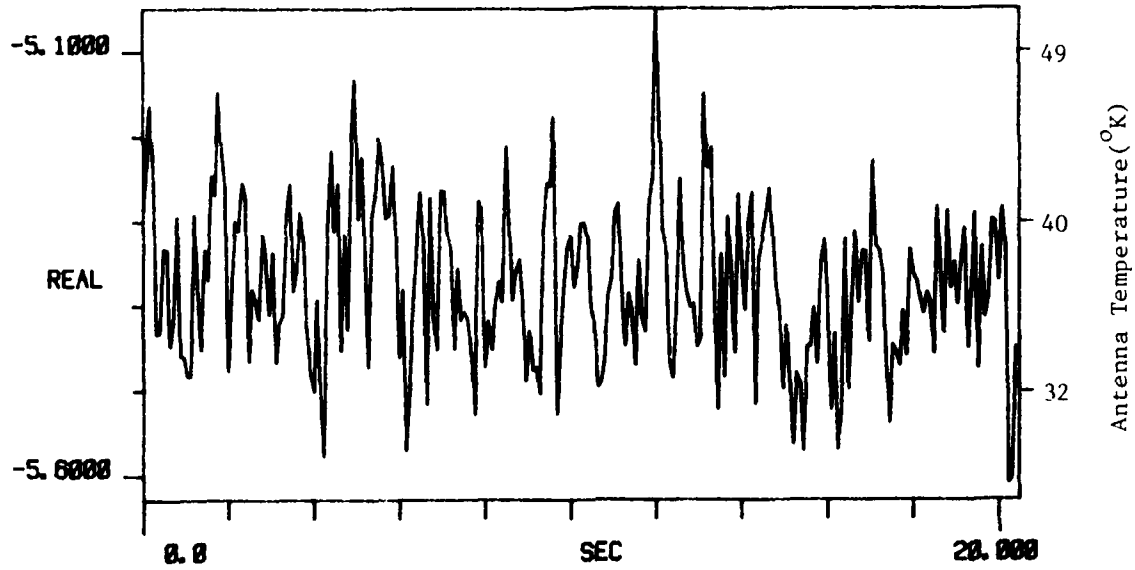


Figure D-3. Zenith Sky Measurement. 2 Mar 80

TI AVG 1

R# 75

#A 1



TI AVG
20.000

R# 75

#A 1

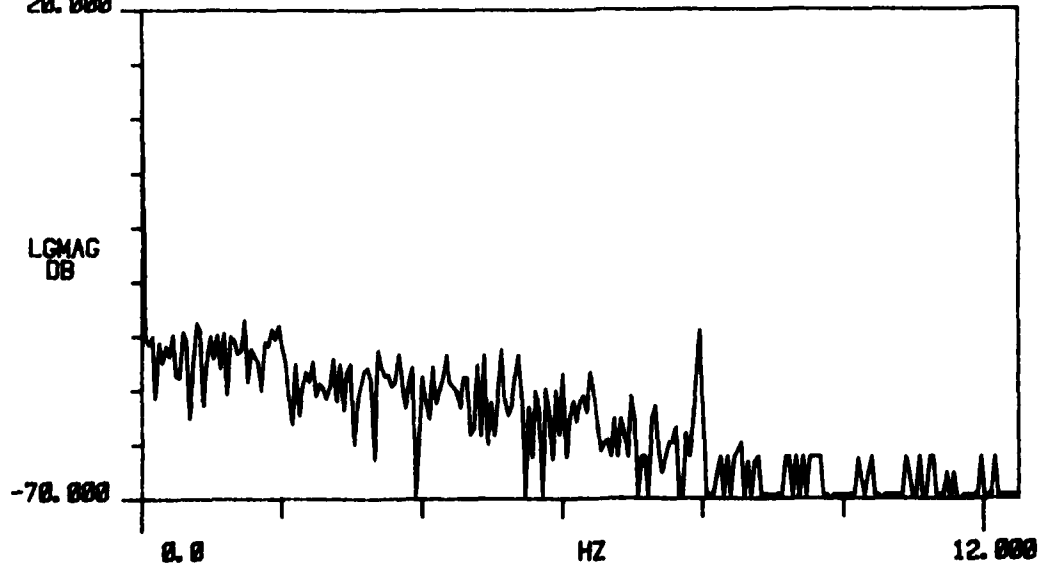


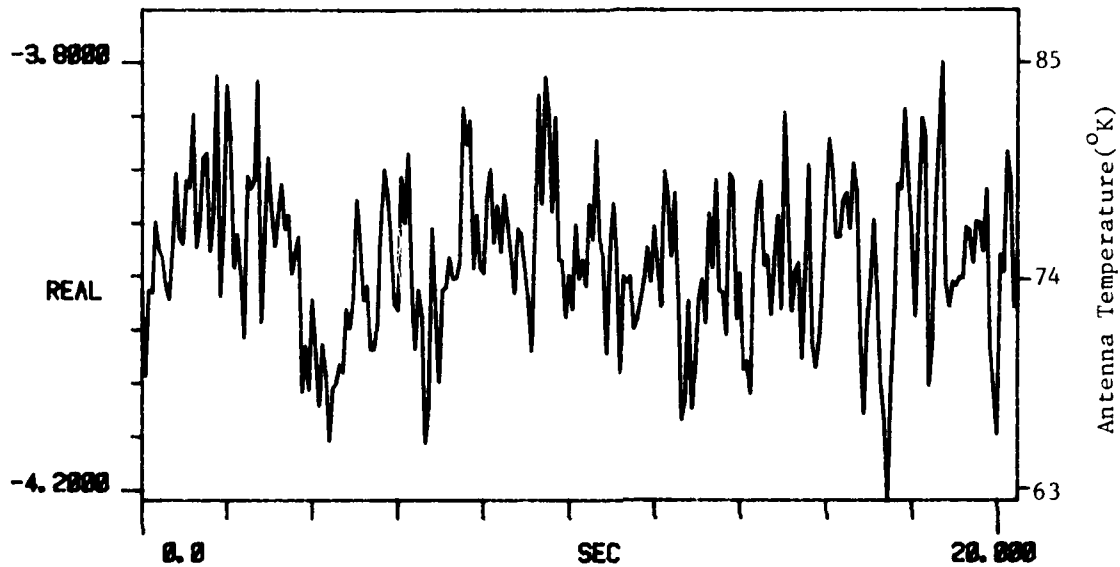
Figure D-3. Zenith Sky Measurement. 2 Mar 80

D-4. 8 March 1980
Zenith Sky Measurements

TI AVG 1

R# 10

#A 1



TI AVG

R# 10

#A 1

20.000

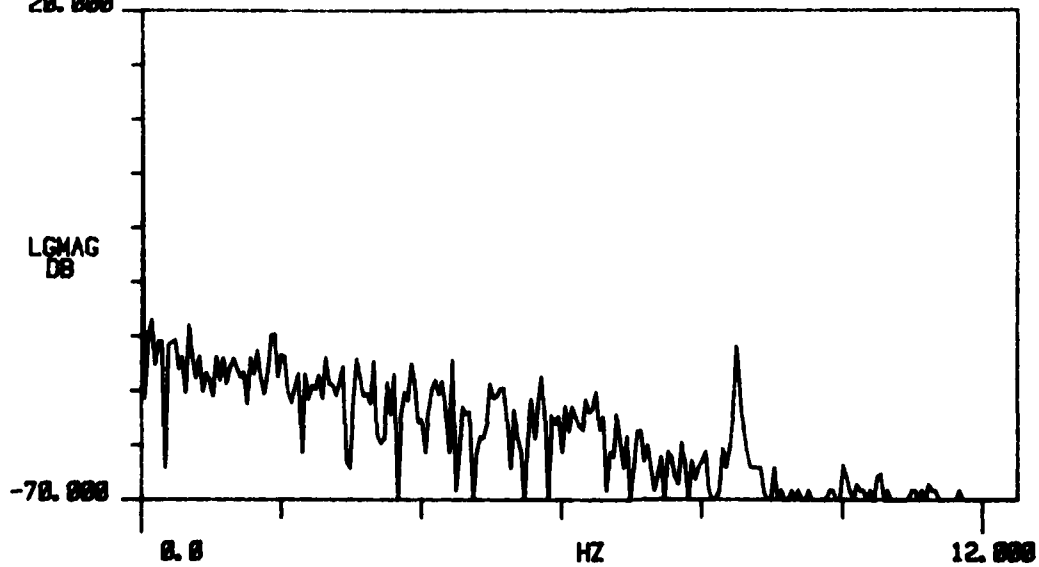
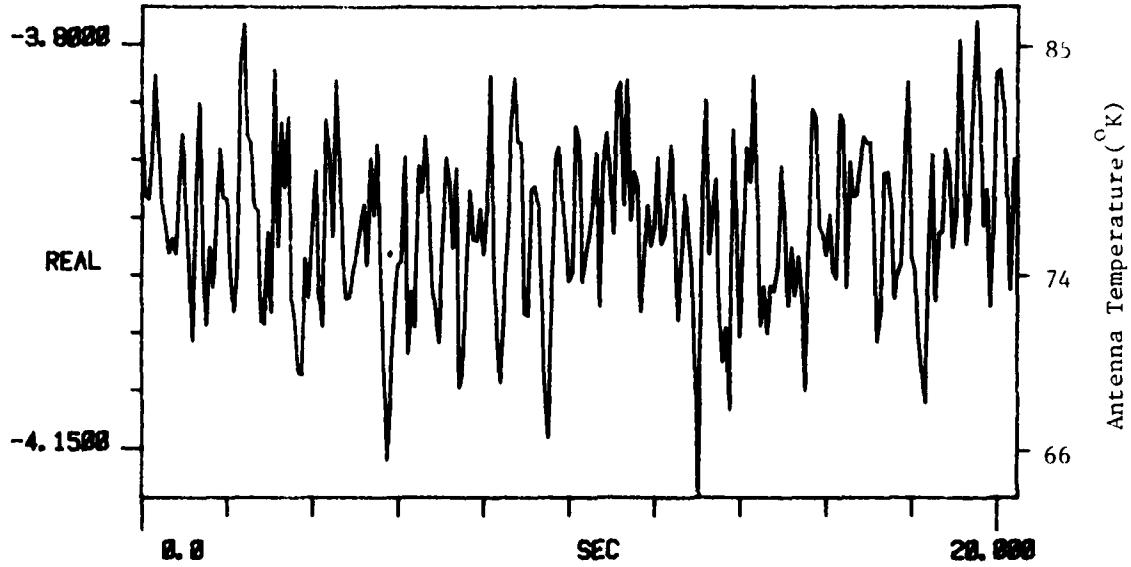


Figure D-4. Zenith Sky Measurement. 8 Mar 80

TI AVG 1

R# 11

#As 1



TI AVG
20.000

R# 11

#As 1

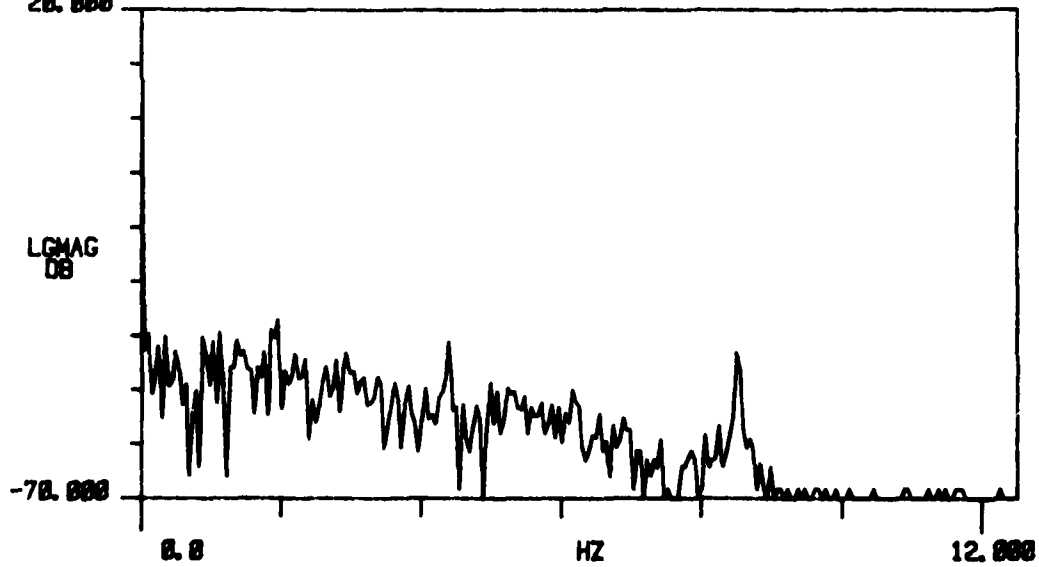
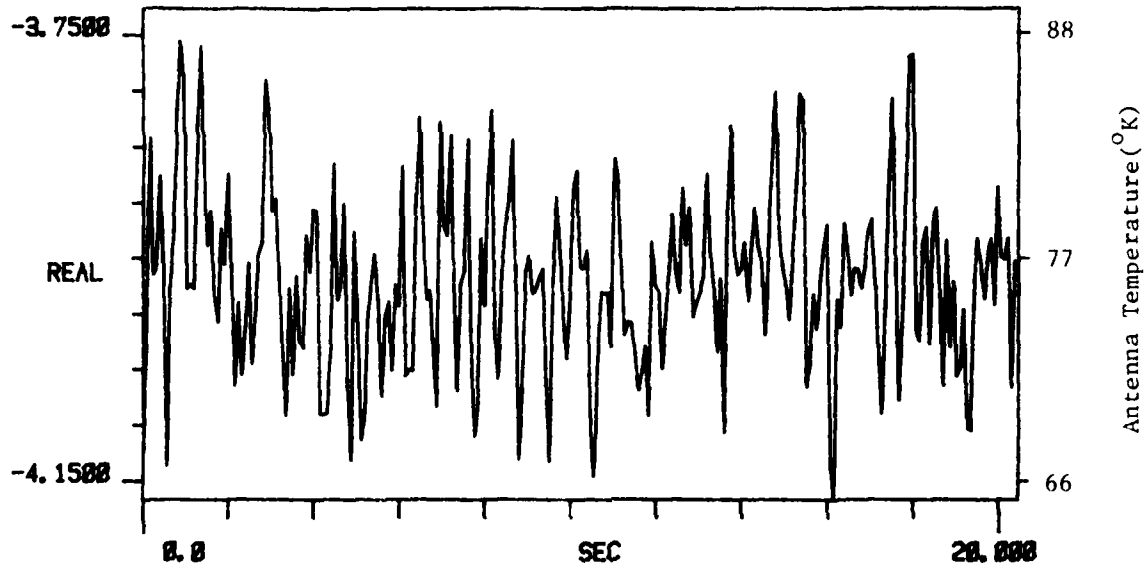


Figure D-4. Zenith Sky Measurement. 8 Mar 80

TI AVG 1

R# 13

#A# 1



TI AVG
20.000

R# 13

#A# 1

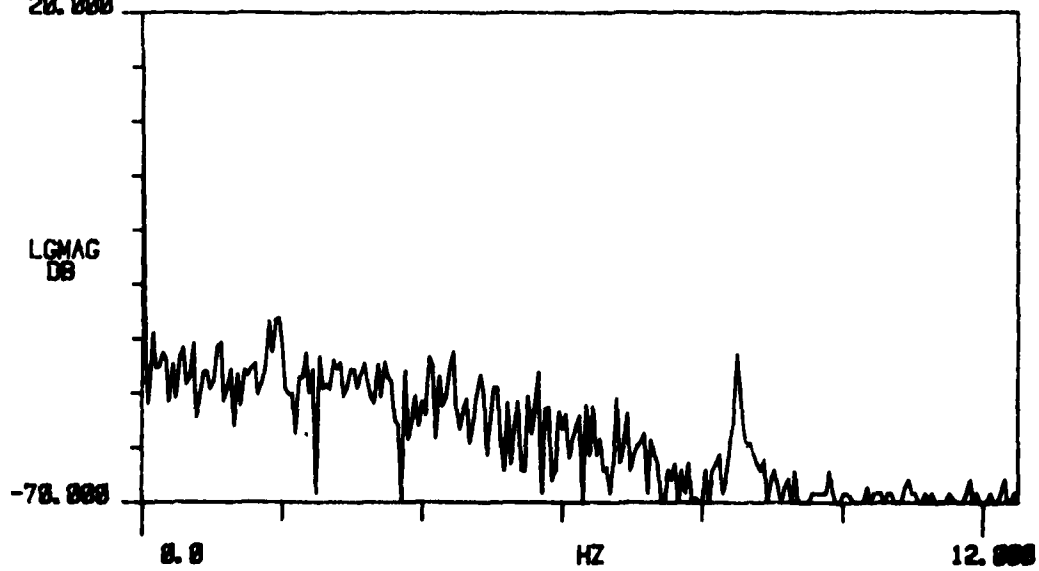
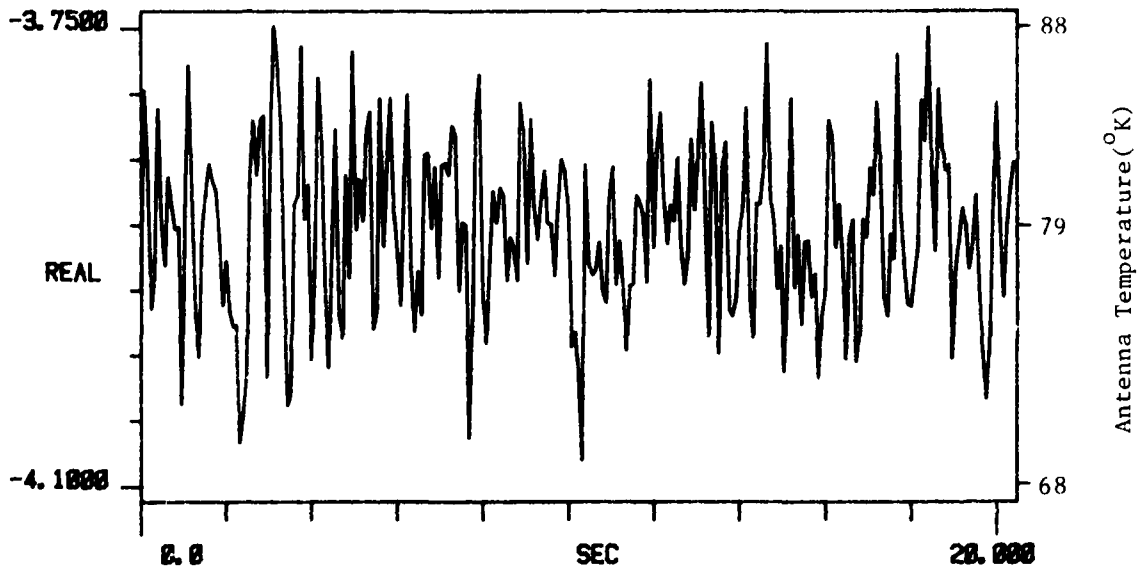


Figure D-4. Zenith Sky Measurement. 8 Mar 80

TI AVG 1

R# 15

#A_s 1



TI AVG
20.000

R# 15

#A_s 1

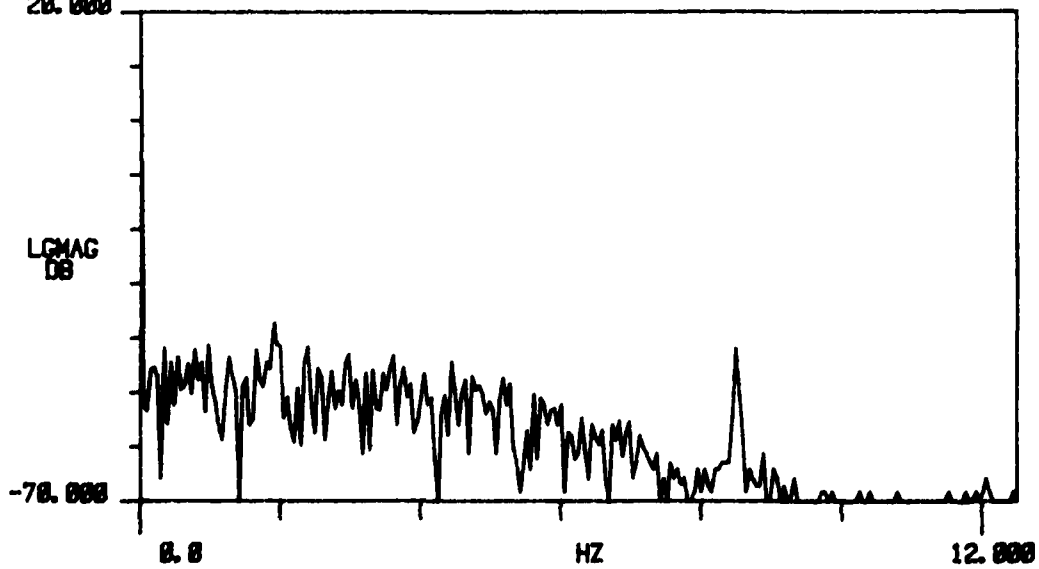


Figure D-4. Zenith Sky Measurement. 8 Mar 80

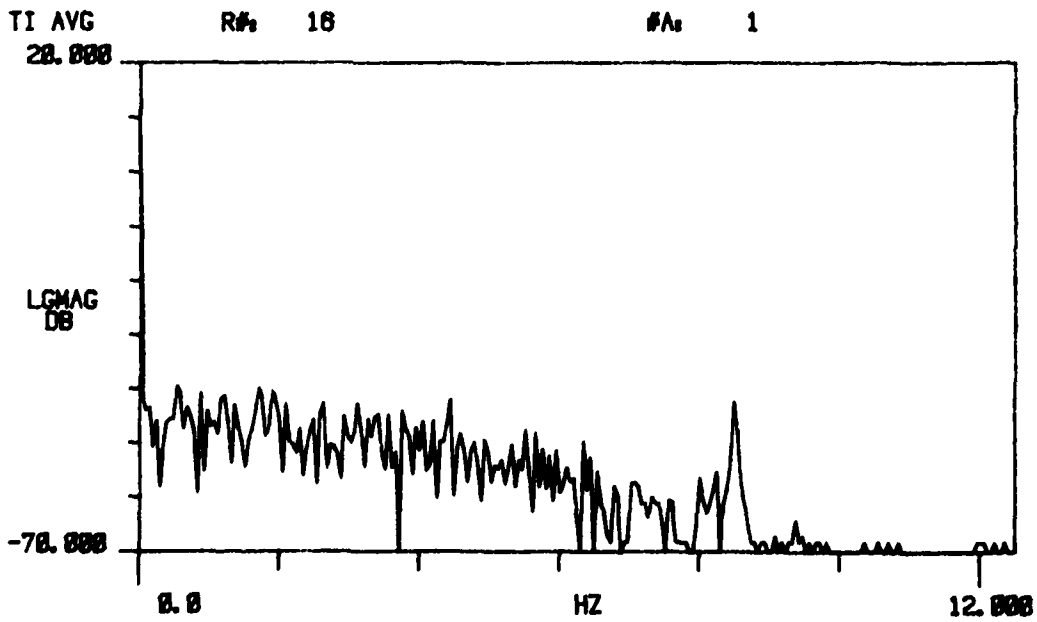
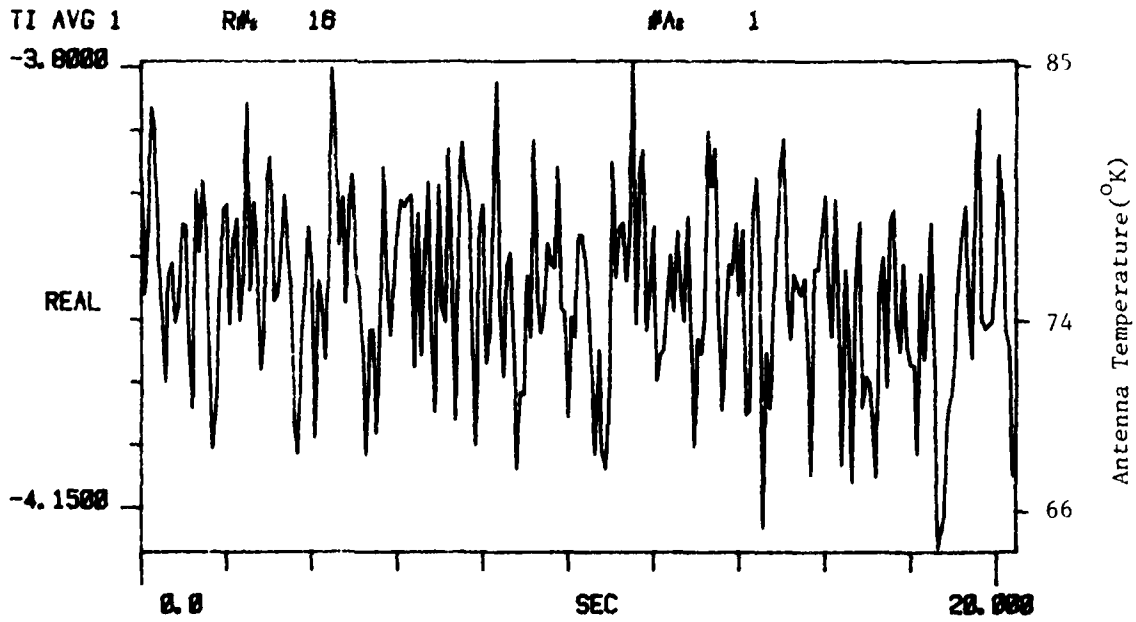
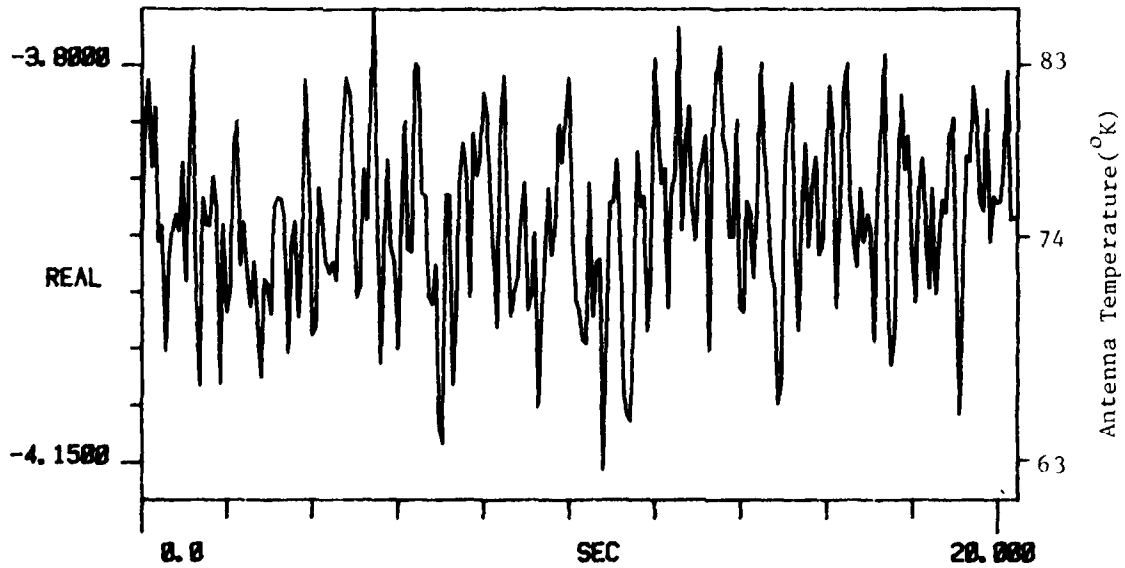


Figure D-4. Zenith Sky Measurement. 8 Mar 80

TI AVG 1

R# 18

#A 1



TI AVG

R# 18

#A 1

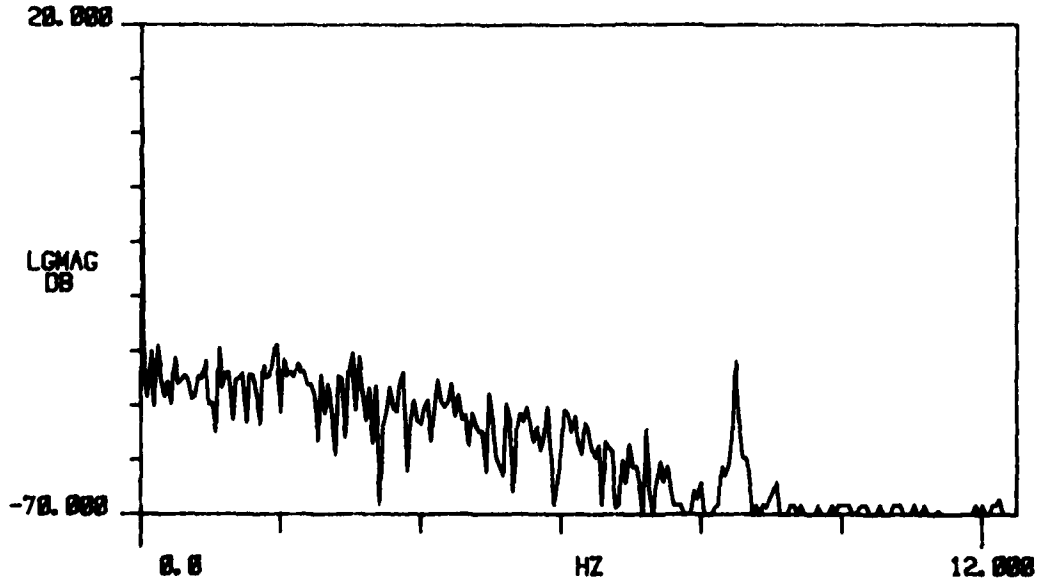


Figure D-4. Zenith Sky Measurement. 8 Mar 80

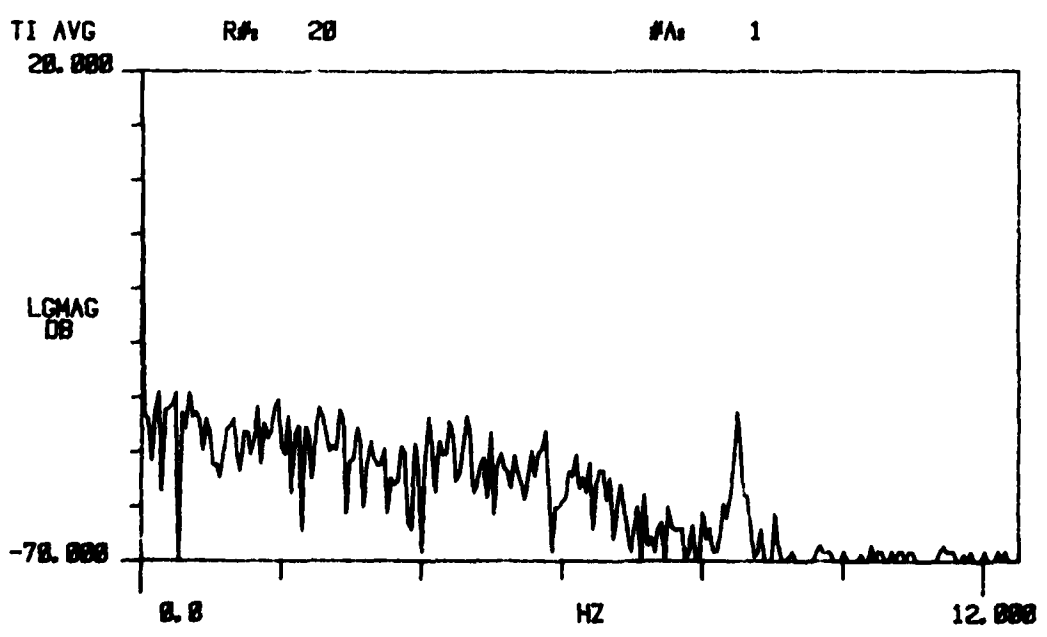
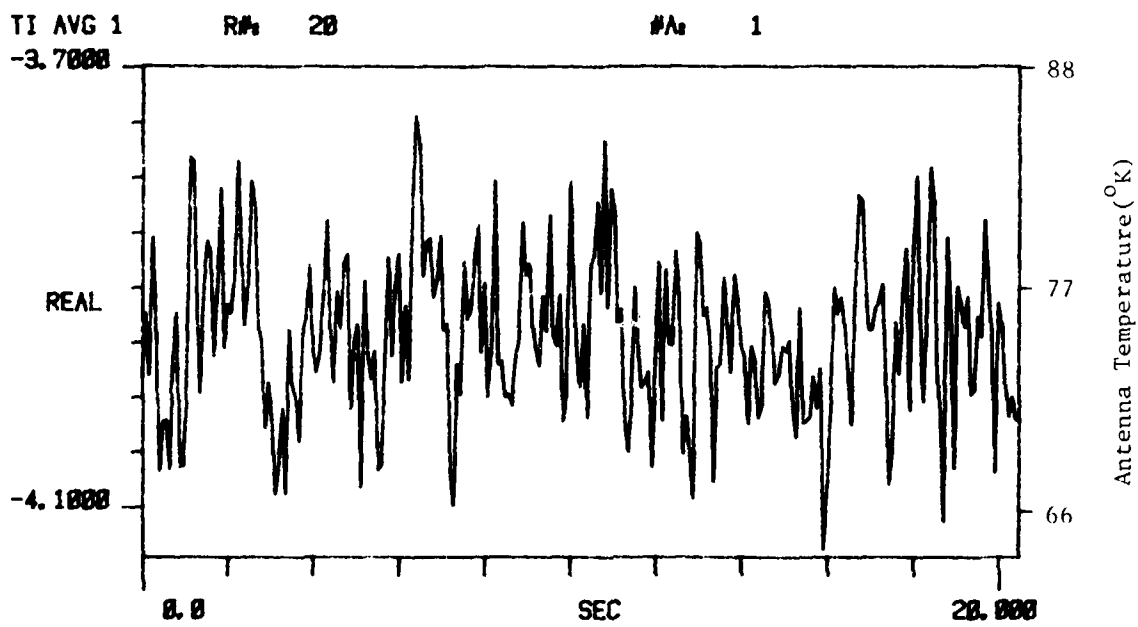


Figure D-4. Zenith Sky Measurement. 8 Mar 80

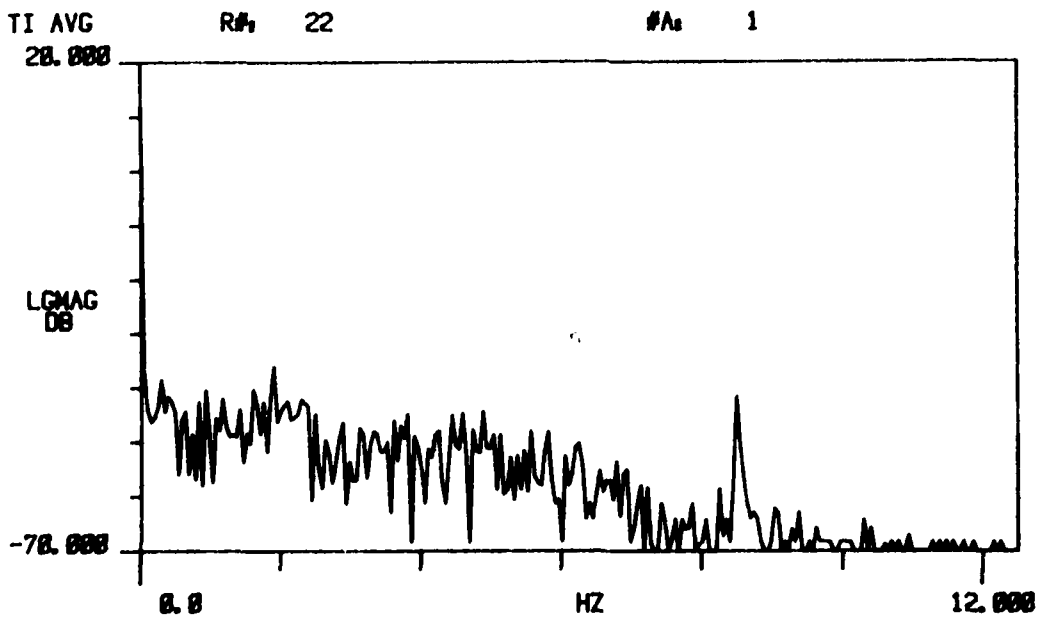
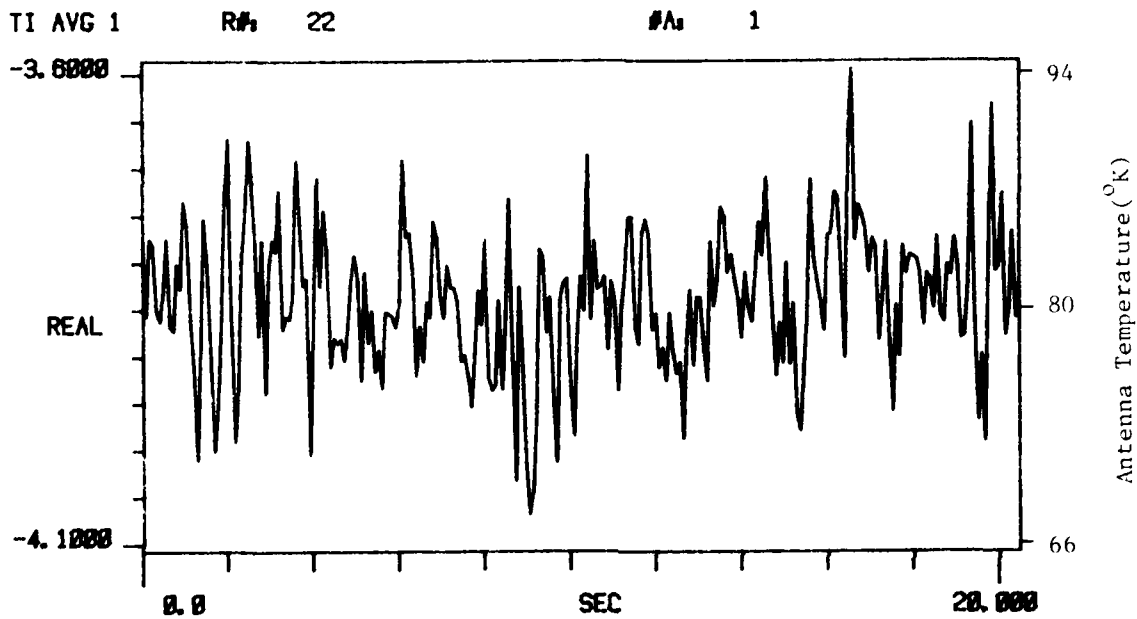


Figure D-4. Zenith Sky Measurement. 8 Mar 80

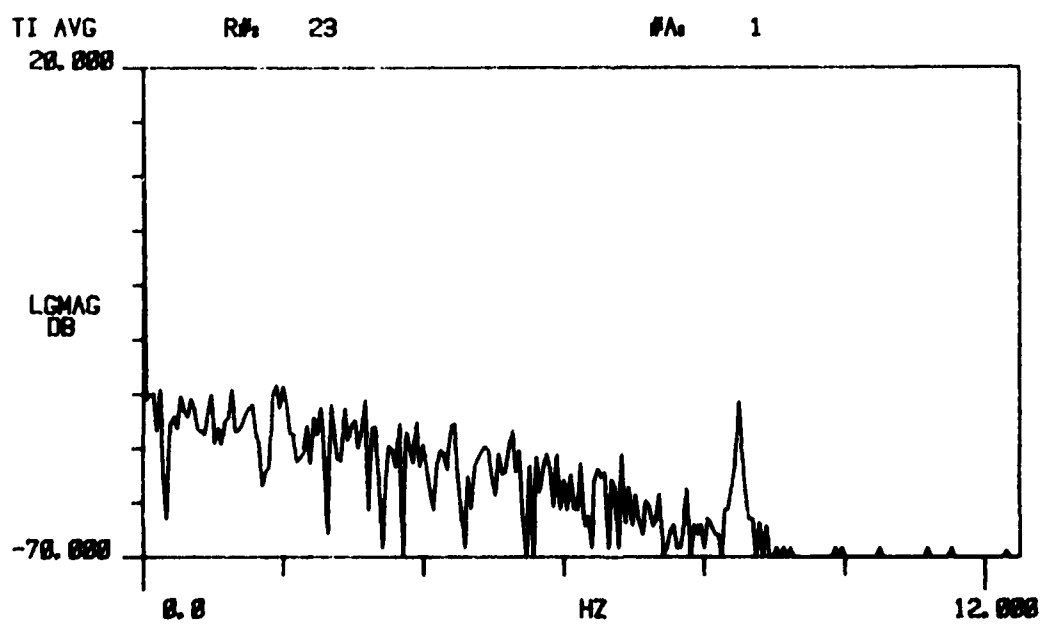
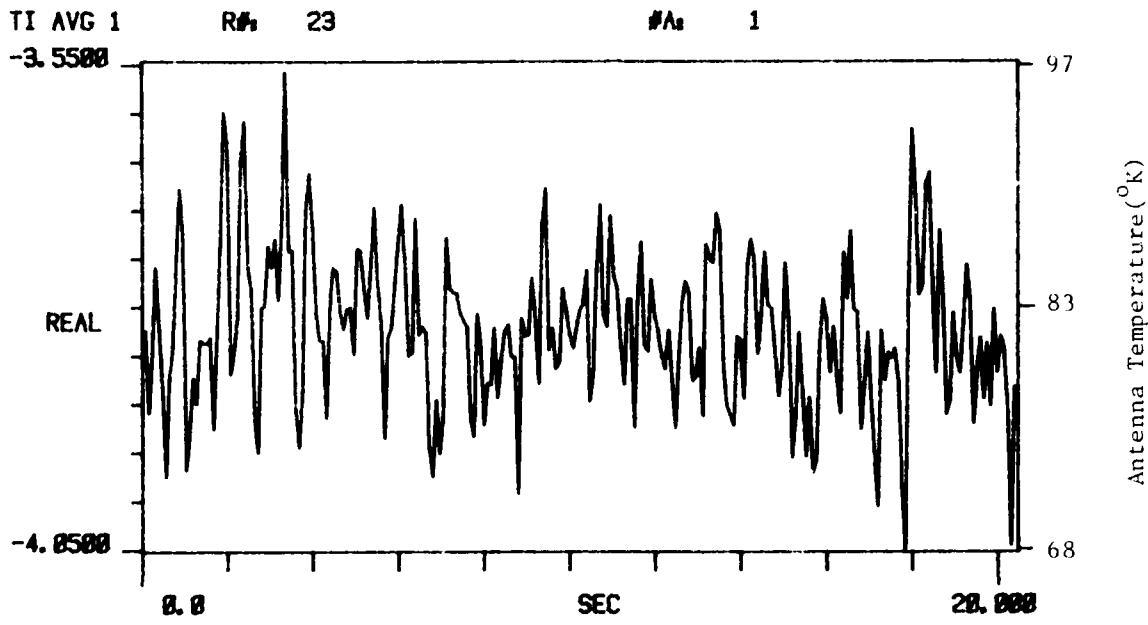


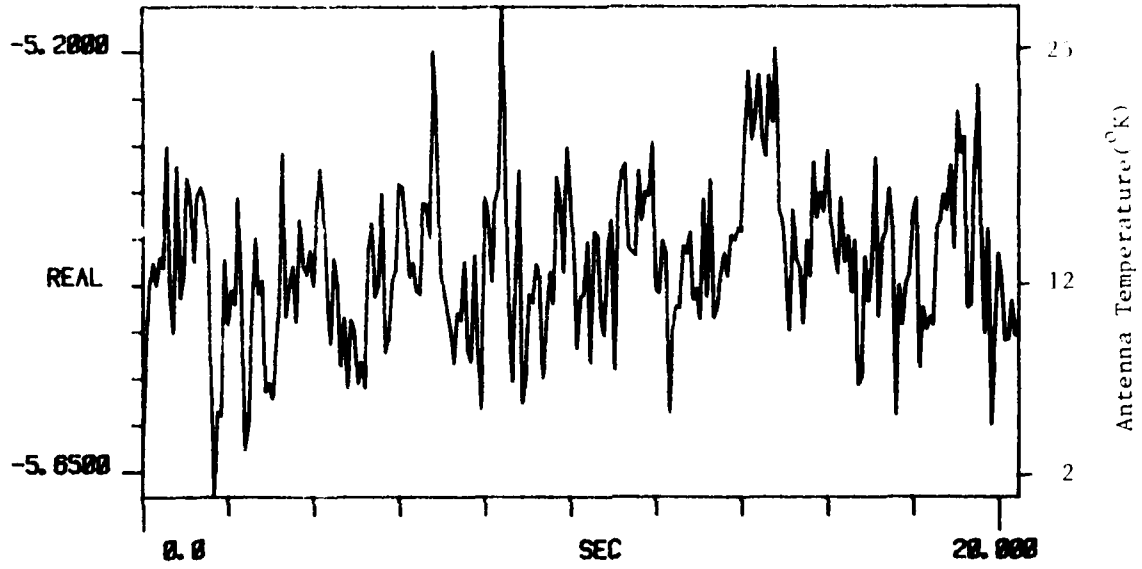
Figure D-4. Zenith Sky Measurement. 8 Mar 80

D-5. 11 March 1980
Zenith Sky Measurements

TI AVG 1

RA 9

FA 1



TI AVG
20.000

RA 9

FA 1

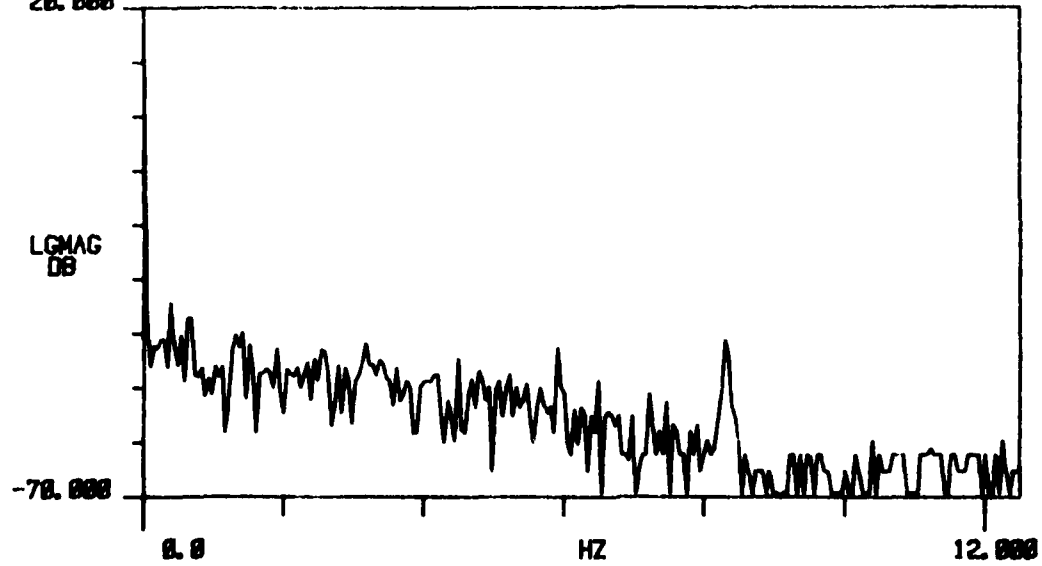
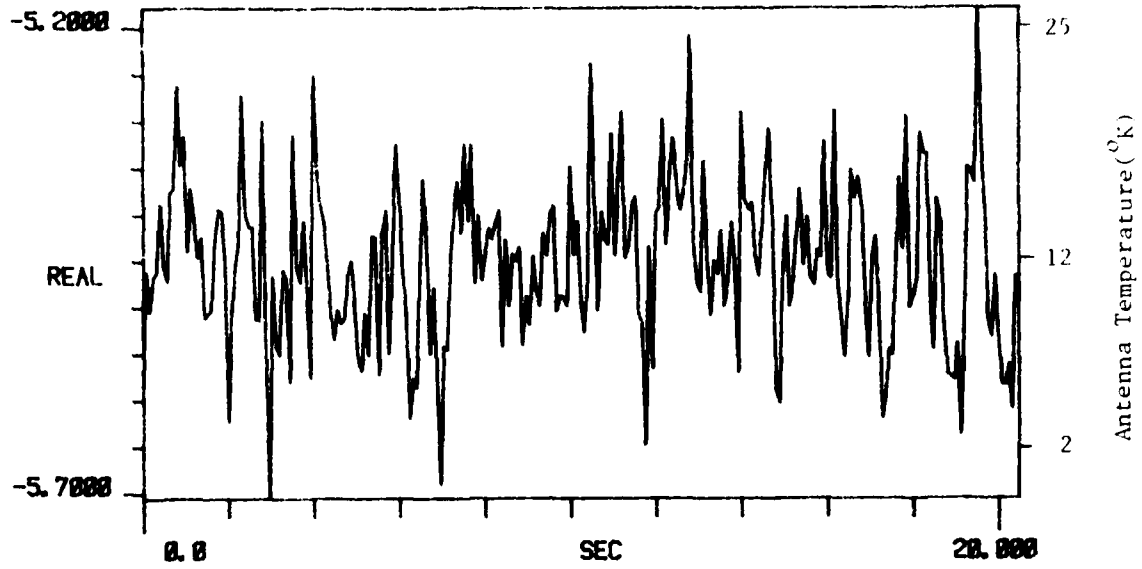


Figure D-5. Zenith Sky Measurement. 11 Mar 80

TI AVG 1

R# 10

#A 1



TI AVG
20.000

R# 10

#A 1

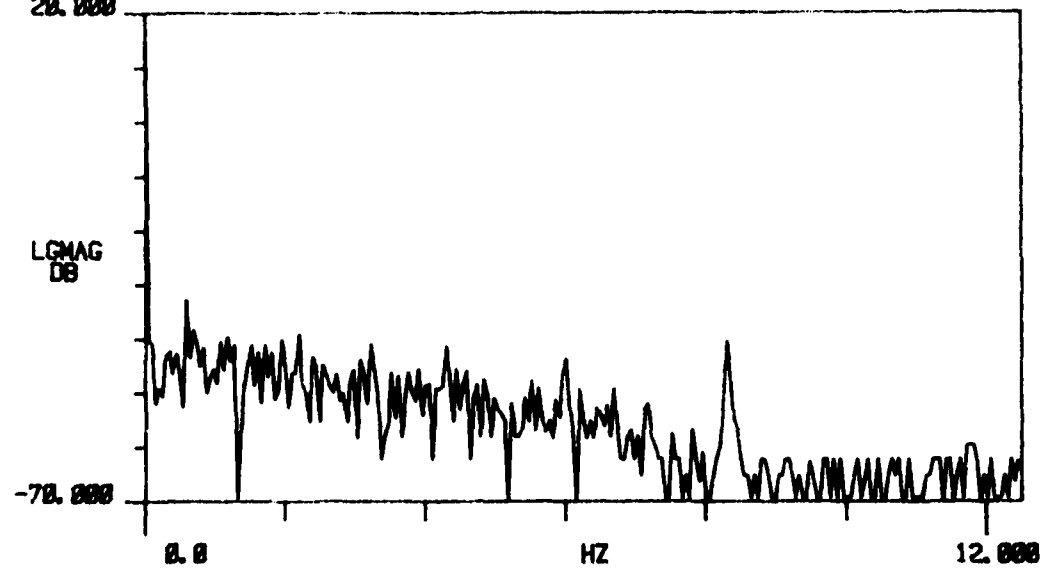
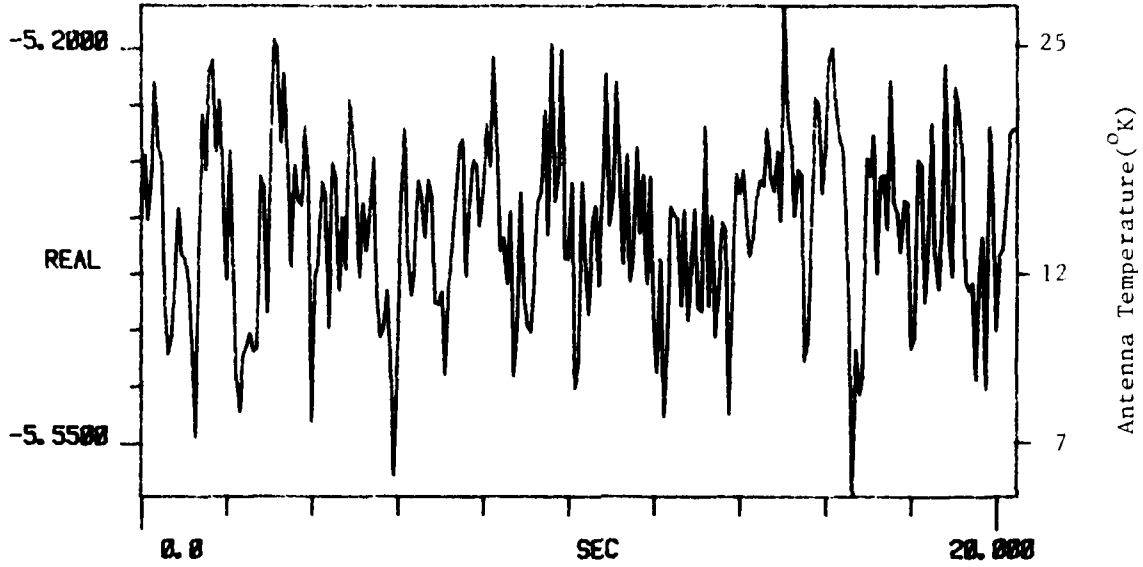


Figure D-5. Zenith Sky Measurement. 11 Mar 80

TI AVG 1

R# 12

#A 1



TI AVG
20.000

R# 12

#A 1

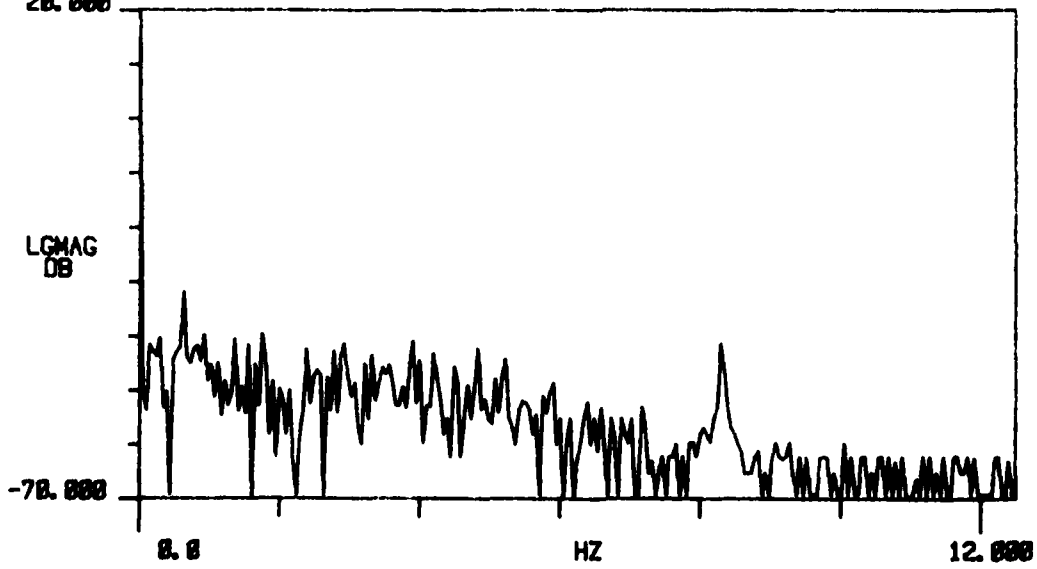
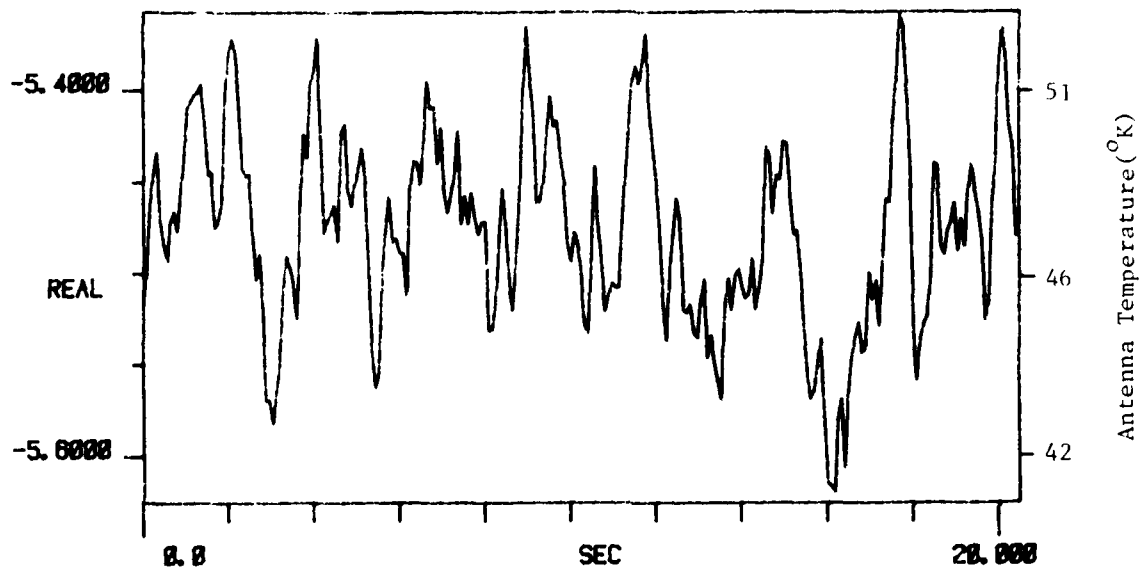


Figure D-5. Zenith Sky Measurement. 11 Mar 80

TI AVG 1

R# 18

#A 1



TI AVG
20.000

R# 18

#A 1

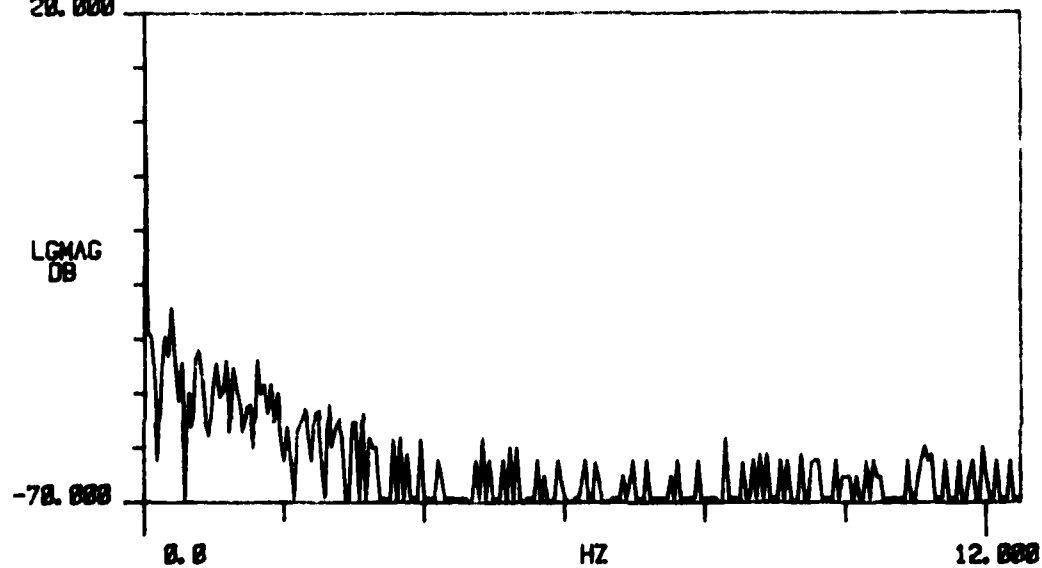


Figure D-5. Zenith Sky Measurement. 11 Mar 80

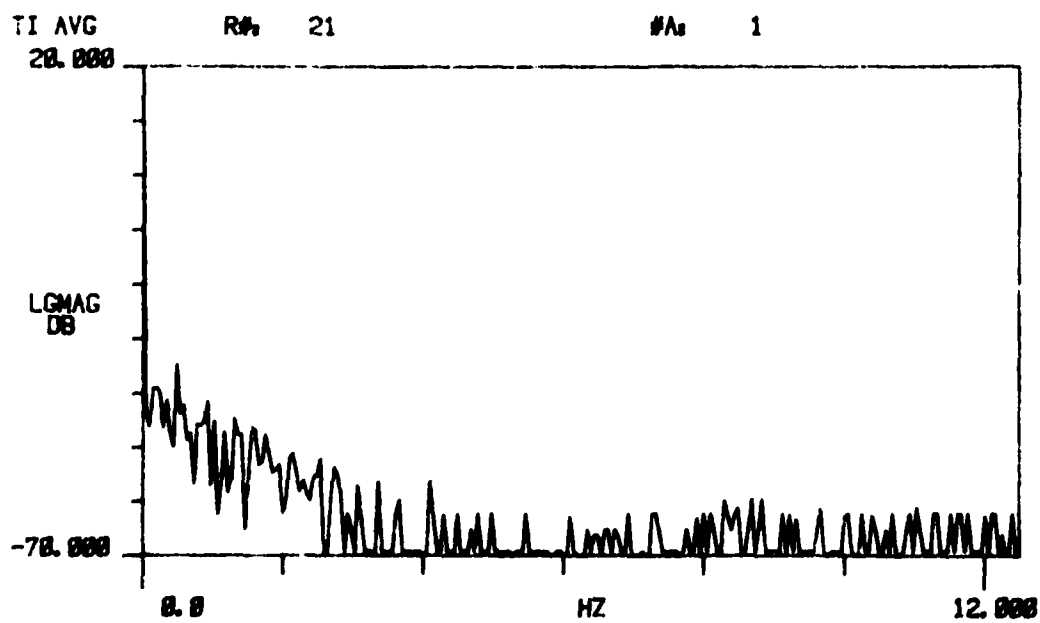
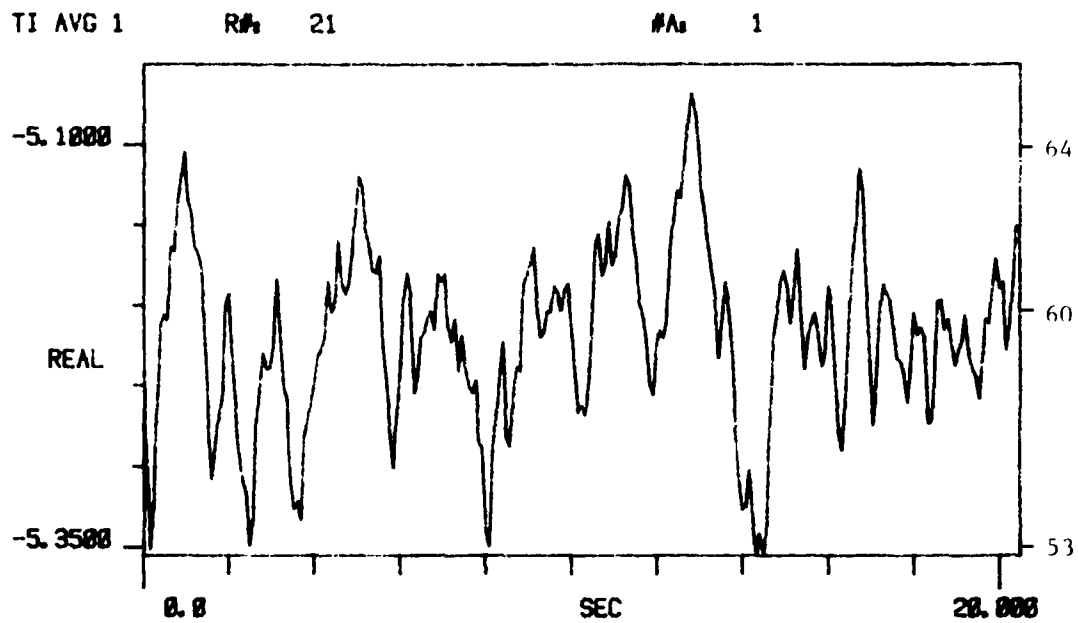
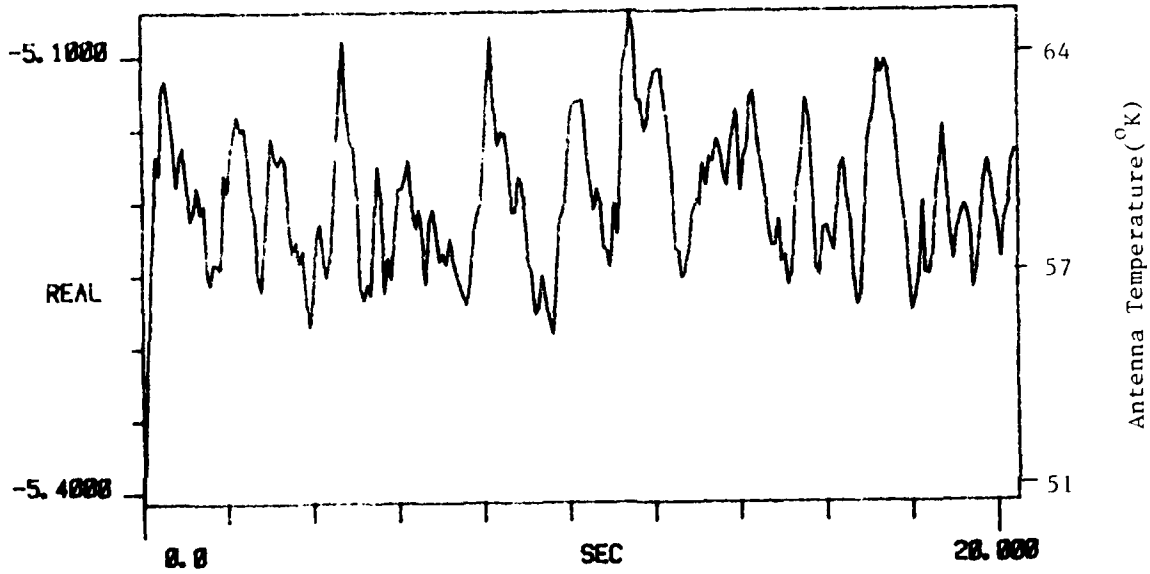


Figure D-5. Zenith Sky Measurement. 11 Mar 80

TI AVG 1

R# 22

#A 1



TI AVG
20.000

R# 22

#A 1

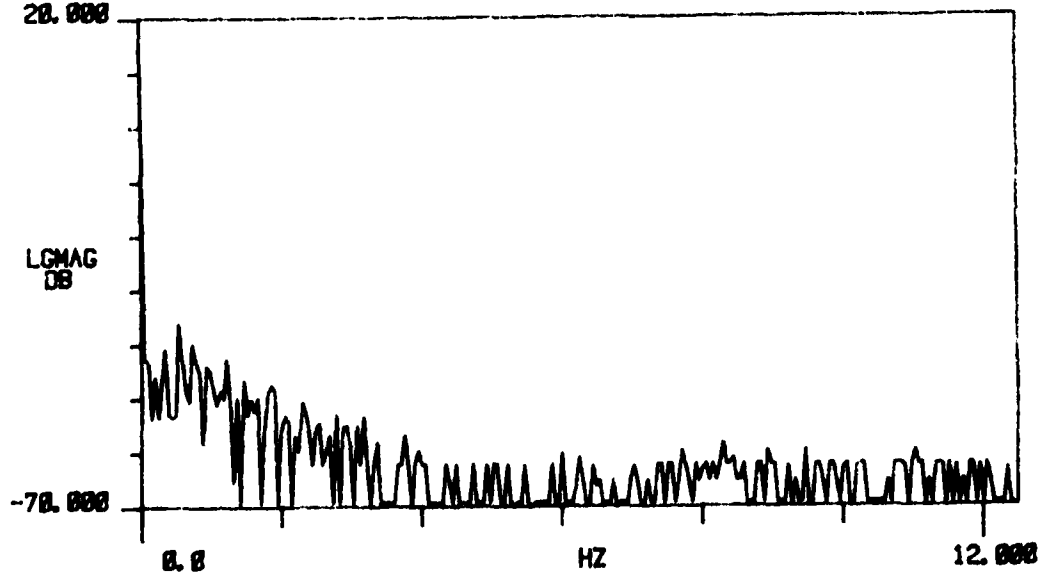
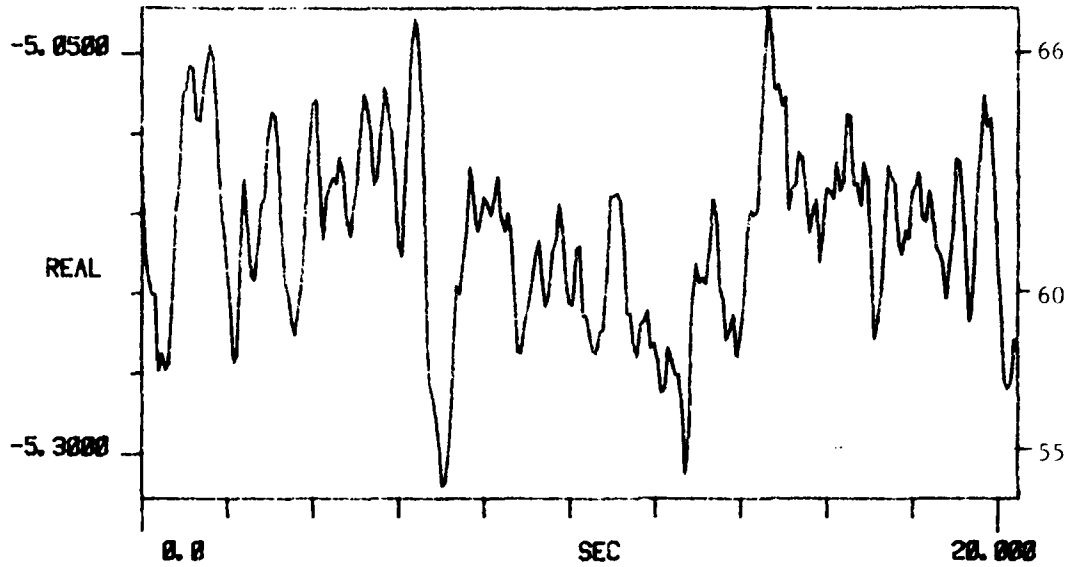


Figure D-5. Zenith Sky Measurement. 11 Mar 80

TI AVG 1

R# 23

#A 1



TI AVG
20.000

R# 23

#A 1

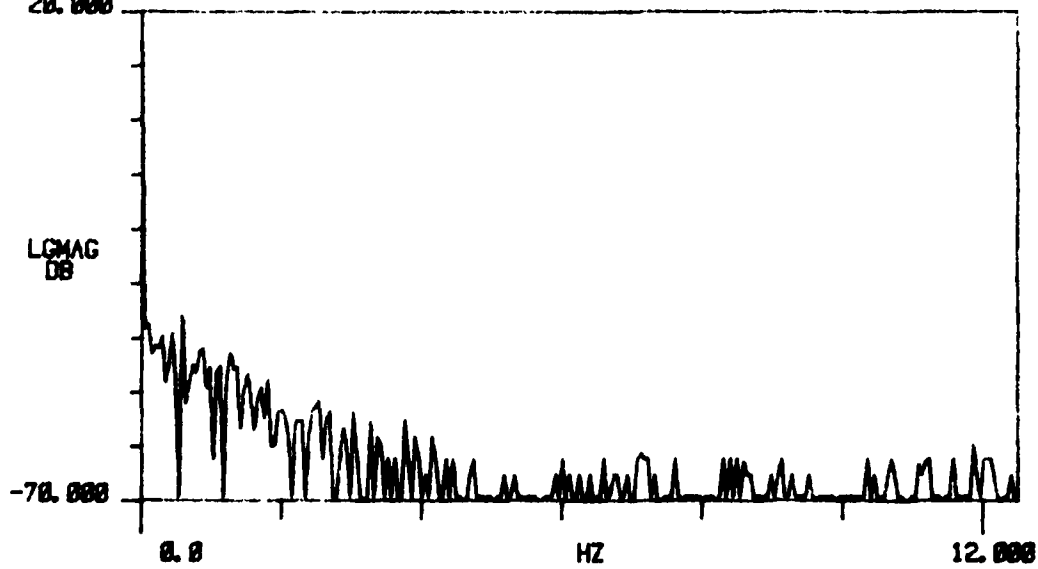
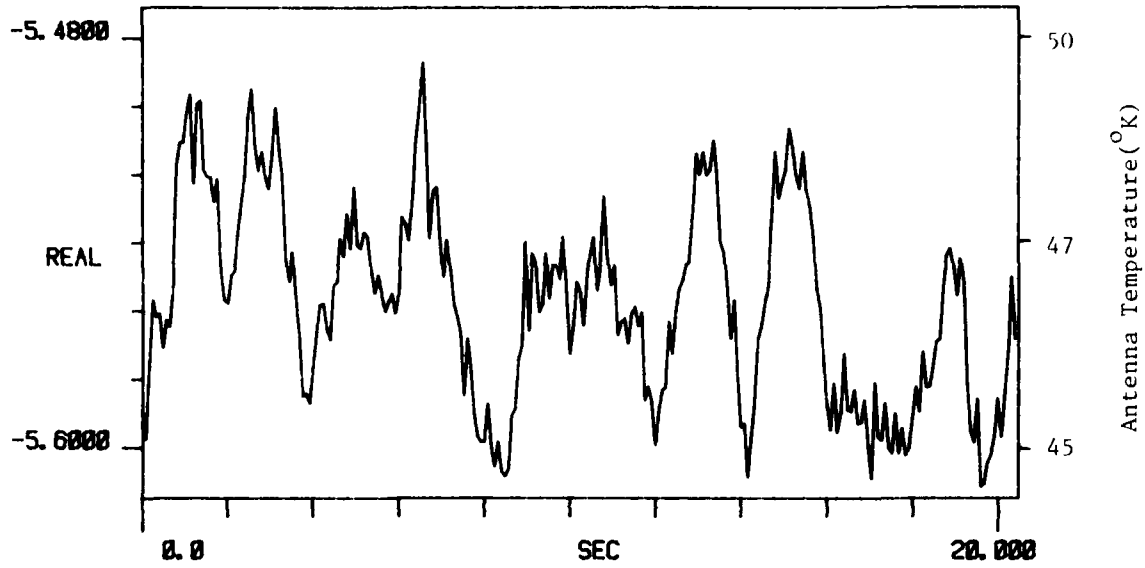


Figure D-5. Zenith Sky Measurement. 11 Mar 80

TI AVG 1

R# 30

#A 1



TI AVG
20.000

R# 30

#A 1

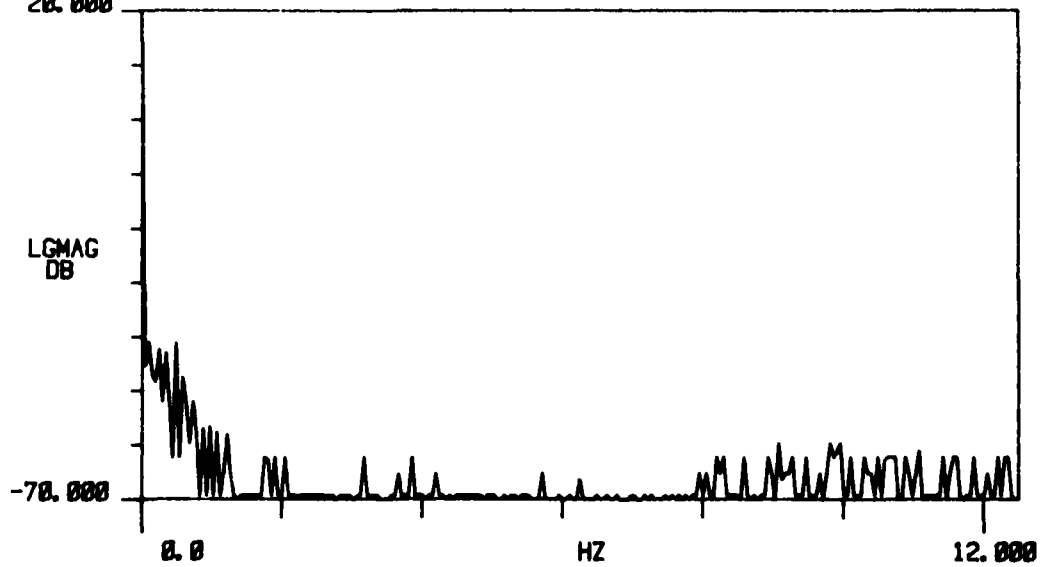
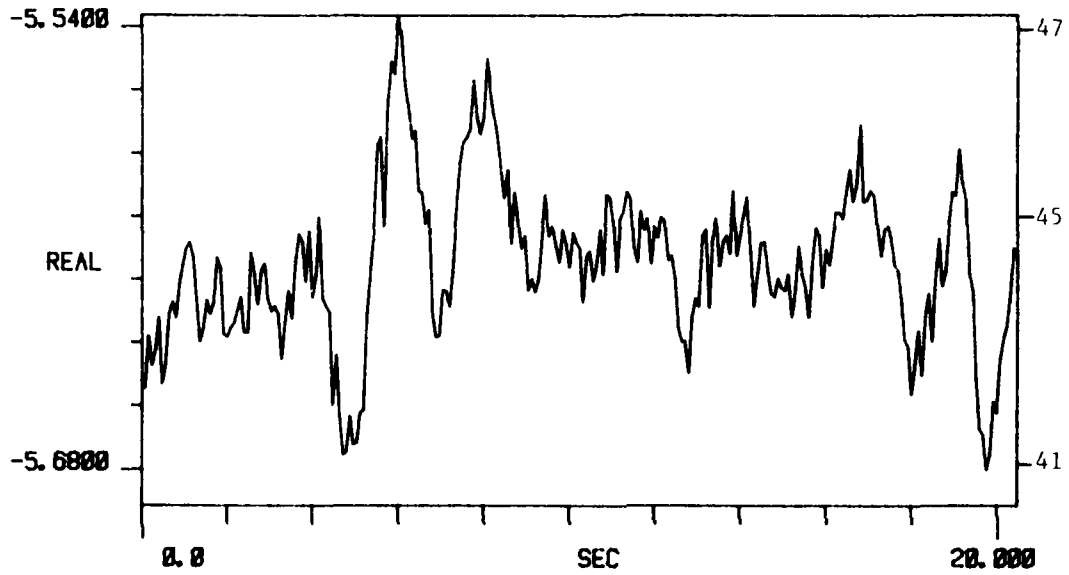


Figure D-5. Zenith Sky Measurement. 11 Mar 80

TI AVG 1

R# 31

#A 1



TI AVG
20.000

R# 31

#A 1

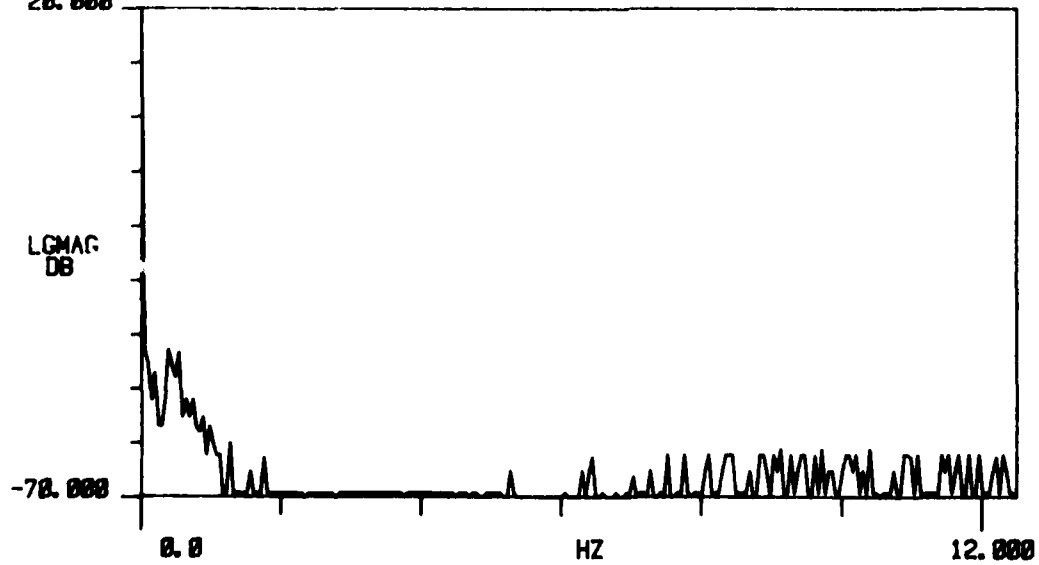
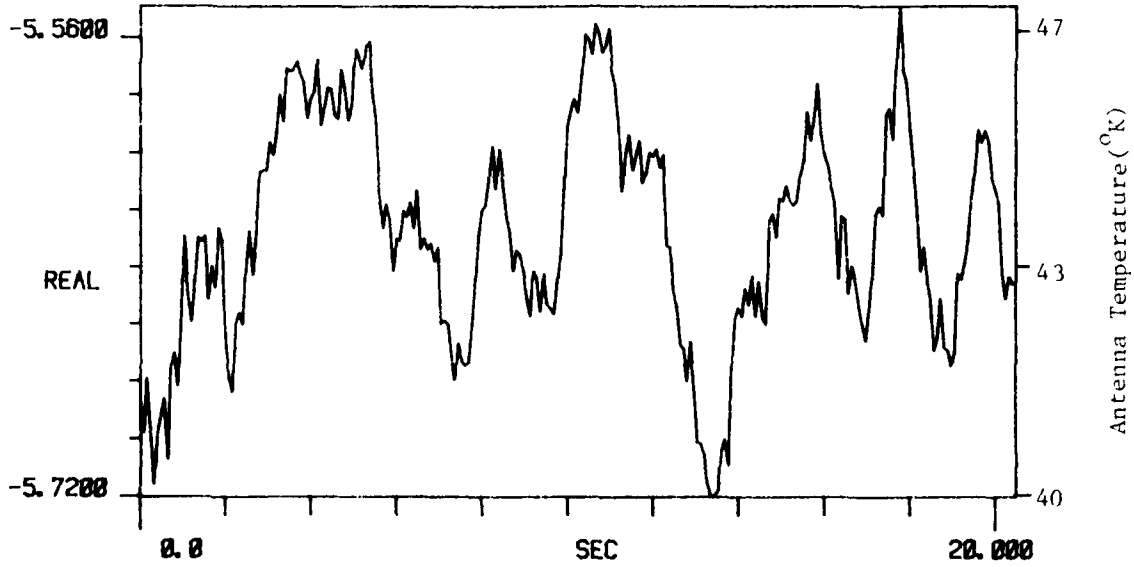


Figure D-5. Zenith Sky Measurement. 11 Mar 80

TI AVG 1

R# 32

#A 1



TI AVG
20.000

R# 32

#A 1

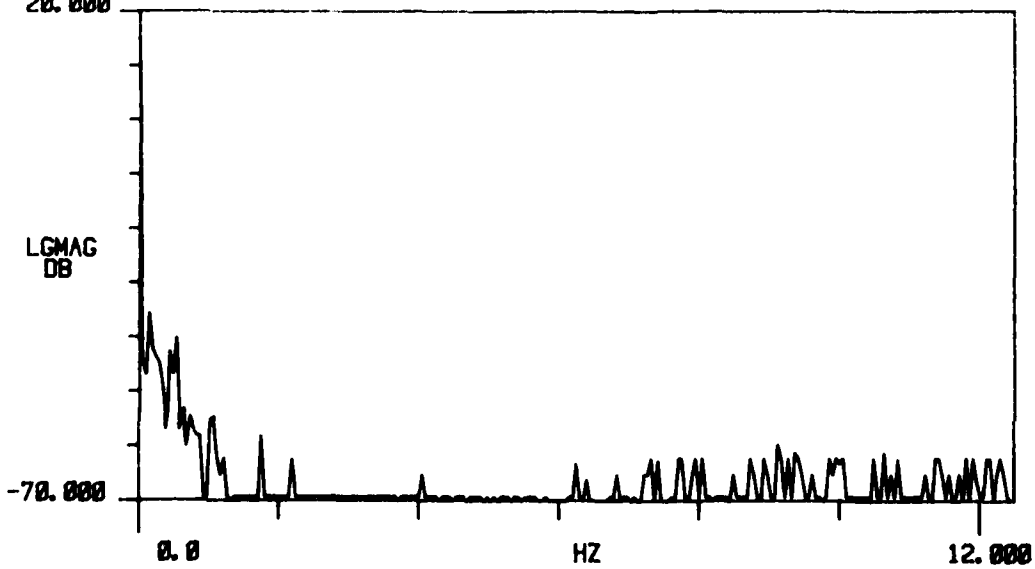
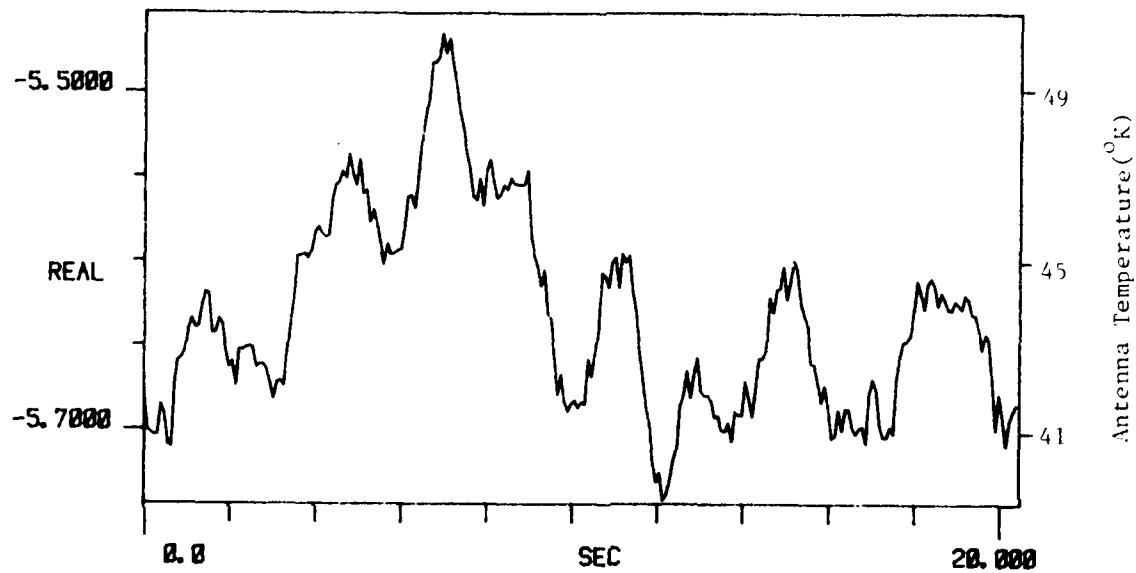


Figure D-5. Zenith Sky Measurement, 11 Mar 80

TI AVG 1 R# 33 #A 1



TI AVG 20.000 R# 33 #A 1

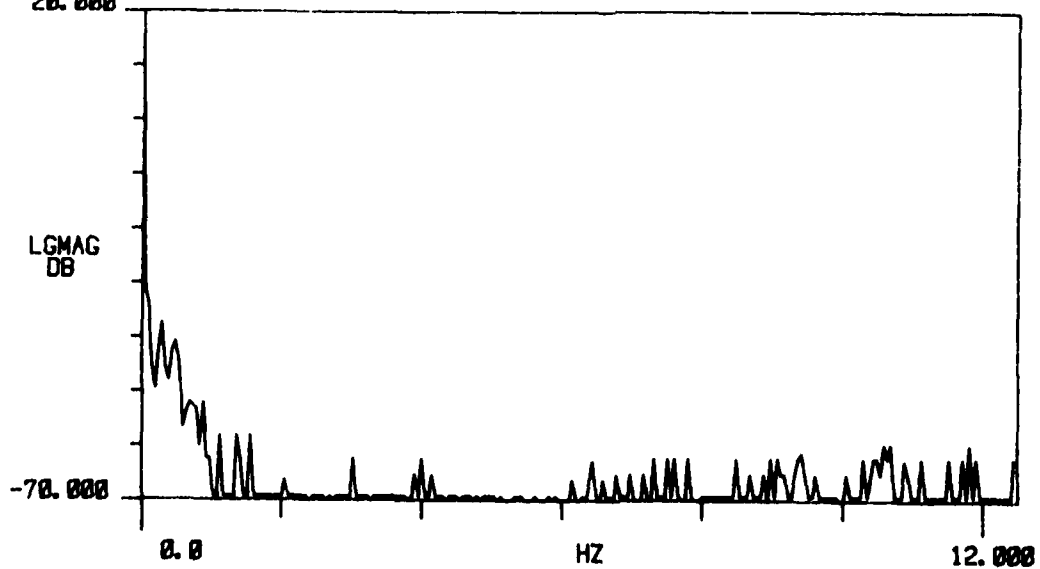


Figure D-5. Zenith Sky Measurement. 11 Mar 80
211

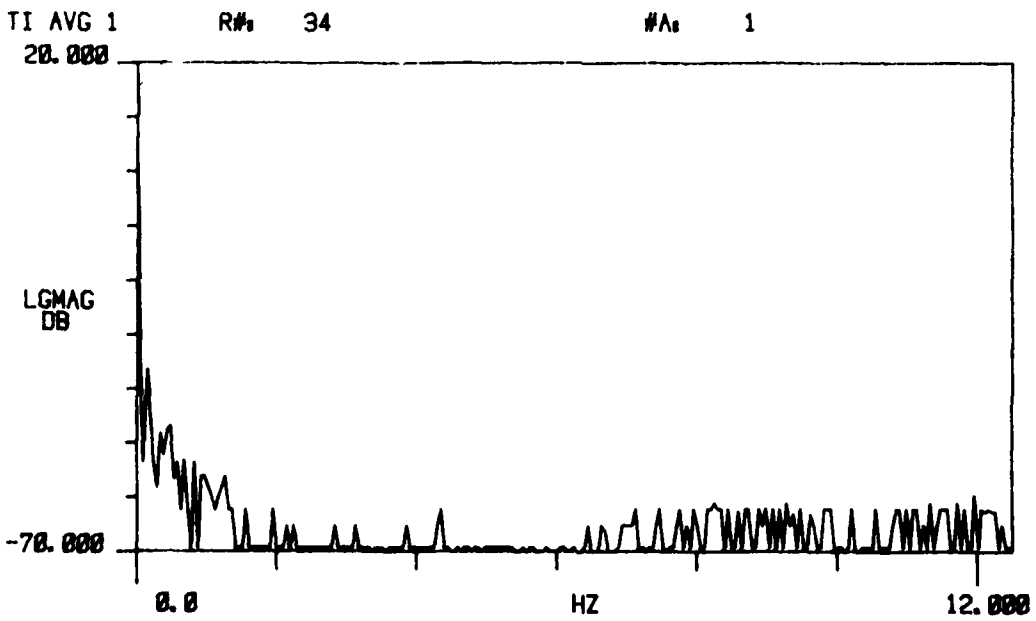
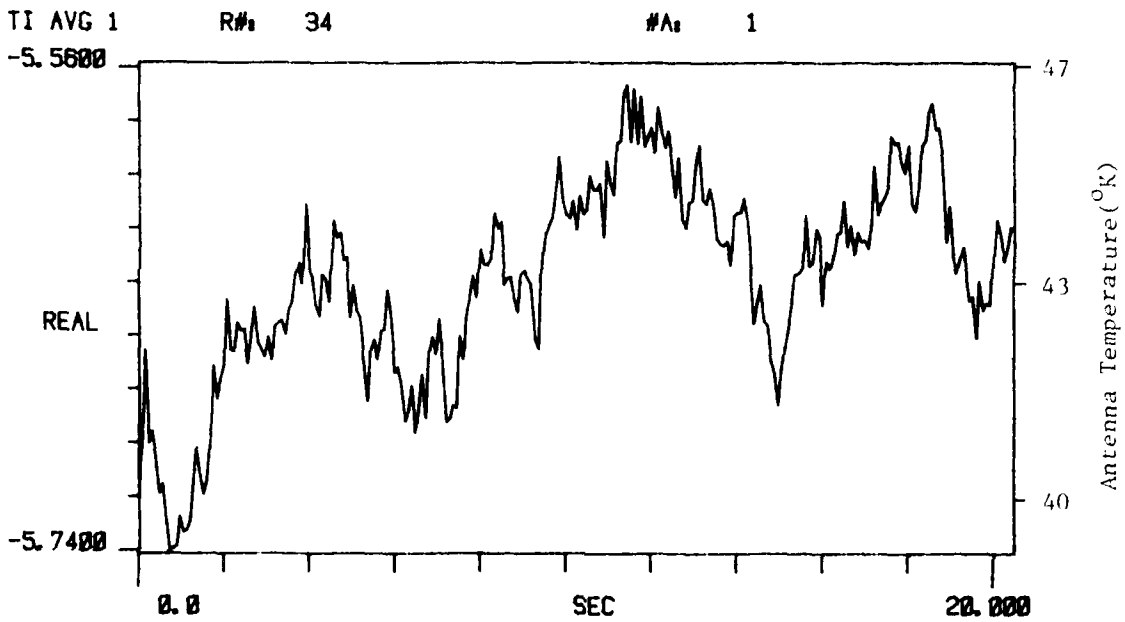
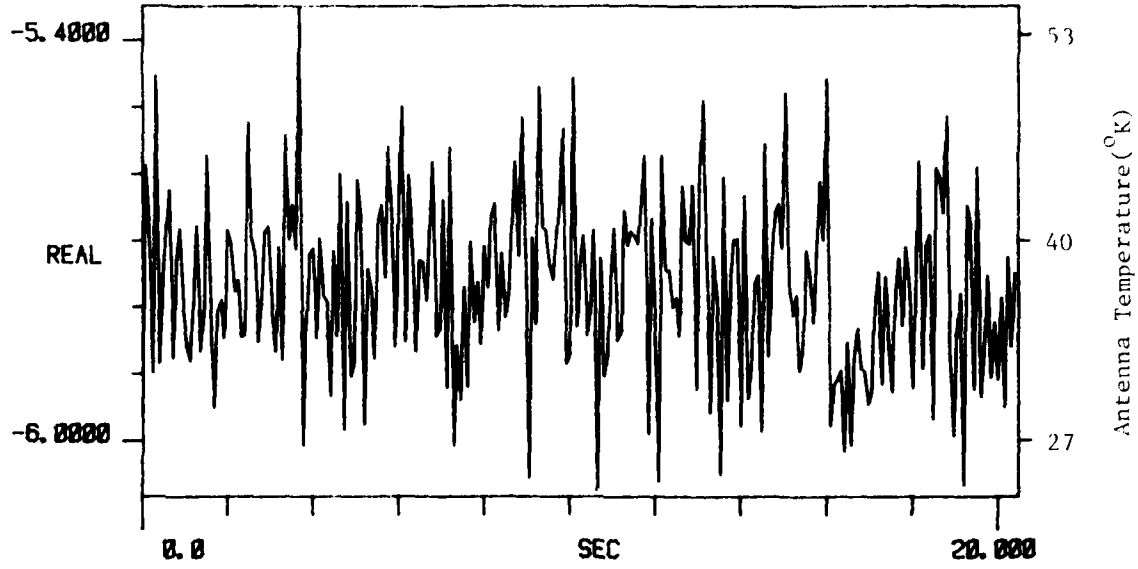


Figure D-5. Zenith Sky Measurement. 11 Mar 80

TI AVG 1

R# 44

#A 1



TI AVG
20.000

R# 44

#A 1

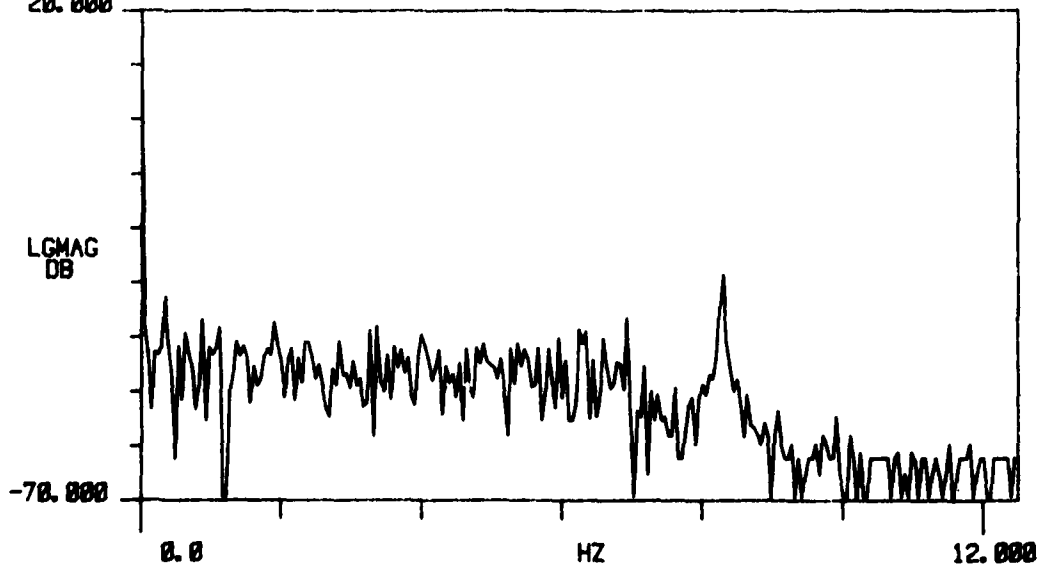
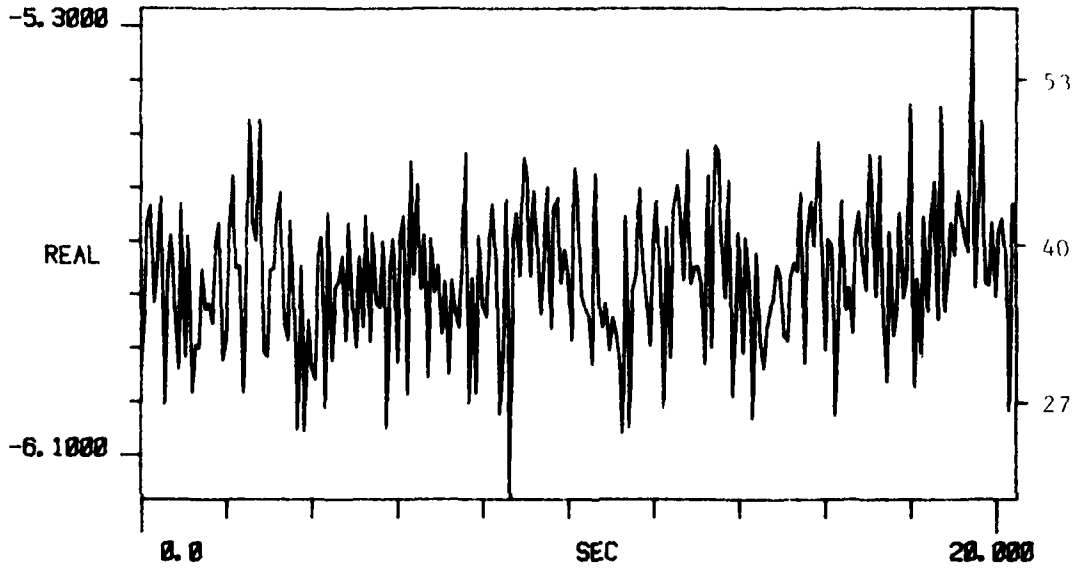


Figure D-5. Zenith Sky Measurement, 11 Mar 80

TI AVG 1

R# 45

#A 1



TI AVG
20.000

R# 45

#A 1

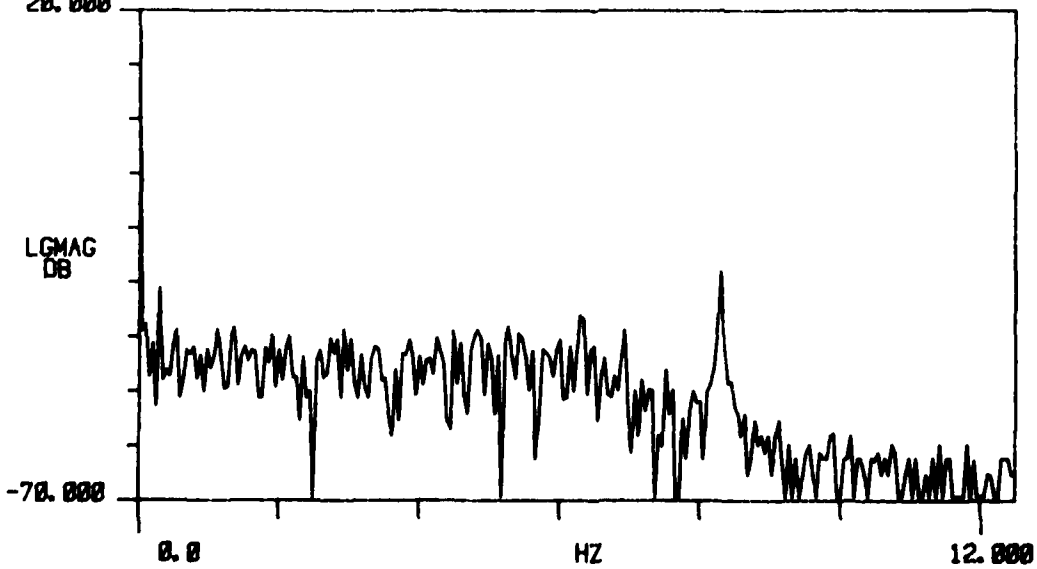


Figure D-5. Zenith Sky Measurement. 11 Mar 80

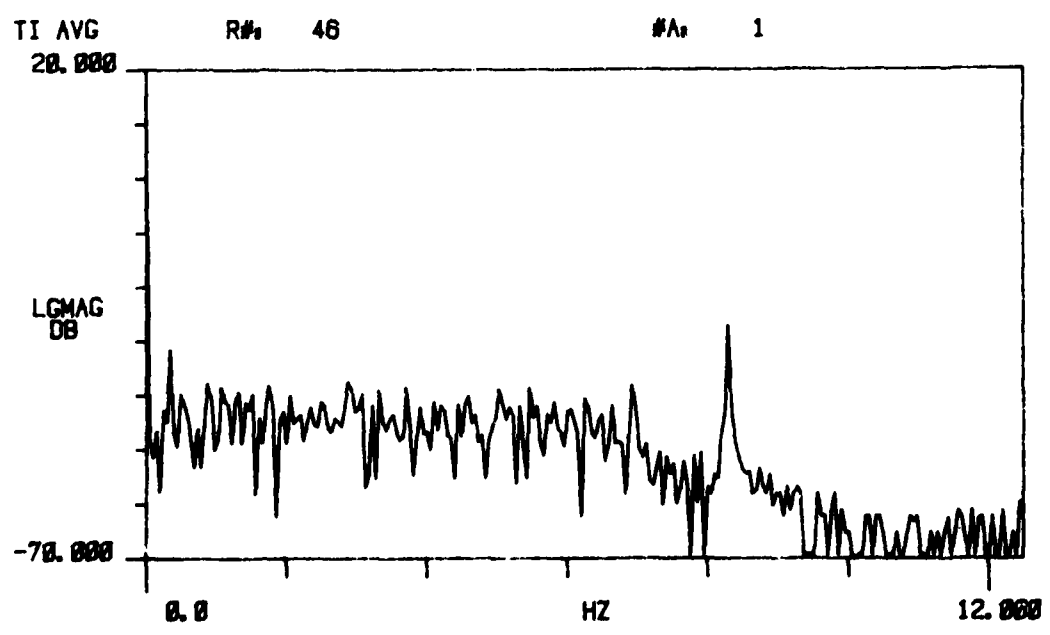
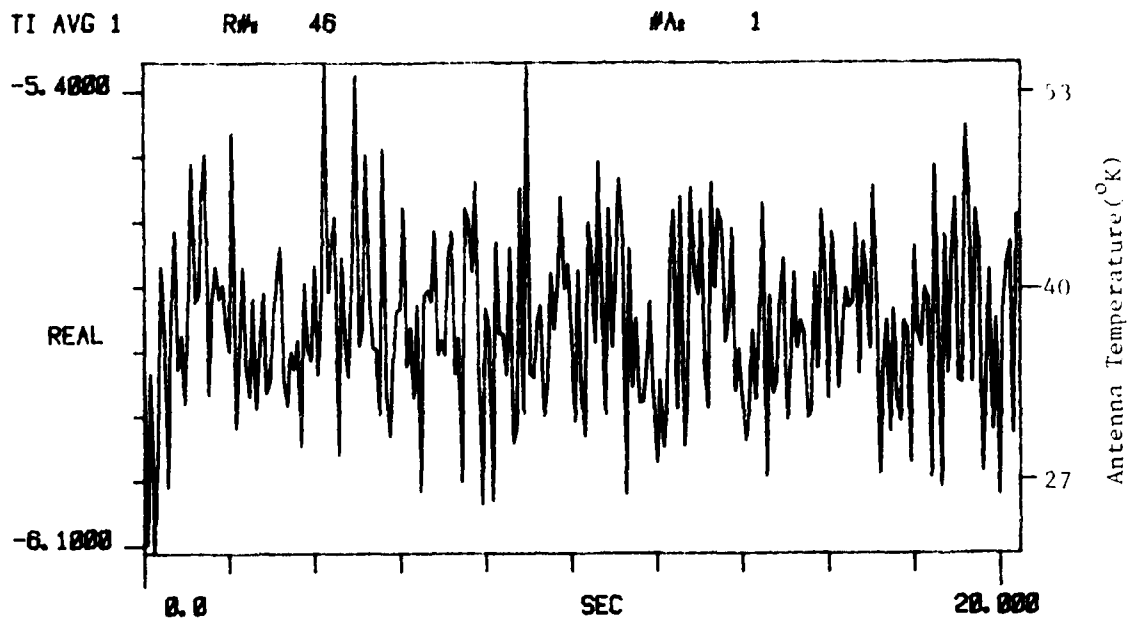


Figure D-5. Zenith Sky Measurement, 11 Mar 80

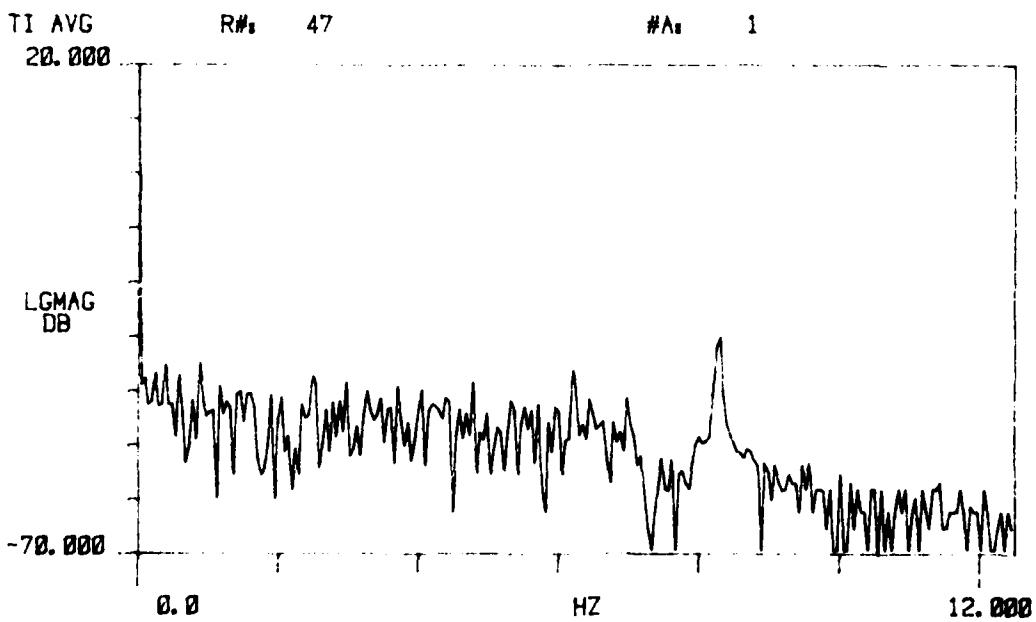
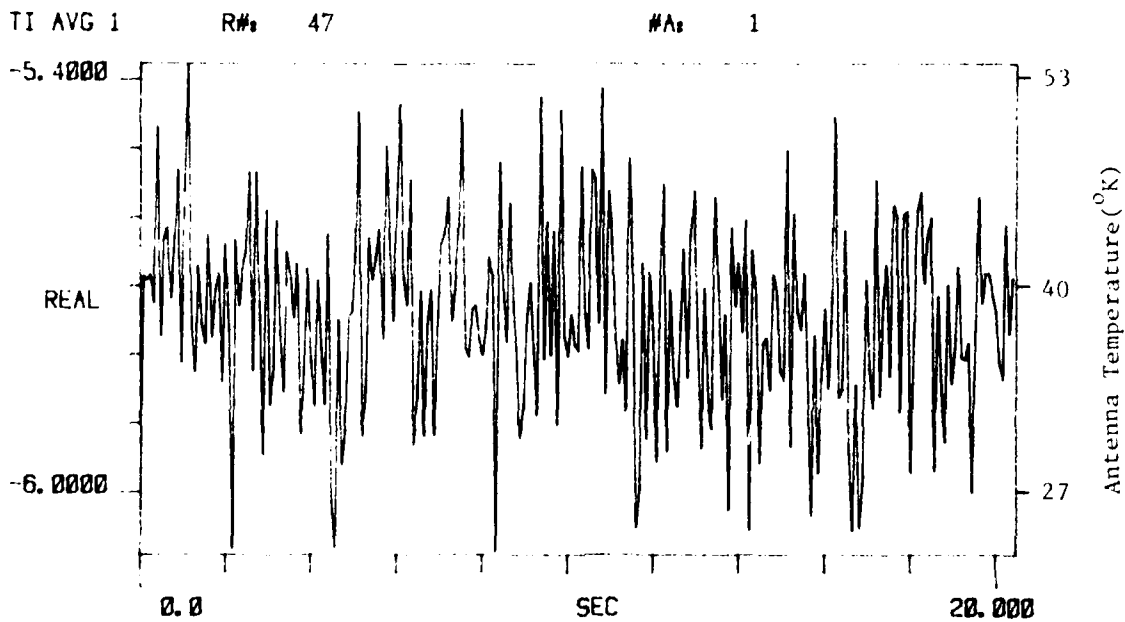
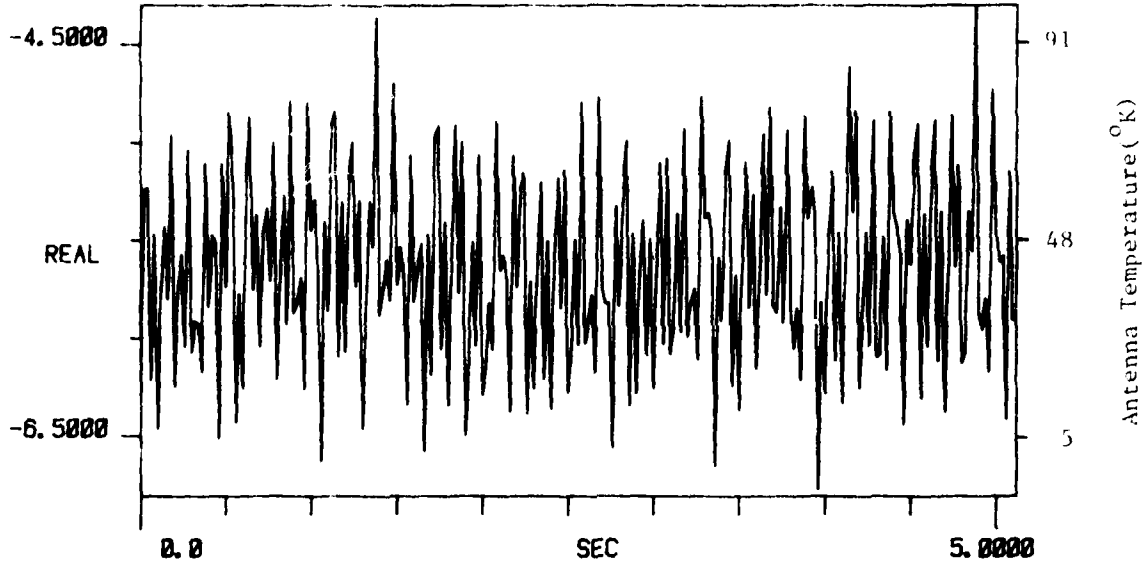


Figure D-5. Zenith Sky Measurement. 11 Mar 80

TI AVG 1

R# 54

#A 1



TI AVG
20.000

R# 54

#A 1

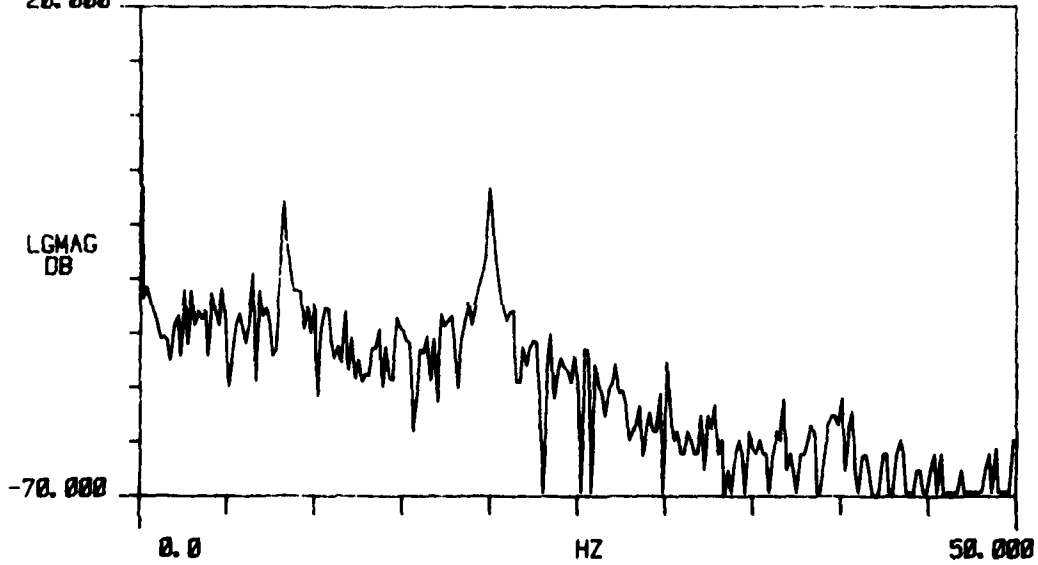


Figure D-5. Zenith Sky Measurement. 11 Mar 80

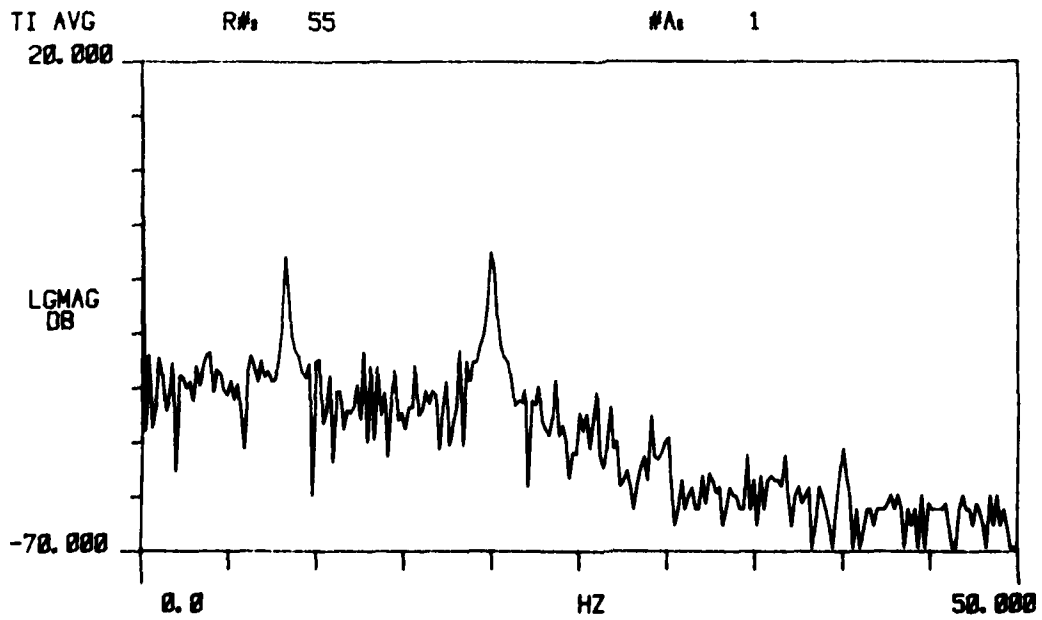
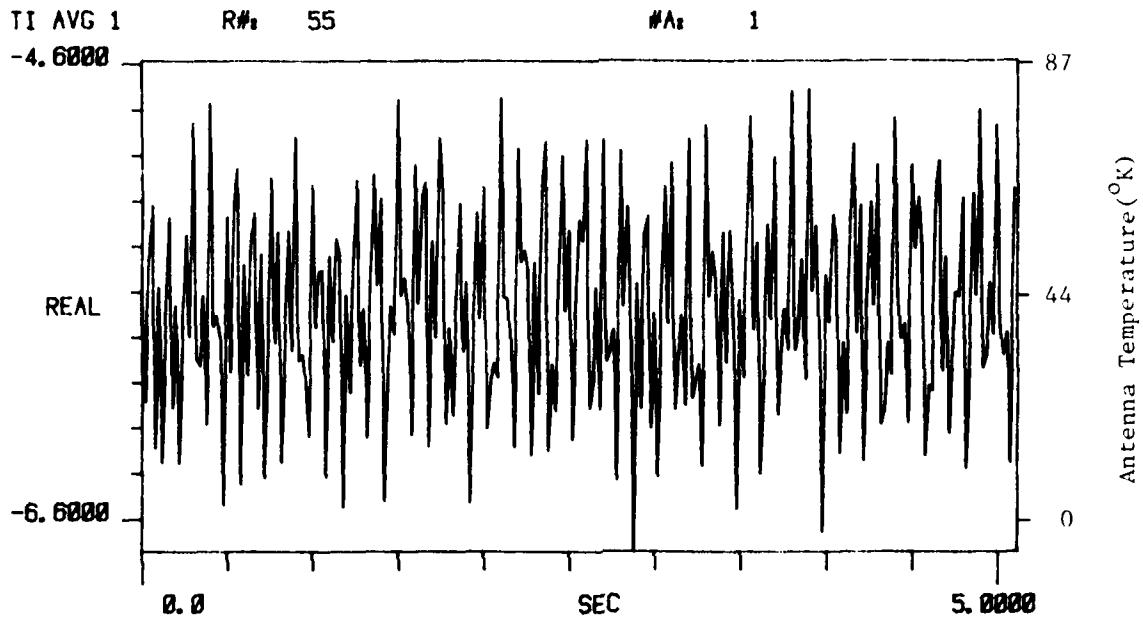


Figure D-5. Zenith Sky Measurement. 11 Mar 80

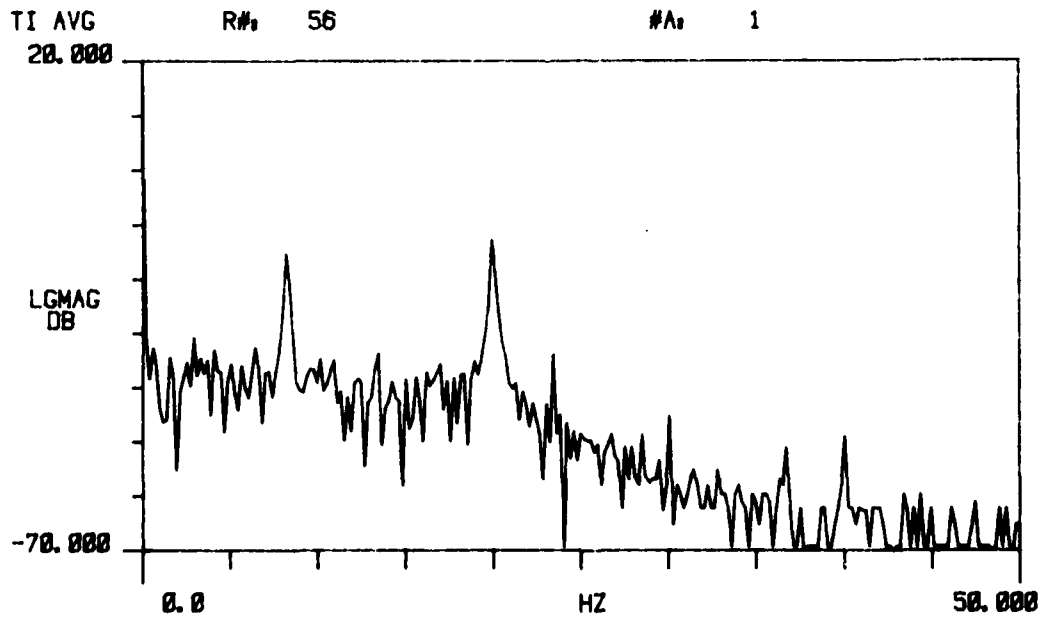
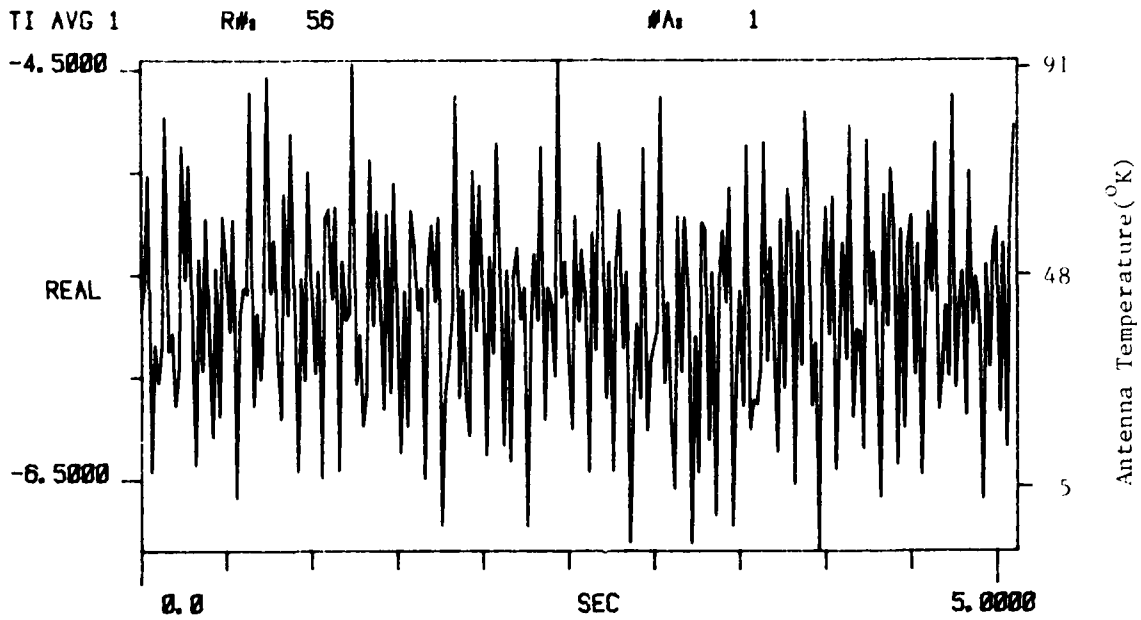
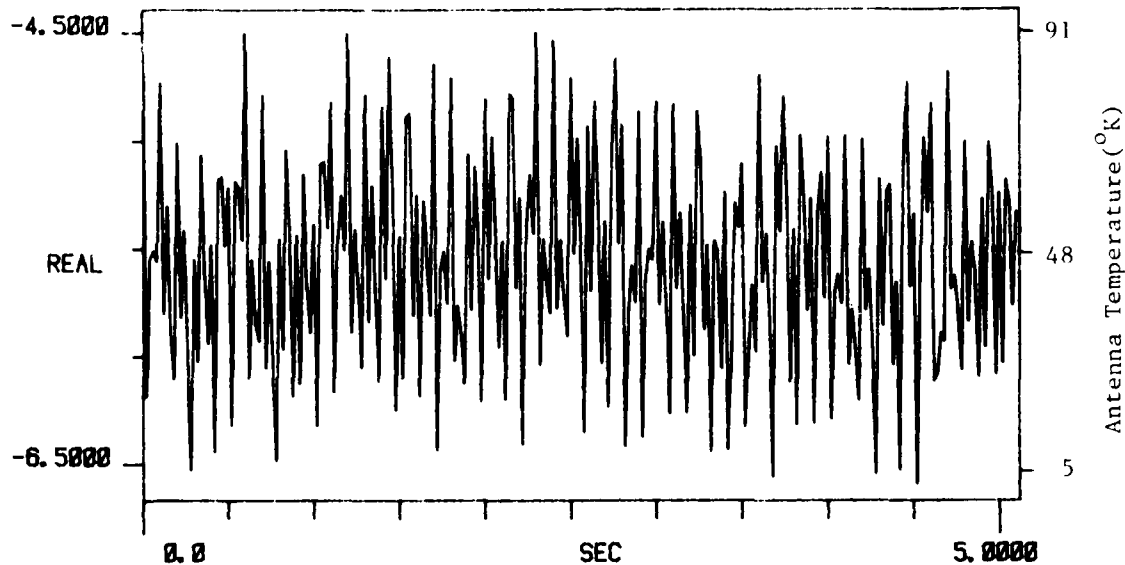


Figure D-5. Zenith Sky Measurement. 11 Mar 80

TI AVG 1

R# 57

#A 1



TI AVG

R# 57

#A 1

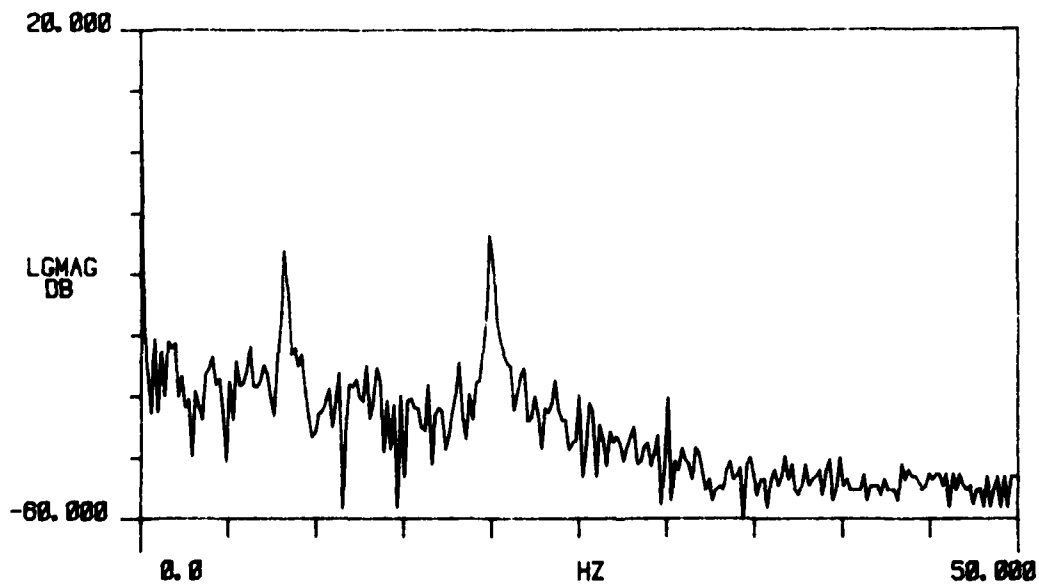
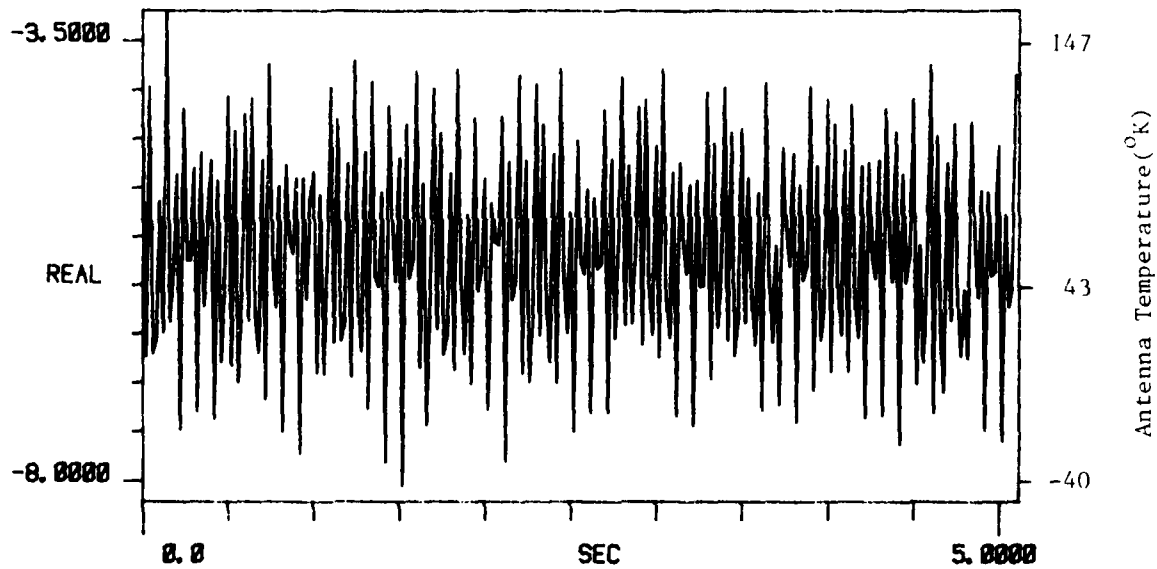


Figure D-5. Zenith Sky Measurement. 11 Mar 80

TI AVG 1

R# 62

#A 1



TI AVG 1

R# 62

#A 1

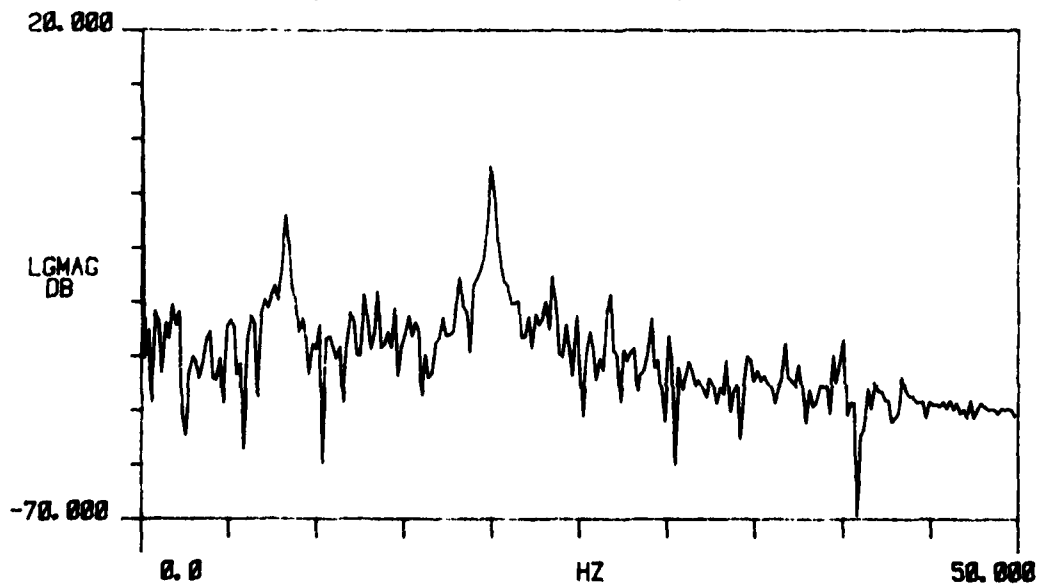
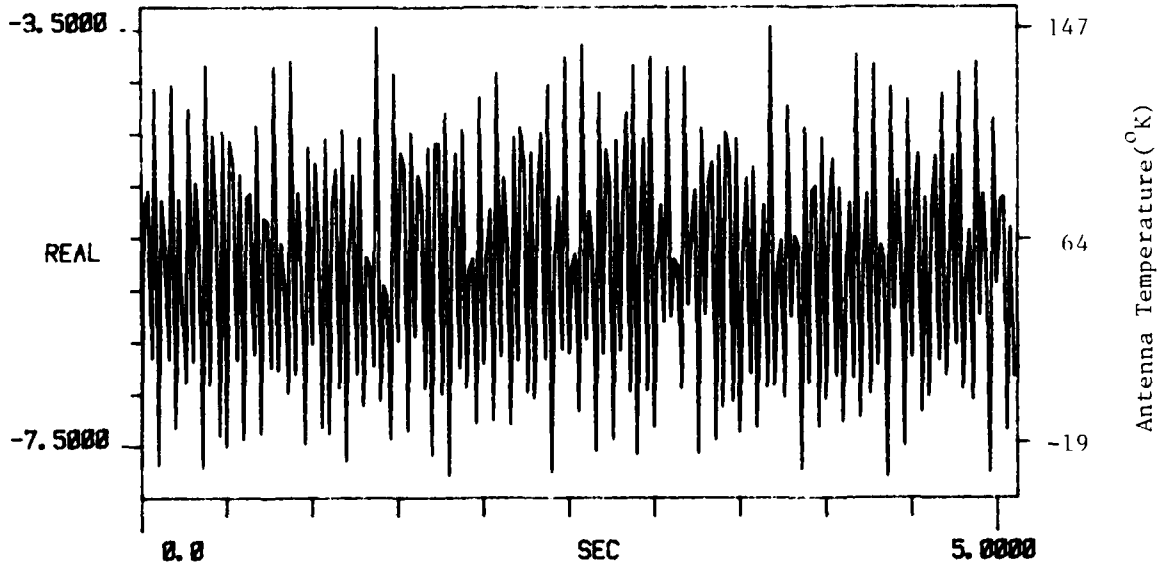


Figure D-5. Zenith Sky Measurement. 11 Mar 80

TI AVG 1

R# 63

#A 1



TI AVG
20.000

R# 63

#A 1

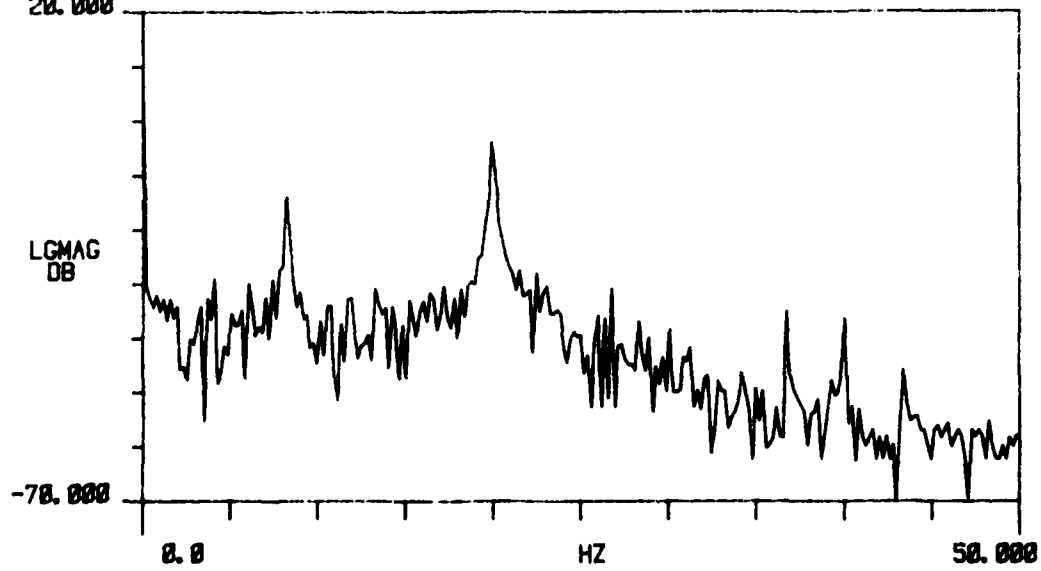


Figure D-5. Zenith Sky Measurement. 11 Mar 80

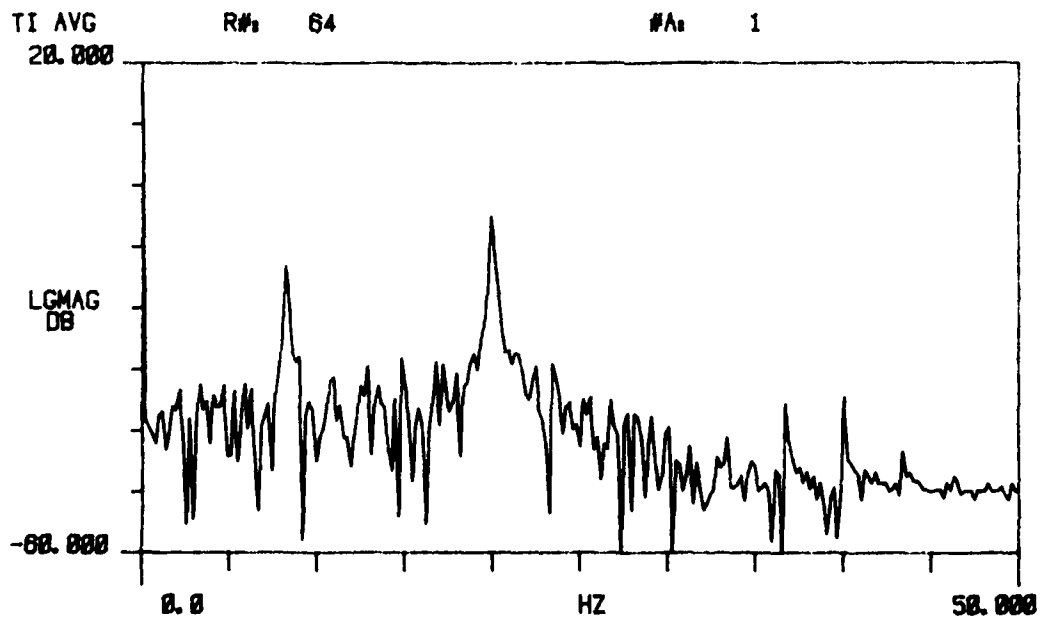
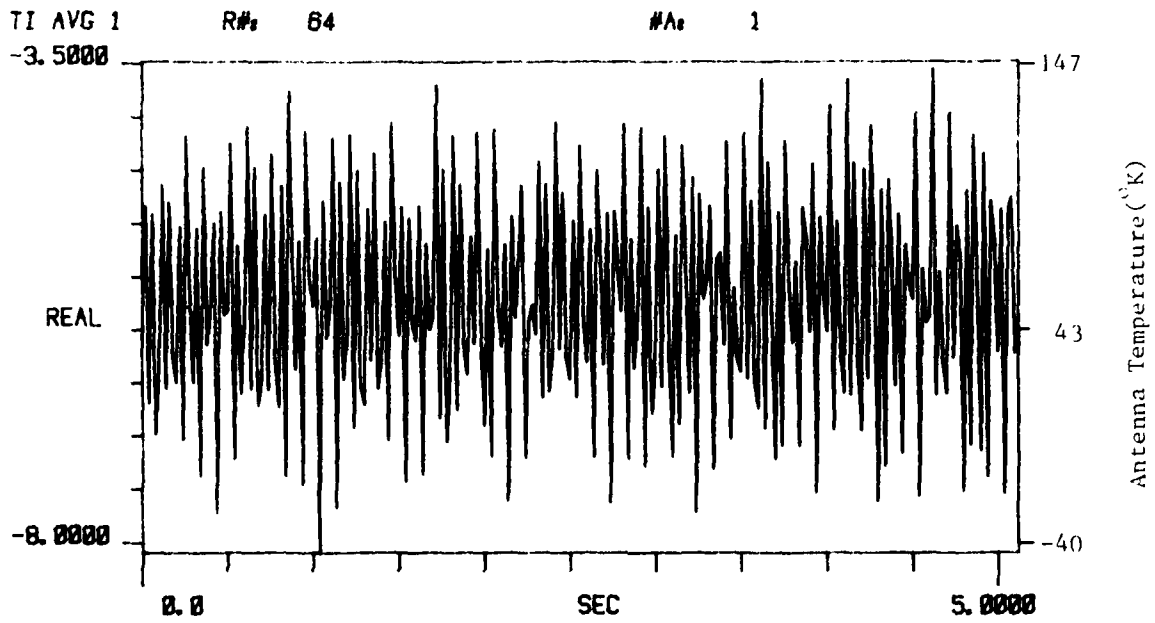
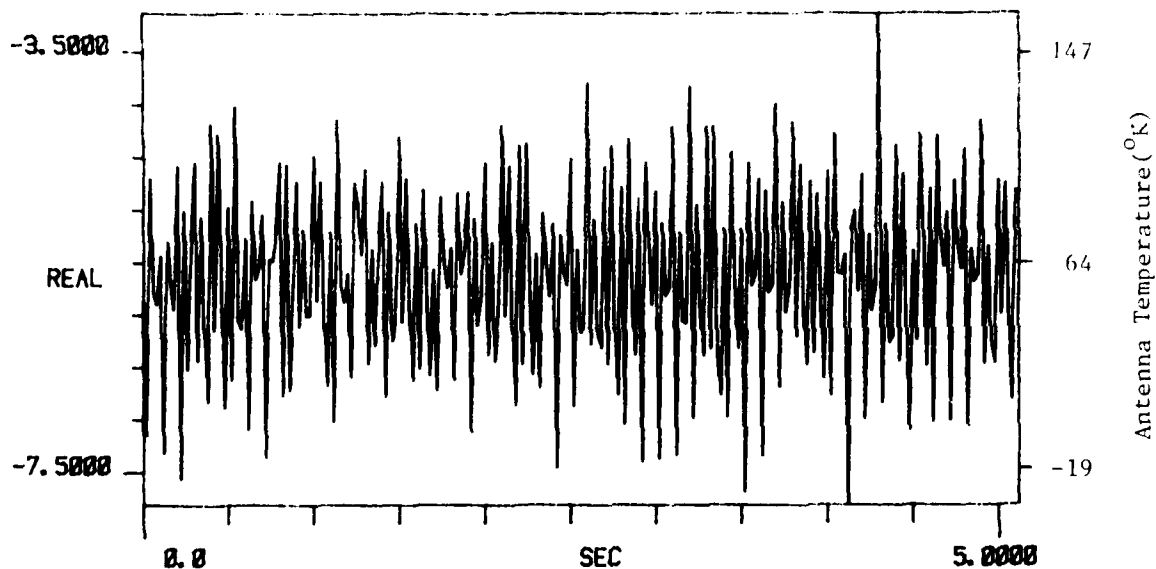


Figure D-5. Zenith Sky Measurement. 11 Mar 80

TI AVG 1

R# 65

#A 1



TI AVG

R# 65

#A 1

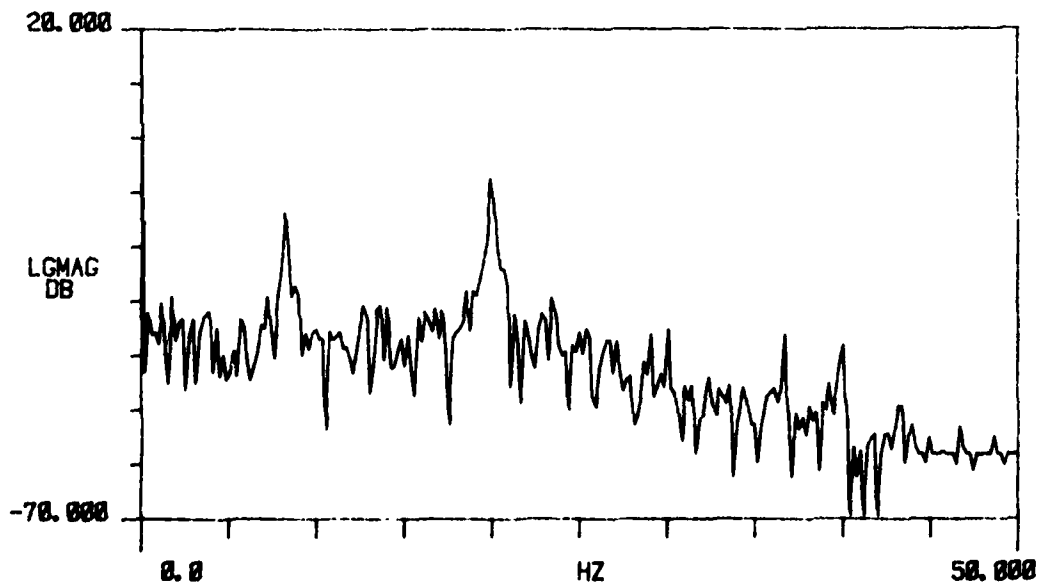


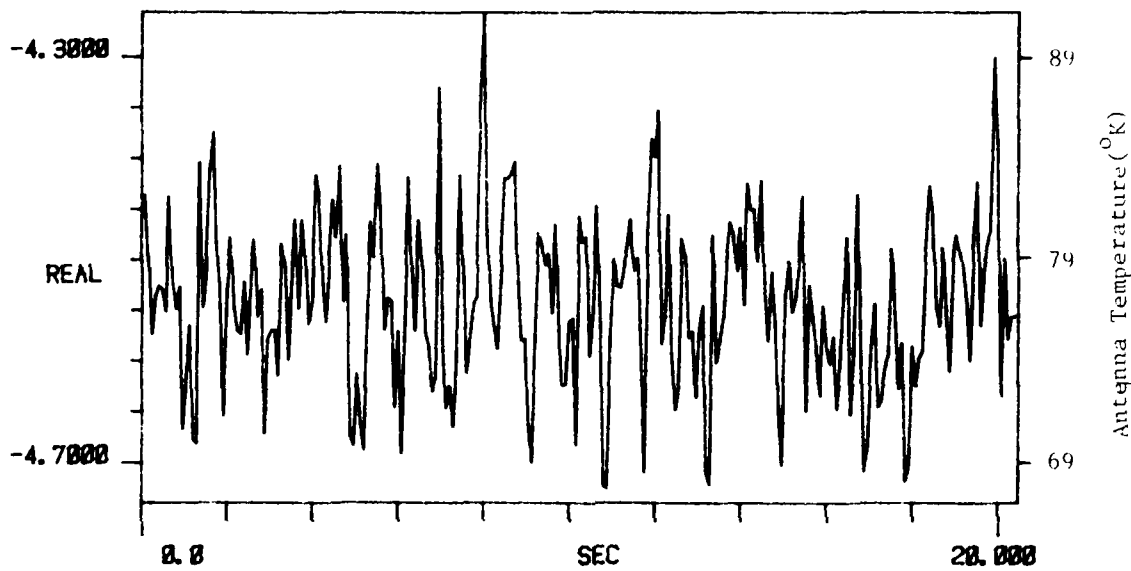
Figure D-5. Zenith Sky Measurement. 11 Mar 80

D-6. 16 March 1980
Zenith Sky Measurements

TI AVG 1

R# 80

#A 1



TI AVG
20.000

R# 80

#A 1

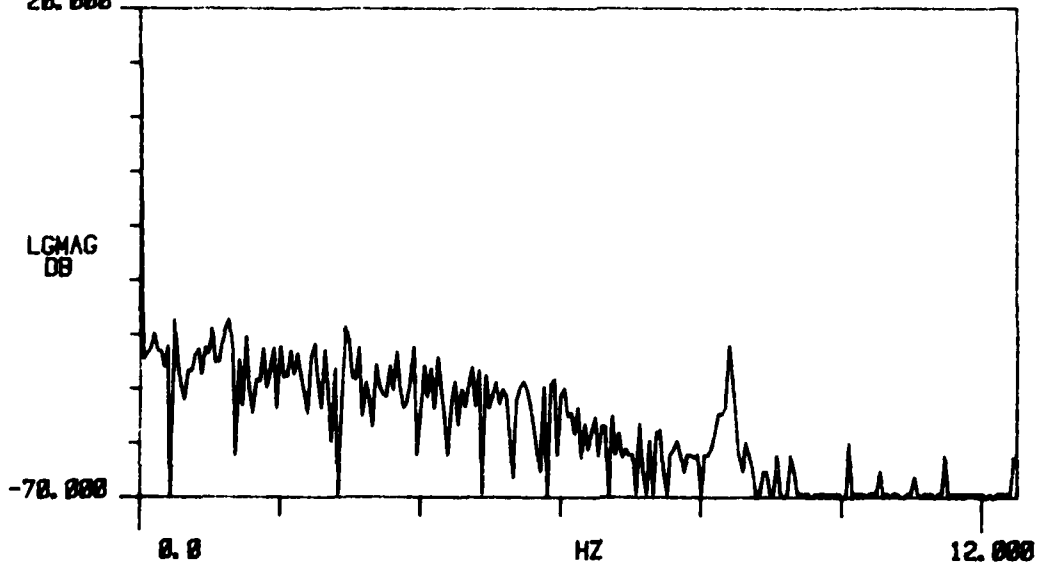
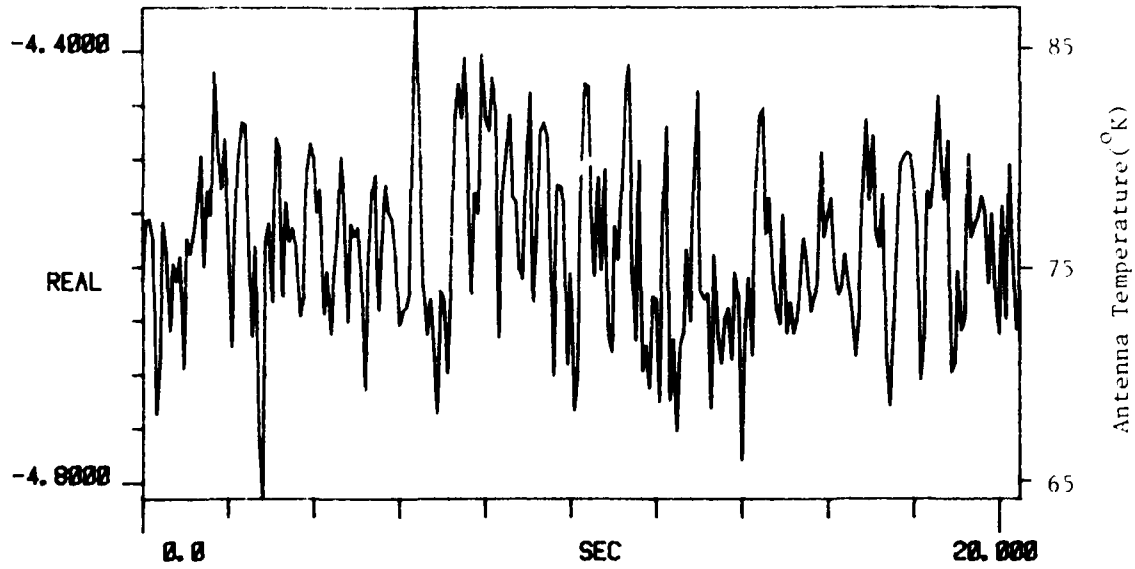


Figure D-6. Zenith Sky Measurement. 16 Mar 80

TI AVG 1

R# 81

#A 1



TI AVG
20.000

R# 81

#A 1

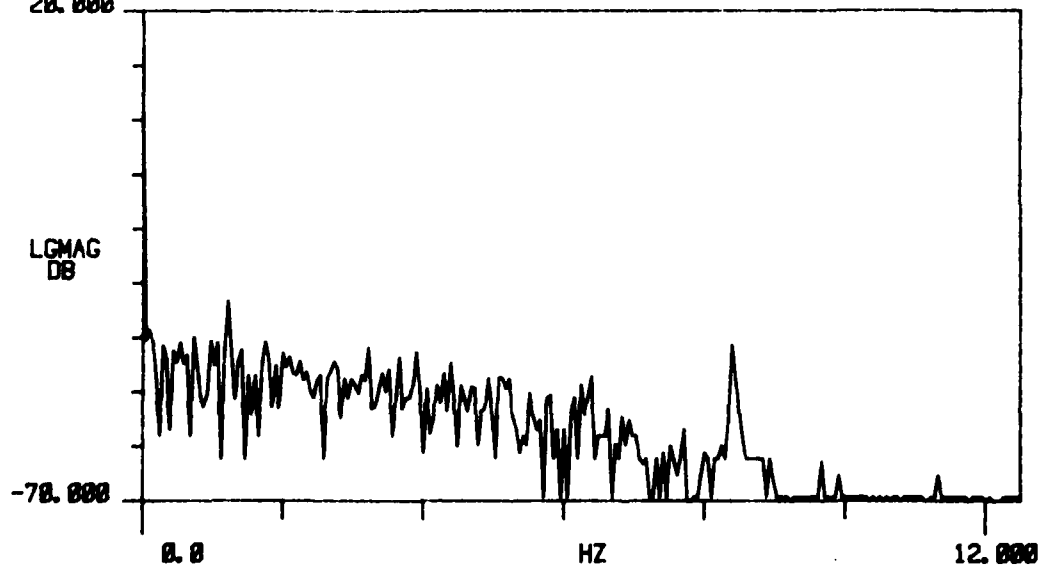
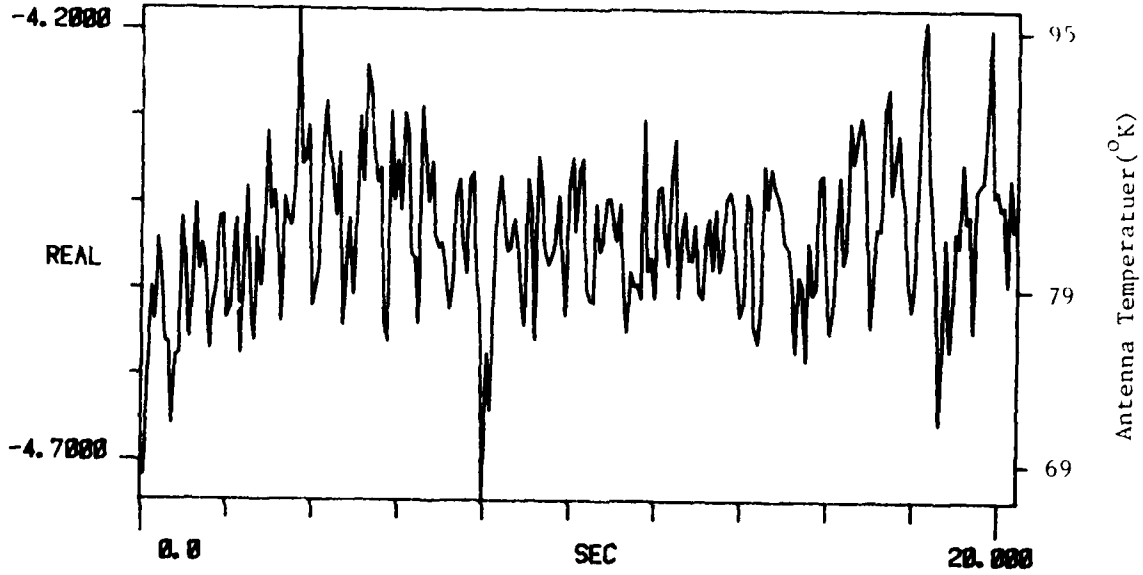


Figure D-6. Zenith Sky Measurement. 16 Mar 80
227

TI AVG 1

R# 82

#A 1



TI AVG

R# 82

#A 1

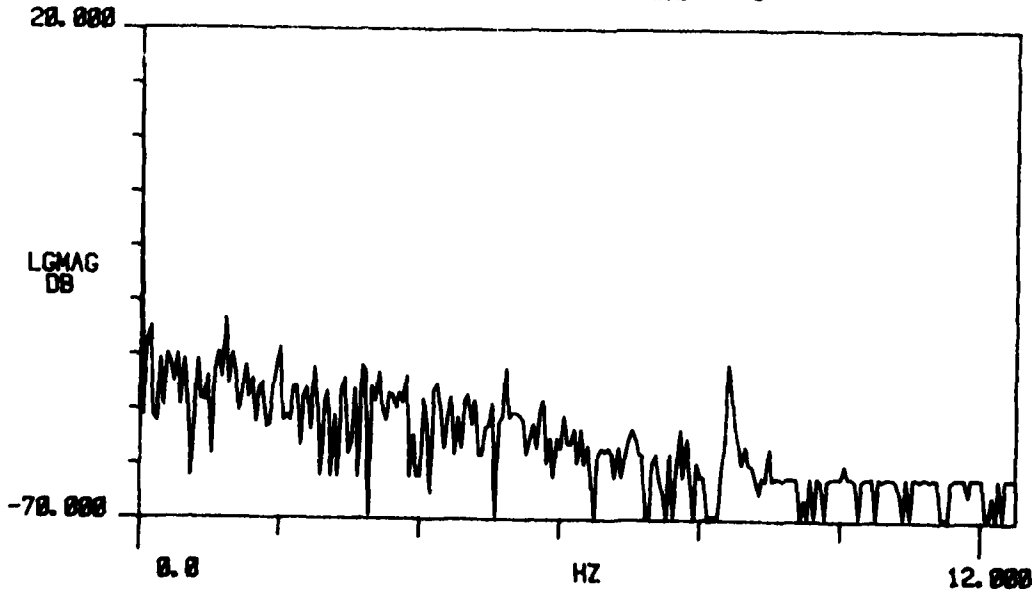
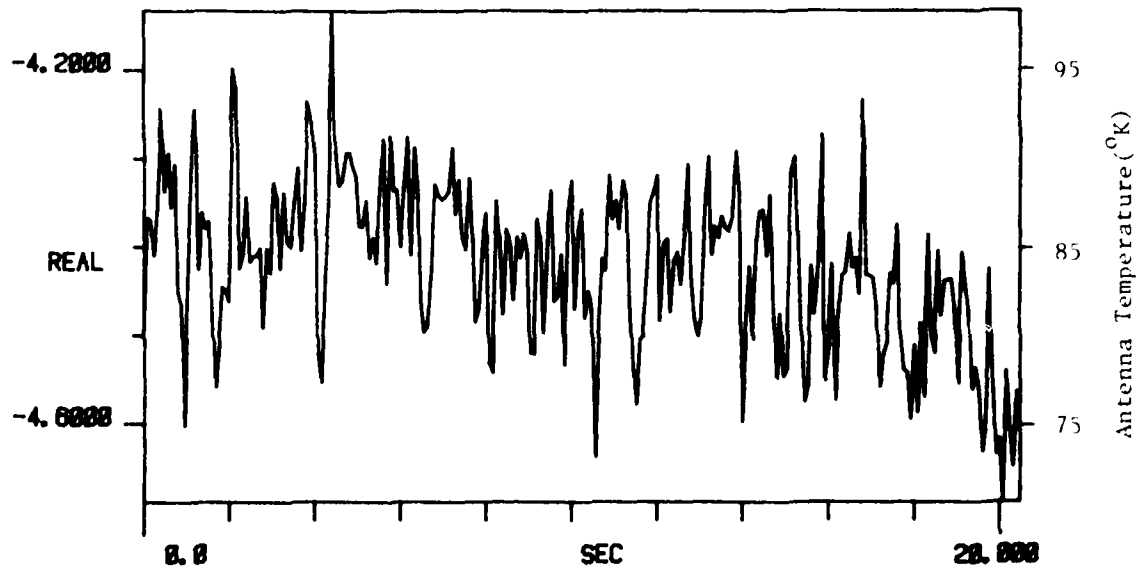


Figure D-6. Zenith Sky Measurement. 16 Mar 80

TI AVG 1

R# 83

CA 1



TI AVG
20.000

R# 83

CA 1

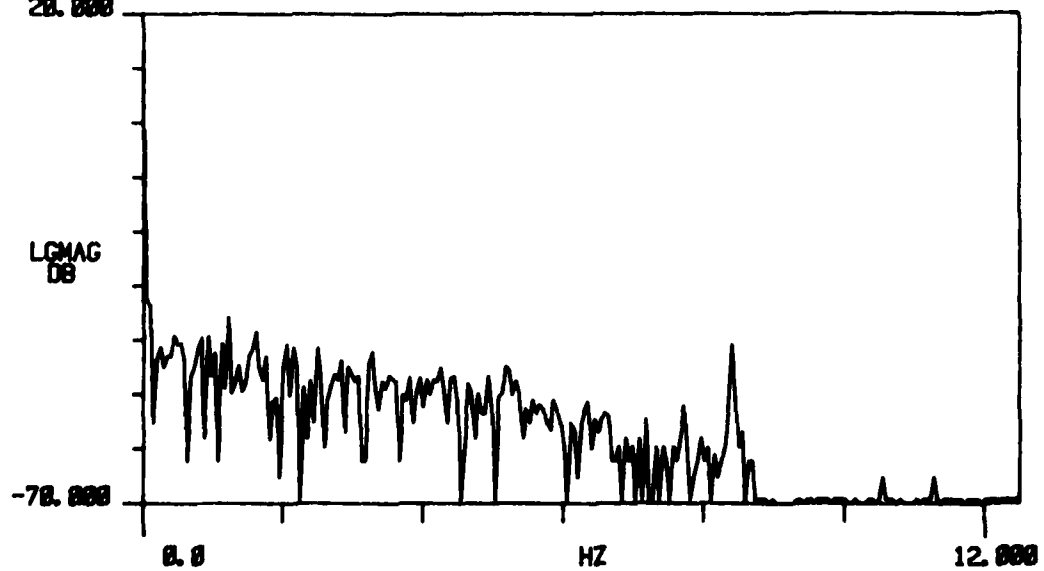
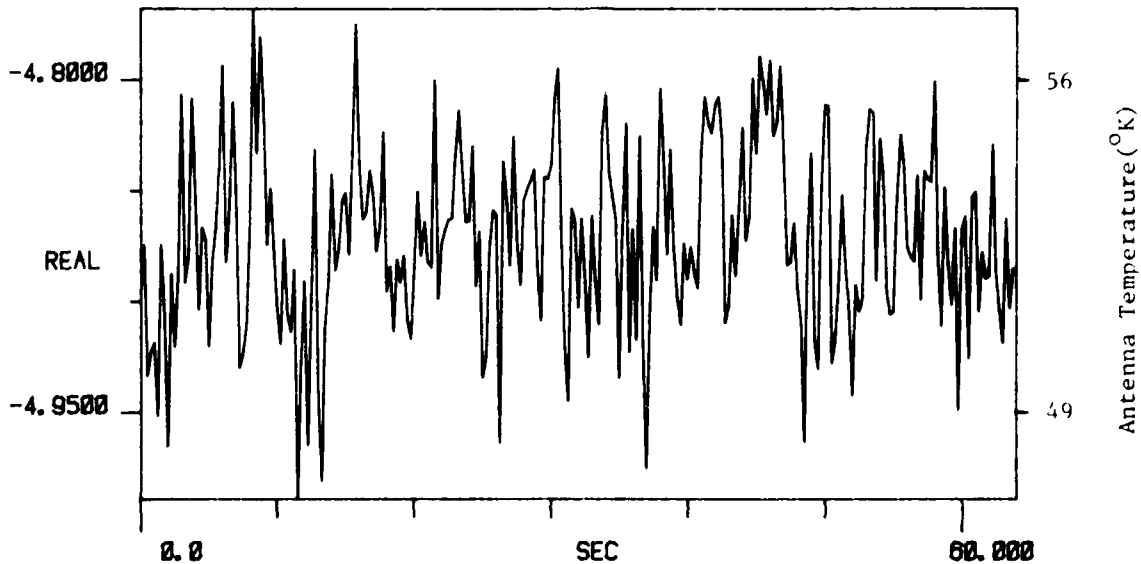


Figure D-6. Zenith Sky Measurement. 16 Mar 80

TI AVG 1

R# 100

#A 1



TI AVG
20.000

R# 100

#A 1

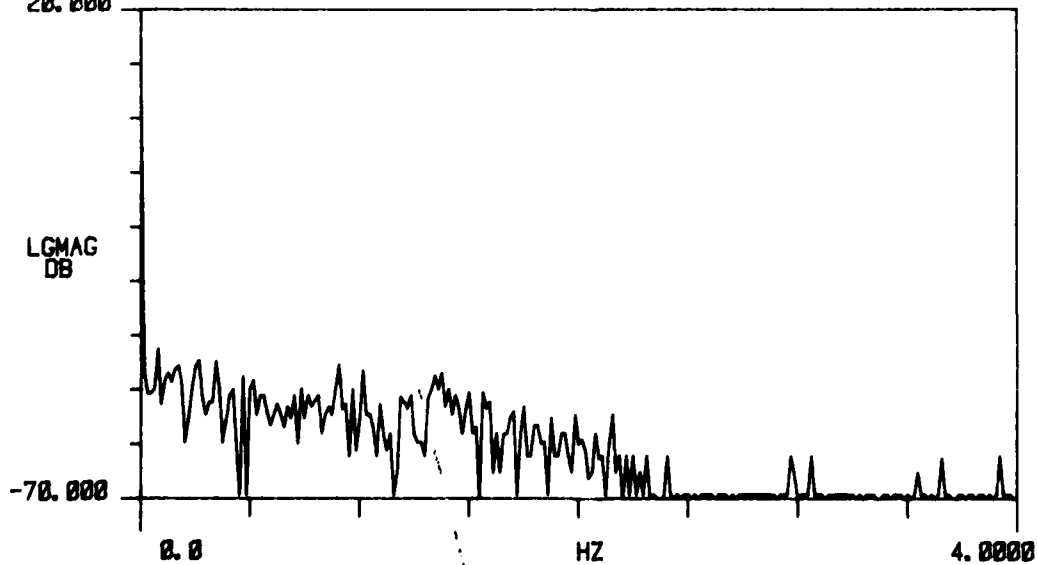
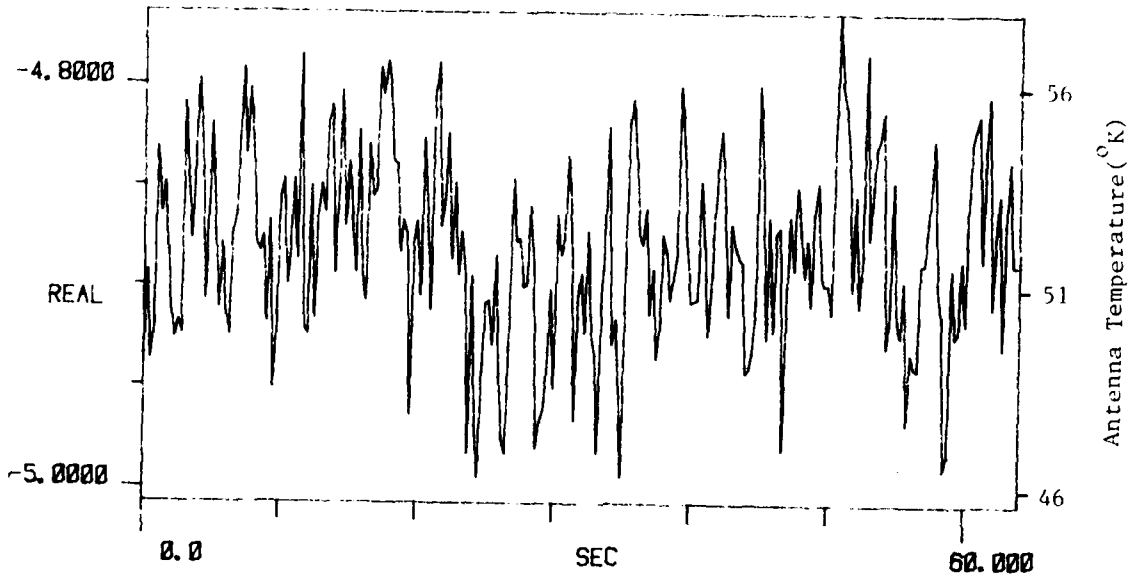


Figure D-6. Zenith Sky Measurement. 16 Mar 80

TI AVG 1

R#s 101

#As 1



TI AVG
20.000

R#s 101

#As 1

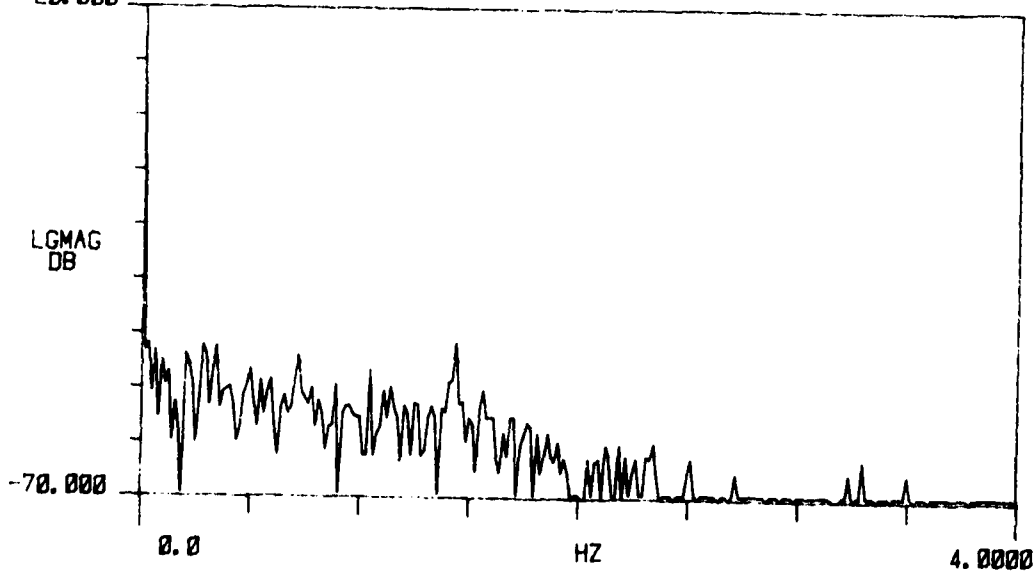
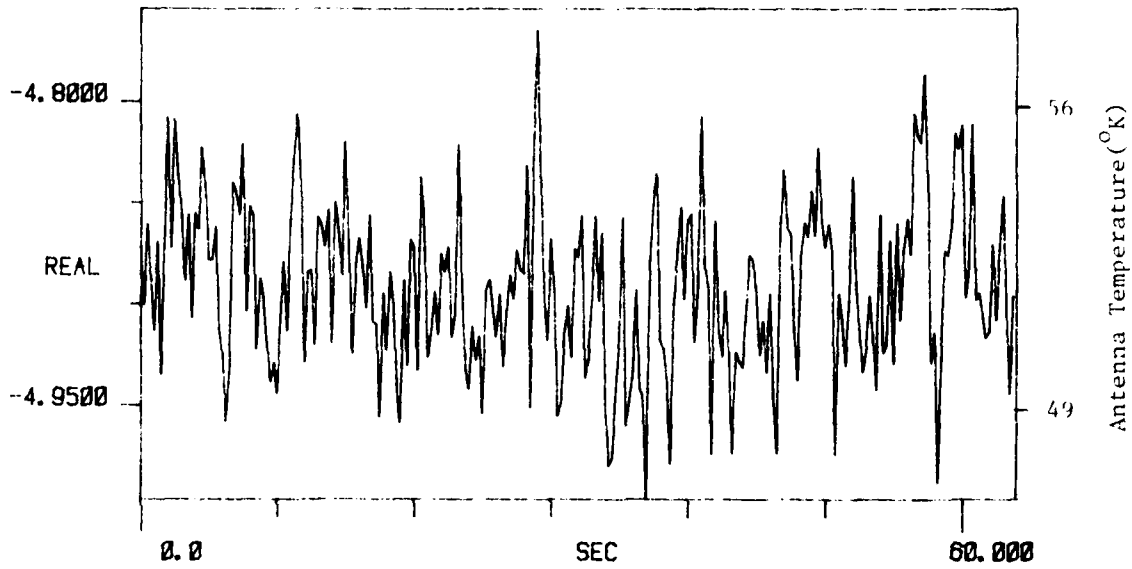


Figure D-6. Zenith Sky Measurement. 16 Mar 80

TI AVG 1

R# 102

#A 1



TI AVG
20.000

R# 102

#A 1

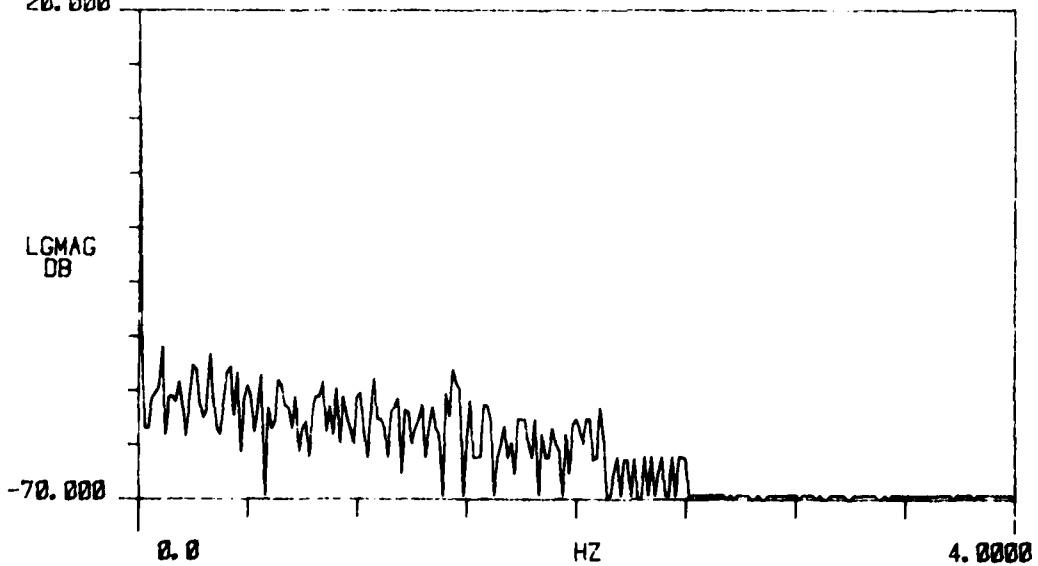
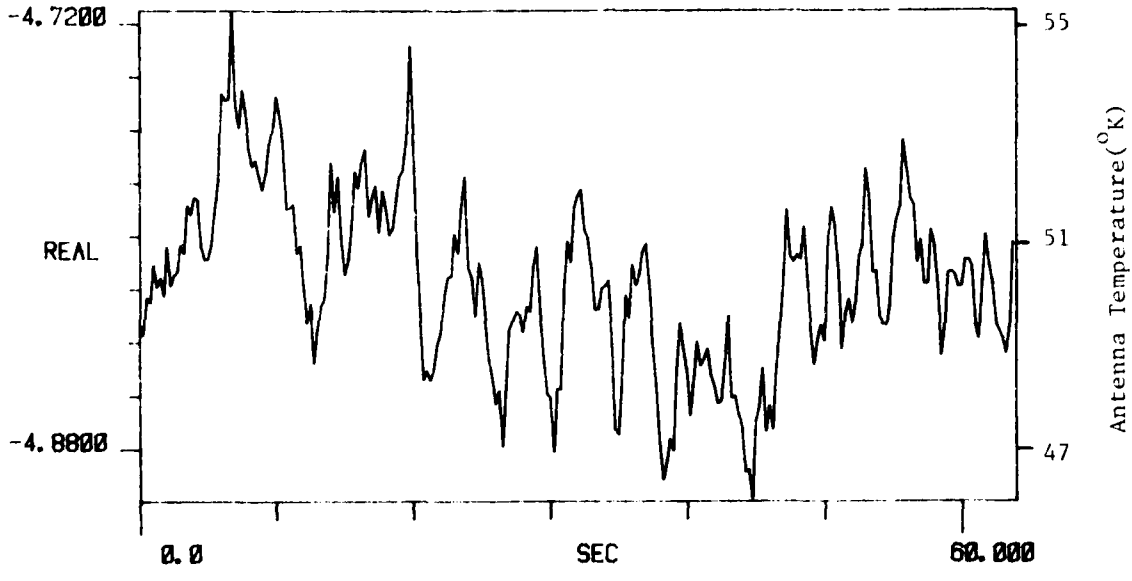


Figure D-6. Zenith Sky Measurement. 16 Mar 80

TI AVG 1

R# 117

#A 1



TI AVG
20.000

R# 117

#A 1

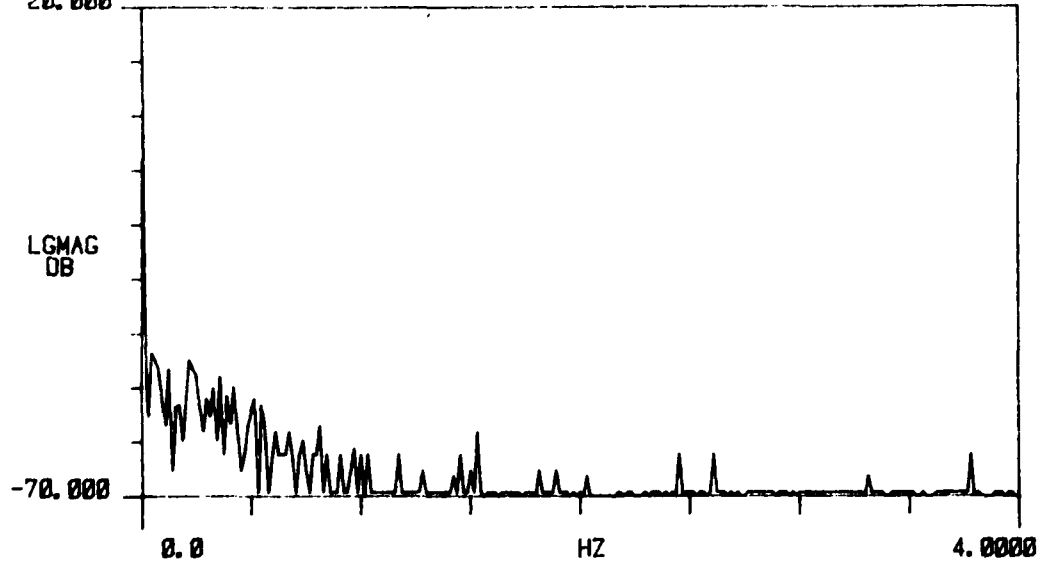
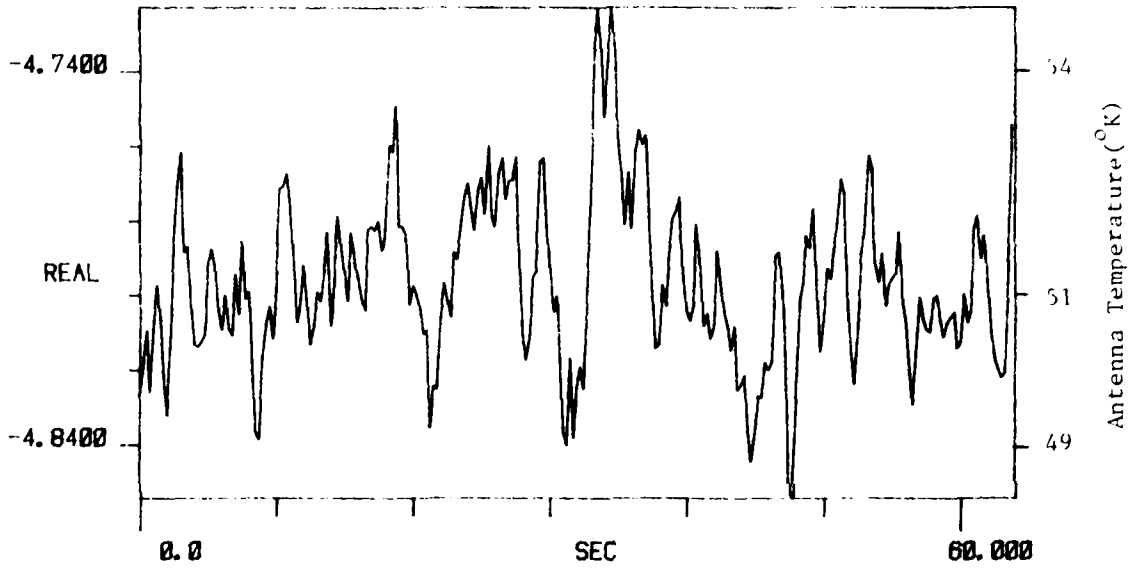


Figure D-6. Zenith Sky Measurement. 16 Mar 80

TI AVG 1

R#: 118

#As 1



TI AVG
20.000

R#: 118

#As 1

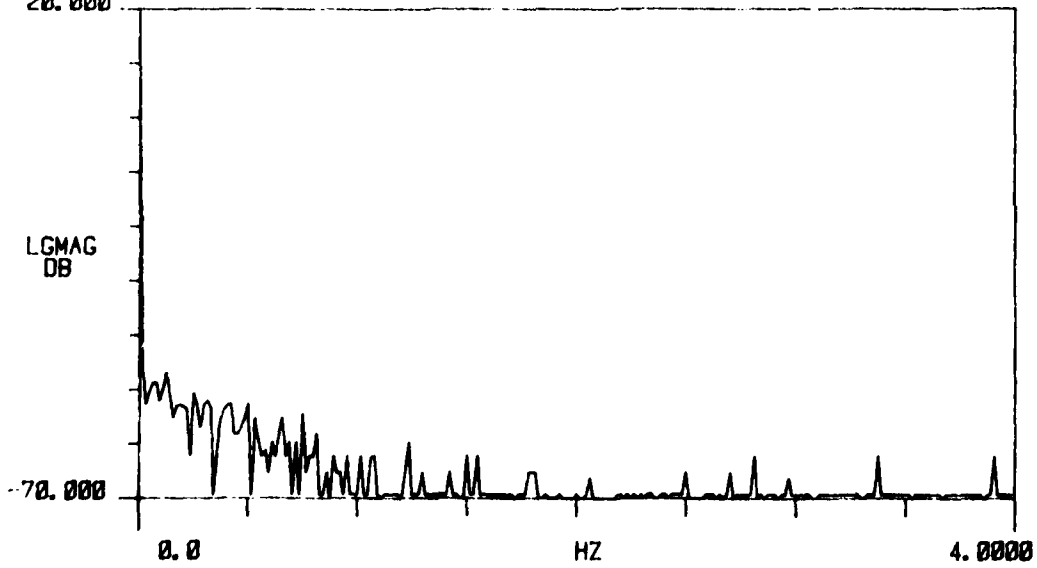
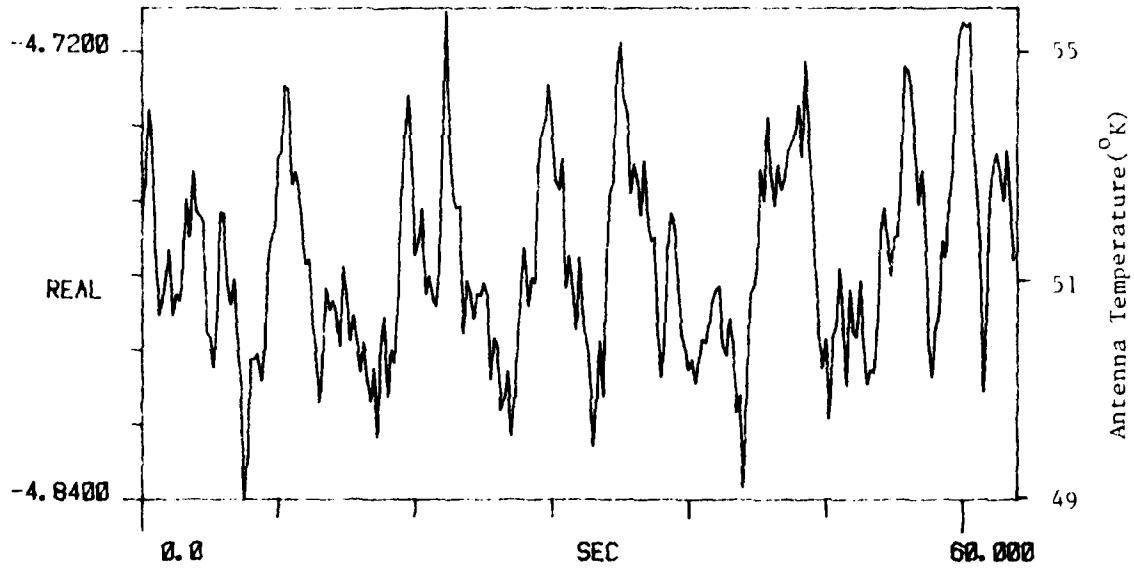


Figure D-6. Zenith Sky Measurement. 16 Mar 80
234

TI AVG 1

R# 119

#A 1



TI AVG
20.000

R# 119

#A 1

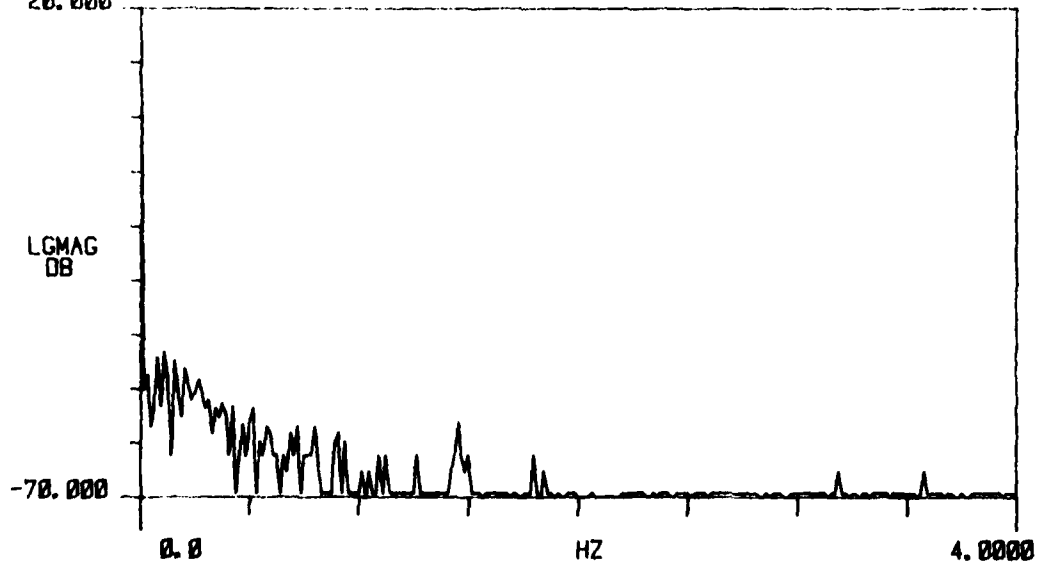
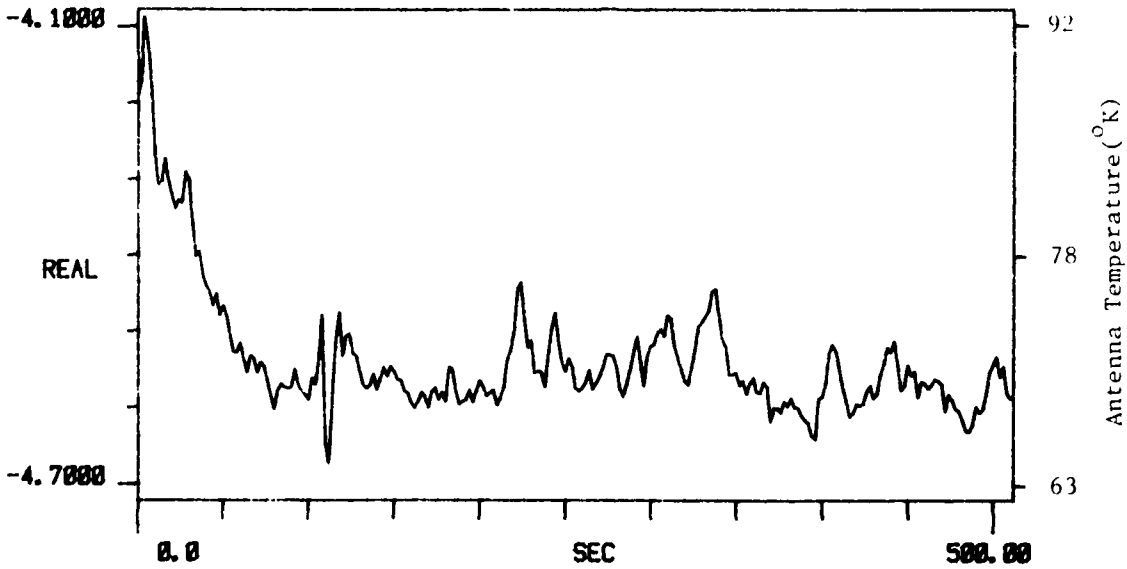


Figure D-6. Zenith Sky Measurement. 16 Mar 80

TI AVG 1

R# 82

#A 1



TI AVG

R# 82

#A 1

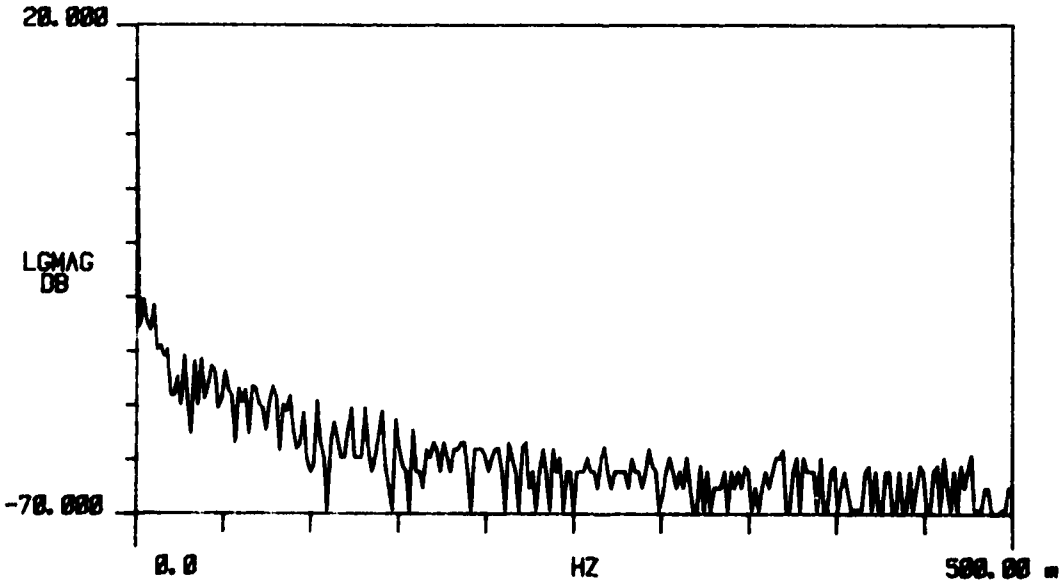


Figure D-6. Zenith Sky Measurement. 16 Mar 80

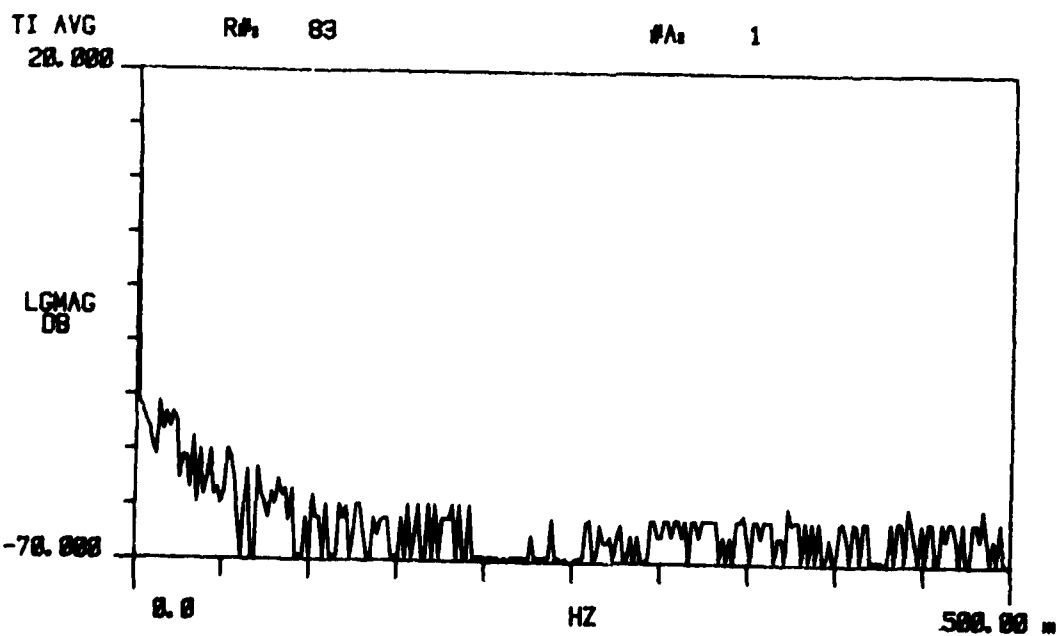
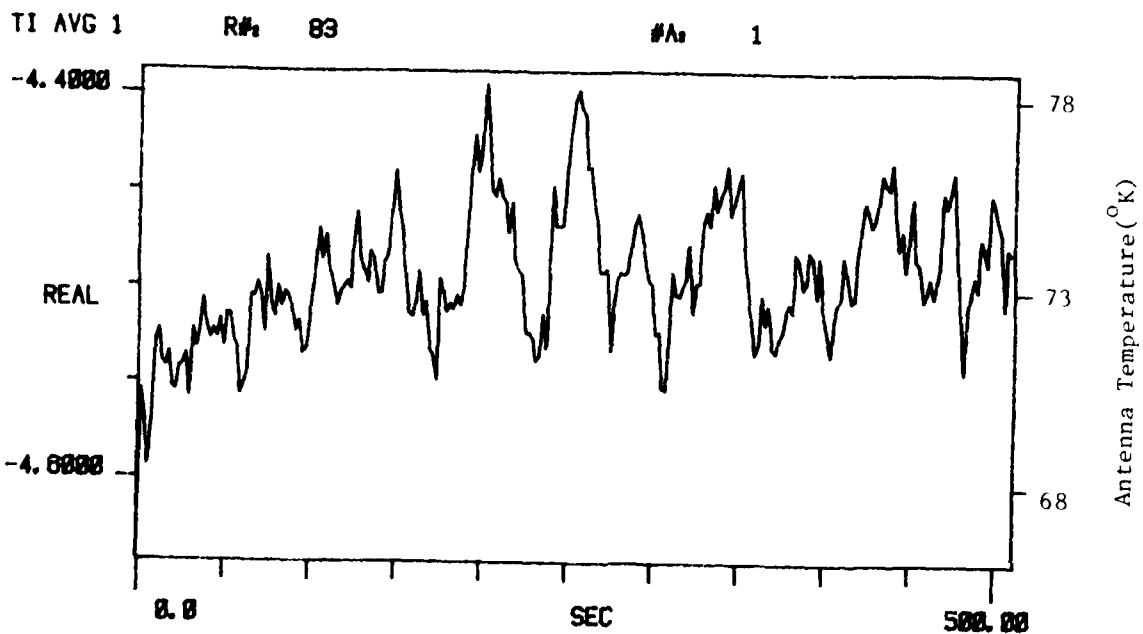
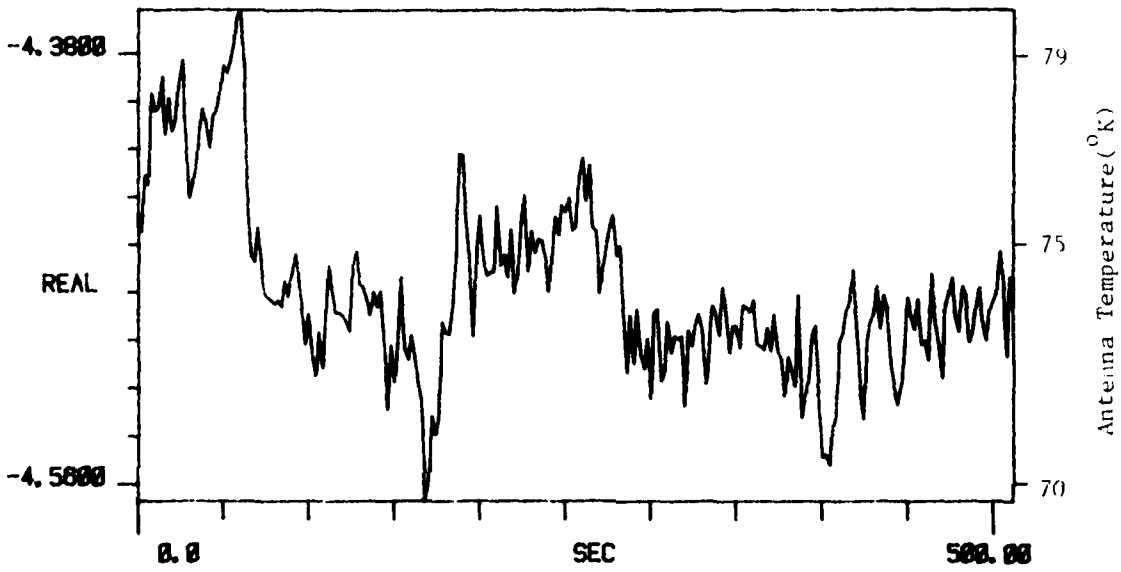


Figure D-6. Zenith Sky Measurement. 16 Mar 80
237

TI AVG 1

R# 84

#A1 1



TI AVG

R# 84

#A1 1

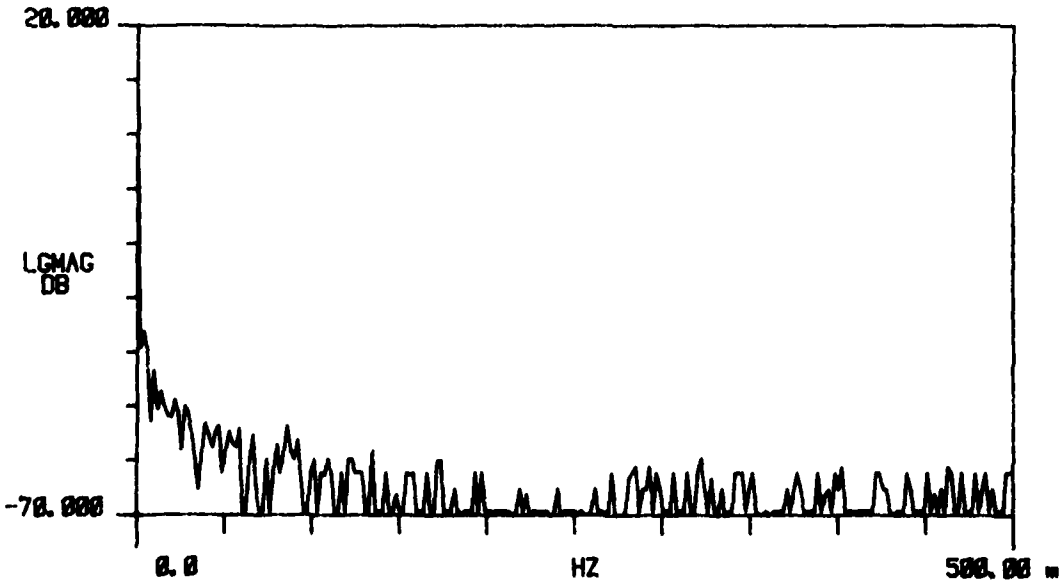


Figure D-6. Zenith Sky Measurement. 16 Mar 80

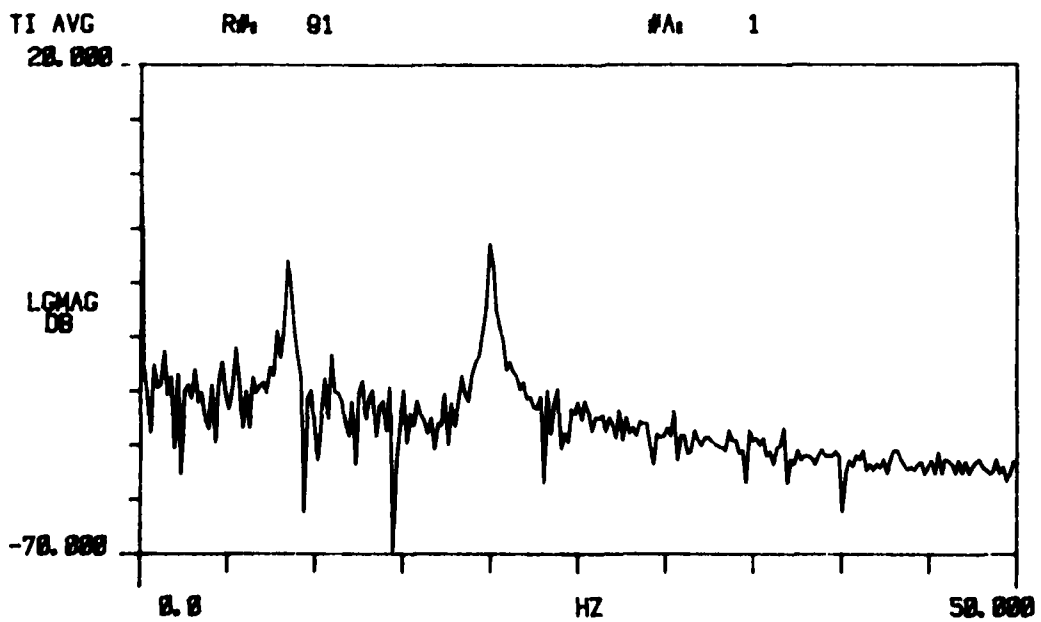
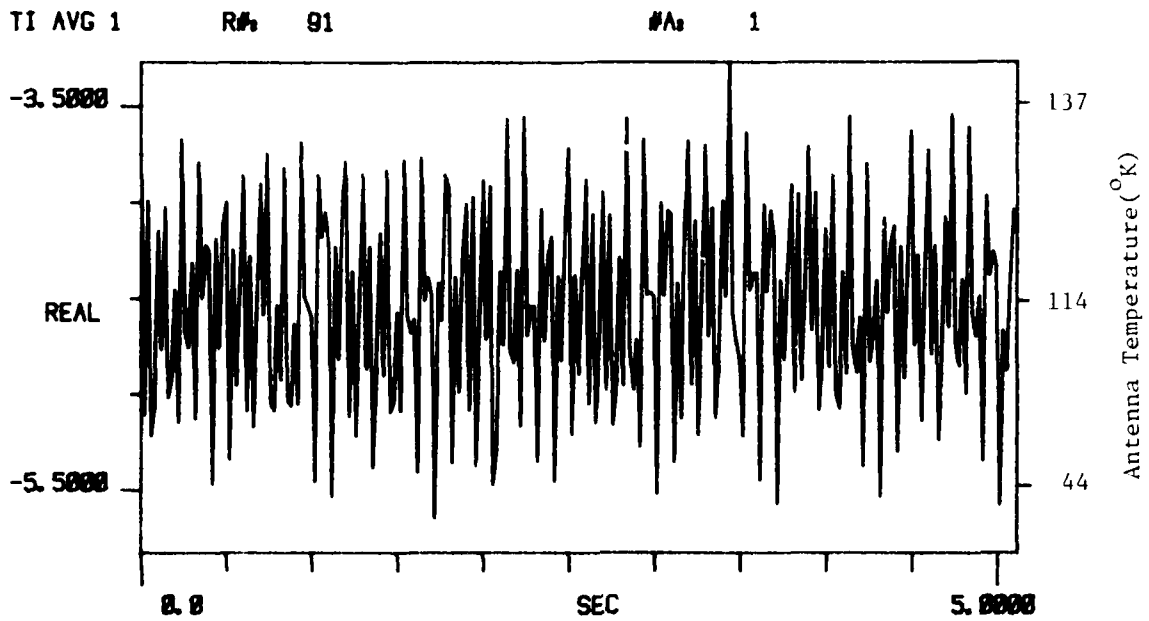
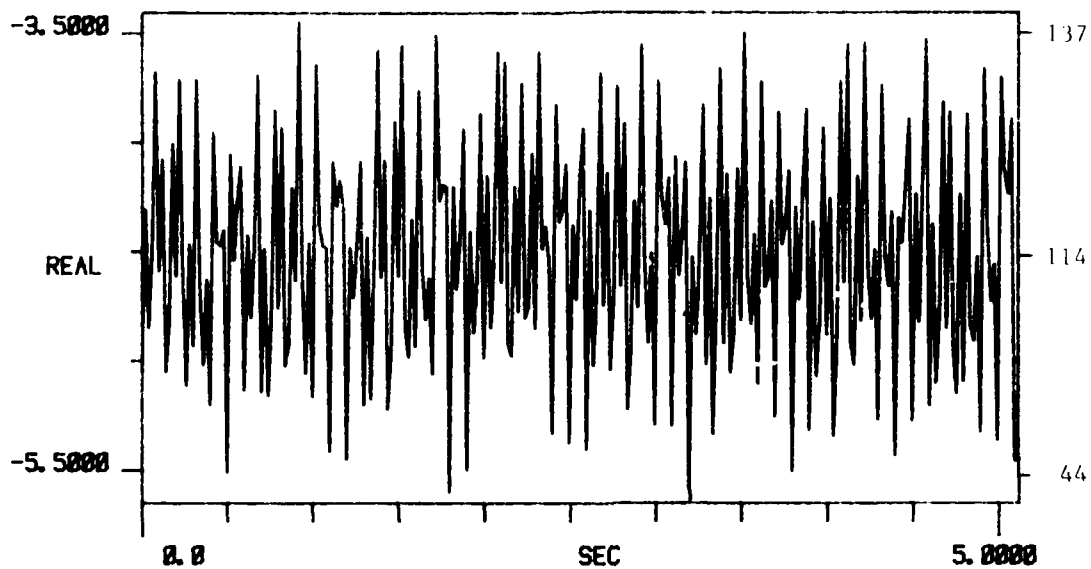


Figure D-6. Zenith Sky Measurement. 16 Mar 80

TI AVG 1

R# 92

#A_s 1



TI AVG

R# 92

#A_s 1

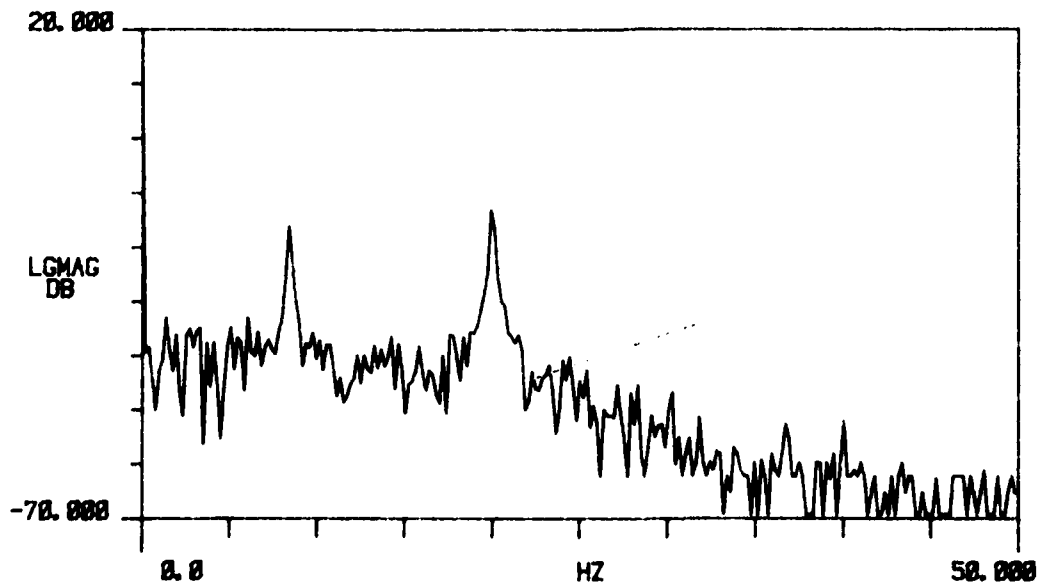


Figure D-6. Zenith Sky Measurement. 16 Mar 80

TI AVG 1

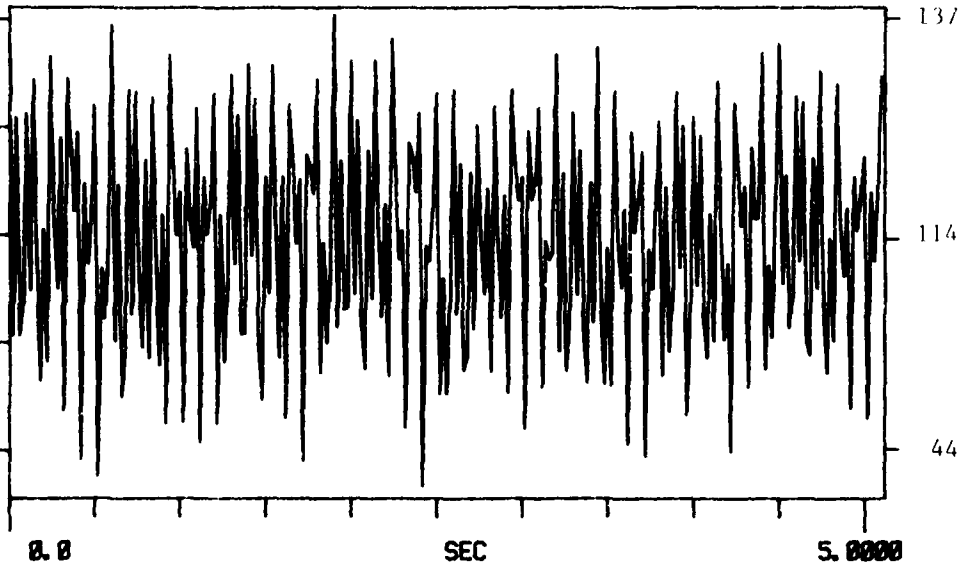
R# 93

#A 1

-3.5000

REAL

-5.5000



Antenna Temperature (°K)

TI AVG

R# 93

#A 1

20.000

LGMAG
DB

-60.000

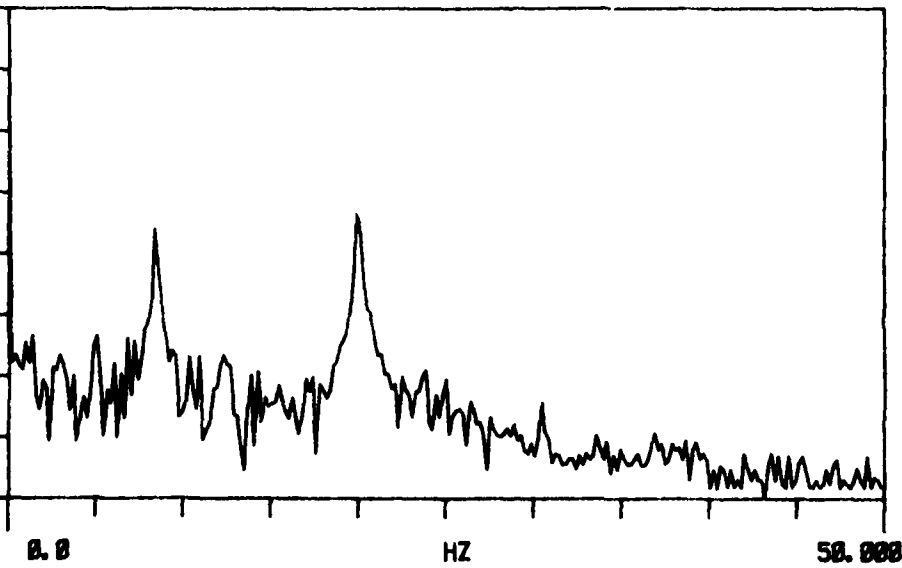


Figure D-6. Zenith Sky Measurement. 16 Mar 80

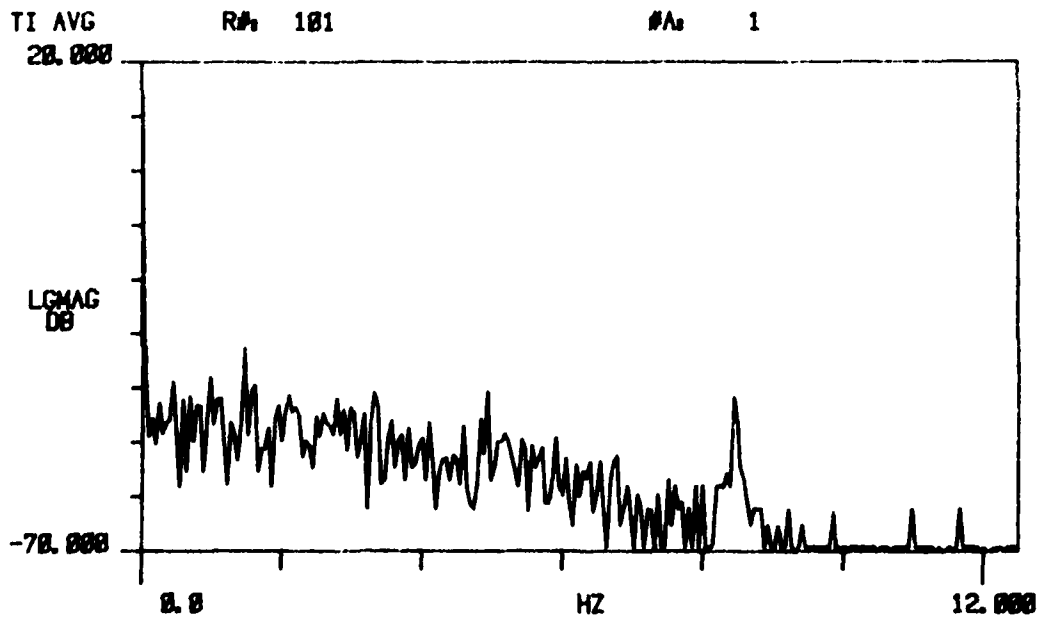
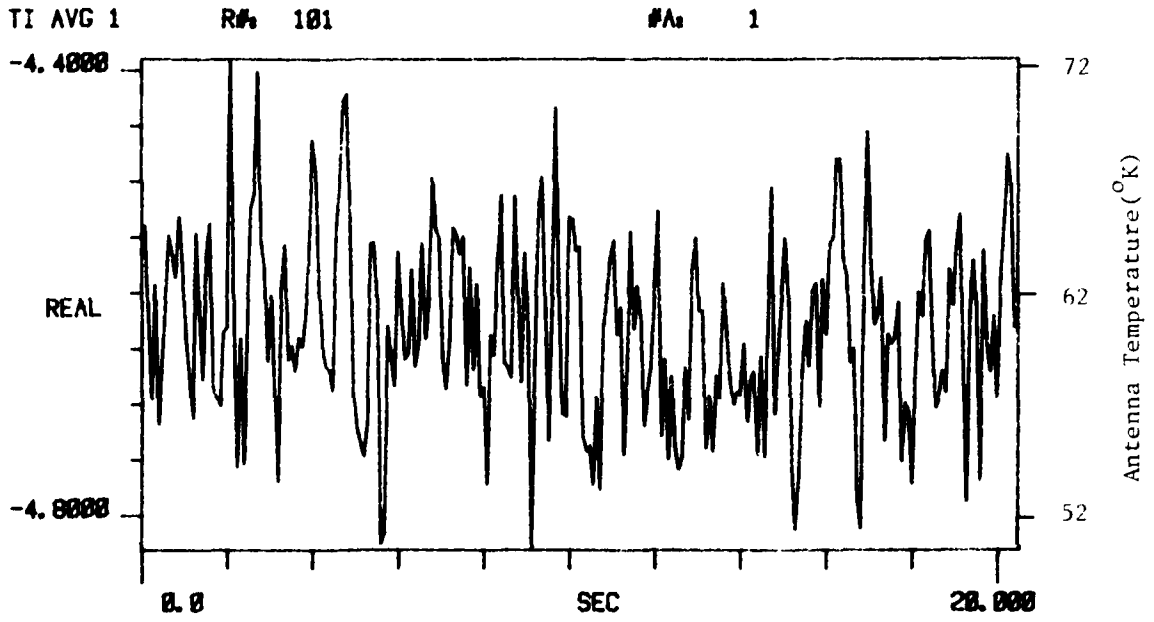
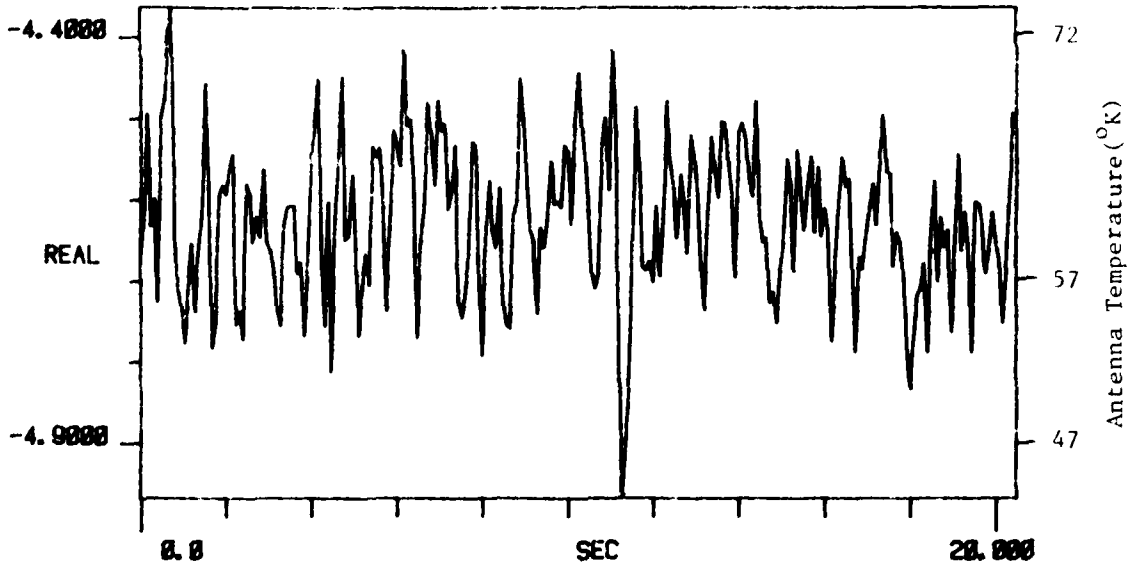


Figure D-6. Zenith Sky Measurement. 16 Mar 80
242

TI AVG 1

R# 182

#A 1



TI AVG
20.000

R# 182

#A 1

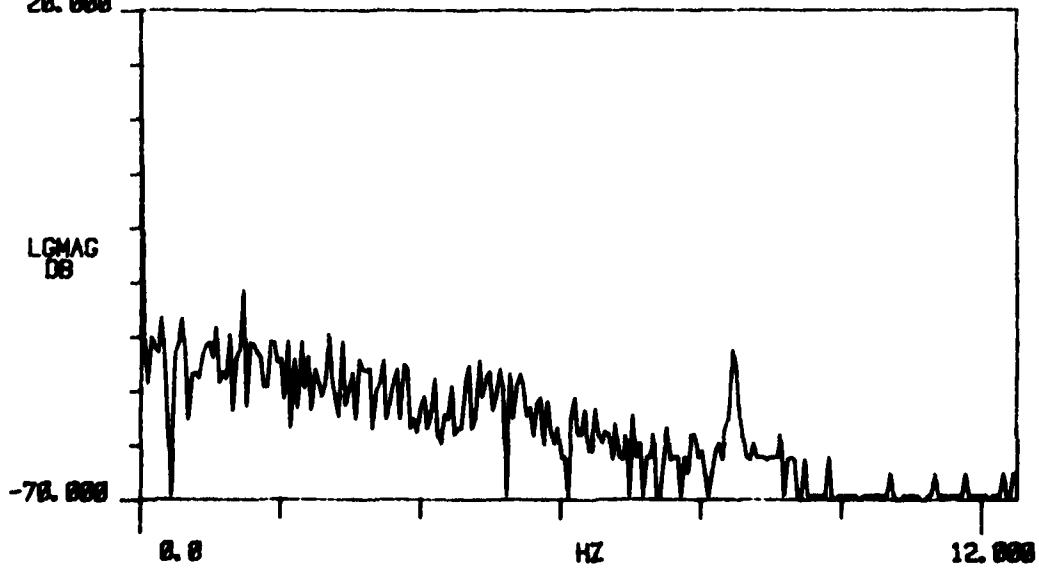
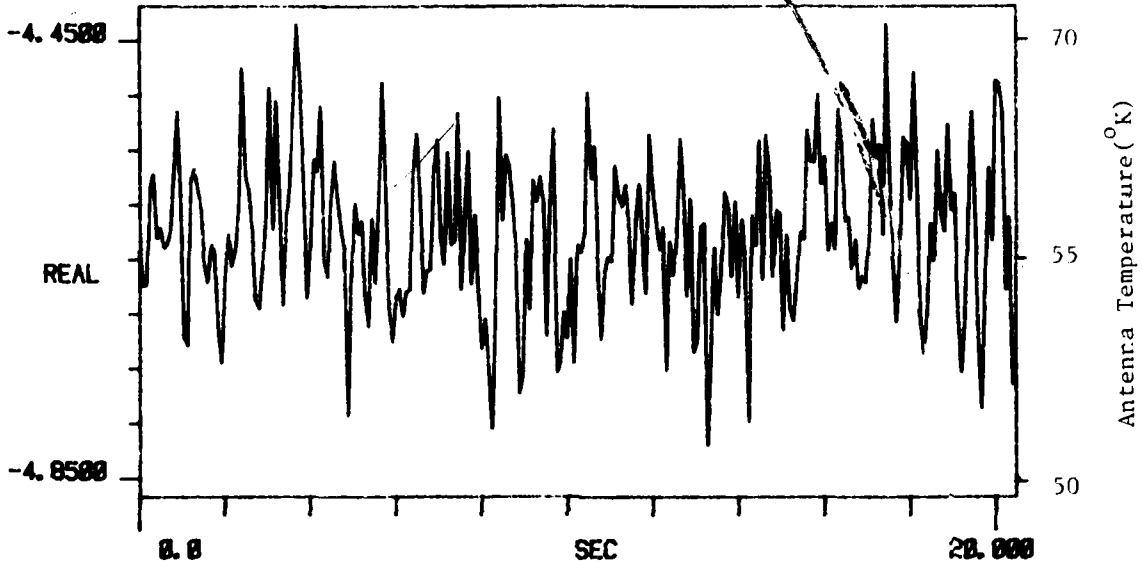


Figure D-6. Zenith Sky Measurement. 16 Mar 80

TI AVG 1

R# 183

#As 1



TI AVG
20.000

R# 183

#As 1

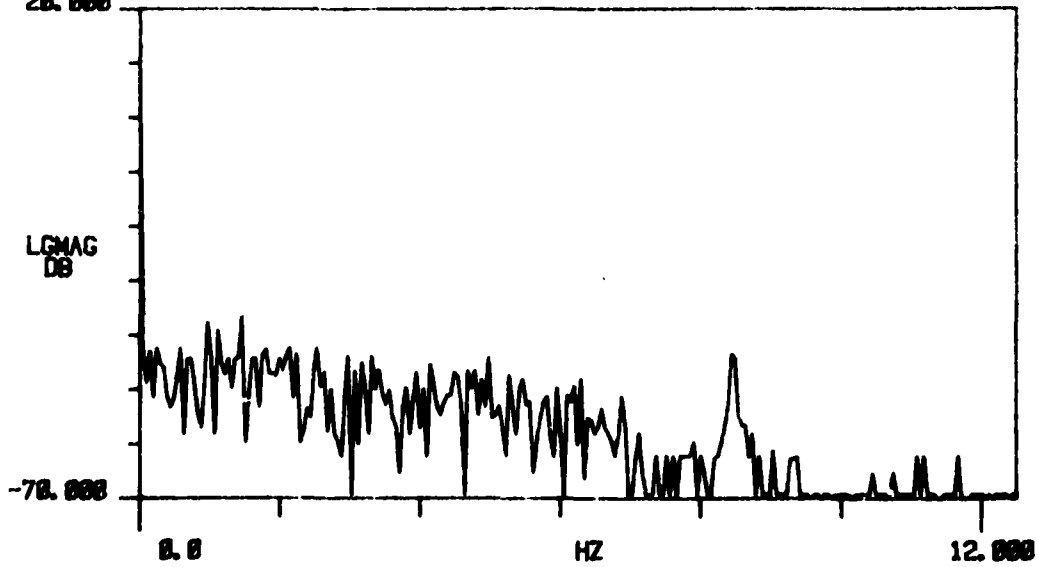


Figure D-6. Zenith Sky Measurement. 16 Mar 80

APPENDIX E

BIBLIOGRAPHY OF ATMOSPHERIC FLUCTUATION EFFECTS

A search of papers relevant to this investigation has been performed. The majority of papers have been concerned with optical propagation experiments of horizontal one-way transmission with coherent sources. Much of the theoretical understanding of turbulence effects originates from these investigations. Only recently have experiments been extended to millimeter wavelengths. Not many publications have treated vertical radiometric observations of atmospheric fluctuations, and most of these have involved fluctuation rates less than 1 Hz. Theory related to vertical passive observations must also be developed in greater detail. In addition to turbulence effects, cloud formations must be included in the formulation of sky brightness temperatures. The importance of wind effects is treated in many publications. Despite the need for advances in both radiometric observations and related theory, most of the papers of the bibliography present various aspects which are important to the fluctuation observations.

BIBLIOGRAPHY

(1) L. Tsang et al, "Theory for Microwave Thermal Emission from a Layer of Cloud or Rains", IEEE Trans. AP, Vol AP-25, No. 5, pp 650-657, Sept. 1977. Formulation of scattering effects of layers of clouds and rain on down-looking radiometers. Derive radiative transfer equations accounting for polarization dependence and drop size distributions. Models clouds and solves resulting equations for brightness versus frequency up to 300 GHz.

- (2) G. G. Haroules, W. E. Brown, "A 60-GHz Multi-Frequency Radiometric Sensor for Detecting Clear Air Turbulence in the Troposphere", IEEE Trans. Aero. Elec. Sys., Vol. AES-5, pp. 712-723, Sept. 1969. -- Model turbulence regions with respect to temperature anomalies.
- (3) A. M. Zavody, "Effect of Scattering by Rain on Radiometer Measurements at Millimeter Wavelengths", Proc. IEEE, Vol. 121 No. 4, pp. 257-263, April 1974. -- Emission from rain due to scattering effects at 37, 72 and 110 GHz discussed. Correction term to antenna temperature for rain in beam area derived.
- (4) R. S. Lawrence, J. W. Strohbehn, "A Survey of Clear-Air Propagation Effects Relevant to Optical Communications", Proc. IEEE, Vol. 58, No. 10, pp. 1523-1545, Oct. 1970. -- Good treatment of how inhomogeneous regions are modeled in the optical region. Large and small scale refractive variations treated.
- (5) J. W. Strohbehn, "Line-of-Sight Wave Propagation Through The Turbulent Atmosphere", Proc. IEEE, Vol. 56, No. 8, pp. 1301-1317, August 1968. -- A review of treatments involving random fluctuations from optical to millimeter wavelengths. Geometrical models of turbulent mediums presented.
- (6) A. Ishimaru, "Fluctuations of a Beam Wave Propagating Through a Locally Homogeneous Medium", Radio Science, Vol. 4, No. 4, pp. 245-305, April 1969. -- Spectral features of index of refraction and its effect on fluctuations.
- (7) H. J. Liebe, J. D. Hoppenen, "Variability of EHF Air Refractivity with Respect to Temperature, Pressure, and Frequency", IEEE Trans. AP, Vol. SP-25, No. 3, pp. 336-345, May 1977 -- Treat 40 to 140 GHz band for simulated atmosphere up to 40 km. Present graphs of refractivity vs. frequency, temperature and pressure. Model O₂ spectral contributions to refractivity variations.

- (8) C. B. Hogge, R. R. Butts, "Frequency Spectra for the Geometric Representation of Wavefront Distortions Due to Atmospheric Turbulence", IEEE Trans. AP-24, No. 2, pp. 144-154, March 1976. -- Frequency spectrum of fluctuations versus wind velocity and antenna aperture derived.
- (9) L. Shen, "Remote Probing of Atmosphere and Wind Velocity by Millimeter Waves", IEEE Trans. AP, Vol. AP-18, No. 4, pp. 493-497, July 1970. -- Effect of wind on C_n^2 discussed and modeled. Limitations concerning knowledge of path wind velocities discussed.
- (10) M B. Kanevskii, "The Problem of the Influence of Absorption on Amplitude Fluctuations of Submillimeter Radio Waves in the Atmosphere", Scientific-Research Radio-Physics Institute, Vol. 15, No. 12, pp. 1939-1949, Dec. 1972. -- Show intensity dependence of amplitude fluctuations on wavelength due to large and small scale turbulence.
- (11) A. O. Izyumov, "Amplitude and Phase Fluctuations of a Plane Monochromatic Submillimeter Wave in a Near-Ground Layer of Moisture-Containing Turbulent Air", Radio Eng. and Elec. Phys., Vol. 13, No. 7, pp. 1009-1013, 1968. -- Increase in fluctuations in window regions compared to absorption line centers discussed.
- (12) A. O. Izyumov, "Frequency Spectrum of Amplitude Fluctuations of a Plane Electromagnetic Wave in Submillimeter Range Propagating in a Surface Layer of Turbulent Atmosphere", Radio Eng. and Elec. Phys., Vol. 14, No. 10 pp. 1609-1611, 1969. -- Presents frequency spectrums for various sizes of inhomogeneities at 300 GHz. Treatment has bearing on 94 GHz modeling.
- (13) L. A. Hoffman, et al, "Propagation Observations at 3.2 Millimeters", Proc. IEEE, Vol. 54, No. 4, pp. 449-454, April 1966. -- Dry, wind atmospheric effects on signal scintillation observed and discussed.

- (14) T. Orhaug, "The Effect of Atmospheric Radiation in the Microwave Region", Publ. of NRAO, Vol. 1, No. 14, pp. 215-250, Oct. 1962 -- Causes for fluctuating component of antenna temperature discussed. Variation formulated in terms of fluctuations in absorption coefficient.
- (15) T. C. L. G. Sollner, "Frequency Spectrum of Fluctuation in Submillimetre Sky Emission and Absorption", Astron. Astrophys., Vol. 55, pp. 361-368, 1977. - Dual beam astronomy investigation of variations in sky emission. Shows power spectra up to 1 Hz for 350 μ window region.
- (16) N. D. Mavroukoulakis et al, "Temporal Spectra of Atmospheric Amplitude Scintillations at 110 GHz and 36 GHz", IEEE Trans. AP, Vol. AP-26, No. 6, pp. 875-877, Nov. 1978. -- Results of propagation experiment over a 4 km London path. Shows spectral density roll-off at 4.5 Hz at 110 GHz. Models atmosphere according to Ishimaru [see reference (6)] formalism. Good theoretical vs. experimental agreement.
- (17) R. S. Cole et al, "The Effect of the Outer Scale of Turbulence and Wavelength on Scintillation Fading at Millimeter Wavelengths", IEEE Trans. AP, Vol AP-26, No. 5, pp. 712-715, Sept. 1978. -- Theoretical treatment of data from reference (16). Show how varying outer scale of turbulence with respect to Fresnel zones effect spectral densities.
- (18) K. L. Ho et al, "Wavelength Dependence of Scintillation Fading at 110 and 36 GHz", Elec. Lett., Vol. 13, No. 7, pp. 181-182, March 1977. - Original British publication of work described in references (16) and (17).
- (19) N. D. Mavroukoulakis et al, "Observation of Millimetre-Wave Amplitude Scintillations In A Town Environment", Elect. Lett., Vol. 13, No. 14, pp. 391-392, July 1977. -- Time records of amplitude fluctuations observed over 4 km London path at 36, 110 GHz. Correlation of fading with wind and temperature changes noted.

- (20) R. W. Lee, "A Review of Line-of-Sight Propagation Studies of the Small-Scale Structure of the Atmosphere", Stanford Electronics Laboratories, May 1969. -- Describes methods of modeling small-scale effects and presents some experimental work on refractivity variations.
- (21) G. T. Wrixon and R. W. McMillan, "Measurements of Earth-Space Attenuation at 230 GHz", IEEE Trans. on Microwave Theory and Techniques, Vol. MTT-26, No. 6, p. 434, 1978. -- This paper is concerned mainly with observations in the 1.3 mm wavelength region but also describes the continuous fluctuations which have been observed on days of high overcast. This data should be further analyzed.
- (22) G. T. Wrixon, "Measurements of Atmospheric Attenuation on an Earth-Space Path at 90 GHz, Using a Sun Tracker", Bell System Tech. Journal, 50, No. 1, p. 103, 1971. -- Has also observed the same effects mentioned in Reference 22.
- (23) L. Lo, B. M. Fannin and A. W. Straiton, "Attenuation of 8.6 and 3.2 mm Radio Waves by Clouds", IEEE Transactions on Antennas and Propagation, AP-23, No. 6, p. 782, 1975. -- Mainly treats attenuation associated with variety of cloud conditions.
- (24) S. Corsi et al, "Atmospheric Noise in the Far Infrared (300-3000 μm)", IEEE Transactions on Microwave Theory and Techniques, MTT-22, No. 12, p. 1036 1974.
- (25) N. A. Armand et al, "Fluctuations of Submillimeter Waves in a Turbulent Atmosphere", Radio Engineering and Electronics Physics, 13, No. 7, p. 1009, 1968. -- Basic theory of fluctuations in an absorbing medium; calculates the ratio of fluctuation variance in absorption to non-absorption fluctuation variance.

- (26) A. S. Gurvich, "Effects of Absorption on the Fluctuation in Signal Level During Atmospheric Propagation", *Ibid.*, 13, No. 11, p. 1687, 1968. -- Paper covers essentially same ground as Reference 25 above from slightly different point of view.
- (27) F. I. Shimabukuro and E. E. Epstein, "Attenuation and Emission of Atmosphere at 3.3 mm", *IEEE Transactions on Antennas and Propagation*, AP-18, No. 4, p. 485, 1980. -- Looked for fluctuations from atmosphere for long integration times > 4 sec, observed no significant contributions.
- (28) J. A. Lane, "Scintillation and Absorption Fading on Line-of-Sight Links at 35 and 100 GHz," in 'Troposphere Wave Propagation', *IEEE Conference Publication* 48, pp. 116-173 (1968).
- (29) "Special Issue on Remote Environmental Sensing," *Proc IEEE* 57, pp 371-742, April 1969.
- (30) R. W. Lee and A. T. Waterman, "Space Correlation of 35 GHz Transmissions over a 28 km path," *Radio Science* 3, pp 135-140 (1968)
- (31) S. F. Clifford and J. W. Strohbehn, "The Theory of Microwave Line-of-Sight Propagation Through a Turbulent Atmosphere," *IEEE Trans. Antennas and Propagation* AP-18, #2, pp. 264-274, March, 1970.
- (32) A. J. Kemp, "A Scintillation Theory for Millimeter and Submillimeter Wavebands," *Digest of the Fourth International Conference on Infrared and Millimeter Waves and Their Applications*, *IEEE Cat. No. 79 CH 1384-7 MTT*, December 10-15, 1979.

- (33) N. A. Armand et al, "Fluctuations of Submillimeter Radio Waves in a Turbulent Atmosphere," Radio Eng. Electronics Physics 16, #8, pp 1259-1266, 1971.
- (34) P. Moffat, "Fluctuations in Atmospheric Transmission at about 3-mm Wavelength," Inter-Union Commission on Radio Meteorology (IVCRM) Colloquium on Probing of Atmospheric Constituents, Bournemouth, England, May 14-21 (1975).
- (35) K. A. Richer, "Environmental Effects on Radar and Radiometric Systems at Millimeter Wavelengths," Proc. Symposium on Millimeter Waves, Polytechnic Institute of Brooklyn, 31 March, 1970.
- (36) E. Jakeman, G. Parry, E. R. Pike and P. N. Bussey, Contemporary Physics 19, 127-145 (1978).
- (37) S. Chandrasekhar, Monthly Notices of the Royal Astronomical Society 112, 475-483 (1952).
- (38) H. G. Brooker, Proceedings of the Institute of Radio Engineers 46, 289-314 (1958).
- (39) R. Hinder and M. Ryle, Monthly Notices of the Royal Astronomical Society 154, 229-253 (1972).
- (40) V. I. Tatarski, "Wave Propagation in a Turbulent Medium," New York: Dover, 1961.
- (41) S. F. Clifford, "Temporal Frequency Spectra for a Spherical Wave Propagating Through Atmospheric Turbulence," Jour. Opt. Soc. Amer 61, #10, pp 1285-1292, 1971.

- (42) A. Ishimaru, "Temporal Frequency Spectra of Multi-frequency Waves in Turbulent Atmosphere," IEEE Trans. Antenna Propagat. AP-20, 10-19 (1972).
- (43) P. A. Mandics, R. W. Lee and A. T. Waterman, Jr., "Spectra of Short-Term Fluctuations of Line-of-sight Signals: Electromagnetic and Acoustic," Radio Science 8, #3, pp 185-201 (1973).
- (44) P. A. Mandics, J. C. Harp, R. W. Lee and A. T. Waterman, Jr, "Multi-frequency Coherences of Short-Term Line-of-sight Signals: Electromagnetic and Acoustic," Radio Science 9, #8, 9, pp 723-731, 1974.
- (45) H. B. Janes, M. C. Thompson Jr., D. Smith, and A. W. Kirkpatrick, "Comparison of Simultaneous Line-of-sight Signals at 9.6 and 34.5 GHz," IEEE Trans. AP-18, #4, pp 447-51 (July, 1970).
- (46) J. S. Bendat and A. G. Piersol, "Measurement and Analysis of Random Data," New York: Wiley, 1966.
- (47) R. W. McMillan, J. C. Wiltse, and D. E. Snider, "Atmospheric Turbulence Effects on Millimeter Wave Propagation," IEEE EASCON, 1979.
- (48) R. W. McMillan and D. E. Snider, "Atmospheric Turbulence Effects on Infrared and Near-Millimeter Wave Propagation," Digest of the Fourth International Conference on Infrared and Millimeter Waves and Their Applications, IEEE Cat. No. 79 CH 1384-7 MTT, December 10-15, 1979.
- (49) H. B. Janes and M C. Thompson, Jr. "Fading at 9.6 GHz on an Experimentally Simulated Aircraft-to-Ground Path," IEEE Transactions on Antennas and Propagation, AP-26 #5, 715 (1978).
- (50) R. W. Lee and J. C. Harp, "Weak Scattering in Random Media with Application to Remote Sensing," Proc. IEEE 57, #4, pp 375-406, April 1969.

- (51) A. N. Kolmogoroo, "The Local Structure of Turbulence in Incompressible Viscous Fluid for Very Large Reynolds' Numbers," Doklady Akad. Nauk SSSR 30, 301 (1941).
- (52) Thompson, M. C., Jr., and Janes, H. B., "Measurements of Phase-Front Distortion on an Elevated Line of Sight Path," IEEE Trans. vol AES-6 no. 5, Sept. 1970, pp 645-55. (x-band).
- (53) Bennett, J. A., "Refractive Errors in Angle-of-Elevation Measurements," IEEE Trans vol AES-7 no. 2, March 1971, pp 243-7. (theory).
- (54) Lees, M. L., "High Resolution Measurement of Microwave Refraction on Short Tropospheric Paths," IEEE Trans vol AP 20 no. 2, March 1972, pp 176-81. (K_a band).
- (55) Valley, G. C., "Angular Jitter in Amplitude Comparison Monopulse Radar Due to Turbulence," IEEE Trans vol AP-23 no. 2, March 1975, pp 274-8. (theory).
- (56) Andreev, G. A. and Chornaya, L. F., "Amplitude and Phase Fluctuations of Millimeter Wave (MMW) Beam Propagating in a Turbulent Atmospheric Atmosphere," Proc. Anglo-Soviet Seminar on Atmospheric Propagation at Millimetre and Submillimetre Wavelengths, Moscow, Nov. 28 - Dec. 3, 1977, pp P1-10. (theory 0.8-10 mm).
- (57) Tukiz, O, "Theory of the Scintillation Fading of Microwaves," IRE Trans vol AP 5 no. 1, Jan. 1957, pp 130-6.
- (58) Muchmore, R. B., and Wheelon, A. D., "Frequency Correlation of Line-of-Sight Signal Scintillations," IEEE Trans vol AP-11 no. 1, Jan. 1963., pp 130-6.
- (59) Crawford, A. B., and Jakes, C. W., Jr., "Selective Fading of Microwaves," BST J vol. 31 no 1, Jan. 1952, pp 68-90 (Measurements: angle of arrival 1.25 cm, fading, S-band).

- (60) Kiely, D. G., "Some Measurements of Fading at a Wavelength of 8MM over a Very Short Sea Path," J. Brit IRE, vol 14, Feb. 1954, pp 89-92.
- (61) Tolbert, C. W., Fannin, B. M., and Straiton, A. W., "Amplitude and Phase Difference Fluctuations of 8.6MM and 3.2 CM Radio Waves on Line-of-sight Paths," Univ. of Texas EERL Rpt 78, March 1956, DDC AD 08810.
- (62) Tolbert, C. W., and Straiton, A. W., "Attenuation and Fluctuation of Millimeter Radio Waves", IRE Nat. Conv Rec vol 5 pt 1, 1957, pp 12-18.
- (63) J. W. Strohbehn and S. F. Clifford, "Polarization and Angle to Arrival Fluctuations for a Plane Wave Propagated Through a Turbulent Medium", IEEE Trans. Antennas and Propagation, Vol. AP-15, No. 3, May 1967, pp. 416-421.
- (64) G. A. Andreyev, V. A. Golunov, A. T. Ismailov, A. A. Parshikov, B. A. Rozanov, and A. A. Tanyigin, "Intensity and Angle of Arrival Fluctuations of Millimetric Radiowaves in Turbulent Atmosphere", Joint Anglo-Soviet Seminar on Atmospheric Propagation at Millimetre and Submillimetre Wavelengths, Institute of Radioengineering and Electronics, Moscow, November, 1977.
- (65) Tolbert, C. W., Britt, C. O., and Straiton, A. W., "Antenna Pattern Fluctuations at 4.3 Millimeter Wavelengths Due to Atmospheric Inhomogeneities", Univ. of Texas EERL Rpt no. 96, 13 Dec 1957.
- (66) Weibel, G. F., and Dressel, H. O., "Propagation Studies in Millimeter-Wave Link Systems," Proc IEEE vol 55 no. 4, April 1967, pp 497-513. (measurements, 3.3mm).
- (67) Lane, J. A., et al, "Absorption and Scintillation Effects at 3mm Wavelength on a Short Line-of-sight Radio Path," IEE Electron. Lett. vol 3 no. 5, May 1967, pp 185-6.
- (68) Matthews, P. A., "Scintillation on Millimetre Wave Radio Links and the Structure of the Atmosphere," Proc. Anglo-Soviet Seminar loc cit, pp H1-8-

END

DATE
FILMED

6-81

DTIC